THE UNIVERSITY OF QUEENSLAND

AUSTRALIA

The Functional Role of Laminins-α4 and -β2 in Development of the Neuromuscular Junction

Kirat Kishore Chand

BSc. (Hons)

A thesis submitted for the degree of Doctor of Philosophy at

The University of Queensland in 2014

School of Biomedical Sciences

Abstract

The precise development and organisation of the neuromuscular junction (NMJ) is critical for the production of efficient neurotransmission signals. Disruption of these specialisations may result in severely altered transmission properties at the NMJ. Signalling and adhesion molecules have long been established to be key mediators in the distribution of synaptic specialisations. The basal lamina acts to maintain stability of the associated tissue and contains a number of these signalling and adhesion molecules. The laminins, a family of large multimeric proteins, are one of the key components of the basal lamina that act as specific cell regulators and provide mechanical stability. Laminins have been shown to form an interconnecting network that assists in stabilisation of the basal lamina and provides attachment sites for other basal lamina components. The synapse specific laminin chains, -α4, -α5, and -β2, play an essential role in differentiation and organisation of the NMJ. These chains form the laminin isoforms, laminin-221 (α2β2γ1), laminin-421 (α4β2γ1), and laminin-521 (α5β2γ1).

Laminin-β2, found in each of the three synapse specific isoforms, has been shown to organise presynaptic specialisations at the developing NMJ. *In vitro* laminin-β2 is able to interact directly with N-type and P/Q-type voltage-gated calcium channels (VGCCs), suggesting a role in organising VGCCs in close proximity to active zones. During NMJ development and maturation different VGCCs mediate neurotransmission, with N-type VGCCs being dominant during early development but later switching to P/Q-type VGCC mediation as the NMJ matures. Mice deficient in laminin-β2 (*lamb2*$^{-/-}$), present severely disrupted neurotransmission properties, and morphological abnormalities including invasion of the synaptic cleft by perisynaptic Schwann cell (PSCs) processes. The poor transmission properties observed at *lamb2*$^{-/-}$ NMJs may be attributed to the entry of the processes into the cleft, with laminin-521, containing the β2 chain, shown to directly prevent invasion of the synaptic cleft by PSCs. The laminin-α4 chain forms the unique short arm laminin-421 heterotrimer. Targeted mutation of the *lama4* gene does not alter formation of active zones and junctional folds, though disruptions in the precise alignment of active zones and postsynaptic folds are seen at NMJs of laminin-α4 deficient mice (*lama4*$^{-/-}$). The functional consequences of loss in laminin-α4 had not been previously reported.

This study examined the role of laminin-β2 in the organisation of N- and P/Q-type VGCCs at active zones of developing postnatal day 8 (P8) and matured, postnatal day 18 (P18) NMJs. The contribution of each channel to the release of transmitter was assessed using intracellular electrode recordings of end-plate potentials (EPPs). The VGCC toxins, ω-conotoxin-GVIA and ω-agatoxin-IVA, were used to specifically target N- and P/Q-type VGCCs respectively in order to assess the relative contribution of each subtype to neurotransmission in wild type (WT) and *lamb*2$^{-/-}$ mice. Utilising live Ca^{2+} imaging techniques we also assessed the capabilities of PSCs at postnatal day 14 (P14) *lamb*2$^{-/-}$ NMJs. The present study also investigated the functional consequences of loss in laminin-α4 at both P8 and P18. Utilising electrophysiological recordings we characterised the neurotransmission properties of mutant mice compared to age-matched wild-type littermates. Immunohistochemical analyses were undertaken to support our functional studies.

This study found that loss of either laminins-α4 or -β2 resulted in markedly different deficits in neurotransmission. *Lamb*2$^{-/-}$ NMJs demonstrated decreased calcium sensitivity with no change in calcium dependence compared to wild-type littermates. Mutants did not display the characteristic change in VGCC subtype involved with mediating neurotransmitter release. These mutants maintained dependence on N-type VGCCs with P/Q-type channels playing a minor role, in contrast to age-matched wild-type NMJs which predominantly relied on P/Q-type VGCCs at P18. Immunohistochemical analyses confirmed this finding with *lamb*2$^{-/-}$ NMJs displaying a significantly higher expression of N-type channels at the presynaptic membrane than wild-type littermates. Laminin-β2 deficient junctions also demonstrate poor maturation of perisynaptic Schwann cells. At *lamb*2$^{-/-}$ NMJs, PSCs fail to mature and remain dependent on the developmental purinergic signalling receptor ($P_{2Y}R$) rather than switch to the muscarinic signalling receptor (MR) family associated with maturation. The failure to switch signalling receptors resulted in poor decoding of neurotransmission signals, as shown by our functional work on the *lamb*2$^{-/-}$ soleus preparation at P14. At *lama*4$^{-/-}$ NMJs, we observed early perturbations in neurotransmission from P8, which became more evident by P18. *Lama*4$^{-/-}$ NMJs displayed significantly higher levels of synaptic depression under high frequency stimuli and altered paired pulse facilitation compared to wild-type littermates. Analysis of the binomial parameters of neurotransmitter release demonstrated a decrease in quantal release as a result of a decrease in the number of active release sites, but not in the average probability of transmitter release from these sites. Our functional findings suggest alterations in the short-term plasticity of the NMJ and possibly defective recycling of

synaptic vesicles and/or the calcium handling at *lama*4$^{-/-}$ NMJs. We propose that alterations to synapsin I and its associated molecules may be partly responsible for the changes in neurotransmission observed at *lama*4$^{-/-}$ NMJs. Our findings demonstrate altered distribution and expression of presynaptic components associated with active zones, specifically an increase in the number of synaptic vesicles and a decrease in the density of the fluorescently labelled Bassoon at the active zone region. Our results suggest that the fewer active release sites may compensate for the deficits of the *lama*4$^{-/-}$ NMJs by alterations to pre- and postsynaptic specialisations.

In conclusion, this thesis has identified that laminins-α4 and -β2 play fundamental roles in establishing efficient neurotransmission properties at the NMJ. Results suggest that laminin-β2 is a key regulator in development of the neuromuscular junction, with its loss resulting in reduced transmitter release due to decreased calcium sensitivity stemming from a failure in the developmental switch from N- to P/Q-type VGCCs in mediation of transmitter release. Associated with this failed switch in VGCCs, we note a failure in the developmental expression and clustering of presynaptic N- and P/Q type VGCCs and associated presynaptic molecules at *lamb*2$^{-/-}$ NMJs. We are also the first to characterise the functional consequences of the loss of laminin-α4, finding subtle changes in neurotransmission properties at mutant NMJs. We suggest laminin-α4 plays a role in organisation of the NMJ during development, with its loss resulting in altered neurotransmission properties that do not significantly compromise the survival of the animal.

Declaration by author

This thesis *is composed of my original work, and contains* no material previously published or written by another person except where due reference has been made in the text. I have clearly stated the contribution by others to jointly-authored works that I have included in my thesis.

I have clearly stated the contribution of others to my thesis as a whole, including statistical assistance, survey design, data analysis, significant technical procedures, professional editorial advice, and any other original research work used or reported in my thesis. The content of my thesis is the result of work I have carried out since the commencement of my research higher degree candidature and does not include a substantial part of work that has been submitted *to qualify for the award of any* other degree or diploma in any university or other tertiary institution. I have clearly stated which parts of my thesis, if any, have been submitted to qualify for another award.

I acknowledge that an electronic copy of my thesis must be lodged with the University Library and, subject to the General Award Rules of The University of Queensland, immediately made available for research and study in accordance with the *Copyright Act 1968*.

I acknowledge that copyright of all material contained in my thesis resides with the copyright holder(s) of that material. Where appropriate I have obtained copyright permission from the copyright holder to reproduce material in this thesis.

Publications during candidature

Chand, K.K., Lee, KM., Schenning, M.P., Lavidis, N.A., and Noakes, P.G. (2014) Loss of β2-laminin Alters Calcium Sensitivity and Voltage Gated Calcium Channel Maturation of Neurotransmission at the Neuromuscular Junction. *The Journal of Physiology.* DOI: 10.1113/jphysiol.2014.284133

Ngo, S.T., Caudron, A.J., Lichanska, A.M., Chand, K.K., Choy, P.T., Lavidis, N.A., Yoneda-Kato, N., Cooper, H.M., and Noakes, P.G. Altered expression of Zyxin and Mlf1 following genetic and physical disruption of neuromuscular synaptic transmission. *Neurological Sciences*. Submitted manuscript, 2014

Conferences and symposiums

National:

Chand K.K., Lavidis N.A., and Noakes P.G. Functional identification of specific voltage gated calcium channel types supporting neurotransmitter release at neuromuscular synapses missing β2-laminin. 31st Annual Meeting of the Australian Neuroscience Society, January 2011. POS-TUE-018. (*Presenting author*)

Chand K.K., Darabid H., Lavidis N.A., Robitaille R. and Noakes P.G. Mice lacking β2-laminin present altered neuromuscular synapses: Functional investigation of Schwann cell activity. School of Biomedical Science International Symposium, October 2013. ORAL SESSION 5-2. (*Presenting author*)

International:

Chand K.K., Darabid H., Lee, KM., Lavidis N.A., Robitaille R. and Noakes P.G. Mice Lacking β2-laminin Present Immature Neuromuscular Synapses: Functional Investigation of Calcium Channel Subtypes Involved in Transmitter Release. 7th Annual International Motoneuron Meeting. Sydney, Australia. July 2012. P30. (*Presenting author*)

Chand K.K., Lee, KM., Lavidis N.A., and Noakes P.G. The role of β2-laminin in localization of voltage-gated calcium channels at active zones of mouse neuromuscular junctions. 42nd Annual Meeting of the Society for Neuroscience. New Orleans, United States of America. October 2012. 743.03/C52. (*Presenting author*)

Darabid H., Chand K.K., Lavidis N.A., Noakes P.G., and Robitaille R. Altered Neuron-Glia Interactions at Neuromuscular Junctions of Beta2-Laminin Deficient Mice. 8th Annual Canadian Neuroscience Meeting. Toronto, Canada. May 2013. 2-B-20.

Chand K.K., Lee, KM., Noakes P.G., and Lavidis N.A. Loss of α4-laminin results in aberrant neurotransmission in multiple skeletal muscle fiber types. 43rd Annual Meeting of the Society for Neuroscience. San Diego, United States of America. November 2013. 229.01/E44. (*Presenting author*)

Lee, KM., Chand K.K., Lavidis N.A., and Noakes P.G. α4-laminin is not involved in the developmental switch of voltage-gated calcium channel subtypes. 43rd Annual Meeting of the Society for Neuroscience. San Diego, United States of America. November 2013. 229.20/F9.

Chand K.K., Lee, KM., Patton, B.L., Noakes P.G., and Lavidis N.A. Loss of laminin-α4 leads to decreased functional capacity in neurotransmission at maturing neuromuscular junctions. 44th Annual Meeting of the Society for Neuroscience. Washington D.C., United States of America. November 2014. 598.08 / C67. (*Presenting author*)

Lee, KM., Chand K.K., Patton, B.L., Lavidis N.A., and Noakes P.G. Loss of laminin-α4 accelerates aging of the neuromuscular junction. 44th Annual Meeting of the Society for Neuroscience. Washington D.C., United States of America. November 2014. 598.25 / D12.

Publications included in this thesis

Chand, K.K., Lee, KM., Schenning, M.P., Lavidis, N.A., and Noakes, P.G. (2014) Loss of β2-laminin Alters Calcium Sensitivity and Voltage Gated Calcium Channel Maturation of Neurotransmission at the Neuromuscular Junction. *J Physiol.* ***The submitted manuscript is incorporated as Chapter 3.***

Contributor	Statement of contribution
Chand, K.K.	Electrophysiology studies – 80% Immunohistochemistry and analysis – 5% Interpretation of results – 50% Manuscript preparation – 80% Reviewing and editing manuscript – 50% Study Design – 10%
Lee, KM.	Histological processing and analysis – 100% Immunohistochemistry and analysis – 95% Interpretation of results – 10% Manuscript preparation – 20% Reviewing and editing manuscript – 15% Study Design – 10%
Schenning, M.P.	Electrophysiology studies – 20%
Lavidis, N.A.	Interpretation of results – 20% Reviewing and editing manuscript – 10% Study Design – 40%
Noakes, P.G.	Interpretation of results – 20% Reviewing and editing manuscript – 25% Study Design – 40%

Contributions by others to the thesis

The majority of work completed throughout this thesis was undertaken by KK Chand. Help was provided for the conception and design of the project as well as interpretation of results and critical revision of work by NA Lavidis and PG Noakes, with R Robitaille contributing to Chapter 4. KM Lee significantly contributed to the immunohistochemistry conducted in Chapters 3 & 5. H Darabid was involved equally with all experimental work contributing to Chapter 4.

Statement of parts of the thesis submitted to qualify for the award of another degree

None

Acknowledgements

I would like to acknowledge the many individuals who have helped me on both a personal and professional level throughout the duration of my candidature. First and foremost, my sincerest thanks to my supervisor, Dr. Nickolas Lavidis, for your generosity, guidance and assistance with all aspects of my project. Your enthusiasm and love for neuroscience drew me to your laboratory during my undergraduate years, and your passion to the field has not waned even in the most difficult of times. You have provided an environment in which I could grow as an individual, develop scientific skills, and learn life lessons while enjoying a few pancakes along the way. All I can simply say is, thank you.

To Kah Meng (Andi) Lee, my dear friend and laboratory colleague, I say thank you. Your assistance with experiments, discussions about the project, and your friendship throughout has made the countless hours in front of the rig fly past. My sincerest gratitude to you for helping make this project what it is.

A special thanks to my Lavidis laboratory members, Elizabeth Butt, Cortina Chen, Carlie Cullen, Cheng Han Goh, Erica Mu, Jessica Soden, and Jereme Spiers. Whether you have assisted me along the way experimentally, had a simple troubleshooting discussion, or a friendly chat over a drink to ease the stress, your friendship has been immeasurable and made this journey so much more fulfilling. Working with each of you over the last few years has resulted in numerous fond memories and has forged friendships that will last many years.

Special thanks must also go to Associate Professor Peter Noakes for providing his expertise and assistance with this project, as well as his comprehensive drafting process. In addition, thank you to all Noakes laboratory members, most especially Matthew Fogarty, John Lee, and Haitao Wang for your friendship and assistance.

Finally, I would like to thank all of my family and friends. Your comfort, support and assistance during my study has allowed me to reach my goals. Apologies for all the missed occasions, I promise to make up for them. Without your unwavering support this would not have been possible.

Keywords

laminins, neuromuscular junction, basement membrane, voltage-gated calcium channels, neurotransmission, perisynaptic Schwann cells, development, maturation

Australian and New Zealand Standard Research Classifications (ANZSRC)

ANZSRC code: 110902, Cellular Nervous System, 40%

ANZSRC code: 110904, Neurology and Neuromuscular Diseases, 40%

ANZSRC code: 110905, Peripheral Nervous System, 20%

Fields of Research (FoR) Classification

FoR code: 1109, Neurosciences, 75%

FoR code: 1116, Medical Physiology, 25%

Table of Contents

List of Figures

List of Tables

List of Abbreviations

α-BTX	alpha-bungarotoxin
ω-Aga IVA	omega-agatoxin VIA
ω-CTX GVIA	omega-conotoxin GVIA
ω-CTX MVIIC	omega-conotoxin MVIIC
ACh	Acetylcholine
AChE	Acetylcholinesterase
AChR	Acetylcholine Receptor
BSA	Bovine serum albumin
CAST	Cytomatrix at the active zone-associated structural protein
CAZ	Cytomatrix Active Zone proteins proteins
CMD	Congenital muscular dystrophy
CMS	Congenital myasthenic syndrome
CNS	Central nervous system
Dia	Diaphragm
EDL	*Extensor Digitorum Longus*
EPCs	End-plate currents
EPPs	End-plate potentials
lama4	Laminin alpha 4 gene
lamb2	Laminin beta 2 gene
LRE	Leucine-arginine-glutamate
MEPCs	Miniature endplate currents
MEPPs	Miniature end plate potentials
MuSK	Muscle Specific Kinase
NTI	Nerve terminal impulse
NMJ	Neuromuscular junction
PBS	phosphate buffered saline

PSCs	Perisynaptic Schwann Cells
RIM	Rab3-interacting molecule
RMP	Resting membrane potential
SOL	Soleus
SNAP-25	Synaptosome- associated protein of 25 kDa
SNAREs	Soluble N-ethylmaleimide sensitive factor attachment protein receptors
STX1A	Syntaxin 1A
SV2	Synaptic vesicle protein 2
Syt2	Synaptotagmin 2
TX-100	Triton X-100
VGCC	Voltage Gated Calcium Channel

CHAPTER 1

Literature Review

INTRODUCTION

The skeletal neuromuscular junction (NMJ) is a highly specialised synapse formed between an innervating motor neuron and a skeletal muscle fibre. The precise molecular and architectural organisation of the NMJ enables efficient electro- chemical communication from the central nervous system (CNS) to the muscle fibres (Wu *et al.*, 2010). The NMJ is composed of three primary structural elements; the presynaptic nerve terminal capped by perisynaptic Schwann cells (PSCs), the synaptic cleft, and the postsynaptic end-plate region. At a mature NMJ the precise structural apposition is necessary for efficient release of neurotransmitter from the presynaptic motor neuron into the synapse. Released transmitter diffuses across the synaptic cleft, a region lined with basal lamina, and binds to ligand gated receptors at the postsynaptic muscle membrane ultimately culminating in muscular activity (Sanes, 1995).

By comparison to other synapses, the accessibility and large structural size of the vertebrate NMJ has enabled a comprehensive understanding of the structure, function, and development of this synapse (Sanes & Lichtman, 1999). During development the NMJ undergoes a switch from polyinnervation to singly innervated synapses, with multiple neuromuscular connexions at birth reducing to single connexions during early postnatal development (Redfern, 1970; Balice-Gordon & Lichtman, 1993; Katz & Shatz, 1996; Tapia *et al.*, 2012; Turney & Lichtman, 2012). Polyneuronal innervation occurs due to excessive axonal branching during embryonic development, with multiple axon branches converging at a single end-plate region on each fibre, leading to innervation from multiple motor neurons (Brown *et al.*, 1976). The reduction in the number of converging axons, termed synaptic elimination, occurs during the early stages of postnatal development, within the first two weeks postnatal in mice. This process essentially entails the withdrawal of multiple axons with only a single innervating axon remaining at the end-plate, resulting in a mono-innervated muscle fibre (Walsh & Lichtman, 2003). Perisynaptic Schwann Cells (PSCs) are suggested to play a role in these remodelling processes by detecting strong versus weak synaptic axonal signalling, and actively ‘pruning’ away weaker axons (Darabid *et al.*, 2013; Smith *et al.*, 2013). During this period of neural development intricate bi-directional exchange of signalling between the motor terminal and target muscle fibres leads to the formation of a functional synapse. As such, synaptic elimination coincides with a change in postsynaptic acetylcholine receptor (AChR) patterning. Nerve terminals are eliminated presynaptically from the same regions that lose AChRs postsynaptically. The occupancy of synaptic territory is highly dynamic and changes during the course of competition and elimination (Turney & Lichtman, 2012).

Recently, NMJ research has focused on a group of signalling and adhesion proteins located in the basal lamina in particular the laminin protein family. These proteins, specifically laminin chains; α2, α4, α5, β2 and γ1 form the three laminin isoforms, 221 (α2 β2 γ1), 421 (α4 β2 γ1), and 521 (α5 β2γ1), which are found exclusively at the synapse of the NMJ (Sanes, 1995; Aumailley *et al.*, 2005). The laminin-α4, -α5, and -β2 chains have been identified to play a critical role in differentiation and function of pre- and postsynaptic regions of the NMJ (Patton *et al.*, 1997; Patton, 2000; Nishimune *et al.*, 2004; Nishimune *et al.*, 2008; Carlson *et al.*, 2010; Chen *et al.*, 2011; Nishimune, 2012). The laminin-β2 chain is found specifically in the basal lamina of the NMJ in each of the three-synapse specific laminin isoforms (221, 421 and 521). It has been shown that laminin-β2 is involved in the organisation of the presynaptic region (Noakes *et al.*, 1995a; Nishimune *et al.*, 2004; Carlson *et al.*, 2010; Nishimune, 2012). The laminin-α4 chain is found concentrated in the basal lamina as part of the laminin heterotrimer, laminin-421 (Patton *et al.*, 1997). It has been suggested that laminin-α4 coordinates precise pre- and postsynaptic differentiation at the NMJ (Patton *et al.*, 2001; Carlson *et al.*, 2010). Laminin chain mutations lead to defects in organisation of pre- and postsynaptic structures that can result in reduced neurotransmission at the NMJ (Knight *et al.*, 2003). Presently, studies of laminin mutations have largely focused on ultra-structural examination utilising electron microscopy and immunohistochemistry to observe alterations in molecular organisation. Consequently, we will investigate aberrations in neurotransmission at the skeletal NMJ in mice lacking the α4, and β2 chains using functional electrophysiological and calcium imaging techniques.

1.1 The Tripartite Structure and Function of the Neuromuscular Junction

The skeletal NMJ is structurally organised to allow efficient communication of an electrical impulse from the motor axon to the muscle fibres via the release of neurotransmitter. The type of neurotransmitter released at the NMJ varies between species. For example, in order to initiate an excitatory response at the NMJ, acetylcholine (ACh) is released in vertebrates whereas in Drosophila glutamate serves the same function. The skeletal NMJ operates at a high safety factor, meaning transmitter is released in excess than that required to excite postsynaptic cells, which in turn aids in the production of strong and reliable neurotransmission under various physiological conditions and stresses (Wood & Slater, 1997, 2001). The NMJ is a tripartite structure comprising of three key cellular elements; the presynaptic nerve terminal, PSCs, and the postsynaptic region of muscle characterised by membrane infolding (termed postjunctional folds) (see Figure 1.1). The nerve terminal is capped by PSCs with both structures separated from the postsynaptic specialisations by the synaptic cleft, a region lined/filled with synaptic basal lamina (see Figure 1.1).

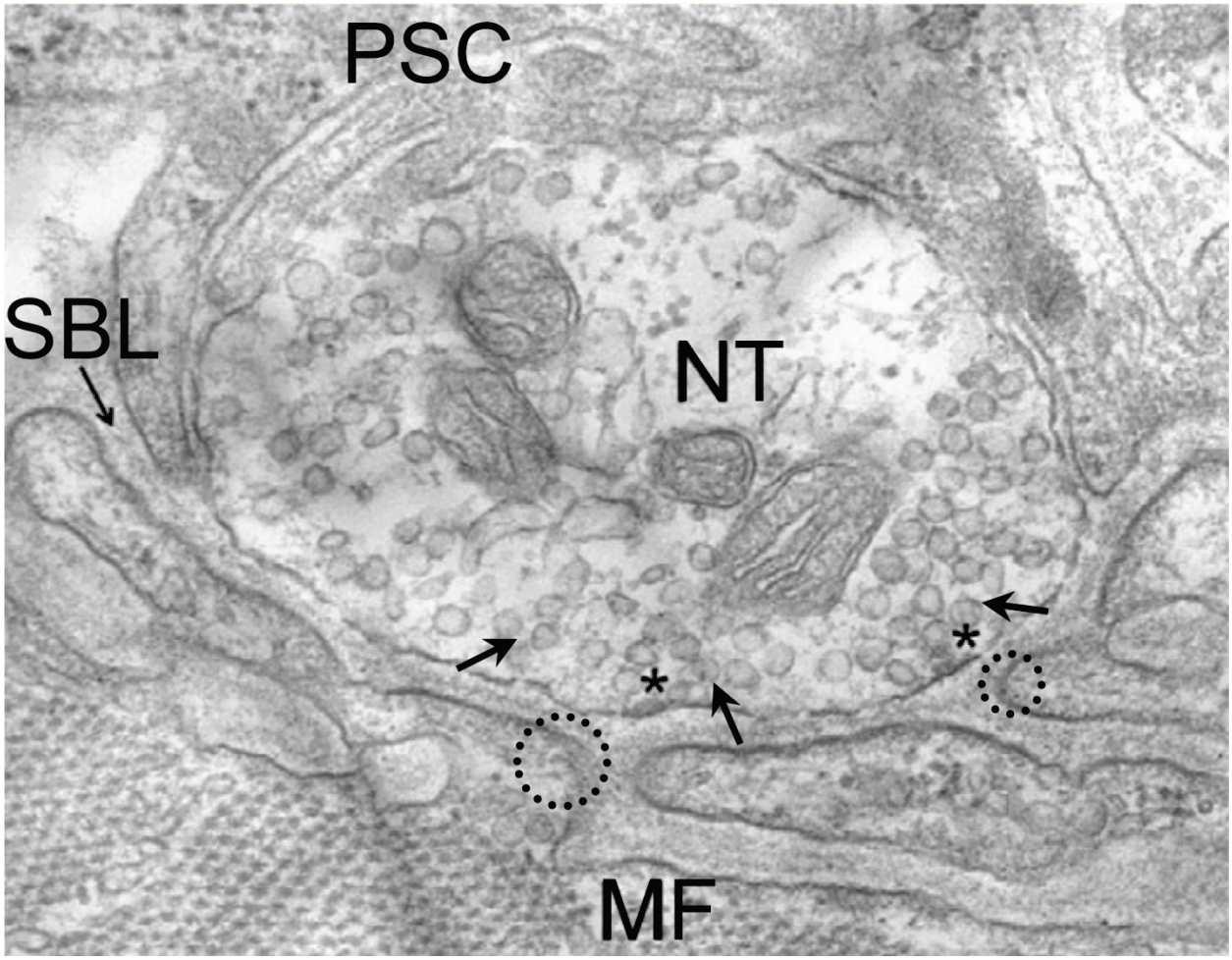

Figure 1.1 Electron Micrograph depicting Ultrastructure of the Mature Rodent Skeletal Neuromuscular Junction

The three main structural components of a mature skeletal NMJ; the nerve terminal (NT) capped by Schwann cells (PSCs), and the muscle fibre (MF). The pre- and postsynaptic regions are separated by the synaptic cleft, which is lined by synaptic basal lamina (SBL). Synaptic vesicles (arrows) containing the neurotransmitter, ACh, are present throughout the nerve terminal, however they are primarily localised to the juxtamuscular half of the terminal. Vesicles form clusters in close proximity to active zones (*) at the presynaptic membrane. The SBL is comprised of adhesion molecules such as laminins, which are capable of modulating differentiation of the synapse. The postsynaptic region is characterised by invagination of the muscle fibre membrane. The peaks of these folds contain high concentrations (~10,000 μm^2) of AChRs (dotted circles). Adapted from Wu *et al.* (2010).

1.1.1 The Presynaptic Region

The presynaptic region is characterised by the nerve terminal containing synaptic vesicles and many structural and functional proteins necessary for the release of chemical neurotransmitters into the synaptic cleft. Upon arrival of the nerve impulse from the motor axon, the nerve terminal undergoes depolarisation. This membrane depolarisation results in the activation of voltage-gated calcium channels (VGCCs) (detailed in section 1.1.3). Following VGCC activation a number of complex interactions involving numerous proteins occurs in order to directly or indirectly aid synaptic vesicle function to release transmitter, and finally culminate in the propagation of the neurotransmission signal (De Laet *et al.*, 2002) (see section 1.2). These complex interactions occur at the highly specialised electron dense regions termed active zones (Couteaux & Pecot-Dechavassine, 1974; Heuser *et al.*, 1979) (see Figure 1.2). At the mammalian NMJ, each active zone is 100-200 nm in length separated by approximately 500 nm of presynaptic membrane, and is highly organised into two double rows of accessory proteins and VGCCs that 'dock' synaptic vesicles between the double rows (Walrond & Reese, 1985; Nagwaney *et al.*, 2009; Ruiz *et al.*, 2011; Meriney & Dittrich, 2013) (see Figure 1.2). The synaptic vesicles interact with VGCCs and numerous accessory proteins to allow formation of nano-domains and micro-domains that facilitate efficient transmitter release (see Figure 1.2*A*).

At each NMJ, the motor nerve terminal itself is capped by three to five PSCs in close apposition to the presynaptic terminal (10-20 nm) (Auld & Robitaille, 2003; Griffin & Thompson, 2008). Numerous studies have demonstrated the key involvement of PSCs in the regulation of synaptic activity at the NMJ (Robitaille, 1998; Feng & Ko, 2007, 2008; Todd *et al.*, 2010). More recent studies have demonstrated the capability of PSCs to influence synaptic inputs during the elimination stage of development, a finding that will be explored in this thesis (Darabid *et al.*, 2013).

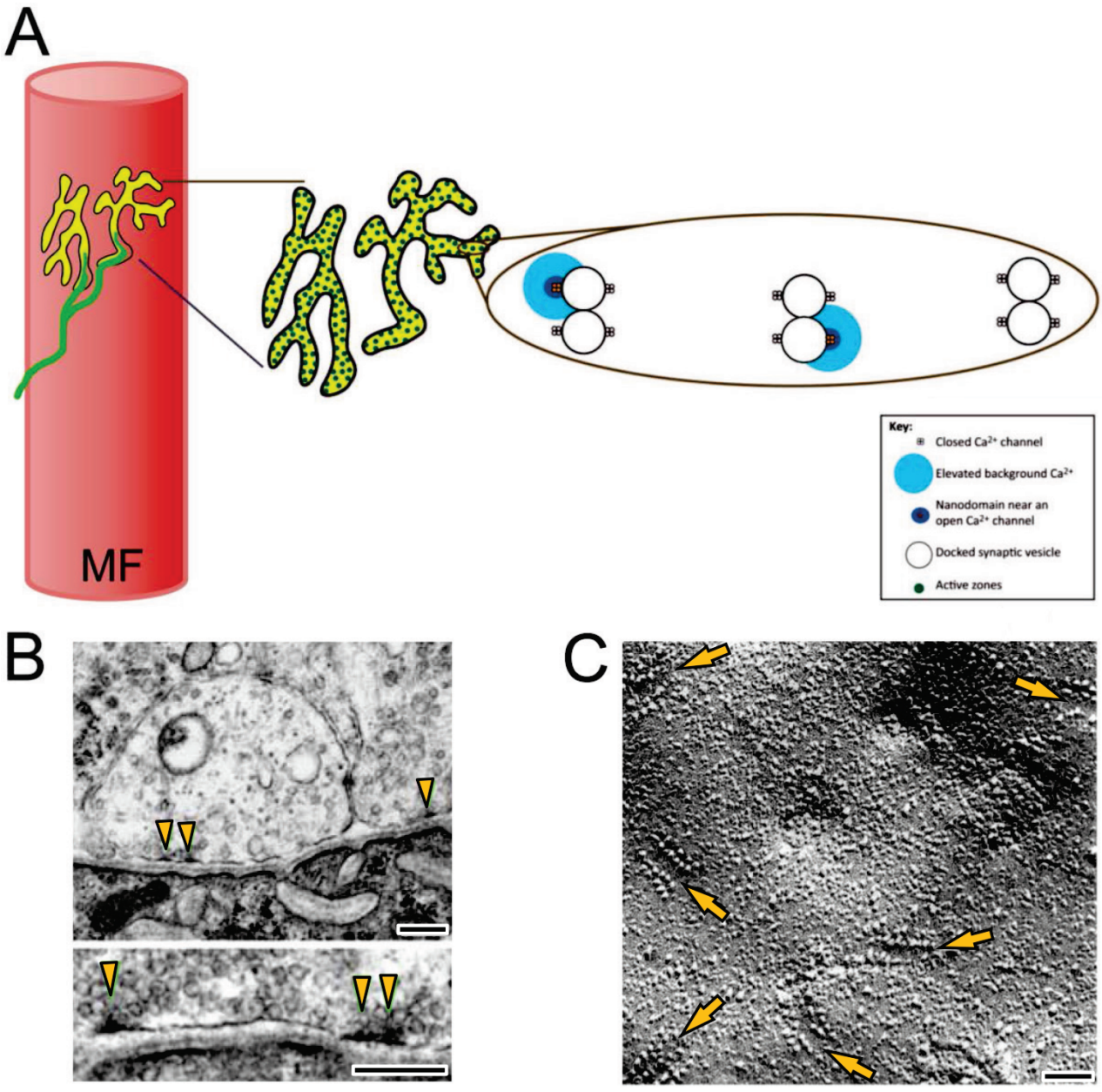

Figure 1.2 Theoretical Arrangement of Active Zones based on Assembly of unreliable single Vesicle Release Sites

***A*,** The mouse neuromuscular junction, innervated by the motor nerve (green trunk), is comprised of hundreds of active zones (green dots) co-localised to the postsynaptic AChR end-plate (yellow region). Each of these active zones, measuring 100-200 nm in length, is organised into linear arrays of double rows and separated from another by approximately 500nm. These double rows comprise of closely associated VGCCs, a number of accessory proteins and synaptic vesicles, which are docked between the rows. Arrival of an action potential at the terminal results in Ca^{2+} influx through VGCCs, which open at a low probability in response to the stimulus, causing elevated background levels of Ca^{2+} (light blue regions). The influx of Ca^{2+}develops into nano-domains of Ca^{2+} (dark blue regions) that in turn trigger tightly associated vesicles to undergo fusion and exocytose transmitter. Differences in

number, size, and vesicles arrangement at active zones are thought to contribute to varied synaptic properties. ***B***, This theoretical arrangement is based on electron micrographs, which show electron dense regions (indicated by yellow arrowheads) tightly apposed to folds at the postsynaptic membrane, and ***C***, freeze-fracture studies of the mouse diaphragm muscle, which displayed double rows of active zones aligned in parallel (indicated by yellow arrows). Scale bars B: 10 μm and C: 0.1 μm. Adapted from A, Tarr *et al.* (2013) B, Nishimune *et al.* (2004) and C, Fukunaga *et al.* (1983).

1.1.2 Perisynaptic Schwann Cells

Regulation of Perisynaptic Schwann Cell Development and Maturation

Immature PSCs present strikingly different morphology than mature PSCs. Immature PSCs display a globular 'fried egg' shape with a high degree of overlap and intermingling of cells. By contrast, mature PSCs present branched morphology and are compartmentalised into tile patterns when covering the NMJ (Brill *et al.*, 2011). These differences are suggested to correspond with the transition in postsynaptic morphology from plaque-like to pretzel shape during maturation (detailed in section 1.1.3.2). Developing NMJs require neuregulin-1 (NRG1) and the ErbB receptors, ErbB2 and ErbB3, to aid in PSC survival and migration, as well as postsynaptic end-plate maturation (Lin *et al.*, 2000; Ngo *et al.*, 2012). The loss of NRG1, ErbB2 or ErbB3 resulted in a deficiency or absence of PSCs at embryonic NMJs of associated knockout mouse models (Erickson *et al.*, 1997; Riethmacher *et al.*, 1997; Lin *et al.*, 2000; Wolpowitz *et al.*, 2000). During synaptogenesis the motor axon reaches target muscles and form nerve-muscle contacts but soon retract and mice die at birth. Brill *et al.* (2011) found PSCs at immature NMJs are highly dynamic, becoming quiescent at mature NMJs. The dynamic exploratory behaviour observed in the study may have implications in the process of axonal elimination during early development of the NMJ, becoming more static as the basal lamina develops at matured NMJs. This is thought to be based on the activity of the associated NMJs, with weak inputs being 'pruned' and strong synapses being capped by the PSCs as the NMJ reaches maturity. Studies have previously shown PSC phagocytosis of retracting axons after elimination from the surface of the muscle fibre (Bishop *et al.*, 2004). During the elimination of polyneuronal innervation, each of the excessive axons is pruned away from the end-plate individually. The retracting nerve bulbs are subdivided and subsequently phagocytised by the surrounding PSCs. The signalling cue responsible for directing this process has not yet been ascertained. Smith *et al.* (2013) observed the direct involvement of PSCs in phagocytosis of innervating nerve terminals during early development, suggesting a role in the process of postnatal synaptic elimination, which leads to a switch from polyneuronal innervation to single innervated NMJs (see Figure 1.3).

Molecules located in the basal lamina, such as laminin-β2, interact and signal with PSCs to determine their state of activity and prevent invasion of the synaptic cleft (Patton *et al.*, 1998). Patton and colleagues (1998) demonstrate an increase in the extension of PSC processes in cultures lacking laminin-β2, while in the presence of laminin-β2 the processes remained rounded. The study concluded that laminin-β2, contained within the

synaptic basal lamina, actively inhibits entry of PSC processes into the cleft allowing close interaction between pre- and postsynaptic regions of the NMJ without disruption to neurotransmission. Loss of such interactions results in altered PSC morphology and function, such as extension of PSC processes into the synaptic cleft as seen at laminin-β2 deficient NMJs. Reddy *et al.* (2003) found ablation of matured PSCs from frog NMJs did not result in any short term changes in structure or functional capacity of the junction. However, several days post ablation, a significant reduction in transmitter release, muscle twitch tension, and partial or complete nerve terminal retraction was observed. These findings suggest PSCs do not play an acute maintenance role at the adult NMJ, but rather are involved in long term maintenance of the adult NMJ. By contrast PSCs at developing NMJs appear to be involved in strengthening of robust synaptic inputs, potentially aiding in synaptic competition (Darabid *et al.*, 2013).

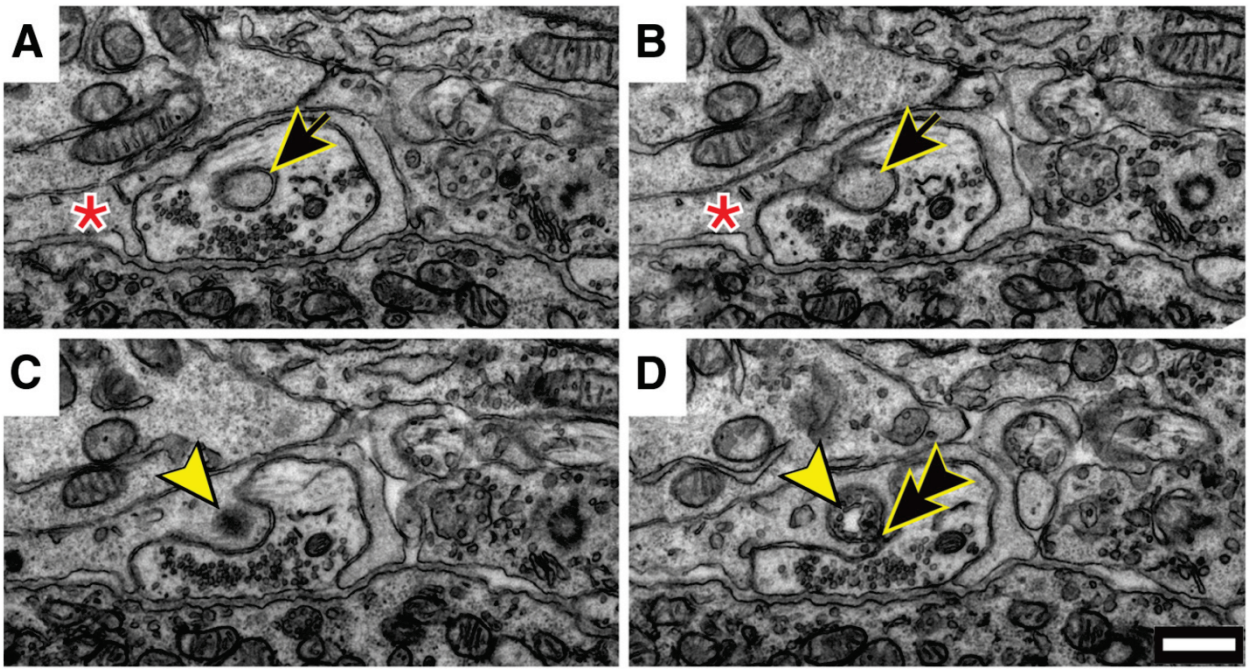

Figure 1.3 Schwann Cell Phagocytosis of a mouse Neuromuscular Junction at Postnatal Day 3
A, Electron microscopic sections of a single PSC (indicated by red asterisk) penetrating the presynaptic nerve terminal (black arrow) during the process of synaptic elimination. ***B***, The site of PSC entry into the terminal is indicated by the black arrow in. ***C***, The edge of a phagocytic vesicle as indicated by the yellow arrowhead can be seen at the base of the PSC. ***D***, The vesicle containing cytoplasm of the nerve terminal (yellow arrowhead) and is being pinched off from the PSC (black arrowheads). A–C, Adjacent 65 ηm sections. C & D, Two 65 nm sections apart. Scale bar: 500 ηm. Adapted from Smith et al. (2013).

Perisynaptic Schwann Cell Modulation of Neurotransmission

Perisynaptic Schwann cells are non-myelinating glial cells capable of releasing internal Ca^{2+} stores in response to different stimulus, with elevations in Ca^{2+} indicating excitation of the cell, a finding conserved in both amphibian and mammalian NMJs (Jahromi *et al.*, 1992; Rochon *et al.*, 2001; Darabid *et al.*, 2013). PSCs are capable of detecting the pattern of neuronal and synaptic activity, and in turn, respond by modulating the synaptic transmission by potentiating or depressing the signal (see Figure 1.4) (Pasti *et al.*, 1997; Todd *et al.*, 2010). Castonguay and Robitaille (2001) found that by increasing intracellular calcium stores in PSCs utilising thapsigargin, they were able to observein an increase in evoked transmitter release. Conversely blockade of this potential increase in PSC calcium resulted in significantly depressed transmitter response. These findings suggest that PSCs are capable of potentiating transmitter release at the NMJ under high frequency stimuli. A growing body of evidence strongly suggests that PSCs are involved in the modulation of synaptic activity at the mature NMJ (Robitaille, 1998; Henneberger *et al.*, 2010; Panatier *et al.*, 2011).

Robitaille and colleagues (2009) have proposed a signalling pathway involving the bi-directional communication between all three cellular bodies at the NMJ that allows facilitation and depression of transmission (see Figure 1.4). The arrival of the action potential at the nerve terminal causes exocytosis of neurotransmitter which binds to the associated receptors at the postsynaptic region. The released transmitter also binds to PSC metabotropic receptors, ACh binds to mAChRs and ATP binds to P_{2Y}Rs, which results in activation of G-proteins at the PSC membrane. To potentiate neurotransmission, the G-Proteins subsequently activate phospholipase C (PLC), in turn cleaving the membrane lipid phosphatidylinositol bisphosphate into diacylglycerol and inositol trisphosphate (IP3). The cleaved IP3s bind to receptors on the endoplasmic reticulum, triggering Ca^{2+} release from internal stores in the PSC. This elevation in Ca^{2+} leads to the release of gliotransmitters such as, prostaglandins and neurotrophins, in conjunction with other molecules not yet identified. These gliotransmitters are thought to act on the nerve terminal and increase the level of transmitter release by unknown mechanisms. In order to depress neurotransmission, activation of G-Proteins activates a signalling cascade that culminates in the release of depressing gliotransmitters, nitric oxide, glutamate, endocannibinoids, and arachidonic acid. These gliotransmitters are suggested to act directly on the nerve terminal to decrease the release of neurotransmitter through unknown means.

A recent study has shown PSCs demonstrate differential activation based on the type of neuronal stimulus (Todd *et al.*, 2010). Using continuous or bursting stimulus patterns in order to mimic endogenous motor neuronal activity, researchers observed changes in internal Ca^{2+} responses. The bursting pattern resulted in post-tetanic depression and oscillatory Ca^{2+} response in the PSCs with a slower and sustained elevation of Ca^{2+}. By contrast, continuous stimulation induced post-tetanic facilitation and a single phasic Ca^{2+} response with a faster rise time and short duration compared to responses observed under bursting stimulus. These different elevations in calcium suggest PSCs are capable of decoding the pattern of synaptic activity, and may have a role in modulation of this signalling process. Rousse *et al.* (2010) observed PSC calcium responses are dependent on muscle fibre type. The calcium response at PSCs from fast twitch fibres displayed faster kinetics compared to those at slow twitch fibres, with PSCs at slow twitch fibres demonstrating a larger Ca^{2+} elevation in response to the same stimuli. Interestingly, the study found that the responses observed at the fast twitch fibres utilised only internal Ca^{2+} stores, while PSCs of slow twitch fibres involved both internal stores and entry of extracellular Ca^{2+}. Though the functional consequences on the NMJ as a result of these differences are yet to be determined, these findings suggest PSC activation is governed in part by the synaptic properties of the associated synapse.

These studies have focused primarily on matured adult synapses despite PSCs being shown to play a vital role in the formation and elimination of synapses during development (Eroglu & Barres, 2010). Darabid *et al.* (2013) demonstrated that PSCs at immature NMJs are capable of interacting with competing inputs during the development of the NMJ, suggesting that PSCs are capable of activity-dependent modulation of synaptic transmission. Developing PSCs are capable of detecting transmitter release primarily via purinergic (P_2) signalling, however at mature NMJs PSCs modulate transmitter release via both muscarinic and purinergic (P_1 and P_2) receptors (Robitaille, 1995; Rochon *et al.*, 2001). At the developing NMJ, PSCs utilize P_{2Y} receptors to detect neurotransmitter release even though muscarinic receptors were found to be present and active (Darabid *et al.*, 2013). The investigators suggest that as the NMJ matures there is a switch from purinergic to a mixed muscarinic-purinergic signalling corresponding to the loss of polyneuronal innervation. This switch is proposed to be based on the change in PSC properties and function during maturation of the NMJ. Developing PSCs are highly dynamic, with exploratory behaviour involving constant repositioning of processes, and dependence on purinergic signalling. This PSC

dynamism during development may allow for flexible changes in function and structure of the still plastic NMJ with suitable detection of the neural signal. As the NMJ stabilises during maturation, the associated PSCs become less variable in their activity and mobility, which aids in stability of the NMJ structure and function. In addition to this, PSCs utilise a combination of both muscarinic and purinergic pathways to modulate the more sophisticated neural signals.

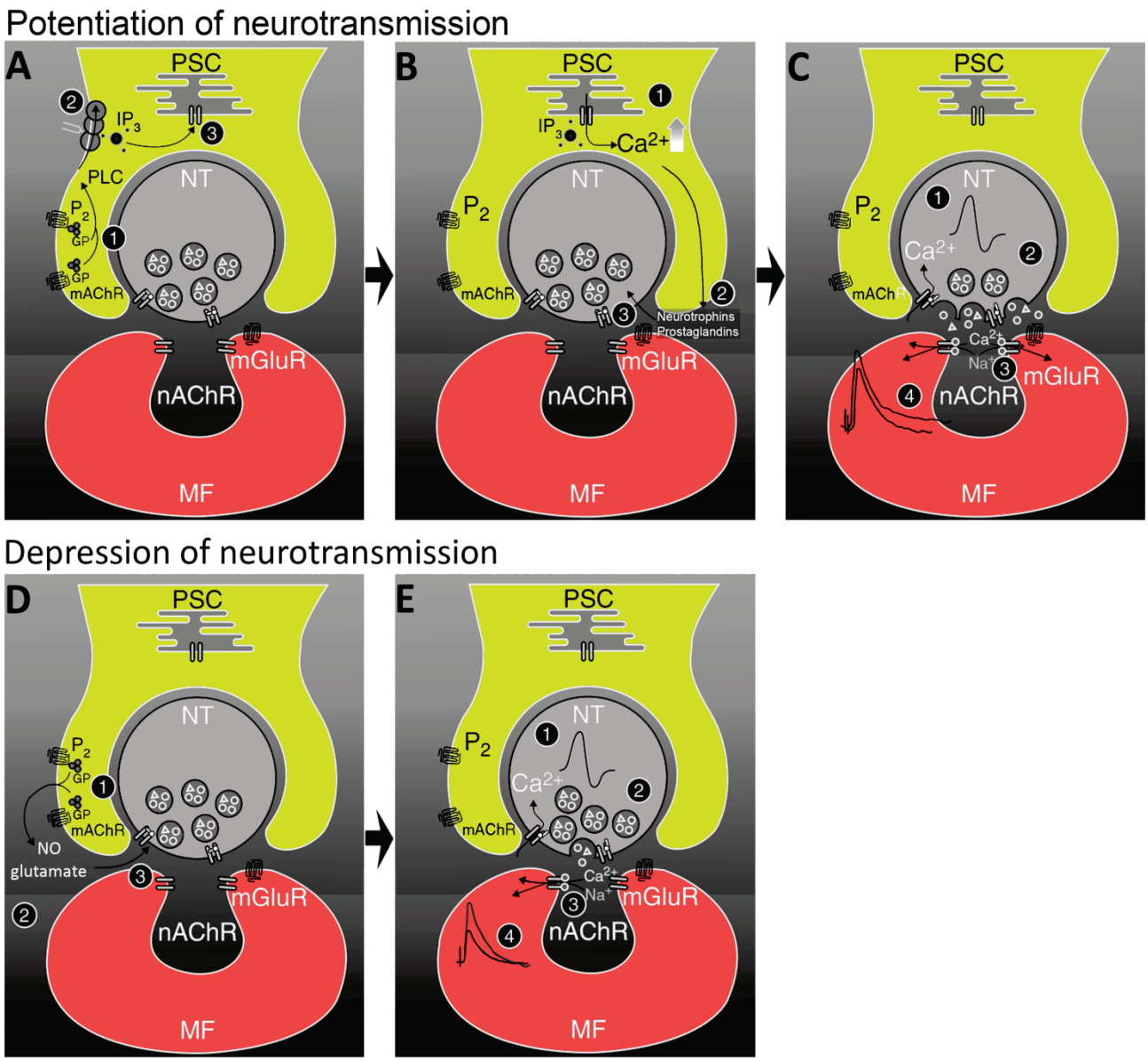

Figure 1.4 Proposed Perisynaptic Schwann Cell Modulation of Neurotransmission

Schematic illustration of signalling between PSCs and the nerve terminal (NT) in modulating synaptic transmission at the muscle fibre (MF). Arrival of an action potential at the presynaptic terminal culminates in the release of acetylcholine (small circles) and ATP (triangles) into the synaptic cleft. Released transmitter binds to associated receptors at the end-plate and to PSC metabotropic receptors (ACh to mAChRs and ATP to P_2Rs) which in turn activate G-proteins (GPs). To potentiate neurotransmission; ***A***, GPs activate phospholipase C (PLC), which produces diacylglycerol and inositol trisphosphate (IP3). ***B***, IP3s bind to receptors on the endoplasmic reticulum, triggering Ca^{2+} release from internal stores in the PSC (1). The elevated Ca^{2+} induces release of gliotransmitters (prostaglandins and neurotrophins) into the synaptic cleft (2), which act on nerve terminals. ***C***, resulting in markedly increased release of transmitter from the terminal by unknown mechanisms (3), which in turn results in a larger end-plate potential (4). To depress neurotransmission; ***D***, activation of GPs at the PSCs (1) results in the release of

gliotransmitters (nitric oxide (NO) and glutatamate) into the synaptic cleft (2), which act on the nerve terminals (3). ***E***, these gliotransmitters act via retrograde and anterograde signalling, to decrease the release of transmitters by unknown mechanisms (2). The reduction in transmitter release leads to generation of a smaller end-plate potential. Figure adapted from Rousse and Robitaille (2006); Belair and Robitaille (2009).

1.1.3 Voltage Gated Calcium Channels

Influx of calcium into the presynaptic nerve terminal following terminal depolarisation occurs through voltage-gated calcium channels (VGCCs). Calcium channels at the vertebrate NMJ are activated by nerve terminal action potentials with a time constant of ~1.3 ms (Stanley, 1993). The VGCCs are multimeric transmembrane protein channels located at the membrane of the presynaptic nerve terminal (Weiss, 2008). Fatt and Katz (1953) first postulated the idea of VGCCs while investigating the electrical properties of crustacean muscle. It was found that removal of calcium from the biological buffer solution bathing the preparations resulted in a marked decrease or abolishment of electrical response, while increasing calcium concentration led to greater amplitude of activity. This finding suggested that an influx of calcium ions may be responsible for the transport of the charge (Fatt & Katz, 1953). Continued investigation of VGCCs has led to the identification of several different VGCC subtypes. Each subtype has been characterised based upon its pharmacological and molecular profiles (for review, seeLacinova, 2005). The VGCCs comprise of a single transmembrane pore forming α_1 subunit ($Ca_v\alpha$) (~190–250 kDa) and associated auxiliary subunits ($Ca_v\beta$), namely an intracellular phosphorylated β subunit (~55 kDa,), a transmembrane γ subunit (~33 kDa) and the disulfide-linked α_2-δ dimer (~170 kDa) (see Figure 1.5) (Singer *et al.*, 1991; Day *et al.*, 1997; Walker *et al.*, 1998; for review, see Klugbauer *et al.*, 2003). Numerous isoforms of the α_1 subunit have been identified and are thought to be the primary cause of variations in calcium currents and determinants for the binding of drugs and toxins (for review, see Moreno Davila, 1999). The auxiliary subunits regulate VGCC function by altering channel properties such as activation and inactivation kinetics, voltage dependency and ligand binding (Walker & De Waard, 1998).

Each VGCC subtype possesses specific α_1 subunits, which are the primary determinant of the pharmacological and electrophysiological properties used during early identification of channels. The five VGCC subtypes identified at present and their associated α_1 subunit isoforms are; L-type ($\alpha_{1S,}$ $\alpha_{1C,}$ $\alpha_{1D,}$ α_{1F}), P/Q-type (α_{1A}), N-type (α_{1B}), R- type (α_{1E}), and T-type (α_{1G}, $\alpha_{1H,}$ α_{1I}) (Birnbaumer *et al.*, 1998; Ertel *et al.*, 2000; Nudler *et al.*, 2003). Channels can be identified in two physiologically distinct groups based on voltage activation; high voltage activated (more positive than -20 mV) or low voltage activated (more positive than -70 mV) (Kostyuk, 1999; Lacinova, 2005). Each channel displays different characteristics; the L-type channels (Ca_v1.1- 1.4) possess high voltage activation and slow kinetics of current decay (Fox *et al.*, 1987), while the T-type channels

(Ca_v3.1- 3.3) have a low voltage activation threshold and fast current decay (Carbone & Lux, 1987). The remaining VGCCs possess current conductance between those of L- and T-type channels. N-type channels can be inhibited by ω-conotoxin GVIA (ω-CTX GVIA) isolated from the venom of the cone shell mollusc (*Conus geographus)* (Kasai *et al.*, 1987). The P/Q-type channels are selectively blocked by the peptides ω-agatoxin VIA (ω-Aga IVA) and ω-conotoxin MVIIC (ω-CTX MVIIC) (Hillyard *et al.*, 1992; Mintz *et al.*, 1992; Katz *et al.*, 1996) as well as inhibition by the isolated toxin FTX from the funnel web spider (Llinas *et al.*, 1989). The R-type channel (Ca_v2.3) is insensitive to ω-CTX GVIA and ω-Aga VIA (Zhang *et al.*, 1993).

Multiple types of VGCCs co-exist at a single synapse with possible interactions to induce release of transmitter (Regehr & Mintz, 1994; Dunlap *et al.*, 1995). The primary VGCC isoforms involved with neurotransmission at the skeletal NMJ are N-type (Ca_v2.2) and P/Q-type (Ca_v2.1). The presence of VGCC isoforms varies as the NMJ undergoes maturation, with each channel supporting specific stages according to their characteristic properties (Rosato-Siri & Uchitel, 1999; Santafe *et al.*, 2001), a similar finding is also observed at central synapses (Takahashi & Momiyama, 1993; Iwasaki *et al.*, 2000). Both N- and P/Q- type channels are present and involved with the mediation of transmission during the early stages of development, approximately eight days postnatal (P8) in mice models (Rosato-Siri & Uchitel, 1999; Santafe *et al.*, 2001; Rosato-Siri *et al.*, 2002; Nudler *et al.*, 2003). As the synapse matures, at approximately fourteen days postnatal (P14), the P/Q-type VGCCs become the dominant mediator of neurotransmitter release (Uchitel *et al.*, 1992; Bowersox *et al.*, 1995; Katz *et al.*, 1997; Rosato-Siri *et al.*, 2002), while N-type are suggested to take on a supporting role in regulating feedback and fine-tuned calcium influx. Studies have shown that G-protein mediated inhibition of P/Q-type VGCCs is less than that exhibited at N-type VGCCs (Currie & Fox, 1997). Investigators suggest that NMJs with P/Q-type VGCC dominance may operate over a smaller inhibition range and are therefore easier to activate, while N-type dominant NMJs have higher inhibition, thus only involved in regulating release under particular conditions (Currie & Fox, 1997, 2002; Zaitsev *et al.*, 2007). Katz and colleagues (1996) have shown that in the presence of the P/Q-type VGCC specific blocker, ω-Aga IVA, evoked neurotransmission was significantly decreased at P8. Rosato-Siri and Uchitel (1999) demonstrated that N- type VGCCs play a lesser role in neurotransmission at the mature NMJ through the use of the N- type channel blocker ω-CTX GVIA. It was found that this toxin significantly impaired neurotransmission, by preventing Ca^{2+} influx through N-type VGCCs at P8 but not at P14,

when the NMJ has developed to maturity and switched to P/Q-type VGCC mediated transmitter release. Both L- and R-type VGCCs have also been implicated in having a minor role in the release of ACh at healthy NMJ (Rosato-Siri & Uchitel, 1999; Correia-de-Sa *et al.*, 2000a, b; Urbano *et al.*, 2003), while L-type VGCCs also play a role in transmitter release under pathological conditions such as amyotrophic lateral sclerosis (Fratantoni *et al.*, 2000) and in botulinum toxic poisoning (Santafe *et al.*, 2000).

The presynaptic membrane is lined with domains, which comprise primarily of VGCCs and the associated calcium receptors and sensors (Augustine, 1990; Llinas *et al.*, 1992; Yoshihara & Littleton, 2002; Koh & Bellen, 2003). Strong evidence suggests an overlapping of these domains. Mintz *et al.* (1995) showed that sequential application of ω-CTX GVIA and ω-Aga IVA resulted in a 27% and 50% decrease respectively in calcium currents. However, it was observed that the same toxins resulted in a 50% and 93% decrease respectively in postsynaptic currents. This finding suggests co-operativity between VGCCs, which has also been observed in other synaptic models (Regehr & Mintz, 1994; Wheeler *et al.*, 1996). It is thought the number of these domains involved in transmitter release varies from synapse to synapse and the animal model being investigated. Amphibian models have shown dense clustering of VGCCs while in the giant synapse of squid channels are spatially separated suggesting little overlap in domains (Adler *et al.*, 1991). The degree of micro-domain overlap is suggested to be indicative of calcium sensitivity of the terminal, which is the ability of the terminal to efficiently release transmitter in response to calcium influx. Thus micro-domains with no overlap require higher concentrations of calcium to initiate the release of transmitter (Augustine *et al.*, 1992). Fogelson and Zucker (1985) suggested that the receptor or molecule(s) responsible for triggering the release of transmitter must be spatially located within a few tens of nanometres of the mouth of the associated VGCC. This close spatial relationship indicates the necessity for the precise localisation of all components involved in transmitter release.

P/Q- type VGCCs are spatially located in closer proximity to release sites than N-type channels (Rosato-Siri *et al.*, 2002; Nudler *et al.*, 2003; Urbano *et al.*, 2003). This close spatial locality may well be the reason P/Q-type VGCCs play a more prominent role in the mature NMJ where efficient bulk release of transmitter is required. Mice lacking P/Q-type VGCCs display decreased quantal content and synchrony of transmitter release, again highlighting the importance of P/Q-type channels in efficient transmitter release (Urbano

et al., 2003; Depetris *et al.*, 2008). It was shown that N-type VGCCs were the primary mediators of transmitter release with R-type VGCCs also playing a role. Investigators suggested that the spatially dispersed but abundant N-type VGCCs interact with presynaptic machinery to mediate transmitter release at a decreased efficiency to P/Q-type channels. This notion is supported by previous studies which have shown that elimination of the primary calcium channel subtype results in compensatory mechanisms to allow calcium entry through alternative channel types at decreased efficiency (Jun *et al.*, 1999; Nudler *et al.*, 2003; Inchauspe *et al.*, 2004; Piedras-Renteria *et al.*, 2004).

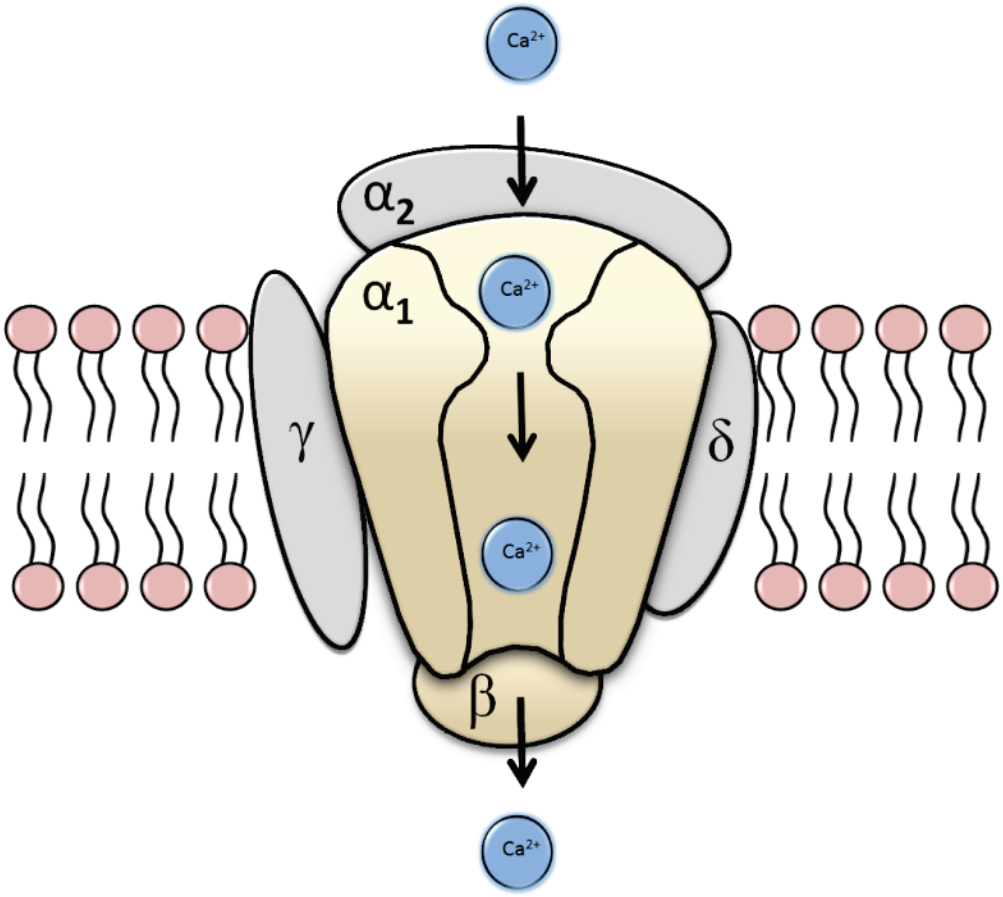

Figure 1.5 Putative Subunit Arrangement of the Voltage Gated Calcium Channel Complex

The VGCC is comprised of a single pore forming α_1 subunit ($Ca_v\alpha$) containing a voltage sensor and binding site for calcium channel blockers. The pore subunit has an estimated diameter of 6 Å (McCleskey & Almers, 1985). Depolarisation of the presynaptic membrane results in activation of the VGCC and influx of Ca^{2+} ions (~2 Å diameter) through the channel. The associated auxiliary subunits ($Ca_v\beta$), namely β, γ and α_2-δ interact with the α_1 subunit to modulate the ion conductance activity through the pore forming subunit. Importantly, the pore forming a_1 subunit of VGCCs has been shown to directly interact with laminin-β2. The α_2 subunit is an extracellular, extrinsic membrane protein linked to the δ subunit via disulphide bridges (S-S). The $\alpha_2\delta$ subunit complex is encoded through post- translational proteolytic processing by the same gene. The intracellular β subunit has no transmembrane segments in contrast to the γ subunit, which possesses four transmembrane segments.

1.1.4 The Synaptic Cleft

The presynaptic nerve terminal and muscle fibre membranes are separated by a space of approximately 50-100 nm, termed the synaptic cleft (see Figure 1.1) (Heuser *et al.*, 1979; Wood & Slater, 2001; Hughes *et al.*, 2006). The entire span of the cleft is comprised of basal lamina, within which are high concentrations of the enzyme acetylcholinesterase (AChE) (Marnay & Nachmansohn, 1938; Rauvala & Peng, 1997; Massoulié & Millard, 2009). The AChE enzymes are anchored to the basal lamina by two heparin sulphate proteoglycan-binding domains within a collagen tail (Krejci *et al.*, 1991; Krejci *et al.*, 1997; Rauvala & Peng, 1997). During early development AChE is expressed asymmetrically by the myotubes over the entire basal lamina surface. However it rapidly accumulates at newly formed synapses as the NMJ matures (Chiu & Sanes, 1984; Ziskind-Conhaim *et al.*, 1984). After synaptic vesicle fusion at the presynaptic membrane (see section 1.3), ACh is exocytosed and quickly diffuses across the cleft due to the high diffusion constant of ACh, and binds to acetylcholine receptors (AChRs) at the postsynaptic membrane (See section 1.1.3) (Land *et al.*, 1984). The exocytosed ACh is degraded by AChE through a process of hydrolysis producing a choline and acetate group, which later undergo re-uptake into the pre-synaptic terminal for recycling. This degradation of ACh occurs in less than a millisecond and diminishes the stimulation of AChR by decreasing presence of ACh, subsequently leading to a decay of the end-plate current and finally termination of neurotransmission (Katz & Miledi, 1965; McMahan *et al.*, 1978; Rosenberry, 1979). Thus decreased expression of AChE will result in prolonged AChR activation, and subsequently a slower decay of the end-plate current will be observed (Katz & Miledi, 1973). Within the basal lamina are a number of signalling and adhesion molecules, which are capable of binding/concentrating ligands on adjacent cell membrane surfaces, thus allowing for signalling between NMJ components (Sanes, 1995; Hughes *et al.*, 2006). These molecules, such as the laminins, are critical for the development and organisation of the neuromuscular junction.

Laminins are a family of glycoproteins forming large (~400 to ~900 kD) heterotrimeric complexes composed of α, β, and γ chains (see Figure 1.6) (Green *et al.*, 1992; Noakes *et al.*, 1995a; Aumailley *et al.*, 2005). Each chain is homologous to the others and possesses similarly arranged sequence domains, contributing to the characteristic three stranded coiled-coil structure of the laminin trimer (for review, see Timpl & Brown, 1994). The first laminin isoform was discovered by Timpl and colleagues in 1979. The study extracted matrix from an Engelbreth- Holm- Swarm (EHS) mouse tumour capable of

producing matrix of the same composition as the basement membrane (Timpl *et al.*, 1979). From this matrix a collagenous protein was isolated as well as a second protein with a large molecular weight, that researchers named laminin. Beck and colleagues (1990) utilized rotatory electron micrographs to show that the EHS laminin formed a cruciform shape, with three short arms comprising of single laminin chains, and one long arm made from each of the chains forming α-helical coiled-coil (see Figure 1.6) (Beck *et al.*, 1990). While numerous molecules have been shown to possess laminin-like domains, a key characteristic for a protein to be classed a laminin chain is the presence of this α-helical coiled-coil domain. To date, five α, three β, and three γ chains have been identified in both mouse and human (Miner & Yurchenco, 2004). Each of the short arms possesses a distal laminin N-terminal (LN) domain, which have been shown to allow interaction with other short arm LN domains to aid in basal membrane stability (see Figure 1.6*A*) (Yurchenco & Cheng, 1993). These interactions demonstrate a strong preference for ternary interactions involving one α, one β, and one γ chain to form a network that stabilizes the basement membrane architecture (Yurchenco & Cheng, 1993). At the C-terminus end of the long arm are five laminin G-like (LG) domains positioned in tandem (Sasaki *et al.*, 1988). These LG domains interact with a number of cellular receptors such as integrins, α-dystroglycan, and heparan sulfate proteoglycans (such as agrin and perlecan), which enable laminin heterotrimers to anchor to the cell surface (Aumailley *et al.*, 1990; Talts *et al.*, 1999; Ido *et al.*, 2004). Specifically, α-dystroglycan, agrin and perlecan bind to the LG4-5 region (Talts *et al.*, 1999), while integrins bind the LG1-3 region (Ido *et al.*, 2004; Ido *et al.*, 2007).

Cell culture and *in vivo* studies suggest that laminins are responsible for organising the assembly of the basement membrane (Yurchenco & Orear, 1994; McKee *et al.*, 2007). During early myogenesis embryonic muscle initially expresses laminin after the formation of the first myotubes with α2, α5, β1, and γ1 found to be the earliest laminin chains expressed in mice (Sorokin *et al.*, 1997). As the embryo develops basal lamina becomes rich in laminin-α4, coinciding with the generation of secondary muscle fibres at approximately embryonic day 14 (Patton *et al.*, 1997). Laminin-β2 is specific to the synapse from the earliest point of expression while in contrast laminin chains α4 and α5 are widely expressed during development but become synapse specific in adults (Miner *et al.*, 1997; Patton *et al.*, 1997).

It has been suggested that basal lamina are capable of functioning directly as both a mechanical superstructure and specific regulator of cell activity as well as providing attachment sites for cell surface receptors, such as dystroglycan, which are anchored to the intracellular cytoskeleton (see Figure 1.6) (Henry & Campbell, 1996). This ability provides structural support to the underlying membrane while distributing mechanical stress of the cell. Delwel *et al.* (1996) found basal lamina is also capable of acting as signalling molecules via receptors such as integrins. Such interactions enable the regulation of cellular proliferation, migration, differentiation and morphology.

The basal lamina ensheathes each muscle fibre as well as passing into, and spanning the synaptic cleft of the NMJ (Hunter *et al.*, 1989; Sanes, 1995; Sanes & Lichtman, 1999). Only a small fraction of the basal lamina, approximately 0.1% of the total lamina, actually separates the motor nerve from a muscle fibre and is termed synaptic basal lamina (Patton *et al.*, 1997; Pedrosa-Domellof *et al.*, 2000). The majority of basal lamina is extrajunctional and in adults is largely comprised of laminins-α2, -β1 and -γ1 (Sanes *et al.*, 1990; Schuler & Sorokin, 1995; Sorokin *et al.*, 1997; Tiger & Gullberg, 1997). Laminin-β2 is found concentrated at the myotendinous junctions and has also been reported to be present in extrajunctional basal lamina at varied levels in multiple species (Sanes *et al.*, 1990; Cohn *et al.*, 1997; Cohn *et al.*, 1998; Sieb *et al.*, 1998). Synaptic basal lamina in the adult NMJ is comprised of several specific laminin isoforms; α2, α4, α5, β2 found only in this region in addition to γ1 (Patton *et al.*, 1997) with the specific exclusion of laminin-β1 (Hunter *et al.*, 1989; Sanes *et al.*, 1990). The relative location of these synaptic laminin chains are presented in figure 1.6*B*. Synaptic basal lamina has previously been shown to play an integral role in the organisation of nerve terminal formation even in the absence of muscle fibres at the synaptic site (Sanes *et al.*, 1978; Kuffler, 1986). The synaptic laminins form three heterotrimers; laminin-221 (α2β2γ1), laminin-421 (α4β2γ1) and laminin-521 (α5β2γ1) (Patton *et al.*, 1997; Aumailley *et al.*, 2005) (see Figure 1.6*C*). These heterotrimers interact with the three main cellular elements that comprise the NMJ; the motor neuron, the muscle fibre and the PSC. Laminin-421 spans the entire synaptic cleft mediating contact between the motor neuron and muscle fibre (Patton *et al.*, 2001). Laminin-221 lines the deep folds at the post-synaptic region mediating contact between invaginated membranes (Cho *et al.*, 1998; Patton *et al.*, 1998), while laminin-521 covers the outer perisynaptic Schwann cell body, thus mediating contact with the perisynaptic space (Patton, 2000). Laminin-521 acts to prevent the intrusion of Schwann cell processes into the synaptic cleft resulting in a capping of the nerve terminal that is suggested to enhance neurotransmission efficacy (Patton *et al.*, 1998).

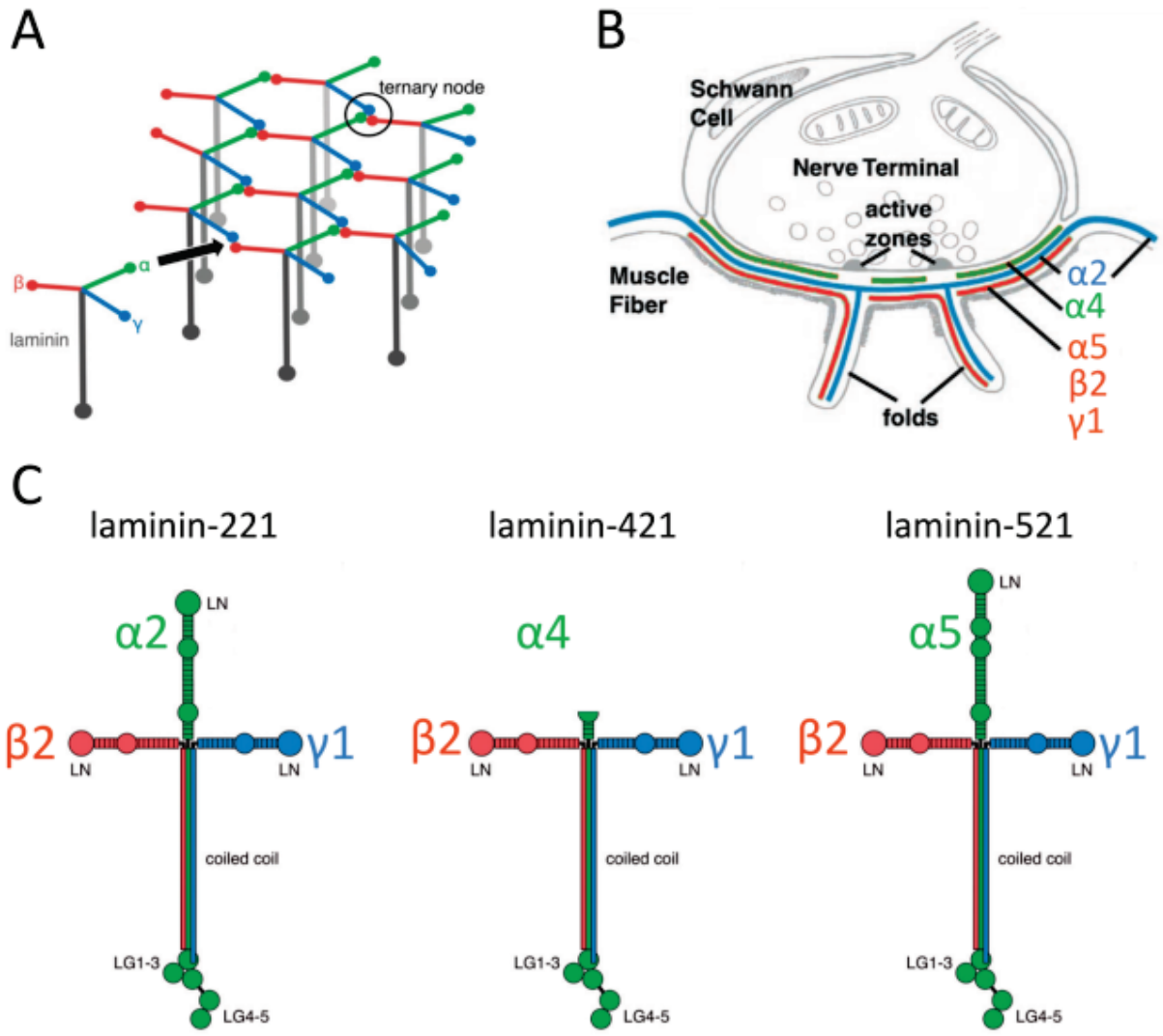

Figure 1.6 Distribution of Laminin Chains at the Skeletal Neuromuscular Junction

Specific laminin chains found within the synapse of the NMJ. ***A***, Laminin heterotrimers interact via the short arms to form a network that aids in the stabilisation of the basal lamina membrane architecture. Long arms do not participate in this lamina network but rather interact with other components of the basal lamina. ***B*****,** Laminin chains α2, α4, α5, β2, and γ1 are found in high concentrations lining specific regions of the synaptic cleft. ***C***, Laminin chains form three predominant heterotrimers; laminin-221 (α2β2γ1), laminin-421 (α4β2γ1) and laminin-521 (α5β2γ1). Laminin- 421 presents as "T" shaped heterotrimers due to the abbreviated short arm of the α4 chain, thus only possesses two LN domains. Of key note is the presence of β2 and γ1 chains in each of the three heterotrimers. Mutation in either of these two chains has been shown to result in severe disruptions in NMJ structure and function. Mutation in the γ1 chain in particular leads to embryonic lethality. Cell surface receptors, such as α-dystroglycan, integrin and perlecan, bind to laminin heterotrimers via the LG sites on the long arms to anchor the complex in the basement membrane. A. adapted from Patton et al., 2001, B & C. adapted from (Hohenester & Yurchenco, 2013).

The laminin subunit common to all three synaptic laminin heterotrimers is laminin-β2. Originally termed s-laminin, laminin-β2 was one of the first laminin chains to be cloned and as such has been highly investigated using *in vitro* experimentation. Laminin-β2 promotes nerve terminal formation and has been shown to possess selectively adhesive properties to motor neurons (Hunter *et al.*, 1989), inhibit neurite outgrowth (Porter *et al.*, 1995; Sann *et al.*, 2008), and is capable of directly inducing presynaptic differentiation of axons (Son *et al.*, 1999). Laminin-β2 is capable of inducing differentiation by regulating the maintenance of active zone components, the assembly of synaptic vesicles in close proximity to active zones, and in preventing Schwann cell processes from invading the synaptic cleft (Noakes *et al.*, 1995a; Cho *et al.*, 1998; Patton *et al.*, 1998; Libby *et al.*, 1999; Sanes & Lichtman, 1999; Knight *et al.*, 2003; Nishimune *et al.*, 2004; Nishimune *et al.*, 2008; Chen *et al.*, 2011).

Laminin-β2 is localised to the synaptic basal lamina approximately twelve hours after synapse formation at embryonic day 14.5 (Sanes *et al.*, 1990; Patton *et al.*, 1997). Laminin-β2 knockout mice (*lamb2*$^{-/-}$) demonstrate normal synaptogenesis and synaptic elimination culminating in singly innervated motor end-plate (Noakes *et al.*, 1995a). Immuno-histochemical staining of acetylcholine receptors (AChRs) and synaptic vesicles using α-bungarotoxin (αBTX) and synaptic vesicle protein 2 (SV2) respectively, showed normal apposition of pre- and postsynaptic regions at *lamb2*$^{-/-}$ NMJs (Noakes *et al.*, 1995a; Knight *et al.*, 2003). Noakes *et al.* (1995b) found mice lacking laminin-β2 compensated for this loss with an up-regulation of laminin-β1, at the synaptic basal lamina. While the basal lamina was structurally intact, the functional ability of mutants was impaired. Mice lacking laminin-β2 presented disrupted presynaptic differentiation at the NMJ with defects including; decreased number of active zones, diffuse distribution of synaptic vesicles at the nerve terminal, and invasion of Schwann cell processes into the synaptic cleft (see Figure 1.7)(Noakes *et al.*, 1995a; Noakes *et al.*, 1995b; Patton *et al.*, 1998; Knight *et al.*, 2003; Nishimune *et al.*, 2004). Laminin- 521, containing the β2 chain, is thought to directly prevent invasion of the synaptic cleft by Schwann cells (Cho *et al.*, 1998; Patton *et al.*, 1998). These studies however did not investigate the role of laminin-421(then known as laminin-9) as a potential stop signal for Schwann cell processes due to the unavailability of purified laminin-421 at the time. Thus the defects in transmission associated with laminin-β2 knockout may be partly attributed to the entry of Schwann cell processes into the cleft.

Knight *et al.* (2003) found *lamb*2$^{-/-}$ mice had a 15- fold decrease in the frequency of spontaneous transmitter release but not in spontaneous amplitude, when compared to wild type NMJs. This decrease was attributed to a reduced ability for transmitter release due to presynaptic differences between wild-type and laminin-β2 deficient NMJs. *Lamb*2$^{-/-}$ NMJs showed a 50% decrease in evoked neurotransmitter release when compared to wild-type, a result supporting the phenotypic morphological disruptions seen in mutants (Knight *et al.*, 2003). Laminins are present in the peri-neural sheathing of peripheral nerves, thus disruption of laminin-β2 expression may also result in diminished action potential propagation to the presynaptic nerve terminal. Knight and colleagues (2003) used extracellular electrophysiological recordings to investigate deficits in the propagation of action potentials along the nerve terminal in *lamb*2$^{-/-}$ NMJs. The study found no significant difference between wild-type and *lamb*2$^{-/-}$ NMJs, concluding that the reduction in quanta of neurotransmitter was due to a breakdown in the presynaptic depolarisation-secretion coupling mechanism. Laminin-β2 was initially believed to be involved in the actual formation of the active zone. However, further studies have found no difference in the number of active zones between wild-type and *lamb*2$^{-/-}$ mice at birth, but a significant decrease has been observed at postnatal day 4 suggesting a role in maturation rather than formation of active zones at the synapse, an observation substantiated by the findings presented in Chapter 3 (Nishimune *et al.*, 2004).

Similar findings have been observed in human subjects suffering from a severe form of congenital myasthenic syndrome (CMS), resulting from truncating mutations of the *LAMB*2 gene (Maselli *et al.*, 2009). The human NMJs of this study displayed similar morphological and functional deficits that have been observed in the NMJs of laminin-β2 deficient mice as previously discussed (Noakes *et al.*, 1995a). Namely, NMJs from the CMS patient presented immature nerve terminals, decreased numbers of active release sites, invasion of the synaptic cleft by Schwann cell processes, and poor formation of the postsynaptic membrane. Functionally, NMJs from the CMS patient showed decreases in quantal content and spontaneous frequency. Investigators suggest that the perturbed postsynaptic folding may be due to the loss of interaction with cell surface receptors such as integrins, dystroglycan and podosomal complexes, which are involved in the maintenance of the synaptic scaffold stability (Tzu & Marinkovich, 2008; Proszynski *et al.*, 2009).

Early studies proposed an interaction between laminin-421 and presynaptic voltage gated calcium channels (VGCCs), which enables the precise alignment and organization of synaptic components (Sunderland *et al.*, 2000; Patton *et al.*, 2001). Subsequent studies by Nishimune *et al.* (2004) found that laminin-β2 is capable of binding directly to the pore-forming subunit of N- and P/Q-type VGCCs (see Figure 1.5). The study showed VGCCs acts as a laminin receptor and that laminins are the first extracellular proteins to act as ligands for VGCCs. Utilising protein pull-down assays, laminin-β2 were identified as the immediately adjacent protein to VGCCs (distance ≤ 2.3 nm). Laminin-β2 showed preference to N- and P/Q-type VGCCs, the primary VGCC subunits involved with neurotransmitter release at the NMJ. Beads coated in laminins containing β2 were capable of binding to cells expressing $Ca_v2.1$ (P/Q-type) and $Ca_v2.2$ (N-type) but not $Ca_v2.3$ (R-type) while beads coated with laminin-111, possessing laminin β1 did not show binding capabilities to any of the Ca_v subunits investigated (Nishimune *et al.*, 2004). These findings demonstrated an interaction between laminin-β2 and VGCCs that appears to be necessary for the development of structurally and functionally mature NMJs (Nishimune *et al.*, 2004; Sann *et al.*, 2008; Carlson *et al.*, 2010; Chen *et al.*, 2011; Nishimune, 2012; Nishimune *et al.*, 2012). The laminin-β2 chain interacts with laminin-α4 to form the unique “T” shaped heterotrimer laminin-421, which is suggested to organise the alignment of pre- and postsynaptic specialisations.

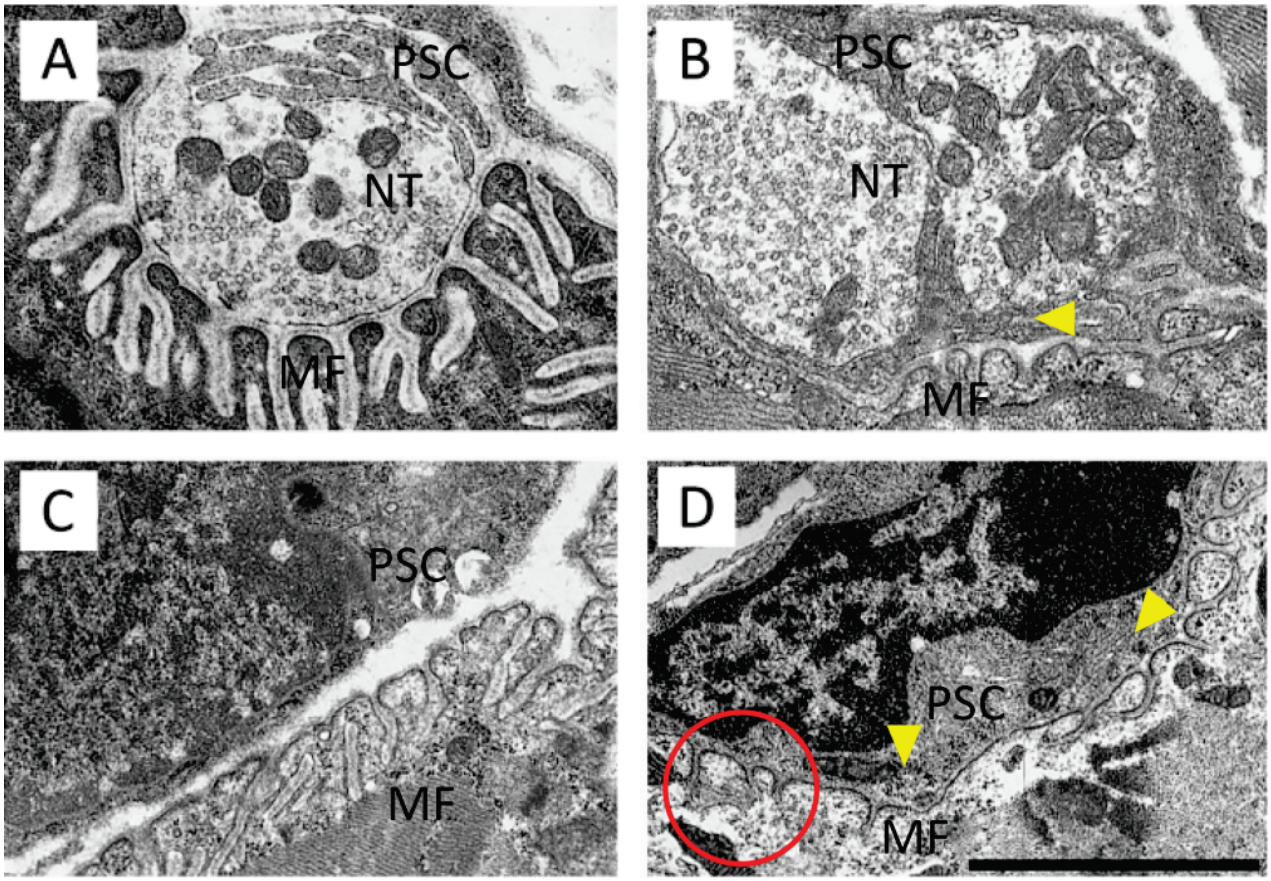

Figure 1.7 Ultrastructure Comparisons of Neuromuscular Junctions of Wild-type and *Lamb2*$^{-/-}$ mice

Electron micrographs illustrating the structural deficits observed in *lamb2*$^{-/-}$NMJs compared to wild-type. ***A***, Wild-type NMJs demonstrate clearly distinguishable regions of the synapse. Active zones appose the highly convoluted postsynaptic folds with no invasion of the synaptic cleft by PSCs. Synaptic vesicles are largely position in the juxtamuscular half of the nerve terminal. ***B***, By contrast, *lamb2*$^{-/-}$ NMJs present severe morphological disruptions such as poorly formed postsynaptic folds (red circle, ***D***) and a decrease in active zone regions. Synaptic vesicles are dispersed throughout the nerve terminal. ***C***, Wild-type NMJs show no aberrant changes in PSC structure or location. ***D,*** Evident invasion of the synaptic cleft by PSC processes which make direct contact with the basal lamina membrane (yellow arrow heads). Scale bar represents 1.5 μm for A & B; 2.0 μm for C & D. Figure adapted from Patton *et al*., 1998.

Laminin-α4 is present extrajunctionally and junctionally during early embryonic stages, with it later being concentrated specifically to the synaptic cleft at embryonic day 14 (Miner *et al.*, 1997; Patton *et al.*, 1997; Patton, 2000; Carlson *et al.*, 2010). The laminin-α4 chain, in contrast to other laminin chains expressed sub-synaptically, is found in highest concentrations at the depths of folds rather than at the crest of folds (Patton *et al.*, 2001). This finding suggests laminin-α4 plays an instructive role in the placement of postsynaptic specialisations, i.e. separating the postsynaptic folds themselves. Thus the presence of laminin-α4 may signal a region where active zones or folds, with dense AChR clusters, will not form during development. Loss of laminin-α4 does not lead to general disruption of synaptic basal lamina components or the distribution of other laminin isoforms.

By contrast, decreased expression of laminin-β2 results in the loss of α5 (Patton *et al.*, 2001). Laminin-α4 may be actively suppressed by laminin-α2 signalling in adults, with loss of laminin-α2 resulting in increased expression of laminin-α4 in the extrajunctional basal lamina of nerves and muscle (Ringelmann *et al.*, 1999). This finding has also been shown in humans afflicted with sufferers of congenital muscular dystrophy (CMD) displaying laminin-α2 deficiency culminating in up-regulation of laminin-α4 (Patton, 2000). Many of the key aspects of synaptogenesis, such as, formation of active zones and junctional folds occur normally in laminin α4 knockout mice (*lama*$4^{-/-}$) as in wild-type mice (Figure 1.8). Loss of laminin-α4 does not influence the number of active zones and postsynaptic folds when normalized per micron of nerve muscle apposition (Patton *et al.*, 2001). However, it has been shown using electron microscopy, that the precise apposition of active zones and post-synaptic folds fails to develop in *lama*$4^{-/-}$ mice, with approximately 70% of active zones displaying a decrease in proper alignment (compare Figure 1.8*A* with 1.8*B*) (Patton, 2000; Patton *et al.*, 2001). This finding indicates that the formation and placement of specific synaptic components is controlled independently (Patton *et al.*, 2001), as well as a potential loss of adhesion between pre- and postsynaptic regions.

Lama$4^{-/-}$ mice appear healthy and grow at a rate similar to wild-type mice. Histological analysis showed no evident signs of myopathy or dystrophy in muscle and muscle fibres with preserved size and shape (Patton *et al.*, 2001). Contractile response of muscle fibres also showed no signs of dystrophic defects. Patton *et al.* (2001) utilised light and electron microscopy to investigate the potential effects on the nerve itself as a result of loss of

laminin-α4, with no defects observed in *lama*4$^{-/-}$ NMJs. Thus the loss of laminin-α4 results in morphological changes isolated to the NMJ. At two months of age, laminin-α4 deficient mice display uncoordinated hindlimb movement when held by the tail, and were noted to occasionally drag their hindlimbs when walking, suggestive of a central deficit leading to neuromuscular dysfunction (Patton *et al.*, 2001). To characterise this potential dysfunction, the study analysed the ability of *lama*4$^{-/-}$ mice to walk along a narrow beam. At two months of age, wild-type mice were capable of crossing the beam with less than two foot slips while only 11% of *lama*4$^{-/-}$ mutants were able to do so. Utilising the same protocol, the same behavioural phenotypes were observed in eight-month old wild-type and mutant mice. These findings suggest that the defects seen in *lama*4$^{-/-}$ NMJs are maintained during ageing but are not progressive in nature (Patton *et al.*, 2001).

Recent research implicates laminin-α4 in playing a crucial role in the maintenance of the NMJ during ageing (Samuel *et al.*, 2012). It was noted that NMJs of *lama*4$^{-/-}$ mice at six months of age morphologically resembled those of 18- 24 month old wild-type NMJs (Valdez *et al.*, 2010). Approximately 50% of *lama*4$^{-/-}$ NMJs presented fragmented AChRs clusters, partial/full denervation, nerve sprouting, axonal swelling, and poly innervation, all of which are characteristic of an ageing NMJ (Valdez *et al.*, 2010; Samuel *et al.*, 2012). Wild-type mice rarely present these alterations in NMJ morphology at six months of age, however as the junction ages (12- 24 months of age) there are marked increases in the number of observed changes (Valdez *et al.*, 2010). These findings strongly indicate that the loss of laminin-α4 may contribute to premature disassembly of the junction normally observed in ageing NMJs. Changes in these knockout junctions also suggest a possible role for laminin-α4 in maintenance of both presynaptic and postsynaptic components during ageing. Samuel *et al.* (2012), found normal protein expression of laminin-α4 at 24 month old wild-type NMJs, however the distribution was often diffuse or lacking with some extrasynaptic expression observed. This finding indicates that during a normal ageing process changes in laminin-α4 distribution may be a factor that initiates the age-related disassembly of the NMJ. Currently, no studies of *lama*4$^{-/-}$ mice have been conducted to characterise the functional synaptic capabilities at the skeletal NMJ.

Mice lacking laminin-α4 do not display severe synaptic defects and abnormalities when compared to *lamb*2$^{-/-}$ mice (Patton *et al.*, 2001). This may be a result of the laminin-β2 chain being present in all three heterotrimers found specifically in the synaptic basal lamina, while the laminin-α4 chain is present only in laminin-421 (Patton, 2000; Carlson *et*

al., 2010). Carlson *et al.* (2010), propose that laminin-421 (α4β2γ1) may interact with both Ca_Vα and α3 integrin to pattern active zones via the ability of individual laminin chains to interact with each component. Laminin-β2 interacts with Ca_Vα to anchor the VGCCs at the presynaptic membrane, which in turn allows other active zone components to localise and tether to, or in proximity to the VGCCs (Nishimune *et al.*, 2004). Such interactions would not only promote stability of the presynaptic region, but would also facilitate organisation of molecular components required for efficient neurotransmitter release. Laminin-α4 has been shown to interact with α3 integrin which is found in proximity to the presynaptic active zones (Suzuki *et al.*, 2005). The integrins provide a link between the cytoskeleton and the extracellular matrix, and in addition are present at both pre- and postsynaptic regions, which aids in stability of the NMJ via interactions with LG1- 3 domains of laminin α chains (Wang *et al.*, 1993; Martin *et al.*, 1996; Colognato & Yurchenco, 2000; Ido *et al.*, 2004). Integrins, α3β1, α6β1, α7β1 and α6β4 have been shown to be the major laminin-binding integrins (Belkin & Stepp, 2000). Loss of interaction between laminin-β2 and Ca_Vα results in poor formation and stabilisation of active zones, while the loss of laminin-α4 leads to misapposition of active zones to postjunctional folds (Patton *et al.*, 2001; Carlson *et al.*, 2010). We propose that this link between pre- and postsynaptic regions, with laminin-421 acting as the primary mediator, is responsible for the stable architecture and organisation at a healthy NMJ, Voltage gated calcium channels act as the presynaptic receptor binding to laminin-β2, which as part of the laminin-421 heterotrimer directly associates with laminin-α4, in turn binding to postsynaptic cell surface receptors such as dystroglycan (see section 1.1.3).

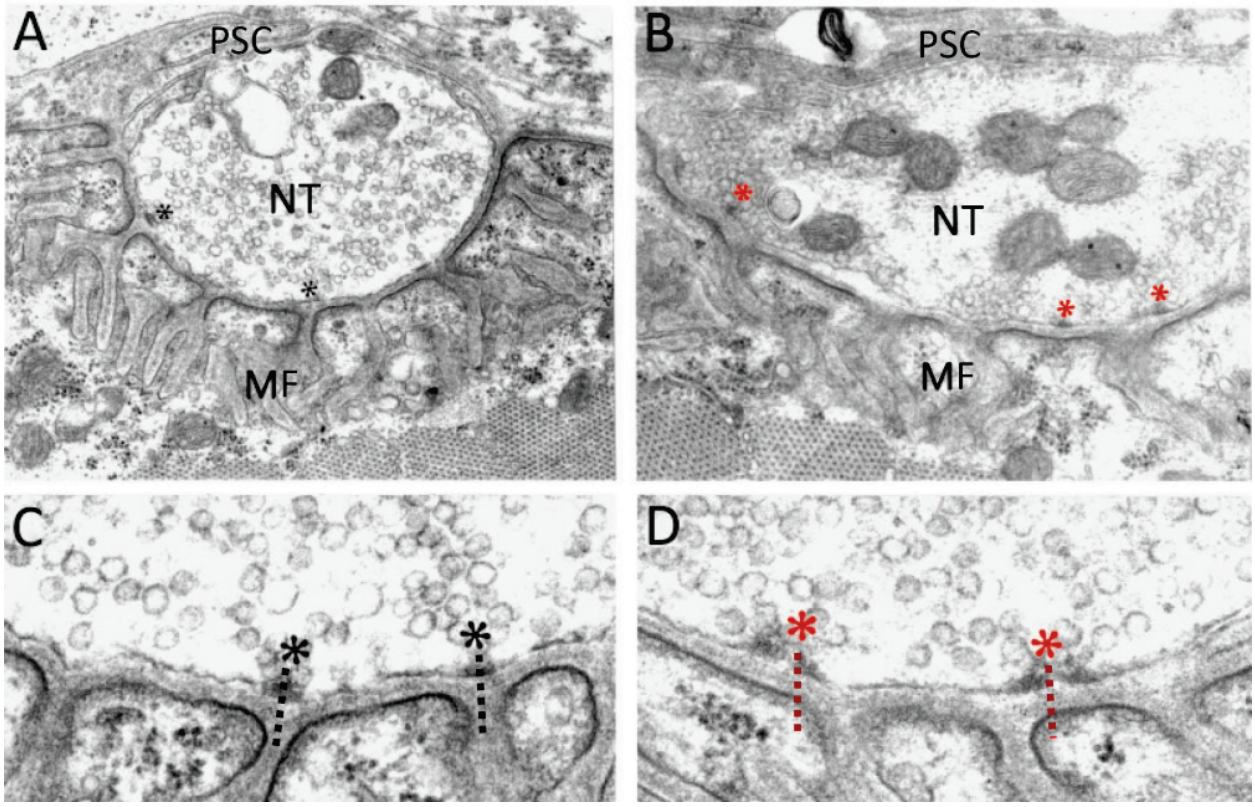

Figure 1.8 Ultrastructure Comparisons of Neuromuscular Junctions of Wild-type and *Lama4*$^{-/-}$ mice

Electron micrographs displaying the morphological changes observed in *lama4*$^{-/-}$NMJs compared to wild-type. ***A***, Wild-type NMJs demonstrate normal morphological structure with capping of the presynaptic nerve terminal by the Schwann cells. Wild-type NMJs also show direct apposition of active zones (black * and dashed lines) to the postsynaptic infolds (see ***C***, for higher magnification). ***B***, *Lama4*$^{-/-}$ NMJs display normal morphology with no change in active zone number or in the folding of the postsynaptic membrane. ***D***, *Lama4*$^{-/-}$ NMJs show misapposition of active zones (red * and dashed lines) to infolds of the postsynaptic region. Wild-type and lama4$^{-/-}$ NMJs show no invasion of the synaptic cleft by PSC processes and synaptic vesicles are primarily positioned in the juxtamuscular half of the nerve terminal near active zones. Scale bar represents 0.6 μm for A & B; 0.25 μm for C & D. Figure adapted from Patton *et al*., 1998.

1.1.5 The Postsynaptic Membrane

The assembly and localisation of postsynaptic structures at the muscle membrane is highly optimised in order to receive and propagate an action potential signal from the presynaptic terminal to the muscle fibre. The most prominent ultra-structural feature of this region is the deep infolds at the membrane surface, termed synaptic folds. Anchored at the crest of these folds are highly dense clusters of AChRs (~10,000 μm^2) (Fertuck & Salpeter, 1974; Fertuck & Salpeter, 1976; Land *et al.*, 1980; Wood & Slater, 1997, 2001; Ngo *et al.*, 2007). Activation of AChRs allows influx of cations through the AChR pore, resulting in generation of a muscle-cell action potential that eventually culminates in muscle contraction. At the depths of the postsynaptic folds are high concentrations of voltage gated sodium channels, which are activated by the depolarisation caused by cations flowing through AChR pores. The opening of these channels propagates electrical activity and results in further depolarisation of the postsynaptic membrane to threshold which triggers the generation of a muscle action potential.

This high density of post-synaptic AChRs is brought about by the action of two nerve derived molecules, neural-agrin and neuregulin-1. During synaptogenesis, contact between the motor nerve terminal and the muscle fibre results in the release of agrin, a heparin sulfate proteoglycan from the terminal itself (Nitkin *et al.*, 1987; Wallace, 1989). Agrin interacts with the transmembrane Muscle Specific Kinase (MuSK) to induce aggregation of AChRs in order to stabilise the synapse during development via binding of its co-receptor, low-density receptor-related protein (LRP4) receptor (Wallace, 1989; Valenzuela *et al.*, 1995; DeChiara *et al.*, 1996; Glass *et al.*, 1996; Mittaud *et al.*, 2004; Zhang *et al.*, 2008; Ghazanfari *et al.*, 2011). The degree of AChR clustering can be altered by the level of activation (phosphorylation) of MuSK, with Ab1 kinases acting to increase the level of MuSK phosphorylation and consequently lead to more AChR clustering (Mittaud *et al.*, 2004). More recently, Ngo *et al.* (2012) demonstrated neuregulin-1 potentiation of MuSK phosphorylation leading to downstream AChR cluster formation. Reduced AChR clustering can be instigated by de-phosphorylation of MuSK by Shp2 (Madhavan & Peng, 2005; Madhavan *et al.*, 2005; Qian *et al.*, 2008). Both MuSK and the receptor associated protein, rapsyn are required for the clustering of AChR at the postsynaptic membrane (Gautam *et al.*, 1995; Qu *et al.*, 1996; Lin *et al.*, 2001; Sanes & Lichtman, 2001). Gervasio and Phillips (2005) suggested that the agrin-MuSK complex may increase the targeting ability of rapsyn, which binds directly to the β-subunit of AChRs, to further aid in synapse stabilisation. Agrin deficient mice demonstrate initial clustering of AChRs however within

days receptors are dispersed throughout the muscle fibre and impaired postsynaptic differentiation is observed (Gautam *et al.*, 1996). Neuregulin-1 increases the transcription of synaptic genes for $AChR_{\alpha}$, $AChR_{\varepsilon}$, $AChR_{\gamma}$ subunit genes, and MuSK genes (Jo *et al.*, 1995; Moscoso *et al.*, 1995; Ngo *et al.*, 2004). These molecules are critical in the clustering and stabilisation of AChRs at the end-plate during maturation.

Numerous other molecules have been shown to bind to or alter the signalling of agrin that may influence the degree of AChR aggregation. These molecules include laminins, integrins, neural-cell adhesion molecule (NCAM), and dystroglycan (Vogel *et al.*, 1983; Sugiyama *et al.*, 1994; Martin & Sanes, 1995; Martin *et al.*, 1996; Martin & Sanes, 1997; Denzer *et al.*, 1998; Sanes *et al.*, 1998; Timpl *et al.*, 2000). Laminin binds to both agrin and the cell surface receptor α-dystroglycan via the γ1 and α subunits respectively (Denzer *et al.*, 1998; Kammerer *et al.*, 1999; Talts *et al.*, 2000; Timpl *et al.*, 2000; Bezakova & Ruegg, 2003; Yurchenco & Patton, 2009). The affinity of agrin for both laminin and dystroglycan may serve to increase laminin anchorage to cell surfaces in some tissues (Yurchenco & Patton, 2009). Importantly, dystroglycan aggregates at the postsynaptic membrane in the presence of laminins-α4 and -α5 to promote maturation of the end-plate (Nishimune *et al.*, 2008; Pilgram *et al.*, 2010). These complex protein interactions demonstrate the multifaceted network that occurs at the postsynaptic membrane to aid in both maturation and stability of the end-plate, which in turn allows for efficient organization of the postsynaptic specialties at the NMJ.

Acetylcholine Receptor Maturation

At developing mammalian NMJs the AChRs comprise of two α-subunits with single β- and δ- subunits, in addition to the foetal γ-subunit. During the first two weeks postnatal the γ-subunit is replaced by the adult ε-subunit (Takai *et al.*, 1985; Gu & Hall, 1988; Horton *et al.*, 1993). Within the first two weeks after birth the γ- are gradually replaced by ε-subunits however, the signals responsible for this switch have not yet been elucidated (Gu & Hall, 1988; Martinou & Merlie, 1991; Yumoto *et al.*, 2005). In addition to the developmental change in AChR subunit expression, the appearance of AChR end-plate distribution also undergoes change with maturation. Prior to muscular innervation (E12-14), AChRs are clustered in the centre of the newly formed embryonic fibre (Ziskind-Conhaim & Bennett, 1982; Creazzo & Sohal, 1983; Lin *et al.*, 2001; Ngo *et al.*, 2007). The clustering of AChRs results in increased metabolic stability, with the turnover of AChRs in adult synapses

occurring at approximately 14 days compared to each day at embryonic stage (Fambrough *et al.*, 1979). As the muscle develops foetal AChR clusters evolve from diffuse oval plaques to mature elongated structures, with invaginated folds containing high and low AChR densities (see Figure 1.9) (Lanuza *et al.*, 2002).

The proteins that drive this change in AChR patterning during maturation are yet to be fully determined, however it is suggested that the synaptic podosome complexes and proteins such as ephexin 1 are crucial for this process (Proszynski *et al.*, 2009; Shi *et al.*, 2010; Shi *et al.*, 2012; Proszynski & Sanes, 2013). Laminins-α5 and -β2 co-localise to the plaque-like AChR end-plate regions at immature NMJs (Proszynski *et al.*, 2009). As the NMJ matures perforations appear at the end-plates, giving the characteristic pretzel shape (Proszynski *et al.*, 2009). These perforations are formed by the presence of synaptic podosomes at the AChR end-plates and coincide with the loss of laminin-α5 from these regions (Proszynski et al., 2009). The edges of these perforations are ringed by laminins and actin-rich focal adhesion molecules such as vinculin. The expression of laminin at the edge of these perforations aids in the stabilisation of the AChR end-plates due to laminin interaction with molecules such as integrin and dystroglycan (Grady *et al.*, 2000; Nishimune *et al.*, 2008). Thus absence of laminins-α5 and -β2 may result in destabilisation of the end-plate and subsequently a loss of AChR clustering. In addition to this, signs of fragmentation and disassembly of the end-plate are associated with a change in expression of laminin-α4, thus it is likely that laminin-α4 interacts with postsynaptic molecules to maintain the integrity of the end-plate complex (Samuel *et al.*, 2012).

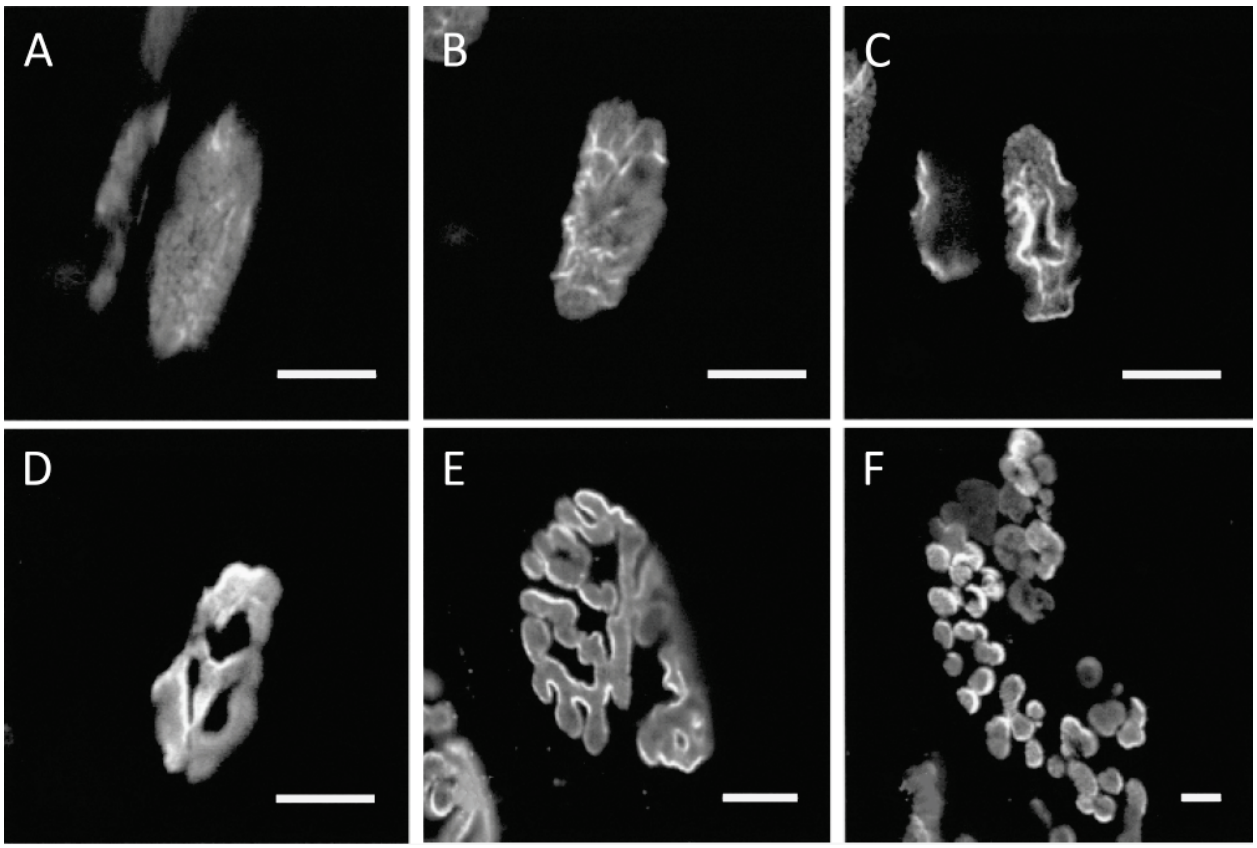

Figure 1.9 Development of Acetylcholine Receptor Clustering Morphology at the Skeletal Neuromuscular Junction from Birth to Adulthood

Synaptic AChR clusters progressively develop from ***A***, diffuse oval plaques with indistinct boundaries found at the foetal NMJ to ***B***, elongated oval plaque with development of non-homogeneity in receptor density. **C**, Plaques begin to form non-innervated regions showing no fluorescence, with the borders of these regions showing higher density of receptors. ***D***, Oval AChRs begin to form convoluted external borders with varying receptor densities. AChR regions show mature branching patterns with varying degrees of receptor density. ***E***, Regions of high AChR density show innervation by nerve terminal branches while other regions are not. ***F***, Intercalary growth of axon terminals results in the discontinuous patterning of AChR gutters as found in adult animals. Scale bars = 10 μm. Adapted from Lanuza *et al.* (2002).

1.2 Mechanisms of Transmitter Release

The NMJ possesses a high safety factor, that is, quanta of ACh are released in excess to that required to induce an end-plate potential (EPP) greater than the threshold required to initiate an action potential (Wood & Slater, 2001). The safety factor of transmission at the NMJ varies between fast and slow twitch fibre muscles as seen in characteristic differences in neurotransmission properties (Gertler & Robbins, 1978; Reid *et al.*, 1999). Differences such as quantal content, AChR density and the degree of postsynaptic folding are factors that may contribute to the varied safety factors observed between muscle fibre types. A number of protein interactions occur at the presynaptic membrane to produce this high safety factor allowing for efficient release of transmitter at the NMJ. The release of transmitter is regulated by release machinery proteins, which interact with VGCCs to coordinate vesicular trafficking, docking and priming, the release of vesicular contents, and membrane retrieval via endocytosis (Ceccarelli *et al.*, 1973; Heuser & Reese, 1973; Hurlbut & Ceccarelli, 1973; for review, see Zheng & Bobich, 1998; Sudhof, 2004).

Transmitter is released from the nerve terminal in quanta of less than 10,000 molecules of ACh, packaged within a single 50 nm diameter synaptic vesicle (Kuffler & Yoshikami, 1975; Reid *et al.*, 1999). Synaptic vesicles are organised and stored in two distinct pools within the presynaptic terminal. The first pool containing the majority of clustered vesicles is termed the reserve pool and is located away from the presynaptic membrane (approximately 150 nm to 200 nm) yet in close proximity to the active zone (Pieribone *et al.*, 1995; Rizzoli & Betz, 2004; Fdez & Hilfiker, 2006). The second distinct cluster is referred to as the readily releasable pool. This pool, originally deriving from the reserve pool, is closely apposed to the presynaptic terminal membrane (see Figure 1.10) (Schikorski & Stevens, 2001). The vesicles from the readily releasable pool are released first with depleted vesicles being replenished from the stores in the reserve pool (for review, see Sudhof, 2004). The size of the reserve pool and consequently the number of vesicles held varies among synapses. The size of the pool is related to the recycling ability and functional requirements of the terminal, thus high frequency activity requires a relatively large reserve pool (Brodin *et al.*, 1997). The regulation of vesicle pool size at these clusters allows for control of quantal release from the presynaptic terminal.

At the matured mouse NMJ there are approximately 850 active zones per terminal, each with two docked vesicles (Nagwaney *et al.*, 2009). Thus it may be assumed that there are approximately 1700 vesicles that are primed in and stored in the readily releasable pool. The same study showed that approximately 3000 quanta are released after a 100Hz train of 1 s duration. This value is equal to all vesicles that are tethered to active zones, i.e. primary and secondary docked vesicles, and non-docked vesicles that are attached to active zone material. Vesicle recruitment is calcium dependent at a rate of 1 vesicle/ ms^{-1} (Hosoi *et al.*, 2007; Neher & Sakaba, 2008) thus vesicle replenishment post high frequency stimulus will be slower due to a global decrease in calcium stores (David & Barrett, 2000). The docking of synaptic vesicles involves a network of proteins that allow for optimal vesicle positioning to facilitate efficient transmitter release.

1.2.1 Synapsin

Synapsins are a family of phosphoproteins capable of binding to actin filaments and synaptic vesicles in a phosphorylation-dependent manner (Petrucci & Morrow, 1987; Greengard *et al.*, 1993; Pieribone *et al.*, 1995; Evergren *et al.*, 2007). Studies have shown that phosphorylation of synapsin by specific protein kinase(s) can regulate their function by altering synapsin affinity for both F-actin and/or synaptic vesicle membranes (Jovanovic *et al.*, 1996; Hosaka *et al.*, 1999; Menegon *et al.*, 2006). There are three distinct synapsin gene variants generally found in vertebrates; synapsin I, II, and III (Hosaka & Sudhof, 1998; Kao *et al.*, 1998; Kao *et al.*, 1999).

Predominantly synapsin I and II are expressed at the synapse (Kao *et al.*, 1998) with preferential localisation to the reserve pool (De Camilli *et al.*, 1983; Torritarelli *et al.*, 1990; Pieribone *et al.*, 1995; Bloom *et al.*, 2003). Deletion of synapsin I results in a decrease in synaptic vesicle number and in the size of the reserve pool (Li *et al.*, 1995; Takei *et al.*, 1995). Ryan *et al.* (1996) found a diminished number of vesicles underwent exocytosis upon nerve stimulation in synapsin I deficient mice. There was also a decrease in the dense clustering of synaptic vesicles at the presynaptic membrane (Bogen *et al.*, 2006; Hvalby *et al.*, 2006). More recent studies comparing wild-type to mice lacking all three forms of synapsin (synapsin I, II, and III) have shown a decrease in synaptic vesicle mobility in addition to the other phenotypes observed in single synapsin knockout models (Gaffield & Betz, 2007).

1.2.2 Rab3

Synaptic vesicles are released from the reserve pool and move to active zones at the presynaptic terminal membrane. Vesicles then undergo a process termed 'docking,' which is the initial contact between vesicular proteins and presynaptic membrane proteins. The precise docking procedure is a targeted process, with the rab protein family implicated in playing a key role. Rab3A is a GTP binding protein that associates with the vesicle membrane (see Figure 1.11) (Johnston *et al.*, 1991). This protein is thought to be involved in targeting, docking and fusion of vesicles (Nonet *et al.*, 1997). Rab3A deficient mice show higher levels of depression during short trains of high frequency stimulation (Geppert *et al.*, 1994a; Nonet *et al.*, 1997) while partial depletion of vesicles and a reduction in synaptic transmission was seen in Rab3 mutants using *C. elegans* models.

Rab3-interacting molecule (RIM) is an active zone protein suggested to be the central organiser of synaptic vesicle docking due to close association with all other known active zone proteins such as CAST and ELKs, as well as its binding to synaptic vesicles via Rab3A (detailed in Figure 1.11) (Wang *et al.*, 1997; Wang *et al.*, 2000; Mittelstaedt *et al.*, 2010; Kaeser *et al.*, 2011). This idea is further supported by studies in mice lacking RIM, where defects in vesicle docking and priming have been documented (Koushika *et al.*, 2001; Castillo *et al.*, 2002; Fourcaudot *et al.*, 2008; Kaeser *et al.*, 2008). A recent study has shown that RIM is crucial for the tethering of P/Q- type VGCCs to the active zone, through observations in RIM-deficient mice (Kaeser *et al.*, 2011). Similar findings have also observed in *Drosophila* (Graf *et al.*, 2012). Investigators proposed that VGCCs bind directly to RIM proteins via a PDZ-domain interaction as well as via an indirect interaction through binding of channels via RIM-binding proteins (Hibino *et al.*, 2002).

1.2.3 Soluble N-ethylmaleimide Sensitive Factor Attachment Protein Receptors

Upon docking at the active zone, synaptic vesicles undergo a priming phase prior to the release of neurotransmitter (see Figure 1.10*B* and insert). The principal proteins involved in this process are the SNAREs (soluble N-ethylmaleimide sensitive factor attachment protein receptors) (Walker *et al.*, 1998). The SNARE protein complex comprises of the vesicular v-SNARE synaptobrevin, and the plasma membrane t-SNAREs, syntaxin 1A and synaptosome- associated protein of 25 kDa (SNAP-25), which collectively dock synaptic vesicles and mediate fusion events at the presynaptic terminal membrane (see Figure 1.10, insert) (Sutton *et al.*, 1998; Catterall, 1999; Chen & Scheller, 2001; Jahn & Grubmuller, 2002; Kidokoro, 2003). Synaptobrevin, also known as vesicular associated

membrane protein (VAMP), binds to both syntaxin 1A and SNAP-25 on the presynaptic membrane in a 1:1:1 ratio to form a stable four helix complex, termed the SNARE complex (Figure 1.10 insert) (Sollner *et al.*, 1993; Xiao *et al.*, 2001). The SNARE complex draws the vesicle into close proximity to the active zones at the presynaptic membrane and primes the vesicle for exocytosis (Weber *et al.*, 1998). It has been shown that the SNARE complex forms prior to stimulus evoked fusion, therefore suggesting that the complex is formed after vesicles have docked but prior to membrane fusion (summarised in Figure 1.10*B*- 1.10*C* and insert) (Xia *et al.*, 2001).

The SNARE complex has also been suggested to interact directly with VGCCs to form a VGCC-active zone complex, through binding of intracellular loops of the α_1 subunits on the channels to syntaxin 1A (see Figure 1.11) (Sheng *et al.*, 1994; Kim & Catterall, 1997; Xiao *et al.*, 2001; Keith *et al.*, 2007). Alteration of this binding is thought to result in modulation of transmitter release. Keith *et al.* (2007) have demonstrated that SNAREs positively modulate VGCCs in the presence of docked vesicles, while channels were inhibited in the absence of docked vesicles. These findings would suggest that calcium influx is likely to occur through VGCCs with docked vesicles, while calcium influx through VGCCs without docked vesicles is minimised.

1.3 Synaptic Vesicle Fusion

Dodge and Rahamimoff (1967) proposed that calcium binds to a critical receptor site in the presynaptic terminal. By measuring the postsynaptic potential at increasing calcium concentrations, it was found that calcium triggers transmitter release in a co-operative manner. The fusion of vesicles occurs within approximately 150 μs after the arrival of an action potential and within 60 μs after calcium entry into the terminal (Sabatini & Regehr, 1996). It has also been demonstrated that a relatively high calcium concentration is required to elicit transmitter release (Uchitel *et al.*, 1992; Neher, 1998; Neher & Sakaba, 2008). These findings indicated that the critical receptor, or calcium sensor, is localised to the active zones in close proximity to VGCCs and demonstrates a low affinity for calcium. One such candidate is synaptotagmin.

Synaptotagmin is a vesicle membrane protein belonging to a family of proteins possessing two calcium and phospholipid binding domains (C_2 domains; C_2A and C_2B) (Perin *et al.*, 1991; Davletov & Sudhof, 1993; Adolfsen & Littleton, 2001).

Synaptotagmin has been shown to directly interact with the regulatory proteins syntaxin, SNAP-25 and Munc 13 (see Figure 1.11) as well as the α1 subunits of both N- and P/Q-type VGCCs (see section 1.1.3) (Sudhof & Rizo, 1996; Charvin *et al.*, 1997; Kim & Catterall, 1997; Schiavo *et al.*, 1997). Early studies by Brose and colleagues (1992) demonstrated the binding capabilities of synaptotagmin to both Ca^{2+} and phospholipids (Brose *et al.*, 1992). More recently it has been suggested that different forms of synaptotagmin will determine the characteristic Ca^{2+} sensitivity of vesicle fusion (Johnson *et al.*, 2010). Numerous studies using synaptotagmin deficient models have found diminished calcium-triggered transmitter release, strongly suggesting synaptotagmins role as the calcium sensor at the presynaptic terminal (DiAntonio *et al.*, 1993; Littleton *et al.*, 1993; Nonet *et al.*, 1993; Geppert *et al.*, 1994b).

Deletion of synaptotagmin has also been implicated in the severe reduction in synaptic vesicle numbers in *C. elegans* and *Drosophila* models suggesting involvement with endocytosis (Jorgensen *et al.*, 1995; Reist *et al.*, 1998; Poskanzer *et al.*, 2003). In the absence of calcium, synaptotagmin is still capable of binding t-SNAREs via the C_2A domain (Verona *et al.*, 2000; Rickman & Davletov, 2003), while in high concentrations of calcium (100-300 μM), binding interaction to SNARE proteins is enhanced (Gerona *et al.*, 2000; Adolfsen & Littleton, 2001). Fernandez-Chacon *et al.* (2002) showed that a point mutation in the C_2A domain resulted in a significant decrease in Ca^{2+} sensitivity of transmitter release. Synchronous transmitter release has been abolished in *Drosophila* mutants that do not express any C_2 domains (*AD4* null) (Yoshihara & Littleton, 2002). Mackler *et al.* (2002) created *Drosophila* mutants in which the C_2B aspartate residues were replaced with asparagines. These mutants showed a >95% decrease in evoked response at the NMJ. This study suggested that the C2B domain plays a key role as the calcium sensing component of synaptotagmin. Together these findings strongly support the proposed role of synaptotagmin as a presynaptic calcium sensor and also suggest a function in stabilisation of the SNARE complex. Close spatial arrangement of VGCCs and syntaxin 1A localises calcium ions to synaptotagmin, which in turn potentiates neurotransmitter release (Xiao *et al.*, 2001; Chapman, 2002; Keith *et al.*, 2007; for review, see Kochubey *et al.*, 2011).

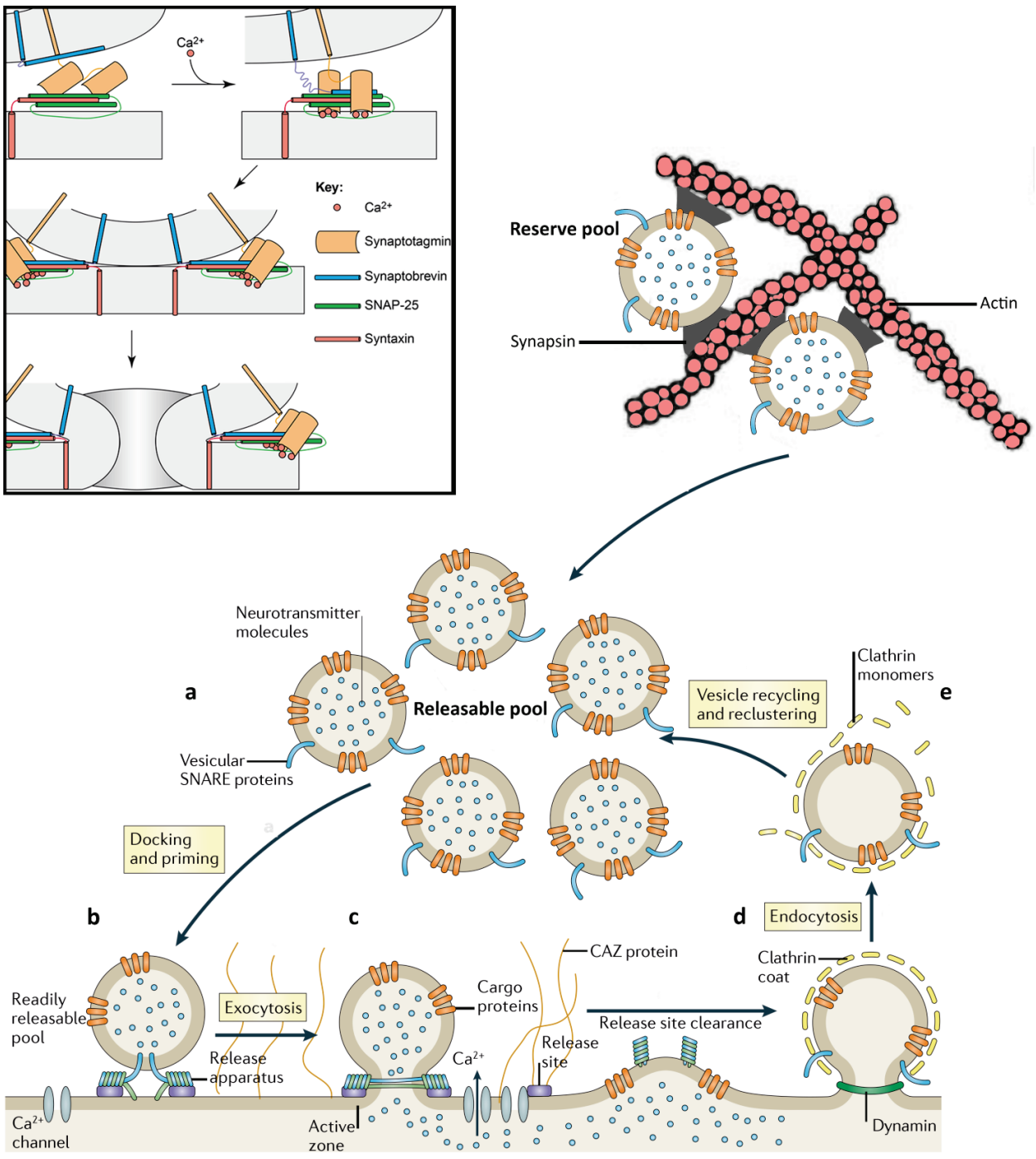

Figure 1.10 Proposed Model of the Mechanism of Neurotransmitter Release from a Motor Nerve Terminal

Synaptic vesicles are separated into two functionally distinct pools: the reserve pool located distal to the presynaptic membrane and, the releasable pool proximal to the active zones at the presynaptic membrane. Vesicles stored in the reserve pool are bound to actin filaments via synapsins. Synaptic vesicles are (***a***) released from reserve pool and targeted to the active zone where they undergo (***b***) docking and priming. Upon nerve terminal depolarisation and subsequent influx of Ca^{2+}, the vesicles (***c***) fuse to the presynaptic membrane and exocytose their contents. Emptied vesicles undergo (***d***) exocytotic retrieval,

mediated by a clathrin- and dynamin-dependent pathway. Finally, (***e***) synaptic vesicle recycling which entails uncoating of clathrin and simultaneous uptake of neurotransmitter before vesicles are re-clustered in one of the two vesicle pools. Rab and Rab effector proteins are involved in multiple events including targeting and docking of SVs. The docking, priming and fusion events involve complex interactions between CAZ (see section 1.3.3) proteins and other active zone proteins; GTP-Rab3 and RIM, Syntaxin-SNAP 25 and VAMP and, synaptotagmin with α1 subunits of VGCCs. Insert shows Ca^{2+} driven synaptic vesicle fusion; Ca^{2+} binding to synaptotagmin results in the latter binding to SNARE proteins, bringing synaptobrevin in closer proximity to SNAP-25 and syntaxin. This complex undergoes Ca^{2+} dependent oligomerisation resulting in the formation of the fusion pore. Synaptotagmin then also undergoes oligomerisation that favours the complete collapse of the vesicle membrane into the presynaptic membrane. Figure adapted from Haucke *et al.* (2011), insert from Koh and Bellen (2003).

1.3.1 Regulating Proteins

The release machinery proteins described previously (see section 1.2) are the primary effectors of vesicular trafficking, docking and priming, and the release of vesicular contents. There are several regulatory proteins present in the presynaptic terminal capable of modulating the release machinery proteins, namely the SNARE complex, which subsequently results in altered transmitter release. The regulatory proteins of key interest are: Munc13 and Munc18 which bind to syntaxin 1A; synaptophysin which binds to VAMP; and SV2 which binds to the calcium sensor synaptotagmin (Schivell *et al.*, 1996; Bean & Scheller, 1997; Betz *et al.*, 1997). Genetic deletion of either Munc13 or Munc18 results in severe deficits in transmitter release, suggesting that they play a role in positioning syntaxin 1A at the docking complex as well as possibly resetting syntaxin 1A on the presynaptic membrane after vesicle fusion (Hosono & Kamiya, 1991; Hosono *et al.*, 1992; Augustin *et al.*, 1999; Varoqueaux *et al.*, 2002). Synaptophysin is a synaptic vesicle glycoprotein that binds to VAMP. This binding has been suggested to prevent the association of VAMP with syntaxin and SNAP-25 on the vesicle membrane (Walchsolimena *et al.*, 1995). The transmembrane synaptic vesicle associated protein (SV2) is found in large abundance within synaptic vesicles (Janz *et al.*, 1998). The exact role of SV2 in transmitter release is not certain, however Pyle *et al.* (2000) found that the phosphorylation of SV2 alters its binding ability to synaptotagmin. This finding supported early suggestions that SV2 may act as a calcium dependent regulator of release machinery proteins (Crowder *et al.*, 1999; Janz *et al.*, 1999).

1.3.2 Cytomatrix at the Active Zone proteins

In addition to the above proteins concentrated at presynaptic release sites (active zones), there are a number of other relatively large proteins collectively termed cytomatrix active zone (CAZ) proteins, which have been suggested to associate with the above release machinery proteins. However, the exact mechanisms by which they regulate the function of the active zone remain unclear (Juranek *et al.*, 2006). The key CAZ proteins include: Bassoon, Piccolo, ELKS and cytomatrix at the active zone-associated structural protein (CAST) (see Figure 1.11). Bassoon and Piccolo are structurally homologous with the later possessing additional PDZ and C2 domains (Dieck *et al.*, 1998; Fenster *et al.*, 2000; Schoch & Gundelfinger, 2006). Both these proteins bind to the Rab3A- associated protein-1 (Pra1), thus suggesting a role in regulation of vesicular trafficking (Shapira *et al.*, 2003; Takao-Rikitsu *et al.*,

2004). It has recently been established that CAST and ELKS are of the same protein family (Wang *et al.*, 2002; Deguchi-Tawarada *et al.*, 2004; Deguchi-Tawarada *et al.*, 2006). Ohtsuka *et al.* (2002) have shown that all currently known active zone proteins are co-immunoprecipitated with CAST, suggesting a coherent network of protein-protein interactions within the active zone region. The direct interaction of CAST to bassoon and RIM1 is essential for efficient transmitter release (Hida & Ohtsuka, 2010). Disruption of this complex network of regulatory proteins can detrimentally affect the release of neurotransmitter at the NMJ.

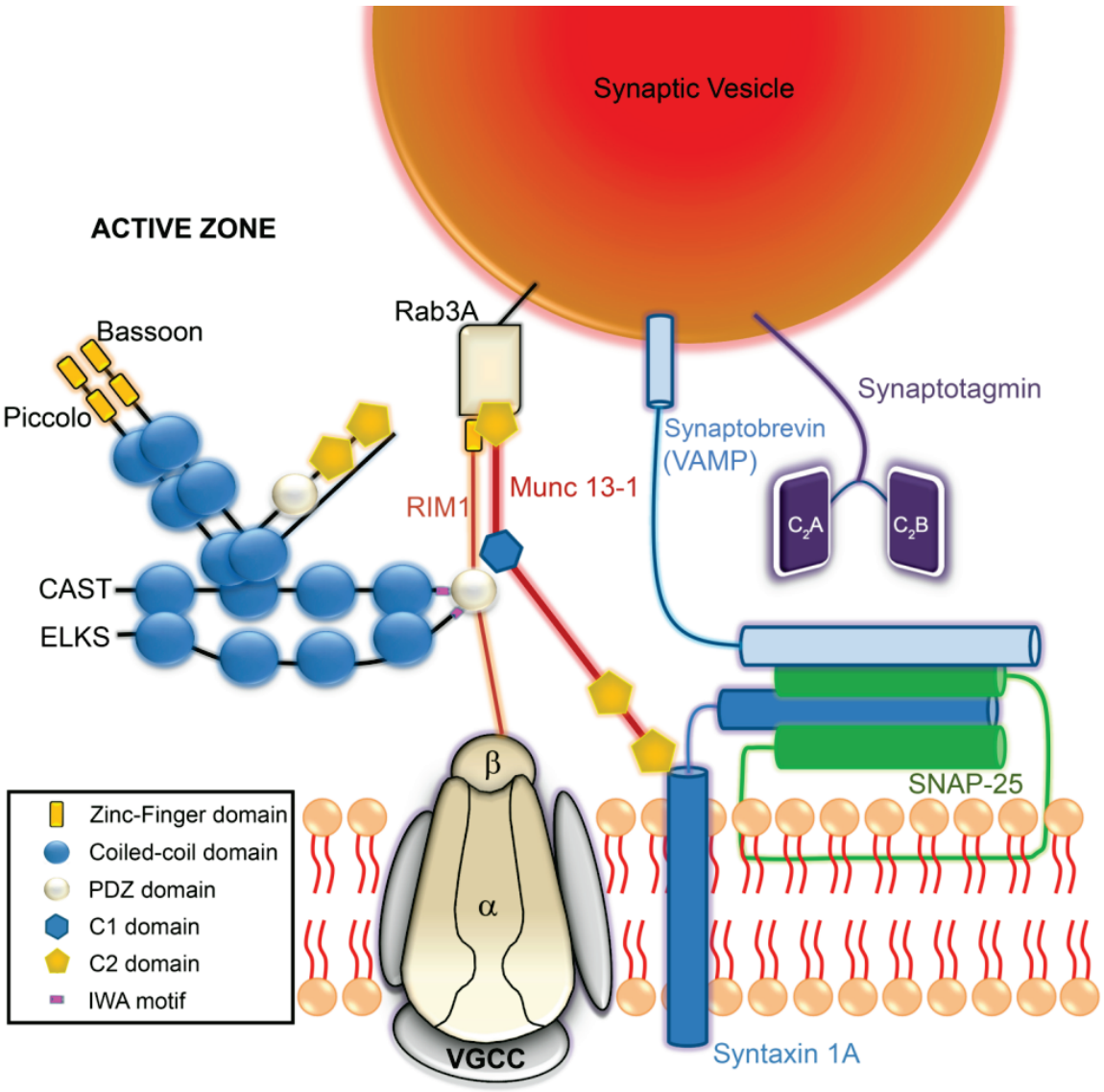

Figure 1.11 Network of Protein-Protein Interactions within the Active Zone Cytomatrix

A number of key proteins within the cytomatrix associate with release machinery proteins at the active zone, termed the CAZ proteins. Cytomatrix at the active zone-associated structural protein (CAST) and ELKs act as a scaffold by binding to the structurally homologous proteins, Bassoon and Piccolo. The COOH -terminal IWA motif of CAST and ELKs binds to the PDZ domain of RIM1. RIM1 binds directly to Munc13-1 via zinc-finger domain, which in turn associates with syntaxin 1A. The syntaxin 1A protein is a major component of the SNARE complex, which is critical in the release of neurotransmitter from the presynaptic terminal. The regulatory proteins, SNAP-25 and synaptobrevin (VAMP), associate with Syntaxin 1A and synaptotagmin to interact with the CAZ proteins to modulate docking, priming and fusion events.

1.4 Rationale

Previous studies have shown that laminins α4, β2, and γ1 play a critical role in development and organisation of the mouse NMJ. There is now growing evidence linking the loss or mutation of specific laminin chains in a wide array of human disorders associated with defects in basal lamina membrane assembly and composition. These disorders include; MDC1A congenital muscular dystrophy, a disorder attributed to mutations in the basal membrane and extracellular matrix at the synapse involving the loss of laminins-α2 and β2 (Helbling-Leclerc *et al.*, 1995; Cohn *et al.*, 1997; Cohn *et al.*, 1998); and Pierson syndrome, a disorder characterised by congenital nephrosis and ocular defects attributed to mutations in genes coding for laminin-β2 (Zenker *et al.*, 2004; Zenker *et al.*, 2005). Recent study by Liu and colleagues (2011) on human amyotrophic lateral sclerosis (ALS) donors observed a wide array of changes in laminin expression. The study found a loss of laminins-α2 and -β2 from extra-ocular muscles of ALS patients as well as a dramatic decrease in expression at limb muscle fibres and the NMJs. Laminin-α4 was found normally expressed at extra-ocular muscles with severely decreased expression at the limb muscles of ALS donors. The pathogenesis of these disorders is influenced by the destabilisation of matrix integrity, and the loss of receptor and ligand interactions. The continued investigation of these laminins will help elucidate their role in spatial organisation and maintenance of the developing and mature NMJs. Study of laminin function may also provide insights into the basis of auto-immune diseases such as Lambert- Eaton myasthenic syndrome (Fukuoka *et al.*, 1987). This disease causes impaired neuromuscular function as a result of auto-immune attack on the extracellular loops of VGCCs, which consequently prevents the binding of laminin-β2 to calcium channels (Fukuoka *et al.*, 1987; Nishimune *et al.*, 2004). Changes in laminin-α4 expression have recently been associated with ageing NMJs and therefore are thought to play a maintenance role at the NMJ (Samuel *et al.*, 2012). At present, study of laminin-α4 has focused solely on characterising the molecular perturbations resulting from the loss of laminin-α4. The functional consequences for neurotransmission, stemming from the loss of laminin-α4, have not yet been investigated. The findings of this study may also provide insight in identifying pharmacological targets that may improve synaptic connections, and promote re-establishment of connections between motor nerves and muscle in the numerous nervous system diseases involving the loss of synaptic connections as well as those attributed to mutations in laminin chains.

1.5 Overall Aims

1. To evaluate the involvement of VGCCs subtype/s in transmitter release at developing (postnatal day 8) and mature (postnatal day 18) neuromuscular junctions in mice lacking laminin-β2.

2. To investigate the properties of perisynaptic Schwann cell activity at the mature neuromuscular junction of laminin-β2 deficient mice.

3. To functionally investigate neurotransmission properties at developing (postnatal day 8) and mature (postnatal day 18) neuromuscular junctions of laminin-α4 deficient mice.

1.6 Overall Hypotheses

1. **a**) *Lamb2*$^{-/-}$ mice would present similar VGCC subtype distribution as wild-type mice at the developing (P8) NMJ.

   b) *Lamb2*$^{-/-}$ mice would present NMJs with altered VGCC dependence and distribution of channel subtypes with respect to wild-types at the mature (P18) NMJ.
   - Loss of laminin-β2 will result in maintained presence of N-type VGCCs and decreased P/Q- type channel expression compared to wild-type NMJs.
   - N-type VGCCs will become the primary regulator of transmitter release at laminin-β2 deficient NMJs.

2. **a**) Loss of laminin-β2 would result in altered PSC activity with properties phenotypic of immature Schwann cells at NMJs of P14 *lamb2*$^{-/-}$ mice.

   b) PSCs would maintain dependence on immature signaling receptor subtype with decreased cell response to stimuli at *lamb2*$^{-/-}$ NMJs.

   c) PSCs would demonstrate decreased ability to modulate high frequency synaptic transmission at *lamb2*$^{-/-}$ NMJs.

3. **a**) *Lama4*$^{-/-}$ mice would display functional disruptions in neurotransmission properties compared to wild-type NMJs at both developing (P8) and mature (P18) age groups.

CHAPTER 2

General Methodology

General methodology

This chapter outlines the general methodology used throughout this thesis. Each method is described here in length; however any specific details pertaining to particular experiments are described in depth in their respective chapters.

2.1 Animals

The present study utilised wild-type mice (with two normal copies of all laminin genes) and homozygous mutant mice (with no normal copies of laminin-α4 or -β2 genes). Mice were obtained from the mating of heterozygous males and females, which were maintained on a defined C57BL/6-129SvJ genetic background. All mice had been backcrossed for over ten generations, thus all mice are C57BL/6 with the mutated locus being 129-SvJ (i.e. recombinant strain). The day of birth was termed postnatal day zero (Theiler, 1989). Identification of wild-type and homozygote mice was established by using a DNA tail assay (Hanley and Merlie, 1991, Noakes *et al*., 1995a). All wild-type and mutant mice used in this study were age-matched littermates for postnatal days 8 or 18 for investigations in Chapters 3 & 5 and, postnatal day 14 for the Schwann cell study of Chapter 4. Mice were anaesthetised with a rising concentration of carbon dioxide and then killed by cervical dislocation. The University of Queensland Animal Care and Ethics Committee approved all procedures undertaken (Ethics number 152/12) and were in accordance with the Queensland Government Animal Research Act 200, associated Animal Care and Protection Regulations (2002 and 2008), as well as the Australian Code for the Care and Use of Animals for Scientific Purposes, 8th Edition (National Health and Medical Research Council, 2013).

2.2 Functional Investigation of Neuromuscular Junctions from mice lacking either Laminin-α4 or Laminin-β2

2.2.1 Tissue Preparation

Whole mouse diaphragms with intact phrenic nerves were dissected free and pinned to a bed of cured silicone rubber (Sylgard, Dow Corning Corp., MI, USA) at the bottom of a 3mL organ bath (see Figure 2.1*A*). For functional study of laminin-α4 mutants (Chapter 5), *extensor digitorum longus* (EDL) and soleus with associated innervating nerves was also dissected free (see Figure 2.1*B* and 2.1*C* for respective muscle pinning). The extracted muscles were immersed in Tyrode's solution (NaCl 123.4 mM; KCl 4.7mM; $MgCl_2$ 1.0 mM; NaH_2PO4 1.3 mM; $NaHCO_3$ 16.3 mM; $CaCl_2$ 0.3 mM; and D-glucose 7.8 mM). Remaining connective tissue was removed from the surface to allow easier manipulation of the

innervating nerve and piercing of muscle fibres. The bath was continuously perfused with Tyrode's at a rate of 2-3mL per minute, at a constant room temperature of 22 ± 2^0C. The reservoir supplying the bath was continuously gassed with 95% O_2 and 5% CO_2. All chemicals unless specified were sourced from Sigma Aldrich (St. Louis, MO, USA).

2.2.2 Stimulation Protocol

The freed nerve, innervating the hemi-diaphragm, was gently sucked into a glass pipette filled with Tyrode's solution. The pipette acted as a stimulating electrode utilizing two silver chloride wires, one passing within the pipette as a positive electrode and the other wrapped around the outside as the negative electrode. A Grass Instruments stimulator (SD48) (Natus Neurology Inc., RI, USA) was used to apply square wave pulses of 0.08ms duration and 10-20 volts strength at a frequency of 0.08-0.1Hz.

2.2.3 Intracellular Electrophysiological Recordings

Fine tipped intracellular glass recording electrode (40 to 60 MΩ) filled with 2 M KCl were used to record end plate potentials (EPPs), miniature end plate potentials (MEPPs) and resting membrane potentials (RMPs) in low calcium concentrations (0.3mM). Recorded signals were amplified using an Axoclamp 2B amplifier with a single head stage (Molecular Devices, CA, USA) and then digitised to 20- 40 kHz sampling rate using MacLab system and Scope software (version 3.5.5, A/D Instruments, CO, USA). The digitised data was stored digitally for later analysis.

Muscular action potentials were prevented by partially blocking nicotinic acetylcholine receptors with 2.5 μM d-tubocurarine (Sigma Aldrich), when necessary. The electrode was positioned within 0.5mm of the motor end-plate. Proximity to end plate region was confirmed through analysis of EPP and MEPP rise times, with sites presenting rise times greater than 1.5 ms being rejected for wild-type and values greater than 2 ms rejected for laminin knockouts. Initial resting membrane potential values ranged between 75-85 mV and 60-80 mV for wild-type and laminin mutants respectively. The RMP underwent gradual decrease to a steady value between 55- 65 mV. The recordings were terminated if the RMP fluctuates by more than 10% from these steady values. At least 100 EPPs and 30 MEPPs were recorded for each NMJ under basal conditions.

2.2.4 Extracellular Electrophysiological Recordings

Coarse microelectrodes (2-10 μm diameter) filled with Tyrode's solution was used for extracellular recordings of the nerve terminal impulse (NTI), end-plate currents (EPCs) and miniature end-plate currents (MEPCs). Recorded signals were amplified as explained for intracellular electrophysiological recordings (see above 2.2.3). The electrode position was manipulated until the rise times of both EPCs and MEPCs was less than 1ms. The frequency of EPCs and MEPCs was monitored as the microelectrode is lowered, as electrode pressure is known to give rise to increased frequency of spontaneous activity (Fatt & Katz, 1952; Bennett *et al.*, 1986a; Bennett *et al.*, 1986b). After a site was located, the stimulus was halted for a five-minute period before commencing recording of MEPCs and EPCs. Five to six NMJ sites were selected from each muscle preparation with at least 30 MEPCs and 100– 200 stimulations recorded at each site.

2.2.5 Toxin Preparation and Application

The use of VGCC specific toxins as a tool to evaluate the contribution of VGCC subtypes in mediating transmitter release is well established (Kasai *et al.*, 1987; Llinas *et al.*, 1989; Hillyard *et al.*, 1992; Katz *et al.*, 1996; Iwasaki *et al.*, 2000; Santafe *et al.*, 2001; Pardo *et al.*, 2006; Depetris *et al.*, 2008). Here, the toxins ω-CTX GVIA and ω-AGA IVA were used to elucidate the VGCC subtypes present and involved in mediation of transmitter release at both, wild-type and *lamb*2$^{-/-}$ NMJs during development. Toxins were prepared as stock solutions dissolved in distilled water with ω-CTX GVIA as 0.5 mM stocks and ω-AGA IVA as 100 μM stocks, and stored at -20^{0}C (Regehr & Mintz, 1994). The concentration of these toxins varies considerably in literature (ω-CTX GVIA; 1-5 μM, ω-AGA IVA; 30-200 ηM), primarily due to preparations investigated ranging from neuronal cells, and neonatal to adult rodent skeletal muscle (Protti & Uchitel, 1993; Katz *et al.*, 1996; Plomp *et al.*, 2003; Depetris *et al.*, 2008). This study required a suitable concentration to be selected given the age groups investigated and the focus on observing the developmental switch from N- to P/Q-type VGCC mediation in transmitter release. The toxin concentrations selected for use in this protocol were 50 ηM ω-Aga IVA and 100 ηM ω-CgTx GVIA, similar to prior studies investigating VGCC mediation of NMJ transmission (Rosato-Siri *et al.*, 2002; Depetris *et al.*, 2008).

Once a stable site was found and control recordings taken, the stimulus was ceased for twenty minutes to allow vesicle replenishment. During this period the perfusion of the bath with Tyrode's solution was also halted to allow toxin incubation. The muscle preparation

was continuously oxygenated during incubation. A single VGCC specific toxin was applied directly to the 3mL organ bath with the tissue left to incubate during this twenty minute period (Protti & Uchitel, 1993). After the incubation period the stimulus commenced and recordings taken for a further twenty minutes at the same site as control recordings were taken. Upon completion of the first toxin phase the stimulus was again stopped for a further twenty minutes. The second VGCC specific toxin was then added during this time and left to incubate for a further twenty minutes. After incubation the stimulus will once again commence and recordings of the second toxin phase taken for twenty minutes. Toxin administration order was randomised in order to observe the effects of each VGCC specific toxin on the NMJ of wild-type and *lamb2*$^{-/-}$ deficient mice.

2.2.6 Cryosectioned Immunohistochemistry

Extensor digitorum longus (EDL) muscle was dissected free from wild-type and mutant mice. Tissue was fixed with 4% paraformaldehyde in 0.1 M phosphate buffered saline pH 7.4 (PBS) at room temperature for 30 minutes, and then washed 3 x 10 minutes with 0.1% glycine in PBS. Muscles were then immersed in 15% sucrose in PBS overnight followed by 30% sucrose in PBS overnight. The muscles were embedded in Tissue-Tek® optimal cutting temperature compound (Sakura Finetek, Torrance, CA, USA) and snap frozen in liquid nitrogen. The frozen muscles were sectioned longitudinally at 30 µm using a Cryostat.

Immunofluorescence double labelling was performed to localise molecular components at the presynaptic nerve terminal, see each Chapter 3 for details regarding antibody dilutions. These presynaptic components were immunolocalised with antibodies with respect to postsynaptic acetylcholine receptors (AChRs) labelled with Alexa Fluor-555-conjugated α-bungarotoxin (αBTX), at the NMJ. Cryosections were blocked in PBS containing 2% bovine serum albumin (BSA), 2% goat serum with 0.1- 0.2% TX-100 for 30 minutes at room temperature. All primary antibodies were diluted in PBS containing 2% BSA and 0.1% TX-100 or 2% BSA and 0.2% TX-100. EDL cryosections were then washed 3 x 10 minutes with PBS prior to incubation with appropriate Alexa Fluor 488-conjugated secondary antibodies (Molecular Probes, Invitrogen, Eugene OR, USA) in combination with Alexa Fluor 555-conjugated αBTX (Molecular Probes , Invitrogen) at room temperature for 2 hours. Sections were then washed with PBS and mounted in Prolong Gold anti-fade reagent (Molecular Probes, Invitrogen) and cover-slipped.

2.2.7 Wholemount Immunohistochemistry

Muscles were dissected free from wild-type and *lama*4$^{-/-}$ mice at P18. The muscles were incubated with Alexa Fluor 555 α-bungarotoxin (αBTX) for 30 minutes followed by washing with Tyrode solution. The tissues were then fixed with 2% paraformaldehyde in 0.1 M phosphate buffered saline, pH 7.4 (PBS) at room temperature for 20 minutes followed by consecutive washing with PBS. Immunofluorescence double staining was performed to determine the localisation and distribution of presynaptic components with respect to postsynaptic AChRs in diaphragm muscles (see Chapter 5 for antibody details). The fixed diaphragm and EDL muscles were blocked with PBS containing 2% bovine serum albumin (BSA), 2% goat serum and 0.5% Triton X-100 (TX-100). The tissues were rinsed with 0.5% TX-100 prior to incubation with the appropriate Alexa Fluor 488-conjugated secondary antibodies (Molecular Probes, Invitrogen, Eugene OR, USA) at 4^{0}C for 5 hours. The tissues were then washed with PBS, mounted in Prolong Gold anti-fade reagent (Molecular Probes, Invitrogen) and cover-slipped.

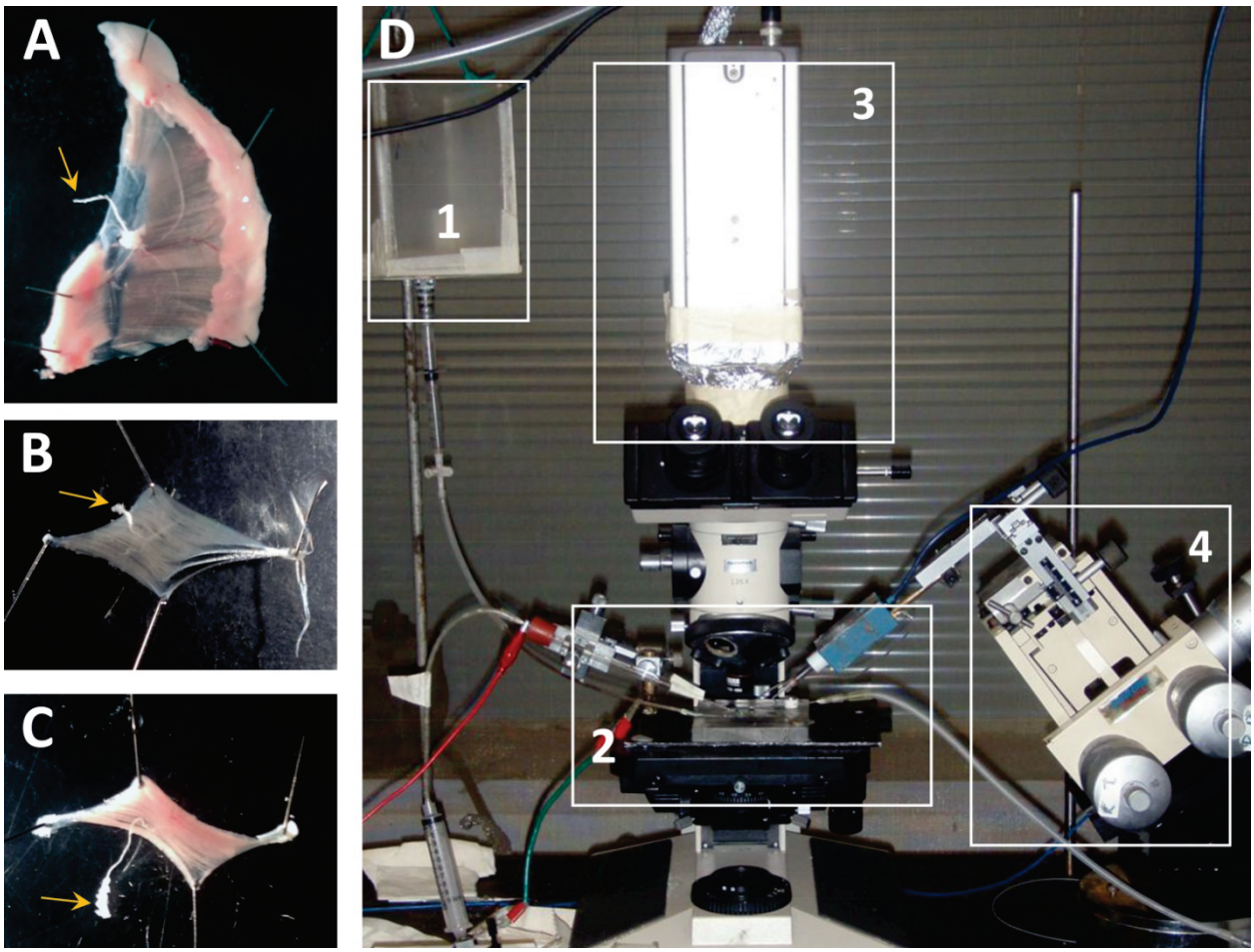

Figure 2.1 Muscle Preparation and Electrophysiological Setup

A, hemi-diaphragm, ***B***, *extensor digitorum longus* (EDL), and ***C***, soleus preparations with intact innervating nerves (yellow arrows) were dissected free and pinned to the Sylgard-coated recording chamber (***D***2). Tissue was stretched and pinned to allow visualisation of the nerve branching by light intensifying camera (***D***3). Connective tissue was excised from the preparations to permit clean electrode piercing during electrophysiology. The electrode manipulator (***D***4) allowed for positioning of the recording electrode to obtain suitable end-plate recordings. Innervating nerves were sucked into glass stimulating electrodes and stimulus patterns applied according to experimental protocol described. Tyrode's solution flows from the reservoir (***D***1) to the organ bath set-up (2). This allowed tissue to be continuously bathed.

2.3 Investigation of Perisynaptic Schwann Cell activity at Neuromuscular Junctions from mice lacking Laminin-β2

2.3.1 Tissue Preparation

The soleus muscle with innervating nerve were dissected free under oxygenated (95% O_2, 5% CO_2) Rees' Ringer's solution (in mM): 110 NaCl, 5 KCl, 1 $MgCl_2$, 25 $NaHCO_3$, 2 $CaCl_2$, 11 glucose, 0.3 glutamate, 0.4 glutamine, 5 BES, 0.036 choline chloride, and 4.34 x 10^{-7} thiamine pyrophosphate. The extracted soleus were pinned to the bottom of a Sylgard-coated recording chamber and innervating nerve stimulated by a suction-stimulating electrode (square wave pulses; 0.2mV-5.0V, 0.1 ms duration) using a Grass Instruments stimulator (SD48) coupled to a Grass stimulus isolator (SIU5).

2.3.2 Electrophysiological Recordings of Synaptic Transmission

Intracellular recordings of end-plate potentials (EPPs) were performed at room temperature using sharp glass microelectrodes (40 to 60 MΩ) filled with 2 M KCl. Proximity to end-plate regions was confirmed through analysis of EPP and MEPP rise times, sites with rise times greater than 1.5 ms were rejected for wild-type mice and times greater than 2 ms rejected for mutant mice. During recordings the initial resting membrane potential (RMP) values were in the range of 70- 85 mV with these values undergoing a gradual decrease to steady values between 45- 60 mV. Recordings were terminated if the RMP fluctuated by more than 10 % from the steady values. Recorded signals were amplified using an Axoclamp 2B amplifier (Axon Instruments) and digitised to 20 kHz sampling rate using MacLab system and Scope software (Version 3.5.5, ADInstruments). The neurotransmission properties of each NMJ were determined by measuring their respective basal quantal content, and post tetanic facilitation after high frequency stimuli (50 Hz for 20 s). These were determined using a modified Ringer's solution with low Ca^{2+} (1 mM)/high Mg^{2+} (6–7 mM) solution. The innervating nerve was stimulated at a frequency of 0.2 Hz with an intensity that was twice the threshold for eliciting EPPs. Quantal content ($\bar{m}$) was determined using method of failures (Del Castillo & Katz, 1954): $\bar{m}$ = $\log_e$ (number of stimuli/number of failures).

2.3.3 Ca^{2+} Imaging of Perisynaptic Schwann Cells

For calcium imaging of the perisynaptic Schwann Cells (PSCs), the extracted soleus muscle and intact innervating nerve were pinned to a Sylgard-coated chamber. The tissue was immersed in Ringer's solution and oxygenated with 95% O_2 and 5% CO_2, as described previously. Muscle preparations were incubated in oxygenated Ringer's solution containing 2mM fluo-4 AM (Invitrogen Inc., NY, USA), 0.02% pluronic acid (Sigma Aldrich), and 1% DMSO (Sigma Aldrich). Following the loading period of forty minutes, tissue was perfused with standard Ringer's solution for twenty minutes. The innervating nerve was gently sucked into a stimulating electrode. Stimulus will be set at twice the threshold level to initiate a visible muscle contraction (Grass Instruments stimulator, SD48) with a frequency of 50Hz for continuous trains of 20 seconds. For imaging purposes muscular contractions will be prevented by partial blocking of nicotinic receptors using 60 μM α-bungarotoxin (Sigma Aldrich).

Tissue was imaged using a Zeiss LSM 510 upright confocal microscope. Excitation of fluo-4 AM was through the use of the 488nm line of an argon laser. Light microscopy with a 40x water immersion objective (Zeiss, BW, Germany) was used for localisation of NMJs. Changes in fluorescence of PSCs were measured and expressed as:

$$\% \, \Delta F / F = (F - F_{rest}) / F_{rest} \times 100$$

In order to standardise across experiments basal fluorescence values were maintained between ranges of 20- 30 pixel intensity values. Experimentation hardware settings were also standardised with offset values between 4.9 and 5.1, and the gain set between 8 and 9. The PSCs were considered responsive when the response amplitude was greater than 5 pixel intensity above resting levels.

CHAPTER 3

Loss of β2-Laminin Alters Calcium Sensitivity and Voltage Gated Calcium Channel Maturation of Neurotransmission at the Neuromuscular Junction

Chand, K.K., Lee, KM., Schenning, M.P., Lavidis, N.A., and Noakes, P.G. (2014) Loss of β2-laminin Alters Calcium Sensitivity and Voltage Gated Calcium Channel Maturation of Neurotransmission at the Neuromuscular Junction. *J Physiol.* DOI: 10.1113/jphysiol.2014.284133 Incorporated as Chapter 3.

Title: **Loss of β2-Laminin Alters Calcium Sensitivity and Voltage Gated Calcium Channel Maturation of Neurotransmission at the Neuromuscular Junction**

Author Names: Kirat K. Chand[1], Kah Meng Lee[1], Mitja P. Schenning[1], Nickolas A. Lavidis[1#], Peter G. Noakes[1,2#]

Affiliations: [1]School of Biomedical Sciences, The University of Queensland, St. Lucia, 4067, Australia. [2] Queensland Brain Institute, The University of Queensland, St. Lucia, 4067, Australia
# Equal contribution by NAL and PGN.

Running Title: β2-laminin regulates calcium channel sensitivity of neuromuscular synapses

Keywords: neuromuscular junction, calcium channels, synaptic transmission.
Number of Words: Key Points summary, 119; Manuscript including Abstract 9,017.

Correspondence should be addressed to: Peter G. Noakes, School of Biomedical Sciences, The University of Queensland, St. Lucia, 4067, Australia. Email: p.noakes@uq.edu.au

ABSTRACT

Laminin-β2 is a key mediator in the differentiation and formation of the skeletal neuromuscular junction. Loss of laminin-β2 results in significant structural and functional aberrations such as decreased number of active zones and reduced spontaneous release of transmitter. *In-vitro* laminin-β2 has been shown to bind directly to the pore forming subunit of P/Q-type voltage gated calcium channels (VGCCs). Neurotransmission is initially mediated by N-type VGCCs, but by postnatal day 18 switches to P/Q-type VGCC dominance. The present study investigated the changes in neurotransmission in mice during the switch from N- to P/Q-type VGCC mediated transmitter release at laminin-β2 deficient junctions. Analysis of the relationship between quantal content and extracellular calcium concentrations demonstrated a decrease in the calcium sensitivity, but no change in calcium dependence at laminin-β2 deficient junctions. Electrophysiological studies on VGCC sub-types involved in transmitter release indicate N-type VGCCs remain the primary mediator of transmitter release at matured laminin-β2 deficient junctions. Immunohistochemical analyses displayed irregularly shaped and immature laminin-β2 deficient neuromuscular junctions when compared to matured wild-type junctions. Laminin-β2 deficient junctions also maintained presence of N-type VGCC clustering within the presynaptic membrane, which supported the functional findings of the present study. We conclude that laminin-β2 is a key regulator in development of the NMJ, with its loss resulting in reduced transmitter release due to decreased calcium sensitivity stemming from a failure to switch from N- to P/Q-type VGCC mediated synaptic transmission.

3.1 INTRODUCTION

The precise alignment of pre- and postsynaptic elements of the neuromuscular junction (NMJ) facilitates efficient and rapid neurotransmission between motor nerve terminals and muscle fibres. Formation of this specialised synapse relies upon an intricate bi-directional exchange of signalling between motor nerve terminals and target muscle fibres during development (Sanes & Lichtman, 1999; Li *et al.*, 2008; Ghazanfari *et al.*, 2011). Numerous molecules are involved in these signalling processes during specific stages of development. Signalling and adhesion proteins located within the basal lamina, in particular the laminin protein family, are capable of influencing development and organisation of the NMJ. Laminin-β2 chain is present in each of the three synapse specific isoforms; laminin-221 (α2β2γ1), laminin-421 (α4β2γ1), and laminin-521 (α5β2γ1) (Patton *et al.*, 1997; Aumailley *et al.*, 2005).

Laminin-β2 is capable of inducing differentiation by regulating the maintenance of active zone components, the assembly of synaptic vesicles in close proximity to active zones, and prevents Schwann cell processes from invading the synaptic cleft (Noakes *et al.*, 1995a; Cho *et al.*, 1998; Patton *et al.*, 1998; Knight *et al.*, 2003; Nishimune *et al.*, 2004; Nishimune, 2012). The interaction between laminin-421 and presynaptic voltage gated calcium channels (VGCCs) enables precise alignment of the synaptic components (Sunderland *et al.*, 2000; Patton *et al.*, 2001; Carlson *et al.*, 2010). Sanes and colleagues have revealed a direct interaction between laminin-β2 and P/Q-type VGCCs (Sunderland *et al.*, 2000; Nishimune *et al.*, 2004). It was also shown that laminin-β2 displayed preference to VGCC subunits involved with neurotransmitter release. Beads coated in laminin-β2 were capable of binding to cells expressing $Ca_v2.1$ (P/Q-type VGCCs) and $Ca_v2.2$ (N-type VGCCs) but displayed poor binding to $Ca_v2.3$ (R-type VGCCs), while beads coated in laminin-β1 did not show binding capabilities to any of the Ca_v subunits investigated (Nishimune *et al.*, 2004). These findings strongly indicate a direct interaction between laminin-β2 and VGCCs that appears to be necessary for the development of a structurally and functionally mature NMJ.

Depolarisation of the nerve terminal results in calcium influx into the terminal via VGCCs, which then triggers neurotransmitter release (Augustine & Charlton, 1986; Hughes *et al.*, 2006). The primary VGCCs involved with neurotransmission at the skeletal NMJ are N-type and P/Q-type. Both N- and P/Q- type VGCCs are present and involved with the mediation of transmission during the early stages of development, at approximately

postnatal day eight (P8) in mouse models (Rosato-Siri & Uchitel, 1999; Santafe *et al.*, 2001; Rosato-Siri *et al.*, 2002; Nudler *et al.*, 2003). As the synapse matures, at approximately postnatal day fourteen (P14) (Uchitel *et al.*, 1992), P/Q-type VGCCs become the dominant mediators of neurotransmitter release (Bowersox *et al.*, 1995; Katz *et al.*, 1996; Rosato-Siri *et al.*, 2002; Urbano *et al.*, 2002), while N-type are suggested to take on a supporting role in regulating feedback and fine-tuned calcium influx. Thus alterations in VGCC sub-type or number may result in significant aberrations in the release of transmitter at the NMJ.

Loss of laminin-β2 results in severely perturbed neurotransmission with a 15- fold decrease in frequency of spontaneous transmitter release but not in amplitude (Noakes *et al.*, 1995a), and a 50% reduction in evoked neurotransmitter release (Knight *et al.*, 2003) when compared to wild-type NMJs. The causative factors presently attributed to the large reduction in quantal release observed in laminin-β2 deficient NMJs are; reduced number of active zones and synaptic vesicles, smaller terminal profiles, reduced nerve-muscle opposition, and invasion of Schwann cell processes into the synaptic cleft (Noakes *et al.*, 1995a; Patton *et al.*, 1998; Knight *et al.*, 2003). Here we propose that altered influx of calcium ions may contribute to the observed decrease in neurotransmission. To test this idea, we examined calcium co-operativity of NMJ synaptic transmission in mice lacking laminin-β2, compared to age-matched control mice. We also functionally determined the contribution, and distributions of VGCCs involved in the release of neurotransmitter at developing and mature NMJs of laminin-β2 deficient and control mice.

3.2 METHODS

3.2.1 Ethics Approval

The University of Queensland Animal Care and Ethics Committee approved all procedures undertaken (Ethics number 152/12) and were in accordance with the Queensland Government Animal Research Act 2000, associated Animal Care and Protection Regulations (2002 and 2008), as well as the Australian Code for the Care and Use of Animals for Scientific Purposes, 8th Edition (National Health and Medical Research Council, 2013).

3.2.2 Animals

Wild-type mice (with two normal copies of all laminin genes) and homozygous mutant mice (with no normal copies of the *LAMB*2 gene) were used in this investigation. Mice were

obtained from the mating of heterozygous males and females and maintained on a defined C57BL/6-129SvJ genetic background. Animals were genotyped using a tail tip DNA tail assay (Hanley & Merlie, 1991). Mice used in this study were age-matched littermates for postnatal days 8, 16-18 of either sex. Mice were anaesthetised with rising concentrations of carbon dioxide and then killed by cervical dislocation. A minimum of five litter-matched pairs was used at each age group for electrophysiology and histological procedures detailed below. All reagents unless specified were supplied by Sigma Chemicals Australia.

3.2.3 Electrophysiology

Tissue Preparation

Mouse diaphragm muscles with intact phrenic nerves were dissected free and pinned to the bottom of a Sylgard-coated recording chamber. The preparation was perfused at a rate of 3 mL min^{-1} with Tyrode's solution (composition (mM): NaCl 123.4; KCl 4.7; NaH_2PO_4 1.3; $NaHCO_3$ 16.3; $MgCl_2$ 1.0; glucose 7.8; $CaCl_2$ 0.1 - 0.3; pH 7.3). The reservoir supplying the bath was continuously gassed with 95% O_2 and 5% CO_2 and maintained at room temperature 22 ± 2^0C.

Electrical Stimulation

The phrenic nerve supplying one hemi-diaphragm was sucked into a glass pipette filled with Tyrode's solution. This pipette acted as a stimulating electrode utilising two silver chloride wires, one passing within the pipette as a positive electrode and the other outside as the negative electrode. The phrenic nerve was stimulated with square wave pulses of 10-20 V intensity, 0.08 ms duration at a frequency of 0.2 Hz, using a Grass Instruments stimulator (SD48) coupled to a Grass stimulus isolator (SIU5).

Extracellular Recordings

Extracellular recordings of nerve terminal impulses (NTI), end-plate currents (EPCs) and miniature end-plate currents (MEPCs) were obtained, as previously described (Knight *et al.*, 2003). In brief, coarse glass micropipettes (~2-10 µm in diameter) filled with Tyrode's solution were positioned on the surface of muscle fibres until sharp rise times of less than 1 ms were detected for both EPCs and MEPCs. The frequency of EPCs and MEPCs were carefully monitored while the electrode was lowered as electrode pressure may give rise to increased frequency of spontaneous activity (Fatt & Katz, 1952; Bennett *et al.*, 1986a; Bennett *et al.*, 1986b). After a recording site was

located, the stimulus was ceased for a five-minute period before commencing recordings of EPCs and MEPCs. This allowed for replenishment of vesicular pools at the nerve terminals. Five to six recording sites were selected from each muscle preparation with 100-200 stimulations and at least 30 MEPCs recorded at each site. Extracellular recordings were used to determine quantal content, calcium dependence and paired pulse facilitation.

Calcium Dependence

Quantal content ($\bar{m}$) was investigated at 0.1, 0.2 and 0.3 mM $[Ca^{2+}]_o$. Tissue was perfused for forty-five minutes between each change in $[Ca^{2+}]_o$ and recording of electrophysiological data. Eleven wild-type and seventeen laminin-β2 deficient mice were examined aged between P16-P18. Calcium dependence was calculated by plotting quantal content against $[Ca^{2+}]_o$ on double logarithmic coordinates. The resulting slope of the curve represents the power relationship (r), which was calculated using linear regression and represents the co-operativity of transmitter release. We further tested the calcium dependence of P18 wild-type NMJs (n = 5) by selectively blocking P/Q-type VGCCs. Dissected wild-type muscles were incubated for forty-minutes with ω-Agatoxin IVA (ω-Aga IVA) (50 nM) at each of the three $[Ca^{2+}]_o$ before electrophysiological studies were performed.

Paired Pulse Facilitation

The facilitation of wild-type and mutant NMJs was investigated by applying twin pulses at 10, 20, 40 ms delays with Tyrode's solution containing 0.3 mM $[Ca^{2+}]$ and 1 mM $[Mg^{2+}]$ and 10 ms delay in 0.6 mM $[Ca^{2+}]$ and 3 mM $[Mg^{2+}]$ Tyrode's . The amount of facilitation was evaluated using the facilitation index (*fi*): $fi = A_2/A_1$ where A_2 is the average of the EPP amplitudes elicited by the second stimulus and A_1 is the average of the EPP amplitudes elicited by the first stimulus (Rosato-Siri *et al.*, 2002). A total of six wild-type and ten laminin-β2 deficient mice aged between P16-P18 were studied for low $[Ca^{2+}]$/high $[Mg^{2+}]$ conditions, and five wild-type and six mutants at the high $[Ca^{2+}]$/high $[Mg^{2+}]$ condition.

Intracellular Recordings

Recordings were performed as per our previous study (Knight *et al.*, 2003). In brief, fine tipped glass microelectrodes (30 to 50 MΩ) filled with 2 M KCl recorded end-plate potentials (EPPs), miniature end-plate potentials (MEPPs) and resting membrane potentials (RMPs). Recorded signals were amplified using an Axoclamp 2B amplifier (Axon Instruments, USA) and digitised to 20-40 kHz sampling rate using MacLab system and Scope software (Version 3.5.5, AD Instruments, CO, USA). Electrodes were manipulated to impale muscle fibres within 0.5 mm of the end-plate region. Proximity to end-plate regions was confirmed through analysis of EPP and MEPP rise times, sites with rise times greater than 1.5 ms were rejected for wild-type mice and times greater than 2 ms rejected for mutant mice. During recordings the initial resting membrane potential (RMP) values were in the range of 70- 85 mV with these values undergoing a gradual decrease to steady values between 55- 60 mV. Recordings were terminated if the RMP fluctuated by more than 10% from the steady values. After a site was located stimulus was ceased for a rest period of ten minutes. Six mice of each genotype were used at P8 with the same number utilised at P18 for intracellular recordings of the toxin studies.

Toxin Preparation and Application

The synthetic polypeptides ω-conotoxin GVIA (ω-CgTx GVIA) and ω-Aga IVA were purchased from Alomone Laboratories (Jerusalem, Israel). Toxins were prepared as stock solutions dissolved in distilled water with ω-CgTx GVIA as 0.5 mM stocks and ω-Aga IVA as 100 μM stocks, and stored at -20^0 C (Regehr & Mintz, 1994). Once a stable site was found and control recordings taken, the stimulus was halted to allow synaptic vesicle replenishment. During this period, the perfusion of the bath with Tyrode's solution was also halted however the muscle preparation was continually oxygenated. A single VGCC specific toxin was applied directly to the tissue with the preparation left to incubate during a forty-minute period. After the incubation period, the stimulus commenced and intracellular recordings were taken for twenty minutes at the same site as the control recordings were initially taken.

Upon completion of the first toxin phase the stimulus was again stopped for forty minutes. The second VGCC specific toxin was added during this time and left to incubate. After incubation the stimulus once again commenced and recordings of the second toxin phase were taken for twenty minutes. Order of toxin administration was randomised to observe the characteristics of each VGCC specific toxin on the junction of wild-type and mutant

mice. The concentrations of toxins used in the protocol were 50 nM ω-Aga IVA and 100 nM ω-CgTx GVIA. The concentrations used for each toxin are similar to prior studies investigating VGCC mediation of NMJ transmission (Rosato-Siri *et al.*, 2002).

Slow Cell-Permeant Calcium Chelator Loading

The extracted diaphragm muscles from P18 wild-type and laminin-β2 deficient mice were incubated for two hours in Ca^{2+}-free Tyrode's solution in the presence of a cell-permeable (-AM) form of the calcium buffer EGTA. After the incubation period, the tissue was washed for fifteen minutes with the Ca^{2+}-free Tyrode's solution followed by a fifteen minute wash with normal Tyrode's, as described above (Urbano & Uchitel, 1999). Electrophysiological recordings were undertaken to observe changes in quantal release at both wild-type and mutant NMJs in the presence of the slow calcium chelator. EGTA-AM was prepared as a 10 mM stock solution dissolved in DMSO, and stored at -20^0 C (Rosato-Siri *et al.,* 2002).

3.2.4 Immunohistochemistry

Extensor digitorum longus (EDL) muscle was dissected free from wild-type and mutant mice at both P8 and P18. Tissue was fixed with 4% paraformaldehyde in 0.1 M phosphate buffered saline pH 7.4 (PBS) at room temperature for 30 minutes, and then washed 3 x 10 minutes with 0.1% glycine in PBS. Muscles were then immersed in 15% sucrose in PBS overnight followed by 30% sucrose in PBS overnight. The muscles were embedded in Tissue-Tek® optimal cutting temperature compound (Sakura Finetek, Torrance, CA, USA) and snap frozen in liquid nitrogen. The frozen muscles were sectioned longitudinally at 30 μm using a Cryostat.

Immunofluorescence double labelling was performed to localise the presynaptic components: i) active zone associated molecules - syntaxin 1A, Bassoon and SNAP25; ii) calcium sensor - synaptotagmin; and iii) calcium channels - N- and P/Q-type VGCCs. These presynaptic components were immunolocalised with antibodies with respect to postsynaptic acetylcholine receptors (AChRs) labelled with Alexa Fluor-555-conjugated α-bungarotoxin (αBTX), at the NMJ. Cryosections were blocked in PBS containing 2% bovine serum albumin (BSA), 2% goat serum with 0.1-0.2% Triton X-100 (TX-100) for 30 minutes at room temperature. This was followed by incubation with the following primary antibodies overnight at 4^{0}C; N-type VGCC with rabbit anti-$Ca_v2.2$ (Alomone Laboratories; Pagani *et al.*, 2004) diluted at 1:1000; active zone associated molecules with mouse anti-Syntaxin 1A (Sigma; clone HPC-1; Pardo *et al.*, 2006) diluted at 1:500; mouse anti-

Bassoon (Enzo Life Sciences; SAP7F407 clone; Nishimune *et al.*, 2004; Chen *et al.*, 2011) diluted at 1:100 and mouse anti-SNAP25 (Sigma; Sadakata *et al.*, 2006; Hata *et al.*, 2007) diluted at 1:5000, and calcium sensor with rabbit anti-Synaptotagmin 2 cytoplasmic domain (Synaptic Systems; Johnson *et al.*, 2010) diluted at 1:100. For the detection of P/Q-type VGCCs at the NMJ, cryosections were blocked with 1% BSA, 5% goat serum and 0.1% TX-100 followed by primary antibody overnight incubation at 4^0C with rabbit anti-$Ca_v2.1$ (Alomone Laboratories; Pagani *et al.*, 2004) diluted at 1:500.

All primary antibodies were diluted in PBS containing 2% BSA and 0.1% TX-100 or 2% BSA and 0.2% TX-100, except for rabbit anti-$Ca_v2.1$ which was diluted in 1% BSA and 0.1% TX-100. EDL cryosections were then washed 3 x 10 minutes with PBS prior to incubation with appropriate Alexa Fluor 488-conjugated secondary antibodies (Molecular Probes, Invitrogen, Eugene OR, USA) in combination with Alexa Fluor 555-conjugated αBTX (Molecular Probes, Invitrogen) at room temperature for 2 hours. Sections were then washed with PBS and mounted in Prolong Gold anti-fade reagent (Molecular Probes, Invitrogen) and cover-slipped.

3.2.5 Image Acquisition and Analysis

Sections were imaged on an Axio Imager microscope equipped with an AxioCamMRm CCD-camera (pixel size 6.45 µm x 6.45 µm, 1388 x 1040 pixels), running AxioVision 4.8 software (Carl Zeiss, Jena, Germany). A 63x/ 1.4 Oil Plan-Apochromat objective was used in combination with ApoTome to provide optical sectioning and improved resolving of fine structures (Bauch & Schaffer, 2006). The images acquired using this configuration had a lateral pixel resolution of 0.1 µm and a Z-step size of 0.3 µm. The point-spread function of this configuration is approximately 0.31 µm in X-Y plane and 0.8 µm in Z plane. This configuration was suitable for distinguishing the large sized VGCC puncta (0.7 to 1.0 µm) and small VGCC sized puncta (0.4 to 0.69 µm). Images were captured using identical exposure times and settings amongst different slides using the same antibody. Imaris x64 7.1.1. (Bitplane, South Windsor, CT, USA) was used to analyse captured Z-stacked images for quantification of VGCC puncta and volume of end-plate. Postsynaptic AChR end-plates stained with Alexa Fluor 555-conjugated αBTX were reconstructed in 3-dimension (3D) using a surface-rendering algorithm based on local contrast in fluorescent z-stacks as previously described (Fogarty *et al.*, 2013). We defined the entire 3D reconstructed AChR end-plate region including its interstitial space as the end-plate volume. Previous literature quantifed

active zone protein expression in relation to the two dimensional measure of postsynaptic AChR area (Chen *et al.*, 2011). However, we utilised end-plate volume as this allowed for a more accurate measure of VGCC puncta in relation to the three dimensional expansion of the postsynaptic end-plate region (Johnson & Connor, 2011). The number of VGCC puncta corresponding to the respective 3D surface-rendered end-plates was measured and categorised based on their diameter; total puncta (≥0.4 μm), large puncta (0.7-1.0 μm) and small puncta (subtraction of large puncta from total puncta). The density of VGCCs at each junction was then determined by dividing the total number of puncta (based on each category stated) over the end-plate volumes. The area of each individual postsynaptic AChR end-plate was also measured using Image J software (Abramoff *et al.*, 2004). This was done in order to compare the area occupied by AChRs in the muscle membrane over time (P8 and P18). All image analysis was completed under double blinded conditions. Two-way ANOVA with Tukey's post-hoc test was used to compare the mean density of VGCCs and area of AChRs between wild-type and mutant junctions. Results are expressed as mean ± SEM with statistical significance accepted at $P < 0.05$.

3.2.6 Data Analysis

Extracellular recording sites were analysed if the frequency of EPCs and MEPCs did not change as a result of electrode pressure and if a single EPC was recorded within the first ten stimuli. Intracellular recordings were included if control and both toxin phases were recorded without interruption. Quantal content ($\bar{m}$) was determined using method of failures (Del Castillo & Katz, 1954b): $\bar{m} = \log_e$ (number of stimuli/number of failures) utilising extracellular electrophysiological recordings. Unpaired two-tailed *t*-tests were performed to compare wild-type and mutant mice for calcium dependence and sensitivity studies. Two-way ANOVA with Tukey's multiple comparisons analysis were utilised to determine statistical significance between wild-type and mutant mice after application of each VGCC toxin and for comparison across both age groups. Results are expressed as mean ± SEM with statistical significance accepted at $P < 0.05$.

3.3 RESULTS

3.3.1 NMJs from Laminin-β2 Deficient Mice show no change in Calcium Dependence of Transmitter Release, but do exhibit lower levels of Calcium Sensitivity

Our electrophysiological recordings of NMJs in laminin-β2 deficient mice showed significant reductions in mean quantal content ($\bar{m}$), and increased number of stimuli that result in failed responses (Table 3.1), supporting our previous results (Knight *et al.*, 2003). Increasing $[Ca^{2+}]_o$ resulted in increased EPC amplitudes at both wild-type and laminin-β2 deficient NMJs at P18, though junctions lacking laminin-β2 were consistently lower when compared to control junctions for the same calcium concentration (Figure 3.1*A*). For example, EPC amplitudes in the presence of 0.3 mM calcium at laminin-β2 deficient NMJs were approximately the same as EPC amplitudes in the presence of 0.1 mM calcium at wild-type NMJs.

We next examined the relationship between transmitter release and $[Ca^{2+}]_o$ in order to better understand the reduced responsiveness to extracellular calcium seen at laminin-β2 deficient NMJs. It has long been established that the relationship between transmitter release and $[Ca^{2+}]_o$ is non-linear, with increasing $[Ca^{2+}]_o$ associated with greater quantal content exhibiting a sigmoidal curve (Jenkinson, 1957; Dodge & Rahamimoff, 1967). When the relationship was plotted on double logarithmic coordinates it forms a straight line (as seen in Figure 3.1*B*), with the line slope representing the power dependence of $[Ca^{2+}]_o$ to transmitter release. Previous research has shown at mammalian nerve terminals, this slope observes a fourth power relationship with transmitter release and calcium concentrations behaving in a co-operative nature (Dodge & Rahamimoff, 1967; Hubbard *et al.*, 1968). In our study, we compared this power relationship between wild-type and laminin-β2 deficient NMJs and found no significant difference (line slope = 3.18 $\pm$ 0.07 for wild-type (n = 11) and 3.52 $\pm$ 0.16 for laminin-β2 deficient NMJs (n = 17), Table 3.1, Figure 3.1*B*). While there appears to be no alterations in the power relationships between the NMJs from laminin-β2 deficient and wild-type mice at P18, we did observe a clear parallel rightward shift (2.3 fold shift) for laminin-β2 deficient NMJs (Figure 3.1*B*), suggesting a reduction in the calcium sensitivity compared to the NMJs from wild-type mice. To assess whether the rightward shift observed at laminin-β2 deficient NMJs was due to the lack of Ca^{2+} dependence on P/Q-type VGCCs, we blocked these channels with ω-Aga IVA at P18 wild-type NMJs (data not shown). By utilising this P/Q-type VGCC blocker, we were able to assess the role of N-type VGCCs in quantal release at P18 wild-type NMJs. In the presence of ω-Aga IVA, we observed a rightward shift (1.6 fold shift) towards the lower

quantal values observed at mutant NMJs and a non-significant change in the slope of the line (wild-type plus ω-Aga IVA, n = 5 : 2.92 ± 0.25 vs. wild-type: 3.18 ± 0.07). These findings suggest that N-type VGCCs are not as proficient in the release of quantal content as P/Q-type channels, and supports our hypothesis that laminin-β2 deficient NMJs possess poor quantal release as a result of maintained dependence on N-type VGCC mediated transmitter release at P18.

To examine NMJ calcium sensitivity further, we then investigated the dissociation constant of calcium, expressed as $K[Ca^{2+}]_o$ (Del Castillo & Katz, 1954a), and the potential maximal quantal content ($\bar{m}_{max}$) of each NMJ. These values were calculated using a double reciprocal plot of $\bar{m}^{1/r}$ vs. $[Ca^{2+}]_o$ (where $\bar{m}$ and r represent quantal content and the power relationship respectively). The plot converted the sigmoidal relationship to a straight line, where the x- and y-intercepts represents K $[Ca^{2+}]_o$ and $\bar{m}_{max}$ values respectively (Figure 3.1*C*). The y-intercept is where there is an infinite $[Ca^{2+}]_o$, and assumes all release sites are active, therefore corresponds to the $\bar{m}_{max}$ (Robinson, 1976; Bennett *et al.*, 1977; Einstein & Lavidis, 1984). If we assume each release site only releases one quanta per stimulation then the $\bar{m}_{max}$ represents the number of release sites. Laminin-β2 deficient NMJs observed a 35% reduction in $\bar{m}_{max}$ and the total number of release sites (Table 3.1, Figure 3.1*C*). The K $[Ca^{2+}]_o$ values were similar for wild-type and laminin-β2 deficient NMJs (Table 3.1), reinforcing that the relationship between quantal content and $[Ca^{2+}]_o$ follows the same calcium dependence in wild-type and laminin-β2 deficient NMJs. This finding also suggests that interaction between the calcium sensor, synaptotagmin (Yoshihara & Littleton, 2002), and Ca^{2+} is not altered at the motor nerve terminals of laminin-β2 deficient NMJs.

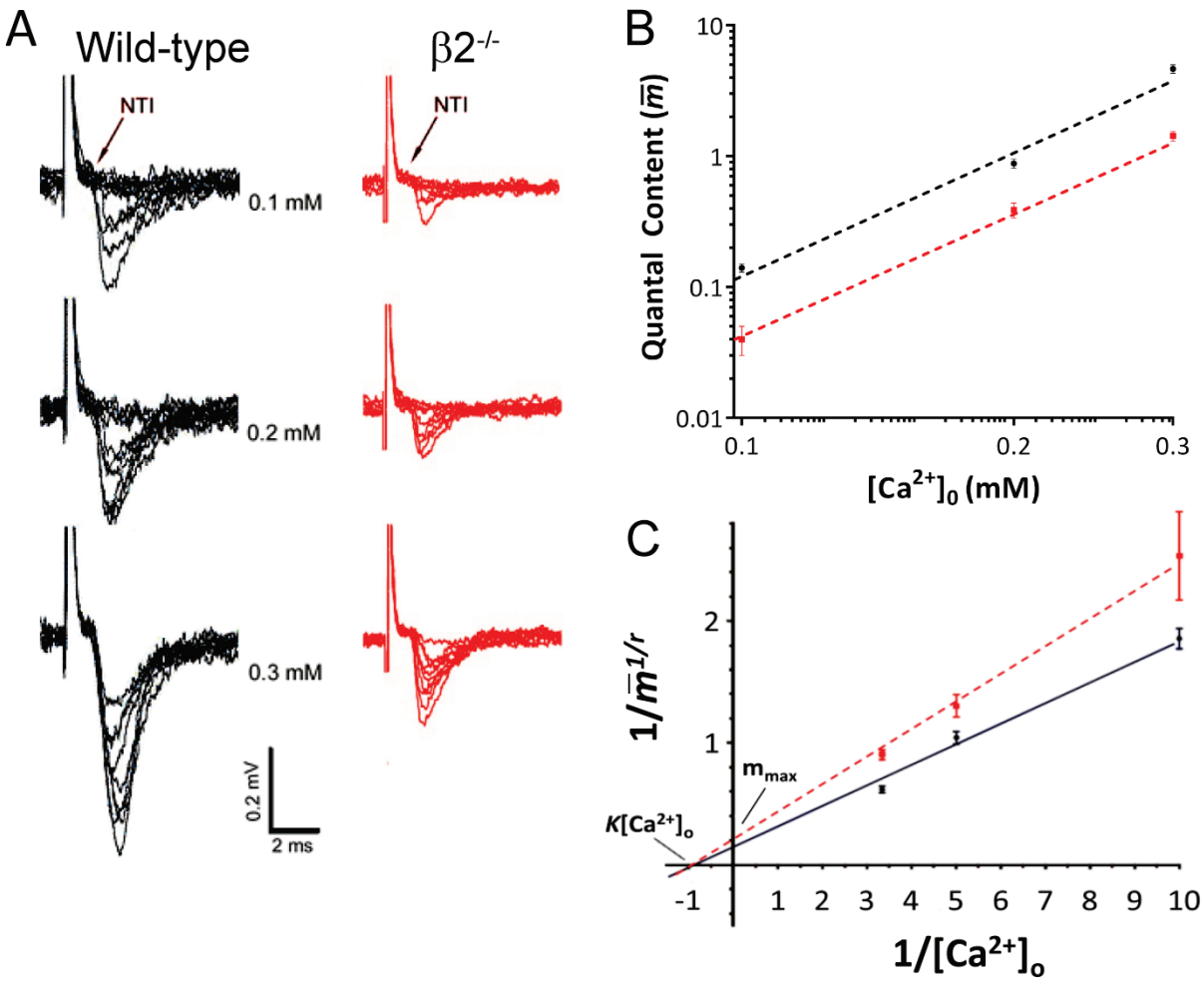

Figure 3.1 The Ca^{2+} Dependence of Transmitter Release was unchanged but exhibited lower Calcium Censitivity at Laminin-β2 deficient Neuromuscular Junctions

A, representative recordings from wild-type (black) and laminin-β2 deficient ($\beta2^{-/-}$) (red) NMJs, showing evoked release increasing with $[Ca^{2+}]_o$ in both genotypes. Laminin-β2 deficient NMJ evoked release was significantly lower in all three recorded $[Ca^{2+}]_o$. ***B***, calcium co-operativity curve plotting mean quantal content ($\bar{m} \pm$ SEM) against $[Ca^{2+}]_o$ of wild-type and $\beta2^{-/-}$ NMJs shown on double logarithmic axes. Double logarithmic plot demonstrated the shift in the position of the unchanged gradient (black to red line plots) as a result of the lower quantal content in mutant NMJs, indicating a change in calcium sensitivity. ***C***, Double reciprocal plot displaying similar K $[Ca^{2+}]_o$ values for wild-type and $\beta2^{-/-}$ NMJs. The potential maximal quantal content values ($\bar{m}_{max}$) correlated to the number of release sites, which are lower in $\beta2^{-/-}$ NMJ ($P < 0.01$). Wild-type, $n = 11$ and $\beta2^{-/-}$, $n = 17$.

Table 3.1 Overall Comparison of Biophysical Properties in Wild-type and Laminin-β2 Deficient Neuromuscular Junctions

	P16-18		
	Wild-type	**Laminin-β2 Deficient**	
Number of animals (*n*)			
Ca^{2+} dependence	11	17	
Low Ca^{2+} facilitation	6	10	
High Ca^{2+} facilitation	5	6	
MEPC amplitude (μV)			
$[Ca^{2+}]_o$ = 0.1 mM	95.2 ± 0.77	97.1 ± 0.59	
$[Ca^{2+}]_o$ = 0.2 mM	99.1 ± 0.61	101 ± 0.89	
$[Ca^{2+}]_o$ = 0.3 mM	105 ± 0.83	97.5 ± 0.52	
Percentage of failures (%)			
$[Ca^{2+}]_o$ = 0.1 mM	73.08 ± 2.93	93.94 ± 1.46	***
$[Ca^{2+}]_o$ = 0.2 mM	10.12 ± 5.56	59.10 ± 7.21	***
$[Ca^{2+}]_o$ = 0.3 mM	0.5 ± 0.08	4.16 ± 3.36	***
Quantal content ($\bar{m}$)			
$[Ca^{2+}]_o$ = 0.1 mM	0.14 ± 0.01	0.04 ± 0.01	
$[Ca^{2+}]_o$ = 0.2 mM	0.88 ± 0.07	0.39 ± 0.05	**
$[Ca^{2+}]_o$ = 0.3 mM	4.66 ± 0.35	1.43 ± 0.12	**
Power relationship (r)	3.18 ±0.07	3.52 ± 0.16	
# Theoretical estimates of:			
$K[Ca^{2+}]_o$ (mM)	0.91	0.91	
$\bar{m}_{max}$	402.20	260.50	**
Paired-pulse facilitation ratio			
Low Ca^{2+}, delay of 10 ms	1.22 ± 0.04	1.17 ± 0.04	
20 ms	1.11 ± 0.03	1.16 ± 0.02	
40 ms	1.01 ± 0.02	1.03 ± 0.03	
High Ca^{2+}, delay of 10 ms	1.23 ± 0.02	1.21 ± 0.04	

* P < 0.05; ** P < 0.01; *** P < 0.001

#Formula used to calculate $\bar{m}_{max}$ and $K[Ca^{2+}]_o$; $\bar{m} = \bar{m}_{max} \bullet \left(\frac{[Ca2+]o}{K[Ca2+]o + [Ca2+]o}\right)$

3.3.2 Facilitation of NMJ Transmitter Release is not affected by the loss of Laminin-β2

Facilitation studies investigate the amount of additional release that occurs as a result of a second stimulus applied to the nerve terminal, causing a further influx of calcium (termed paired pulse facilitation; Rosato-Siri *et al.*, 2002). The closer in time the two stimuli are the more calcium is present to cause facilitation of transmitter release. Given this, we conducted paired pulse facilitation experiments to determine if the drop in calcium sensitivity at laminin-β2 deficient NMJs resulted from disturbances to the VGCC sub-type and their localisation to the presynaptic release machinery, and/or alterations in either calcium sequestration or release probabilities. These experiments were done in mice lacking laminin-β2 and wild-type littermates at P16-P18, and were conducted in Tyrode's solution containing 0.3 mM [Ca^{2+}] and 1 mM [Mg^{2+}] at 10, 20 and 40 ms delays (Figure 3.2*C*); and 0.6 mM [Ca^{2+}] and 3 mM [Mg^{2+}] at 10 ms delay (Figure 3.2*A*, 3.2*B*) in wild-type and laminin-β2 deficient junctions. The latter conditions accentuate facilitation and evoked amplitudes. Our findings showed an average of 70% decrease in evoked pulse amplitudes at laminin-β2 deficient NMJs compared to wild-type NMJs (Figure 3.2*A,* 3.2*B*). No statistical significant differences were observed in the facilitation ratios at all delay times and conditions investigated (Figure 3.2*B*, 3.2*C*; Table 3.1). These findings suggest that although there were severe perturbations in transmission at mutant NMJs under these conditions, the facilitation capabilities of active release sites in laminin-β2 deficient NMJs were comparable to release sites at wild-type NMJs.

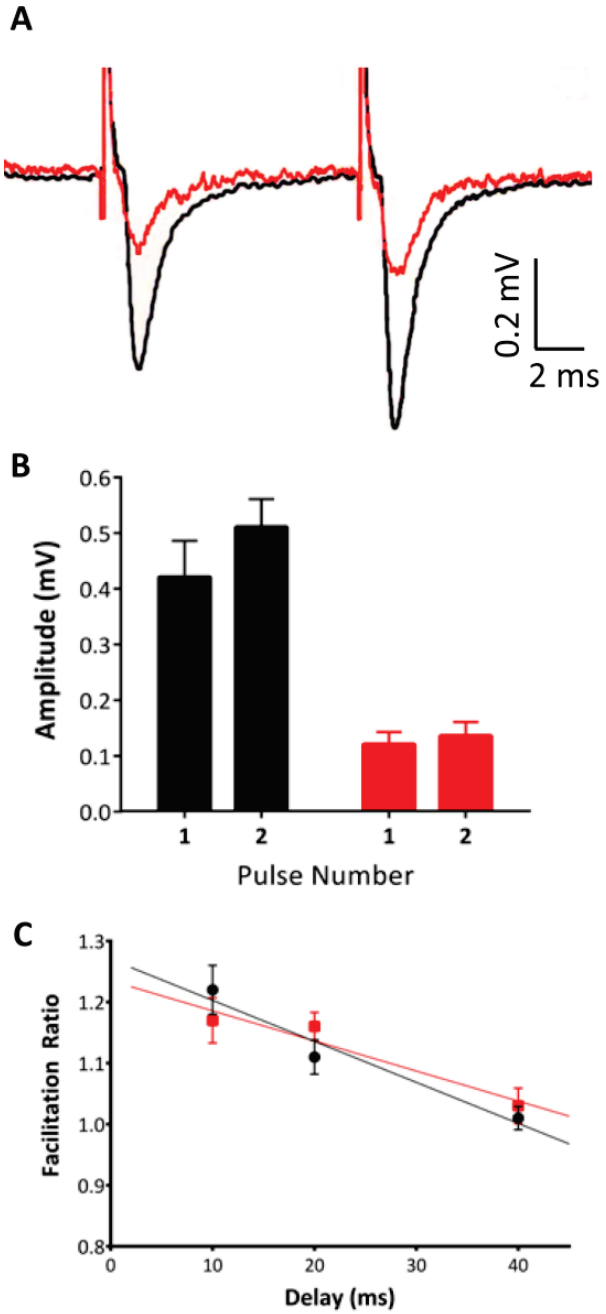

Figure 3.2 The Facilitation of Laminin-β2 Deficient Release Sites was comparable to those in Wild-type Neuromuscular Junctions

A, sample traces of paired pulse facilitation at 10 ms delay for wild-type (black) and laminin-β2 deficient (red) NMJs. ***B***, corresponding plot of paired pulse facilitation data shown for 10 ms delay. ***C***, plot of facilitation ratio against paired pulse delay times for 10, 20, and 40 ms delays. As delay times increase the facilitation ratio decreased, clearly visible in the control animals (C; black line). There were no significant differences with the ratios in both conditions and all delay times. Laminin-β2 deficient NMJs consistently show similar trends but with lower amplitudes in comparison to wild-type mice (A and B). The stimulus artefact was decreased for better visibility in A. For B wild-type n = 5 and $\beta2^{-/-}$ n = 6; for C, n = 6 and n = 10 respectively.

3.3.3 Neuromuscular Junctions from Laminin-β2 Deficient mice fail to switch from N- to P/Q- type VGCC Dominance of Transmitter Release as they Mature

The study of VGCC specific antagonists on neurotransmission is an established tool in evaluating changes in sub-type/s of channels involved in the mediation of transmitter release (Nudler *et al.*, 2003). Utilising this technique, we investigated the role of N- and P/Q-type VGCCs in mediating the release of transmitter at P8 and P18 NMJs lacking laminin-β2 due to their ability to bind laminin-β2 and their role in mature neurotransmission (Nishimune *et al.*, 2004). At P8 both laminin-β2 deficient and wild-type mice demonstrated similar contribution of N- and P/Q- type VGCC in mediation of transmitter release (Figure 3.3*A,* 3.3*B*). For wild-type NMJs, application of the N-type VGCC blocker, ω-CgTx GVIA, produced a 40% drop in EPP amplitudes (59.66 ± 14.94% compared to EPP amplitudes from untreated wild-type NMJs; 100%, represented by dashed line to black filled bar in Figure 3.3*A*; $P < 0.05$, $n = 6$). Subsequent addition of P/Q-type VGCC blocker, ω-Aga IVA, resulted in a further 20 % reduction in amplitude ($P < 0.05$, $n = 6$) to 39.32 ± 10.61% of control EPP amplitudes (Figure 3.3*A*, black filled bar to black checked bar). For laminin-β2 deficient NMJs, application of ω-CgTx GVIA resulted in EPP responses at 53.15 ± 2.41% of control EPP values (Figure 3.3*A*, dashed line to red filled bar; $P < 0.001$, $n = 6$). And for ω-Aga IVA, we saw a further 26% decrease in EPP responses to 27.36 ± 3.66% of control EPP amplitudes (Figure 3.3*A*, red filled bar to red-black checked bar; $P < 0.001$, $n = 6$). No statistical significance was observed between responses of wild-type and laminin-β2 deficient junctions after addition of each toxin at this age group.

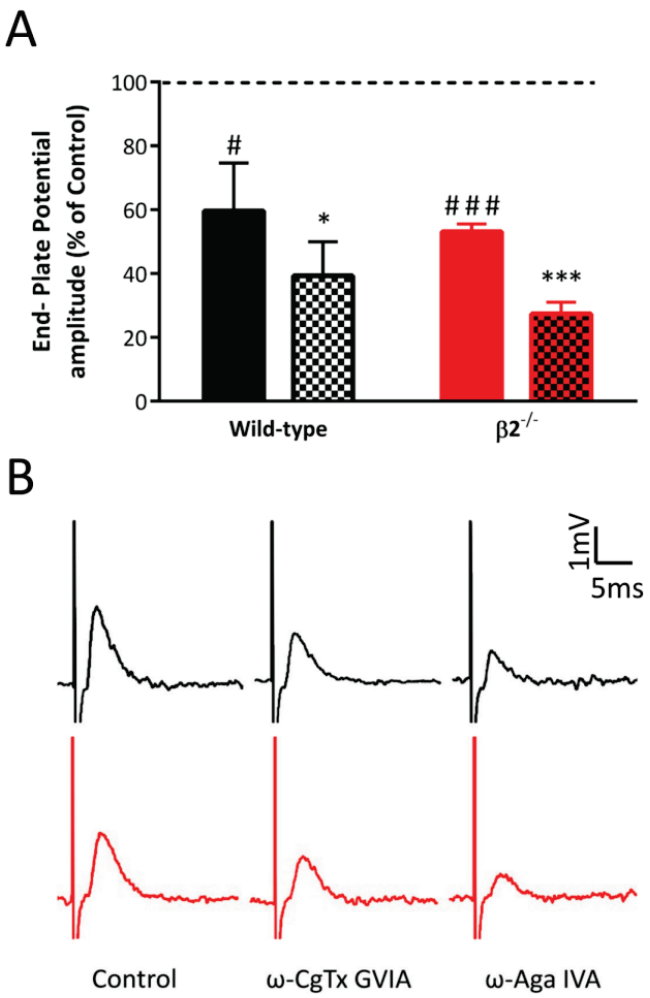

Figure 3.3 During Development there was a similar contribution of N- and P/Q- type VGCCs to Transmitter Release in Wild-type and Laminin-β2 Deficient Neuromuscular Junctions

A, normalised mean evoked end-plate potentials (EPP) responses (± SEM) of wild-type (black) and laminin-β2 deficient ($\beta2^{-/-}$) (red) at P8 NMJs after sequential addition of N- and P/Q-type VGCC specific toxins, ω-CgTx GVIA (filled bars) and ω-Aga IVA (checkered bars) respectively. Black dashed line represents base recordings (100%) prior to toxin administration for associated genotype. In wild-type NMJs (n = 6), application of ω-CgTx GVIA resulted in a 40% decrease in EPP amplitude ($P < 0.05$) from control values with subsequent addition of ω-Aga IVA resulting in a further 20% decrease in EPP amplitude ($P < 0.05$). In P8 $\beta2^{-/-}$NMJs (n = 7), addition of ω-CgTx GVIA produced a 47% decrease in EPP amplitude ($P < 0.001$) from control values. Subsequent addition of ω-Aga IVA resulted in a further 26% reduction in amplitude ($P < 0.001$). ***B***, representative recordings of EPP responses during control, after ω-CgTx GVIA application and subsequent ω-Aga IVA application for wild-type (black) and $\beta2^{-/-}$(red) mice. $^{\#}P < 0.05$, $^{\#\#\#}P < 0.001$ compared to control recordings. $^{*}P < 0.05$, $^{***}P < 0.001$ compared to response in the same NMJ after addition of previous calcium channel blocker.

At matured NMJs (P18), wild-type mice displayed a switch in VGCC sub-type with P/Q-type VGCCs becoming dominant mediator of transmitter release. Addition of ω-CgTx GVIA resulted in a 22% decrease in EPP amplitude to 77.77 ± 11.01% of control EPP amplitudes (Figure 3.4*A*, dashed line to black filled bar; $P > 0.05$, $n = 6$; Figure 3.4*B*). Subsequent application of ω-Aga IVA displayed a further 57% decrease in response to 20.16 ± 6.01% of control EPP amplitudes (Figure 3.4*A*, black filled bar to black checked bar; $P < 0.0001$, $n = 6$; Figure 3.4*B*). These responses to ω-CgTx GVIA and ω-Aga IVA were significantly different from those seen in the developing wild-type junctions (compare Figure 3.3*A* with 3.4*A*; Table 3.2, $P < 0.05$). This finding suggests that wild-type NMJs demonstrate a change from N- to P/Q-type VGCC dominance in transmitter release, a finding established in previous studies (Rosato-Siri *et al.*, 2002; Urbano *et al.*, 2002). By contrast, laminin-β2 deficient NMJs maintained its dependence on N-type VGCCs for mediation of transmitter release at P18. Application of ω-CgTx GVIA resulted in a 60% decrease in EPP amplitude to 43.26 ± 3.02% of control EPP amplitudes (Figure 3.4*A*, dashed line to red filled bar; $P < 0.001$, $n = 6$; Figure 3.4*B*). Addition of ω-Aga IVA resulted in a further 24% decrease to 19.31 ± 4.30% of control EPP responses (Figure 3.4*A*, red filled bar to red-black checked bar; $P < 0.01$, $n = 6$; Figure 3.4*B*). This percentage drop in EPP amplitude was similar to that seen at P8 laminin-β2 and wild-type NMJs, suggesting that laminin-β2 may be required for the switch from N- to P/Q-type VGCC dominance for transmitter release, as seen during NMJ maturation from P8 to P18. To eliminate possible confounding effects of toxin specificity for VGCC sub-type and their target binding efficiencies, we conducted reverse order toxin administration to the NMJs of both age groups for each genotype. We observed the same percentage drops in EPP amplitudes for the given toxins as we have seen with the original administration order, detailed in Table 3.2.

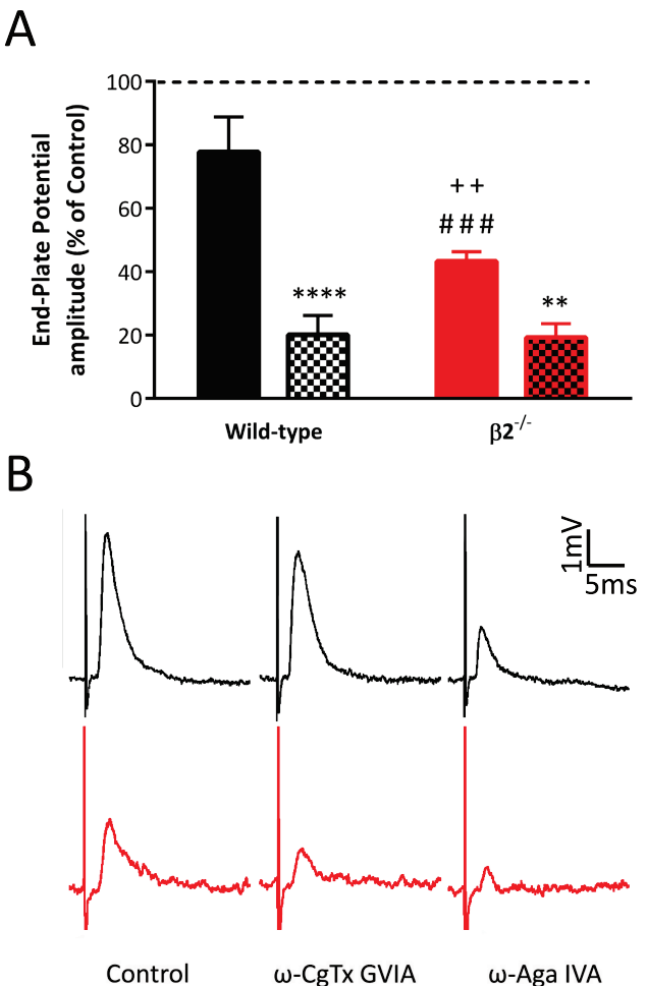

Figure 3.4 N-Type VGCCs remained the Dominant Mediator of Transmitter Release at Postnatal Day 18 Laminin-β2 Deficient Neuromuscular Junctions

A, normalised mean evoked end-plate potentials (EPP) responses (± SEM) of wild-type (black) and laminin-β2 deficient ($\beta2^{-/-}$) (red) at P18 NMJs after sequential addition of N- and P/Q-type VGCC specific toxins, ω-CgTx GVIA (filled bars) and ω-Aga IVA (checkered bars) respectively. Black dashed line represents base recordings (100%) prior to toxin administration for associated genotype. In wild-type NMJs (*n* = 6), application of ω-CgTx GVIA resulted in a 22% decrease in EPP amplitude ($P > 0.05$) from control values with subsequent addition of ω-Aga IVA resulting in a further 57% decrease in evoked response amplitude ($P < 0.0001$). In P18 $\beta2^{-/-}$ NMJs (*n* = 6), addition of ω-CgTx GVIA produced a 57% decrease in EPP amplitude ($P < 0.001$) from control values. Subsequent addition of ω-Aga IVA resulted in a further 24% reduction in amplitude ($P < 0.01$). ***B***, representative recordings of EPP responses during control, after ω-CgTx GVIA application and subsequent ω-Aga IVA application for wild-type (black) and $\beta2^{-/-}$ (red) mice. $^{###}P < 0.001$ compared to control recordings. $^{****}P < 0.0001$ compared to response in the same NMJ after addition of previous calcium channel blocker. $^{++}P < 0.01$ compared to other genotype after application of specific calcium channel blocker.

Table 3.2 Overall Comparison of Responses to VGCC Specific Toxins at Developing and Mature Neuromuscular Junctions in Wild-type and Laminin-β2 Deficient mice

		Genotype			
		Wild-type		Mutant	
	Age(postnatal day)	P8	P18	P8	P18
		EPP amplitudes (% of control)			
Application Order	ω-CgTx GVIA	59.66 ± 14.94	77.77 ± 11.01 *	53.15 ± 2.41	43.26 ± 3.02##
	ω-Aga IVA	39.32 ± 10.61	20.16 ± 6.01 *	27.36 ± 3.66	19.31 ± 4.30
	ω-Aga IVA	67.22 ± 8.70	29.11 ± 5.36 *	72.12 ± 9.36	84.42 ± 5.21###
	ω-CgTx GVIA	26.86 ± 12.61	15.19 ± 2.27	29.52 ± 11.79	18.44 ± 2.74

* $P < 0.05$; significance between age groups within a genotype for corresponding toxin, ## $P < 0.01$, ### $P < 0.001$; significance for corresponding toxin and age between genotypes (two-way ANOVA with Tukey's multiple comparisons test)

We next used EGTA-AM as a Ca^{2+} chelator with slow Ca^{2+} binding kinetics to further investigate the VGCCs involved with transmitter release at P18 (Adler *et al.*, 1991; Augustine *et al.*, 1991). Loading of P18 wild-type NMJs with EGTA-AM resulted in a non-significant decrease (~4%) in normalised quantal content from control values (compare sample traces in Figure 3.5*A*; 96.05 ± 3.42%, $n = 5$). By contrast, incubation of laminin-β2 deficient NMJs with EGTA-AM caused a 65% reduction from control values (compare sample traces in Figure 3.5*B*; 34.39 ± 6.64%, $n = 5$). This reduction in quantal release was significantly greater than that observed at age-matched wild-type NMJs (Figure 3.5*C*; $P < 0.0001$, $n = 5$).

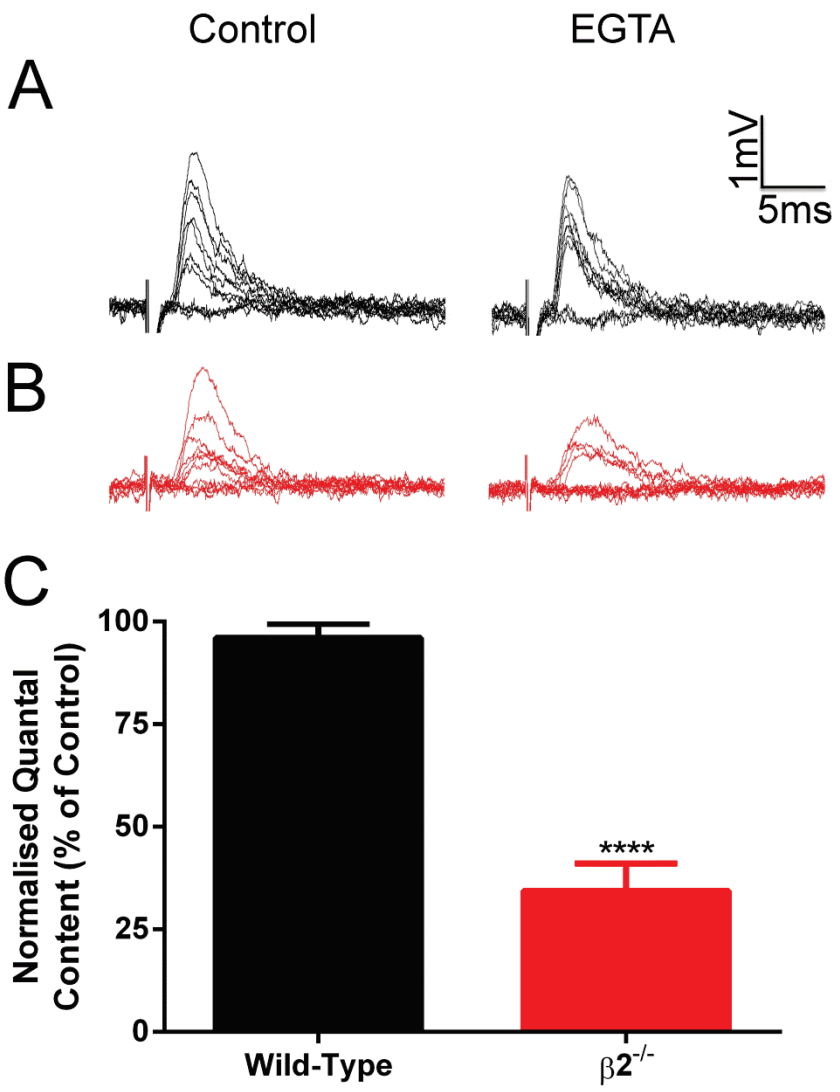

Figure 3.5 The Effect of a slow Cell-Permeant Calcium Chelator (EGTA-AM) on the Quantal Release at Postnatal Day 18 Wild-type and Laminin-β2 Deficient Neuromuscular Junctions

A and ***B***, representative traces of ten consecutive EPPs from wild-type (black traces) and mutants (red traces) under control conditions and in the presence of EGTA-AM (incubation in 10 μM). ***C***, histogram comparing normalised quantal content (mean ± SEM), where 100% represents quantal release in the absence of EGTA-AM (control) and in the presence of EGTA-AM. Wild-type NMJs did not show a significant decrease in quantal content when incubated in the slow cell-permeant calcium chelator. By contrast, mutant NMJs displayed significant decreases in quantal release when incubated with EGTA-AM. **** $P < 0.0001$. For both wild-type and $\beta2^{-/-}$, $n = 5$. Stimulus artefacts have been reduced from sample traces for clarity.

3.3.4 The Motor Nerve Terminals from Laminin-β2 Deficient mice fail to up-regulate the expression of P/Q-type VGCCs clusters and down-regulate N-type VGCCs clusters as they mature

Since NMJs from laminin-β2 deficient mice failed to switch from N- to P/Q-VGCC dominance of transmitter release from P8 to P18, we examined the expression of these channels at NMJs from laminin-β2 deficient and age-matched control littermates. This was investigated using immunohistochemistry. At P8, both wild-type and laminin-β2 deficient NMJs displayed a similar level of discrete punctate staining of N-type VGCCs (Figure 3.6*A*, 3.6*B* top panels). There were no significant differences in the densities of small, large and therefore total puncta of N-type VGCCs, between the two genotypes at this age (Figure 3.6*C*). Nor did we observe any difference in the overall size of their postsynaptic area between the two genotypes at this age (end-plate area for P8; Figure 3.6*E*). For P/Q-type VGCCs at P8, we observed similar staining intensity to that seen for N-type VGCCs, at NMJs from both laminin-β2 deficient and wild-type littermates (compare Figure 3.6*A*, 3.6*B* top panels for N-type with Figure 3.7*A*, 3.7*B* top panels for P/Q-type). Quantification of P/Q-type VGCC puncta showed no differences between genotypes at developing NMJs (P8, Figure 3.7*C*).

We next compared the densities of small and large N- and P/Q-type VGCC stained puncta at this developing age (P8), which is indicative of the degree of VGCC clustering. For N-type, we observed more total puncta when compared to P/Q-type, but for both VGCC sub-types, the contributions by small and large puncta was similar, with the majority of total puncta made up by small stained puncta (0.4- 0.69 μm) (Figure 3.6*C* for N-type, and Figure 3.7*C* for P/Q-type). These findings suggest that aggregations of small and large N- and P/Q-type VGCC puncta do not seem to be affected by an absence of laminin-β2, at this early stage of NMJ maturation. The observation that there were more total N-type VGCC puncta at P8 for both genotypes supports our functional findings that show N-type VGCC as the dominant contributor to transmitter release for both laminin-β2 deficient and wild-type NMJs (Figure 3.3).

At P18 wild-type NMJs showed a significant drop in the number of large N-type VGCC puncta (compare Figure 3.6*C* with 3.6*D*; black bars, $P < 0.001$, $n = 6$), but at both ages these NMJs maintained a high density of small N-type puncta (Figure 3.6*C,* 3.6*D*; black bars). By contrast, P18 laminin-β2 deficient NMJs retained the same level of large N-type VGCC puncta to that seen at P8 (Figure 3.6*C*, 3.6*D*; red bars), however when comparing

the large N-type VGCC puncta at P18, we observed a higher density of large N-type VGCC puncta at laminin-β2 deficient NMJs (0.068 ± 0.004 puncta/ μm^3) when compared to wild-type NMJs (0.051 ± 0.014 puncta/ μm^3) (Figure 3.6*D*; black and red bars, $P < 0.05$, $n = 6$). These observations suggest that N-type VGCC clustering failed to be down-regulated at NMJs lacking laminin-β2 at P18.

Examination of P/Q-type VGCCs at wild-type NMJs showed increased staining intensity from P8 to P18 (Figure 3.7*A* left panels), consistent with increased P/Q-type VGCC expression and its emerging dominance to NMJ synaptic transmission (Figure 3.4). However in terms of P/Q-type VGCC puncta density, our analyses revealed that while there appeared to be an increase in small and large puncta from P8 to P18 this was not statistically significant (compare black bars in Figure 3.7*C* to those in 3.7*D*). By contrast, staining intensity of P/Q-type VGCCs at the NMJs from laminin-β2 deficient mice appeared not to change from P8 to P18 (Figure 3.7*B*, left panels), remaining at a comparative level to that seen at P8 wild-type NMJs (compare Figure 3.7*A* top left, with 3.7*B* left panels). When we quantified P/Q-type VGCC puncta densities, laminin-β2 deficient NMJs displayed a significant decrease in the total density of P/Q-type VGCC puncta from P8 to P18 (Figure 3.7*C*, 3.7*D*; red bars, $P < 0.05$).

Analysis between the two genotypes showed significantly less total puncta density at laminin-β2 deficient NMJs compared to wild-type NMJs at P18 (wild-type; 0.305 ± 0.022 puncta/ μm^3 vs. $\beta 2^{-/-}$; 0.205 ± 0.012 puncta/ μm^3, $P < 0.01$). This decrease was also observed for both small puncta (wild-type; 0.219 ± 0.018 puncta/ μm^3 vs. $\beta 2^{-/-}$; 0.156 ± 0.009 puncta/ μm^3, $P < 0.05$), and for large puncta (wild-type; 0.086 ± 0.005 puncta/ μm^3 vs. $\beta 2^{-/-}$; 0.050 ± 0.004 puncta/ μm^3, $P < 0.001$) (Figure 3.7*D*; black and red bars).

These observations support our functional studies that show N-type VGCC dominance to synaptic transmission persists at P18 laminin-β2 deficient NMJs. By comparison, wild-type NMJs displayed a decrease in the presence and reliance on N-type VGCCs and an increase in P/Q-type VGCCs, consistent with an emergence of P/Q-type VGCC dominance of neurotransmitter release. Loading of P18 wild-type NMJs with EGTA-AM (10 μM) did not cause a significant effect on evoked amplitudes. By contrast, at mutant NMJs, incubation with EGTA-AM caused a significant reduction in evoked amplitude, demonstrating maintained dependence on N-type VGCCs.

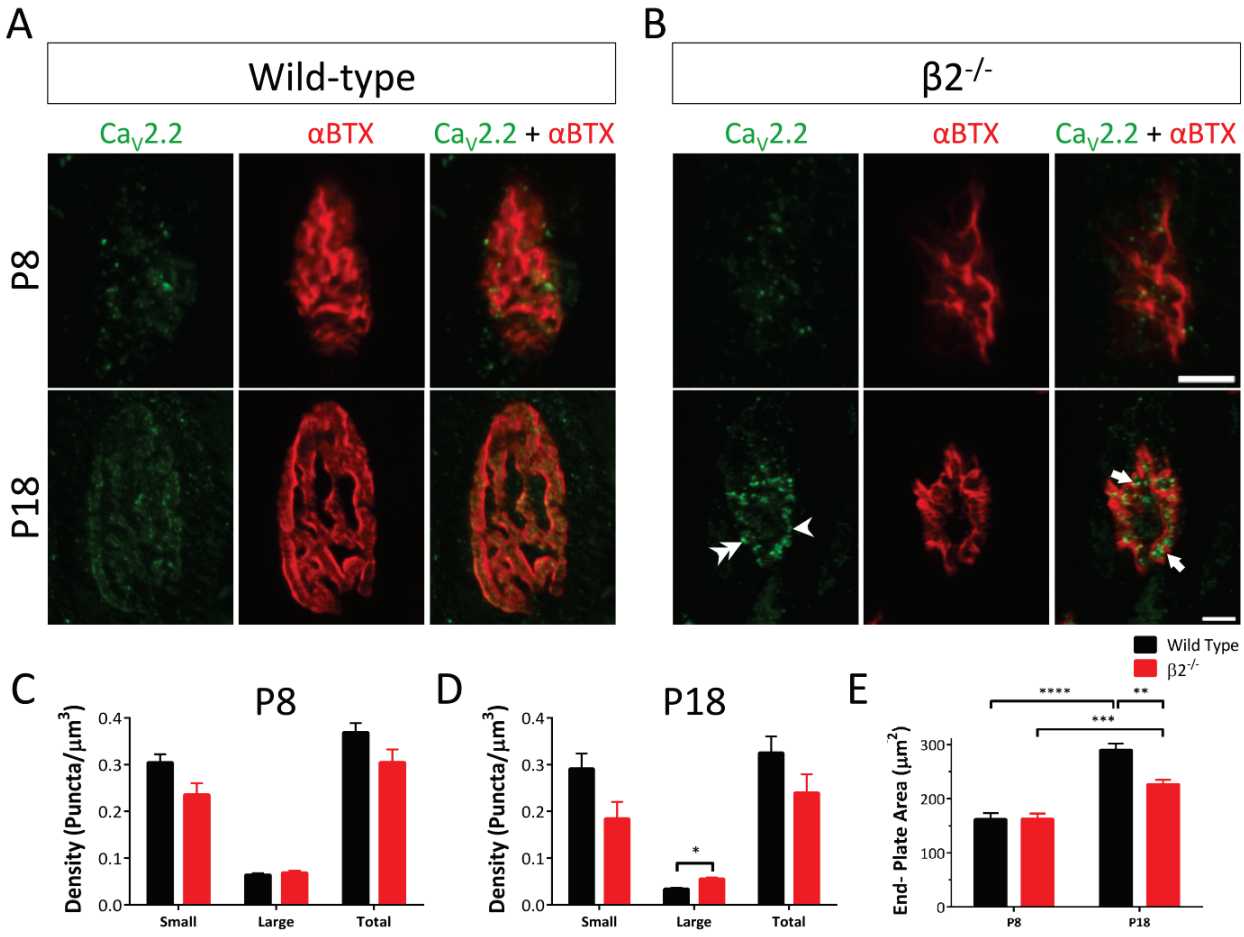

Figure 3.6 Laminin-β2 Deficient Neuromuscular Junctions displayed higher levels of N-Type VGCCs staining compared to Wild-type mice at Postnatal Day 18 Junctions

Immunohistochemical analysis of wild-type (***A***) and laminin-β2 deficient (β2$^{-/-}$) (***B***) junctions doubly labelled for N-type VGCCs ($Ca_v2.2$) and αBTX at P8 and P18. Developing wild-type and laminin-β2 deficient NMJs displayed similar discrete punctate staining of N-type VGCCs (A and B top panels). At P8 wild-type and β2$^{-/-}$NMJs showed plaque-like AChR end-plates, however mutant junctions appeared to be less convoluted. At P18 β2$^{-/-}$NMJs displayed clear punctate staining of N-type VGCCs with strong co-localisation to postsynaptic AChRs (indicated by arrows; B bottom right panel). P18 β2$^{-/-}$NMJs also maintained its AChR plaque-like appearance. Size of punctate staining was characterised as small (single arrowhead), large (double arrowhead), and total puncta per volume calculated. ***C***, density of N-type ($Ca_v2.2$) puncta at P8 (± SEM) showed no significance between genotypes for any of the puncta measurements. ***D***, density of N-type puncta at P18 (± SEM) revealed that laminin-β2 deficient NMJs displayed higher levels of large puncta (*P < 0.05) compared to wild-type junctions. P18 wild-type NMJs demonstrate a significant decrease in large puncta density compared to P8 wild-type junctions (P < 0.001, black bars in C and D for large puncta). ***E***, area of AChR end-plates (± SEM) for P8 and P18 wild-type and β2$^{-/-}$ NMJs, showed increased end-plate area with age for both genotypes, with wild-type NMJs showing greater growth when compared to β2$^{-/-}$ NMJs at

P18. For P8 (C), WT (*n* = 5, NMJs = 65) and mutants (*n* = 6, NMJs = 80). For P18 (D), WT (*n* = 6, NMJs = 83) and mutants (*n* = 6, NMJs = 72). For P8 (E), WT (*n* = 6, NMJs = 191) and mutants (*n* = 6, NMJs = 174). For P18 (E), WT (*n* = 9, NMJs = 139) and mutants (*n* = 9, NMJs = 185). Panel E ** $P < 0.01$, *** $P < 0.001$, and **** $P < 0.0001$. Scale bars = 5 μm for corresponding age group.

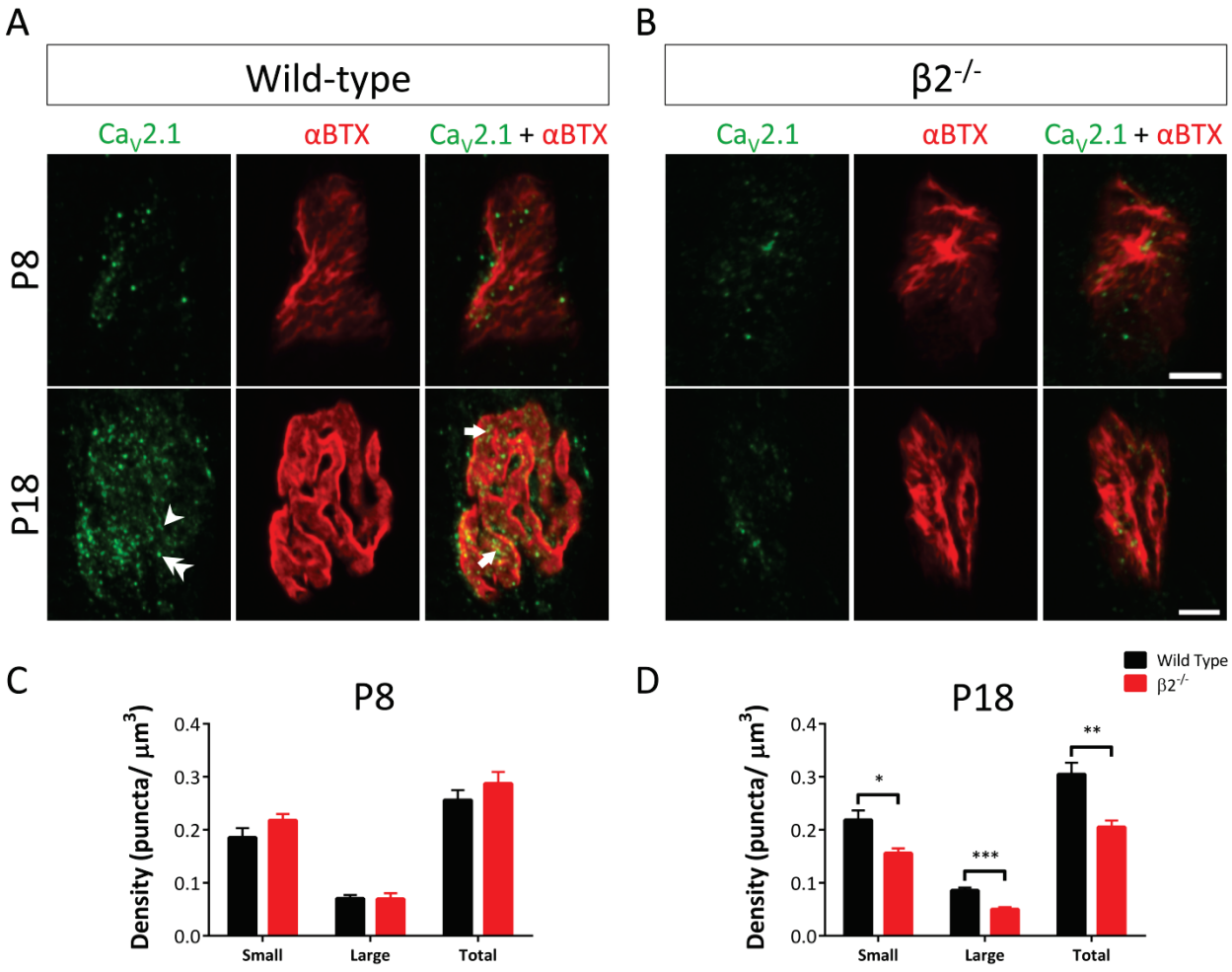

Figure 3.7 Laminin-β2 Deficient Neuromuscular Junctions displayed lower levels of P/Q-Type VGCC staining compared to Wild-type mice as the Neuromuscular Junction Matures from Postnatal Day 8 to Postnatal Day 18

Immunohistochemical analysis of wild-type (***A***) and laminin-β2 deficient ($\beta2^{-/-}$) (***B***) NMJs doubly labelled for P/Q-type VGCCs ($Ca_v2.1$) and αBTX at P8 and P18. Developing wild-type and $\beta2^{-/-}$NMJs displayed similar discrete punctate staining of P/Q-type VGCCs (A and B top panels). β2 laminin deficient NMJs maintained low levels of P/Q-type staining at P18 NMJs in contrast to wild-type junctions, which displayed high levels of puncta co-localised to AChRs (indicated by arrows; A bottom right panel). Size of punctate staining was characterised as small (single arrowhead), large (double arrowhead), and total puncta per volume calculated. ***C***, density of P/Q-type ($Ca_v2.1$) puncta at P8 (± SEM) showed no significance between genotypes for any of the puncta measurements. ***D***, density of P/Q-type puncta at P18 (± SEM) revealed lower levels of small (*$P < 0.05$), large (***$P < 0.001$) and total puncta per volume (**$P < 0.01$) of $\beta2^{-/-}$ compared to wild-type NMJs. Density analysis of total puncta showed a decreased density for $\beta2^{-/-}$ NMJs from P8 to P18, whereas for wild-type NMJs increased in density (red and black bars respectively in C and D; $P < 0.05$, significance not indicated). For P8 (C), WT ($n = 6$, NMJs = 95) and mutants ($n = 5$, NMJs = 67). For P18 (D), WT ($n = 9$, NMJs = 102) and mutants ($n = 9$, NMJs = 100). Scale bars = 5 µm for corresponding age group.

3.3.5 Loss of laminin-β2 results in perturbed Maturation of Motor End-Plates

Our immunohistochemical studies revealed distinct differences in the development of postsynaptic specialisations (AChR end-plates) between wild-type and laminin-β2 deficient NMJs, at P18. While the area of NMJ end-plates for each genotype were approximately the same at P8, wild-type NMJs doubled in size from P8 to P18 (from 166.5 ± 4.94 μm^2 at P8 to 294.5 ± 8.02 μm^2 at P18; $P < 0.0001$, Figure 3.6*E*; black bars). The expansion of NMJ end-plates in laminin-β2 deficient mice also occurred from P8 to P18, but it was significantly less when compared to wild-type NMJs (from 162.0 ± 4.78 μm^2 at P8 to 230.4 ± 6.50 μm^2 at P18; $P < 0.001$; Figure 3.6*E*; red bars). This resulted in P18 laminin-β2 deficient NMJs being significantly smaller than corresponding wild-type junctions (wild-type; 294.5 ± 8.02 μm^2 vs. laminin-β2 deficient; 230.4 ± 6.50 μm^2, $P < 0.01$; Figure 3.6*E*; red and black bars). At P18 wild-type NMJs develop characteristic pretzel shaped end-plates dense in AChRs. By contrast laminin-β2 deficient junctions maintain the plaque-like formation observed at P8 NMJs. These findings indicate that laminin-β2 deficient NMJs suffer from a significant delay or cessation of developmental maturation, a feature that we have detailed in our original publication (Noakes *et al.*, 1995a).

3.3.6 Morphological examination of Laminin-β2 Deficient NMJs revealed altered Arrangement and Localisation of selected Pre- and Postsynaptic Components

We next examined the arrangement of pre- and postsynaptic components implicated in synaptic transmission in wild-type and laminin-β2 deficient NMJs using immunohistochemistry at P8 and P18. Molecules that are able to associate with the presynaptic VGCCs such as syntaxin 1A, Bassoon, synaptotagmin and SNAP25 were qualitatively examined (minimum 30 NMJs from $n = 3$ at each age and genotype) for their molecular organisation within the motor nerve terminal with respect to the underlying postsynaptic AChRs (Kim & Catterall, 1997; Sheng *et al.*, 1998; Zhong *et al.*, 1999; Chen *et al.*, 2011).

Developing NMJs from both wild-type and laminin-β2 deficient mice at P8 displayed no overt differences in the staining intensities or organisation within their motor nerve terminals, for syntaxin 1A, synaptotagmin or SNAP 25 (Figure 3.8, left panels). However, Bassoon staining at the NMJ of laminin-β2 deficient mice was reduced compared to wild-type control at P8 (Figure 3.8, left Bassoon panels). This is consistent with the findings by Nishimune *et al.* (2004) who showed decreased expression of Bassoon staining at the NMJ of laminin-β2 deficient mice at P4. As wild-type NMJs matured from P8 to P18, we

observed enlargement and transition from plaque-like to pretzel shaped AChR end-plates. These end-plates showed good co-localisation of presynaptic components, syntaxin 1A, Bassoon, synaptotagmin, and SNAP 25 (Figure 3.8, right panels). By contrast, laminin-β2 deficient NMJs at P18 showed little if any development of their end-plates beyond P8. The AChRs remained plaque-like with poor co-localisation of presynaptic molecules; syntaxin 1A, Bassoon, synaptotagmin and SNAP 25 (Figure 3.8). These findings suggest that laminin-β2 deficient NMJs failed to develop beyond P8, which supports our functional data.

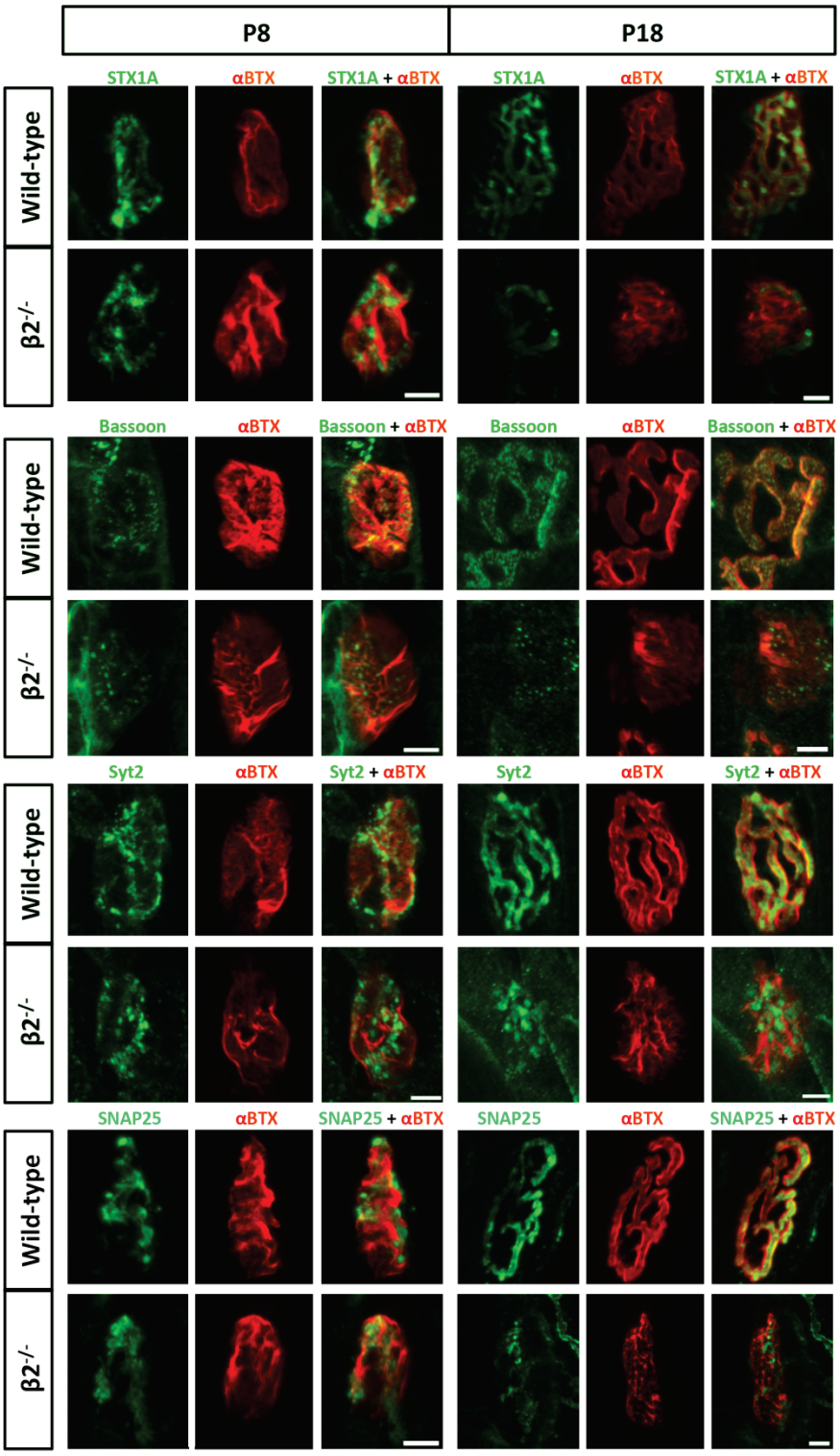

Figure 3.8 Laminin-β2 Deficient mice demonstrated decreased Co-localisation of Presynaptic Components to Acetylcholine Receptors as the Neuromuscular Junction Matures

Wild-type and laminin-β2 deficient ($β2^{-/-}$) NMJs doubly labelled with either syntaxin 1A (STX1A), Bassoon, synaptotagmin 2 (Syt2) or SNAP25 (green) against acetylcholine receptors labelled with Alexa Fluor 555-conjugated αBTX (red). At P8, similar staining patterns were observed for syntaxin 1A, synaptotagmin 2 and SNAP25 with good co-localisation to postsynaptic AChRs stained end-plates in both wild-type and $β2^{-/-}$ NMJs.

However, reduced Bassoon staining was observed in $\beta2^{-/-}$ NMJs compared to wild-type. At P18, wild-type NMJs displayed extensive co-localisation of these presynaptic components with respect to AChR stained end-plates. By contrast, P18 $\beta2^{-/-}$ NMJs showed decreased levels of presynaptic co-localisation with AChR stained end-plates, for these pre-synaptic components. These NMJ immunostaining examples typify what we observed over ~ 30 NMJs per age across and *n* = 3 per genotype. Scale bars = 5 μm.

3.4 DISCUSSION

Here we have shown a clear change in calcium sensitivity at P18 laminin-β2 deficient NMJs compared to wild-type junctions. We also functionally demonstrate a change in the VGCC sub-types involved in mediation of transmitter release at P18 laminin-β2 deficient junctions. These functional changes were supported by our immunohistochemical findings, which display maintained presence of N-type VGCCs at P18 laminin-β2 deficient NMJs. We also observed that loss of laminin-β2 resulted in altered distribution of molecular components known to associate with VGCCs.

3.4.1 Laminin-β2 Deficient mice demonstrate no change in Calcium Dependence but lower Calcium Sensitivity compared to Wild-type Junctions

Studies have previously established that laminin-β2 deficient mice display significant alterations in the release of transmitter at the NMJ (Noakes *et al.*, 1995a; Knight *et al.*, 2003). The loss of laminin-β2 results in significantly increased intermittence of transmitter release, as well as reduced mean quantal content, as supported by findings of the present study (Knight *et al.*, 2003). Laminin-β2 deficient mice display higher failure rate than wild-type littermates but normal nerve terminal impulses, suggesting a defect in the depolarisation-secretion coupling mechanism at laminin-β2 deficient junctions.

The depolarisation-secretion coupling mechanism occurs in a precise sequence involving multiple components that comprise a micro-domain at the active zones. The micro-domains primarily involve the interaction of VGCCs and the calcium sensor, synaptotagmin, localised close to the active zones (Augustine, 1990; Augustine *et al.*, 1992). Mammalian NMJs demonstrate a fourth order power relationship for binding of Ca^{2+} to synaptotagmin (Dodge & Rahamimoff, 1967; Hubbard *et al.*, 1968). The VGCCs lining the active zone form micro-domains of Ca^{2+} when activated by depolarisation of the nerve terminal. The degree of micro-domain overlap is suggested to be indicative of calcium sensitivity of the terminal, which is the ability of the terminal to efficiently release transmitter in response to calcium influx. Thus micro-domains with no overlap require higher concentrations of calcium to induce the release of transmitter (Augustine *et al.*, 1992).

Analysis of the double reciprocal plot indicates a reduction in the number of release sites with a 35% reduction in laminin-β2 deficient junctions compared to wild-type junctions. The similar $K[Ca^{2+}]_o$ values in wild-type and laminin-β2 deficient junctions indicates that the probability of release remains similar and the interaction between synaptotagmin and calcium remains dependent on the fourth power. The decreased number of release sites at mutant junctions may be the result of a selective loss of active sites not participating in regular transmitter release. The NMJ contains an abundance of active sites with only a small number actively participating in neurotransmission, while the majority remain relatively silent (Bennett & Lavidis, 1979; Robitaille & Tremblay, 1991). This non-uniform probability of transmitter release has been demonstrated in both amphibian and mammalian NMJs. Our findings indicate that given the large reduction in release sites at laminin-β2 deficient junctions, only functional sites that possess a similar probability of transmitter release to that of wild-type junctions remain. This finding is consistent with a previous study which found a decrease in the number of active release sites but no change in the probability of release at laminin-β2 deficient NMJs (Knight *et al*., 2003).

In the present study, wild-type and laminin-β2 deficient junctions display similar slopes when quantal content is compared to $[Ca^{2+}]_o$. However, while the slopes are similar, laminin-β2 deficient mice demonstrate an evident parallel shift to the right (2.3 fold) compared to wild-type mice. This finding indicates a decrease in calcium sensitivity but not in calcium dependence. The decrease in calcium sensitivity observed means more calcium influx is required in laminin-β2 deficient junctions to release equal quantal content to wild-type junctions. A decrease in sensitivity of transmitter release in relation to extracellular calcium may be as a result of decreased density of VGCCs and therefore a decrease in overlap between micro-domains or potentially a greater distance between VGCCs and active zones (Augustine *et al.*, 1992).

3.4.2 Laminin-β2 Deficient Neuromuscular Junctions maintained dependence on N-type VGCCs throughout Development

Given that the spatial locality or density of VGCCs in relation to active zones may potentially influence calcium sensitivity, we investigated the relative contribution of VGCC sub-types involved in transmission by utilising specific VGCC blockers such as ω-CgTx GVIA and ω-Aga IVA to block N- and P/Q-type channels respectively (Katz *et al.*, 1996; Rosato-Siri & Uchitel, 1999). Nishimune *et al.* (2004) demonstrated that both

N- and P/Q-type VGCCs interact with the leucine-arginine-glutamate (LRE) tripeptide sequence of laminin-β2 via binding of α_{1a} ($Ca_v2.1$) and α_{1b} ($Ca_v2.2$) subunits. This interaction has been implicated in the clustering of VGCCs at the presynaptic membrane of the nerve terminal (Nishimune *et al.*, 2004). Thus it is expected that the loss of laminin-β2 will result in changes of VGCC sub-types distribution and involvement in transmitter release as the NMJ matures. Multiple VGCCs sub-types co-exist at a single synapse and interact to induce release of transmitter (Regehr & Mintz, 1994; Dunlap *et al.*, 1995). P/Q- type VGCCs are spatially located in closer proximity to release sites compared to the more abundant N-type VGCCs (Rosato-Siri *et al.*, 2002; Nudler *et al.*, 2003; Urbano *et al.*, 2003; Nishimune *et al.*, 2012). This close spatial localisation may well be the reason P/Q-type VGCCs play a more prominent role in the mature junction where efficient bulk release of transmitter is required (Rosato-Siri *et al.*, 2002).

At the developing (P8) NMJs we demonstrate that both wild-type and laminin-β2 deficient junctions exhibit similar dependence on N-type VGCCs with P/Q-type playing a secondary role in the mediation of transmitter release. Previous studies have shown both N- and P/Q-type VGCCs are present and functionally involved at developing NMJs, as observed in our study of both wild-type and laminin-β2 deficient junctions at P8 (Rosato-Siri & Uchitel, 1999; Rosato-Siri *et al.*, 2002; Nudler *et al.*, 2003). Knight *et al.* (2003) found that the probability of transmitter release is the same for both wild-type and laminin-β2 deficient NMJs at P8. Our functional data suggests that N-type VGCCs are the dominant channel for transmitter release for both genotypes but only allow for low levels of quantal release compared to P18 NMJs. At P18 wild-type junctions, we observed an evident switch from N- to P/Q-type VGCC dominance in the mediation of transmitter release. P18 laminin-β2 deficient junctions did not display this switch, but rather remain primarily dependent upon N-type VGCCs in the mediation of transmitter release. At the mature NMJ the switch from N- to P/Q-type VGCCs in wild-type mice is associated with an increase in quantal release, suggesting that P/Q-type VGCCs are co-localised with active zones to facilitate efficient transmission (Nishimune *et al.*, 2012).

Urbano *et al.* (2003) investigated synaptic activity in mice lacking P/Q-type VGCCs. These mutant mice demonstrated similar characteristics to laminin-β2 deficient mice, with decreased quantal content and synchrony of transmitter release. The same study

observed a compensatory mechanism by which N-type VGCCs became the primary mediators of transmitter release in mice lacking P/Q-type VGCCs, a finding supported by numerous studies which demonstrate that elimination of the primary calcium channel sub-type results in calcium entry via an alternate channel at decreased efficiency (Jun *et al.*, 1999; Nudler *et al.*, 2003; Inchauspe *et al.*, 2004; Piedras-Renteria *et al.*, 2004). Investigators suggest that the spatially dispersed but abundant N-type VGCCs interact with presynaptic machinery to mediate transmitter release at a decreased efficiency to P/Q-type VGCCs. The activation threshold and opening times of both N- and P/Q-type VGCCs has been shown to be similar thus the changes in sensitivity are not likely due to these factors influencing influx of calcium ions into the terminal (Inchauspe *et al.*, 2004). These findings may explain the maintained functional presence of N-type VGCCs that was observed in the present study. Functionally the N-type VGCCs become the primary mediators of transmitter release but are not capable of sustaining efficient release of transmitter that is required as the junction matures (post-P15; Marques *et al.* (2000))

As the NMJ develops and enlarges, new release sites are added with a predominance of P/Q-type VGCCs lining the membrane. Laminin-β2 deficient NMJs display smaller end-plate size compared to P18 wild-type NMJs. As the NMJ matures, these newly added sites may not be as active as the sites during development. We propose that these less active sites require the presence of laminin-β2 to maintain the clustering of P/Q-type VGCCs. Thus the loss of laminin-β2 contributes to the dispersal of P/Q-type VGCC clustering and the decrease in efficient release of transmitter observed in laminin-β2 deficient mice at P18.

3.4.3 Laminin-β2 Deficient Junctions displayed maintained N-type VGCC expression at Matured Neuromuscular Junctions

In order to investigate this potential change in expression of VGCCs, we examined the distribution of the primary VGCC sub-types known to mediate transmitter release at the NMJ. Immunohistochemical findings displayed maintained levels of clustering of N-type VGCCs from P8 to P18 in junctions lacking laminin-β2. Mutant NMJs displayed strong co-localisation of N-type VGCC staining to postsynaptic AChRs at P18. Wild-type NMJs demonstrated similar staining levels to laminin-β2 deficient NMJs at P8, however they did not exhibit the increased expression seen at P18 mutant NMJs. For P/Q-type VGCCs, both wild-type and laminin-β2 deficient NMJs displayed similar levels of

discrete punctate staining at P8. These findings support our functional analysis, which demonstrate similar dependence on N- and P/Q-type VGCCs at P8 NMJs for both genotypes.

At P18, wild-type NMJs displayed increased levels of P/Q-type VGCC staining corresponding to the normal functional switch from N- to P/Q-type VGCC dependence for neurotransmitter release as the motor nerve terminal develops (Rosato-Siri & Uchitel, 1999; Santafe *et al.*, 2001). By contrast, laminin-β2 deficient NMJs maintained discrete punctate staining of P/Q-type VGCCs, similar to expression levels seen at P8 (no increase observed with age). The maintained N-type clustering observed in laminin-β2 deficient mice from P8 to P18 may suggest that the clustering of N-type VGCCs occurs independently of laminin-β2. We propose that the loss of this VGCC switching and maintained presence of N-type VGCCs observed in laminin-β2 deficient junctions contributes to the decreased transmission capabilities displayed in these mutants.

In order to further our findings of maintained N-type VGCC dependence at mutant NMJs, we investigated neurotransmission in the presence of the membrane permeable slow calcium chelator, EGTA-AM at P18. The use of Ca^{2+} chelators provides an insight into the spatial organisation of VGCCs involved in transmitter release (Robitaille *et al.*, 1993). EGTA is known to bind Ca^{2+} with a slow on-rate (K on ≈ 3–10 $\mu M^{-1} \cdot s^{-1}$) (Naraghi, 1997; Nagerl *et al.*, 2000), and thus does not influence evoked transmission at matured NMJs, which predominantly rely on P/Q-type VGCCs. This finding is likely due to the close proximity of P/Q-type VGCCs to active zones and thus allowing less time and distance for EGTA to buffer the entering Ca^{2+}. At P18, we propose based on functional findings already discussed here, that laminin-β2 deficient NMJs maintain dependence on N-type VGCCs, which are located distally to the active zone regions (Nudler *et al*., 2003; Urbano *et al*., 2003). In the presence of EGTA-AM, neurotransmission at mutant NMJs was found to be significantly impaired. This observation is likely due to the larger diffusion distance that calcium entering via N-type VGCCs must undergo to bind to the calcium sensor in order to initiate transmitter release (Robitaille *et al.*, 1993). These findings therefore support the idea that N-type VGCCs are the primary mediators of transmitter release at P18 laminin-β2 deficient NMJs.

3.4.4 Laminin-β2 Deficient mice displayed defects in Pre- and Postsynaptic Structures as the Neuromuscular Junction Matures

Immunohistochemical staining of wild-type and laminin-β2 deficient terminals demonstrated perturbations in the distribution of the presynaptic molecules; syntaxin 1A, Bassoon, synaptotagmin and SNAP25 at the P18 age group. At P8, Bassoon expression and co-localisation was found to be decreased compared to age-matched wild-type littermates. This finding is consistent with previous studies which have shown a decrease in active zones from as young as P4 in laminin-β2 deficient mice (Nishimune *et al*., 2004). Here we show normal expression and cellular localisation of syntaxin 1A, synaptotagmin and SNAP25 at P8 in both wild-type and laminin-β2 deficient NMJs. This finding suggests that the active zone associated molecules of laminin-β2 deficient mice maintain a structural integrity comparable to wild-type littermates at P8 NMJs. As the NMJ matured from P8 to P18 in laminin-β2 deficient mice this structural integrity failed to develop. We observed a significant decrease in the levels of co-localisation of these presynaptic molecules with respect to postsynaptic specialisations, when compared to P18 NMJs from wild-type mice. It appeared that the development of laminin-β2 deficient NMJs had not developed beyond that seen at P8.

Prior research has shown that the maintenance of active zone composition, and the molecular organisation of key components is strongly influenced by P/Q-type VGCCs (Nishimune *et al.*, 2004; Nishimune *et al.*, 2012). Previous research suggests that P/Q-type VGCCs interact directly with SNAP25 and syntaxin via the pore forming α-subunits, while Bassoon is capable of interacting with the β1b and β4 subunits of VGCCs (Kim & Catterall, 1997; Zhong *et al.*, 1999; Chen *et al.*, 2011; Nishimune *et al.*, 2012). Thus the failure to up-regulate P/Q-type VGCC expression at P18 NMJs from laminin-β2 deficient mice, may have resulted in reduced expression of these active zone molecules with respect to postsynaptic AChRs. Our findings also indicate that the maintained presence of N-type VGCCs seen at P18 laminin-β2 deficient NMJs, was not capable of organising the molecular components at the active zone of the cytomatrix.

Defects at the postsynaptic region were also observed in P18 laminin-β2 deficient NMJs. Normal pretzel-like AChR clusters with high convolution and branching were observed at NMJs from P18 wild-type mice. By contrast, the NMJs from P18 laminin-

β2 deficient mice retained the plaque-like AChR end-plates seen for both genotypes at P8, suggesting a decline in or arrest of postsynaptic maturation in laminin-β2 deficient mice. The proteins involved with AChR postsynaptic end-plate maturation are yet to be fully determined, but researchers have proposed that the focal adhesion complexes termed podosomes together with selected RhoA activators such as ephexin 1 are critical in this process. End-plate AChRs become perforated in the presence of podosomes that give the characteristic pretzel shape associated with matured end-plates (Proszynski *et al.*, 2009), and mice lacking ephexin 1 develop fewer pretzel shaped AChR end-plates (Shi *et al.*, 2012). At immature AChR end-plates, laminin-β2 and laminin-α5 co-localise to the AChR end-plate region (Proszynski *et al.*, 2009). As the podosomes form within the AChR end-plate perforations appear. At these perforations there was a corresponding loss of laminin-α5 from these regions (Proszynski *et al.*, 2009). Given that β2 laminin can interact with laminin-α5 to form laminin-521 (Aumailley *et al.*, 2005), it is likely that laminin-β2 is also lost at podosomes. This idea is aided by the observation that at laminin-β2 deficient NMJs there is also a loss of laminin-α5 (Patton *et al.*, 1997), and supports an earlier hypothesis that the loss of laminin-α5 results in delayed postsynaptic maturation (Nishimune *et al.*, 2008). At the edges of these perforations, a ring of laminins remain suggesting that these laminins through their known interactions with other postsynaptic molecules such as dystroglycan can aid in AChR end-plate stability and growth (Grady *et al.*, 2000; Adams *et al.*, 2004; Nishimune *et al.*, 2008). Together these findings along with our own suggest that both laminin-α5 and -β2 are required for postsynaptic maturation.

3.5 CONCLUSION

The findings of this investigation strongly support previous literature implicating laminin-β2 in the organisation of key synaptic components necessary for efficient synaptic communication and function. We demonstrate that the loss of laminin-β2 results in a delay or halt in maturation of both pre- and postsynaptic apparatus, more specifically the presence of VGCC sub-types involved in mediation of neurotransmission and the optimal organisation of postsynaptic AChR end-plates. Combined these findings suggest that laminin-β2 is an integral synaptic component necessary for the proper development and maturation of the skeletal neuromuscular junction.

CHAPTER 4

Altered Neuron-Perisynaptic Schwann Cell Interactions at Neuromuscular Junctions of Laminin-β2 Deficient Mice

ABSTRACT

Laminin-β2 is a key mediator in the differentiation and formation of the presynaptic region of the skeletal neuromuscular junction (NMJ). Mice lacking laminin-β2 (*lamb*2$^{-/-}$) present disrupted presynaptic differentiation with fewer active zones, dispersed synaptic vesicles and defective neurotransmission properties. *Lamb*2$^{-/-}$ NMJs demonstrate invasion of peri-synaptic Schwann cell (PSC) processes into the synaptic cleft. This PSC disorganisation may also contribute to the decreased transmission seen in mutants as PSCs have been shown to regulate NMJ stability, synaptic activity and plasticity. Here we functionally characterised PSC activity following laminin-β2 ablation by observing changes in Ca^{2+} responses and transmission properties in *lamb*2$^{-/-}$ and wild-type mice. Electrophysiological recordings of P14 soleus NMJs showed that *lamb*2$^{-/-}$ NMJs release less neurotransmitter than wild-type. Our findings also demonstrate a reduced ability of PSCs to detect transmission in *lamb*2$^{-/-}$ NMJs, as revealed by smaller Ca^{2+} responses and fewer responding cells to high frequency stimuli. This reduced PSC excitability may be due to changes in purinergic or muscarinic receptors, P_{2Y}Rs and MRs respectively. *Lamb*2$^{-/-}$ NMJs display decreased muscarinic receptor signalling activation with smaller Ca^{2+} responses and fewer responding cells after local application of muscarine. *Lamb*2$^{-/-}$ and wild-type NMJs display similar responses in ATP-induced P_{2Y}R activity. *Lamb*2$^{-/-}$ NMJs display poor synaptic plasticity after high frequency stimuli by undergoing greater depression and demonstrating no facilitation of transmitter release compared to wild-type NMJs. Communication between nerve terminal structures and PSCs may play a vital role in the development of properly functioning synapses. It is not clear what comes first, the decrease in transmission or the decline in PSC function. These observations suggest that laminin-β2 is involved in establishing mature and structured PSCs that are capable of detecting and decoding synaptic activity, which consequentially possess the ability to appropriately modulate neurotransmission.

4.1 INTRODUCTION

Schwann cells (SCs), peripheral glial cells, myelinate the length of the motor axon along the peripheral nerve to the muscle fibre. The ending of these motor axons are covered by a number of non-myelinating SCs, termed the perisynaptic Schwann cells (PSCs) (Love & Thompson, 1998). At the neuromuscular junction (NMJ), PSCs envelop most of the presynaptic nerve terminal but leave windows that allow the presynaptic face of the terminal to transmit to the postsynaptic membrane of the muscle. A single NMJ may be capped by three to five PSCs in close apposition to the presynaptic terminal (10-20 nm) with no basal lamina between (Auld & Robitaille, 2003; Griffin & Thompson, 2008; Darabid *et al.*, 2013). The close association of these cellular bodies would suggest an intimate intracellular interaction to facilitate the ability of PSCs to influence neurotransmission. This idea is supported by several studies which have shown that PSCs are capable of regulating the development and functional properties of the NMJ, as well as responding to perturbations at the NMJ (Miledi & Slater, 1968; Georgiou *et al.*, 1994; Robitaille, 1998; Feng & Ko, 2008; Todd *et al.*, 2010). Recently, Darabid and colleagues (2013) have demonstrated that PSCs can help regulate the elimination of excess synaptic inputs at the developing NMJ, a developmental stage of interest to the investigation presented in this chapter.

During development PSCs present a globular morphological pattern with intermingling of cells, which mature into highly branched and compartmentalised patterning that cover the NMJ (Brill *et al.*, 2011). This segregation of PSCs appears to be caused by spatial competition between individual Schwann cells as well as the interaction between the nerve terminal and PSCs, with disruption in coverage leading to axonal degeneration and breakdown of the synapse. This territorial development coincides with maturation of the postsynaptic end-plate region, with both processes requiring neuregulin-1 and the ErbB receptors to successfully form (detailed in Chapter 1) (Lin *et al.*, 2000; Ngo *et al.*, 2012). During synaptogenesis the motor axon reaches target muscles and forms nerve-muscle contacts. Deletion of PSCs during synaptogenesis leads to a cessation in growth of nerve terminal (Reddy *et al.*, 2003). At immature NMJs, PSCs are highly dynamic and are thought to be involved in the process of axonal elimination, with weaker inputs being ‘pruned’ away from the end-plate region while strong inputs become stabilised as the PSCs become more static and cap the terminal (Brill *et al.*, 2011). This finding is strongly supported by recent work which demonstrated the direct involvement of PSCs in phagocytosis of innervating nerve terminals during early development, suggesting a role

in the process of postnatal synaptic elimination, which leads to a switch from polyneuronal innervation to single innervated NMJs (Smith *et al.*, 2013). By employing live Ca^{2+} imaging of PSC activity, Darabid *et al.* (2013) found PSCs at developing NMJs are involved in strengthening of robust synaptic inputs, potentially aiding in synaptic competition.

As discussed above, studies have demonstrated that perisynaptic Schwann cells are able to detect and regulate the synaptic transmission properties of the NMJ, a finding conserved in both amphibian and mammalian NMJs (Jahromi *et al.*, 1992; Reist & Smith, 1992; Robitaille, 1995; Rochon *et al.*, 2001; Darabid *et al.*, 2013). In response to the release of neurotransmitters such as ACh, ATP, and substance P during synaptic activity, the PSCs display elevated intracellular Ca^{2+}. PSCs are capable of detecting the pattern of neuronal and synaptic activity, and in turn, respond by modulating the synaptic transmission by potentiating or depressing the signal via manipulation of G-protein pathways or internal calcium stores (Pasti *et al.*, 1997; Robitaille, 1998; Henneberger *et al.*, 2010; Todd *et al.*, 2010; Panatier *et al.*, 2011). Robitaille (1998) induced a reduction in neurotransmitter release during 0.2Hz stimulation by activating G-proteins via injection of $GTP_{\gamma}S$. Interestingly, inhibition of G-proteins with GDPβS did not alter neurotransmission under the same low-frequency stimulus conditions. This finding suggests that PSCs are not involved in the modulation of neurotransmission under tonic firing conditions. By contrast, inhibition of PSC G-proteins under high frequency conditions reduced the associated depression in neurotransmission (Robitaille, 1998). This finding suggests PSC involvement in the noted depression of neurotransmission after high frequency stimulus. Studies have since aimed to investigate whether these PSC responses are actively involved in modulation of neurotransmission.

Castonguay and Robitaille (2001) found that increasing intracellular calcium stores in PSCs utilising Thapsigargin, an inhibitor of Ca^{2+}-ATPase pumps of internal stores, resulted in an increase in evoked transmitter release. Conversely chelation of intracellular Ca^{2+} stores using BAPTA injection resulted in significantly depressed transmitter response after high frequency stimulus. These findings suggest that PSCs are capable of potentiating transmitter release in a Ca^{2+}-dependent manner at the NMJ. This ability of PSCs to both potentiate and depress neurotransmission based on synaptic activity aids in short-term plasticity of the NMJ.

These functional studies have primarily focused on matured adult synapses despite the vital involvement of PSCs in the formation and elimination of synapses during development (Eroglu & Barres, 2010). Darabid *et al.* (2013) demonstrated that PSCs at immature NMJs are capable of interacting with competing inputs during the development of the NMJ. Developing PSCs are capable of detecting transmitter release primarily via purinergic (P_2) signalling, however at mature NMJs PSCs modulate transmitter release via both muscarinic and purinergic (P_1 and P_2) receptors (Robitaille, 1995; Rochon *et al.*, 2001). At the developing NMJ, PSCs utilise P_{2Y} receptors to detect neurotransmitter release even though muscarinic receptors were also found to be present and active (Darabid *et al.*, 2013). The investigators suggest that as the NMJ matures there is a switch from solely purinergic to mixed muscarinic-purinergic signalling corresponding to the loss of polyneuronal innervation. Darabid and colleagues (2013) propose that the switch in signalling from the purinergic signalling pathway during development to a combination of muscarinic and purinergic at matured NMJs, may be due to a change in the properties and function of PSCs. In conjunction with findings by Brill *et al.* (2011), developing PSCs are highly dynamic, with exploratory behaviour involving constant repositioning of processes, and dependence on purinergic signalling. This PSC dynamism during development may allow for flexible changes in function and structure of the still plastic NMJ. As the NMJ stabilises during maturation, the associated PSCs become less variable in their activity and mobility, which aids in stability of the NMJ structure and function. These changes are of particular importance in the present study.

Signalling and adhesion molecules located within the basal lamina spanning the synaptic cleft act as cues to direct PSCs. Of particular interest is laminin-β2, which has been shown to interact and signal with PSCs to determine their state of activity and prevent invasion into the synaptic cleft (Patton *et al.*, 1998). A key morphological characteristic associated with the loss of laminin-β2 is the dramatic invasion of the synaptic cleft by Schwann cell processes (Noakes *et al.*, 1995a; Patton *et al.*, 1998). In addition to this morphological phenotype, these mutant NMJs demonstrate severely perturbed neurotransmission, which to some degree is thought to be associated with PSC processes penetrating into the synaptic cleft (Noakes *et al.*, 1995a; Knight *et al.*, 2003). In conjunction with findings presented in Chapter 3, which suggest immature pre- and postsynaptic elements at P18 laminin-β2 deficient NMJs, I propose that each of the three cellular bodies comprising the NMJ; the perisynaptic Schwann cells, presynaptic nerve

terminal, and the postsynaptic end-plate, maintain immature functional and morphological characteristics compared to wild-type littermates. To examine this idea, we compared the calcium transients within the perisynaptic Schwann cells of wild-type and laminin-β2 lacking NMJ's. We also identified the receptors involved with modulating such calcium transients both during development and maturity.

4.2 METHODS

4.2.1 Animals and Ethics Approval

Wild-type mice and homozygous mutant mice (with no normal copies of the laminin-β2 gene) age-matched littermates for P14-P16 were used in this investigation. Mice were obtained from the mating of heterozygous males and females and maintained on a defined C57BL/6-129SvJ genetic background. Animals were genotyped using a tail tip DNA tail assay (Hanley & Merlie, 1991). Mice were anaesthetised with rising concentrations of carbon dioxide and then killed by cervical dislocation. The University of Queensland Animal Care and Ethics Committee approved all procedures undertaken (Ethics number 152/12) and were in accordance with the Queensland Government Animal Research Act 200, associated Animal Care and Protection Regulations (2002 and 2008), as well as the Australian Code for the Care and Use of Animals for Scientific Purposes, 8th Edition (National Health and Medical Research Council, 2013).

4.2.2 Muscle Preparation

The soleus muscle with innervating nerve were dissected free under oxygenated (95% O_2, 5% CO_2) Rees' Ringer's solution (in mM): 110 NaCl, 5 KCl, 1 $MgCl_2$, 25 $NaHCO_3$, 2 $CaCl_2$, 11 glucose, 0.3 glutamate, 0.4 glutamine, 5 BES, 0.036 choline chloride, and 4.34 x 10^{-7} thiamine pyrophosphate. The extracted soleus were pinned to the bottom of a Sylgard-coated (Dow Corning Corp., MI, USA) recording chamber and innervating nerve stimulated by a suction-stimulating electrode (square wave pulses; 0.2mV-5.0V, 0.1 ms duration) using a Grass Instruments stimulator (SD48) (Natus Neurology Inc., RI, USA) coupled to a Grass Instruments stimulus isolator (SIU5).

4.2.3 Electrophysiological Recordings of Synaptic Transmission

Intracellular recordings of end-plate potentials (EPPs) were performed at room temperature using sharp glass microelectrodes (40 to 60 MΩ) filled with 2 M KCl. Proximity to end-plate regions was confirmed through analysis of EPP and MEPP rise times, sites with rise times greater than 1.5 ms were rejected for wild-type mice and times greater than 2 ms rejected for mutant mice. During recordings the initial resting membrane potential (RMP) values were in the range of 70- 85 mV with these values undergoing a gradual decrease to steady values between 45- 60 mV. Recordings were terminated if the RMP fluctuated by more than 10 % from the steady values. Recorded signals were amplified using an Axoclamp 2B amplifier (Axon Instruments, USA) and digitised to 20 kHz sampling rate using MacLab system and Scope software (Version 3.5.5, ADInstruments, CO, USA).

The neurotransmission properties of each NMJ were determined by measuring their respective basal quantal content, and post tetanic facilitation after high frequency stimuli (50 Hz for 20 s). These were determined using a modified Ringer's solution with low Ca^{2+} (1 mM)/high Mg^{2+} (6–7 mM) solution. The innervating nerve was stimulated at a frequency of 0.2 Hz with an intensity that was twice the threshold for eliciting EPPs. Quantal content ($\bar{m}$) was determined using method of failures (Del Castillo & Katz, 1954b): $\bar{m}$ = $\log_e$ (number of stimuli/number of failures).

4.2.4 Calcium imaging

The extracted soleus muscle and intact innervating nerve were pinned to a 3 mL Sylgard-coated chamber. The tissue was immersed in Ringer's solution and oxygenated with 95% O_2 and 5% CO_2, as described previously. Muscle preparations were incubated in oxygenated Ringer's solution containing 10 μM fluo-4 AM (Invitrogen Inc., NY, USA), 0.02% pluronic acid (Sigma Aldrich, MO, USA), and 1% DMSO (Sigma Aldrich). Following the loading period of forty minutes, tissue was perfused with standard Ringer's solution for twenty minutes. The innervating nerve was gently sucked into a stimulating electrode. Stimulus was set at twice the threshold level to initiate a visible muscle contraction (Grass Instruments stimulator, SD48) with a frequency of 50Hz for continuous trains of 20 seconds.

Tissue was imaged using a Zeiss LSM 510 upright confocal microscope. Excitation of fluo-4 AM was through the use of the 488 nm line of an argon laser with emitted fluorescence detected through a long-pass filter at 590 nm. Light microscopy with a 60x water immersion objective (Zeiss, BW, Germany) was used for localisation of NMJs. Changes in fluorescence over PSCs soma were measured and expressed as:

$$\% \Delta F / F0 = (F - F_{rest}) / F_{rest} \times 100$$

In order to standardise across experiments basal fluorescence values were maintained between ranges of 20- 30 pixel intensity values. Experimentation hardware settings were also standardised with offset values between 4.9 and 5.1, and the gain set between 8 and 9. The PSCs were considered responsive when the response amplitude was greater than 5 pixel intensity above resting levels.

For experiments where Ca^{2+} responses in PSCs were elicited by agonists, a PV800 Pneumatic PicoPump (World Precision Instruments Inc., FL, USA; positive pressure pulses of 10 PSI, 150 ms) with a glass pipette (5 MΩ, ~2-µm-tip diameter) positioned in close proximity of the PSCs was used to locally apply the agonists. The agonists, ATP (10 µM, Sigma) and muscarine (10 µM, Sigma) were diluted in the extracellular Ringer solution used for the experiment. All Ca^{2+} imaging experiments were performed in normal Ca^{2+}/ Mg^{2+} concentration Ringer's solution at room temperature (~22^0C). Muscle contractions were prevented by blocking postsynaptic AChRs with D-tubocurarine chloride (~3.5 µM, Sigma Aldrich).

4.2.5 Immunohistochemistry

Immunohistochemical labeling was performed in whole by Houssam Darabid (collaborator from the Robitaille Laboratory, University of Montreal). The protocol used has previously been described in Todd *et al*. (2010). Dissected SOL muscles were pinned in a Sylgard-coated dish and fixed for 10 min in 4% formaldehyde at room temperature. Muscles were then permeabilised in 100% cold methanol for 6 min at -20°C. Nonspecific labeling was minimized by incubating the muscles in a solution of 10% normal donkey serum (NDS) and 0.01% Triton X-100 for 20 min. Rabbit, anti-S100β (1:250, Dako) with 0.01% Triton X-100 and 2% NDS was incubated overnight at 4°C, then washed in normal serum muscles, to be then incubated in goat, anti-neurofilament (1:250; SC16143, Santa Cruz Biotechnology) for 90 min. Secondary antibodies (Alexa 488 α-goat and 647 α-rabbit, 1:500) were incubated together for 60 min at room temperature. Muscles were then incubated with α-bungarotoxin (Alexa 594) for 45 min. After each step, muscles were rinsed in PBS containing 0.01% Triton X-100 for 5 min. The preparations were then mounted in the Prolong Gold antifade reagent containing DAPI (Invitrogen) to visualize nuclear material. All labels were observed simultaneously using the spectral detection feature of an Olympus FV1000 confocal microscope.

4.2.6 Data analysis

Results are presented as mean ± SEM, and *n* represents the biological number for electrophysiology studies and the number of PSCs for calcium imaging. Unpaired *t*-tests were performed when comparing responses between genotypes. Analyses were deemed significant at $P < 0.05$.

4.3 RESULTS

4.3.1 Laminin-β2 Deficiency leads to decreased Neurotransmission at Neuromuscular Junctions of Soleus Muscles

We have previously shown that loss of laminin-β2 results in significant decrease in neurotransmission in the diaphragm muscle, a mixed fibre type muscle (Knight *et al.*, 2003). Here, the functional characteristics of the soleus, a predominantly slow twitch fibre muscle, were investigated using intracellular electrophysiology recordings of EPPs and MEPPs. We observed significant deficits in synaptic transmission at laminin-β2 mutant synapses compared to wild-type (Figure 4.1*A*). Evoked amplitude was decreased at *lamb*2$^{-/-}$ NMJs compared to wild-type junctions (wild-type; 1.34 ± 0.15 mV, *n* = 8, junctions = 37 vs. *lamb*2$^{-/-}$; 0.76 ± 0.10 mV, *n* = 10, junctions = 53, *P* < 0.01; Figure 4.1*B*). Quantal size was also reduced at *lamb*2$^{-/-}$ synapses (wild-type; 1.04 ± 0.06 mV, *n* = 8 vs. *lamb*2$^{-/-}$; 0.77 ± 0.08 mV, *n* = 10, *P* < 0.05; Figure 4.1*C*). Quantal content was significantly reduced by approximately 49% in *lamb*2$^{-/-}$ NMJs when compared to wild-type synapses (wild-type; 1.12 ± 0.19, *n* = 8 vs. *lamb*2$^{-/-}$; 0.55 ± 0.06, *n* = 10, *P* < 0.01; Figure 4.1*D*). The frequency of spontaneous transmitter release was found to be 49% lower in *lamb*2$^{-/-}$ NMJs (wild-type; 17.65 ± 2.78 min^{-1}, *n* = 8 vs. *lamb*2$^{-/-}$; 8.68 ± 1.64 min^{-1}, *n* = 6, *P* < 0.05 Figure 4.1*E*). Intermittence of transmitter release was increased at mutant synapses compared to wild-types (wild-type; 36.11 ± 5.49%, *n* = 8 vs. *lamb*2$^{-/-}$; 58.26 ± 3.30%, *n* = 10, *P* < 0.01; Figure 4.1*F*).

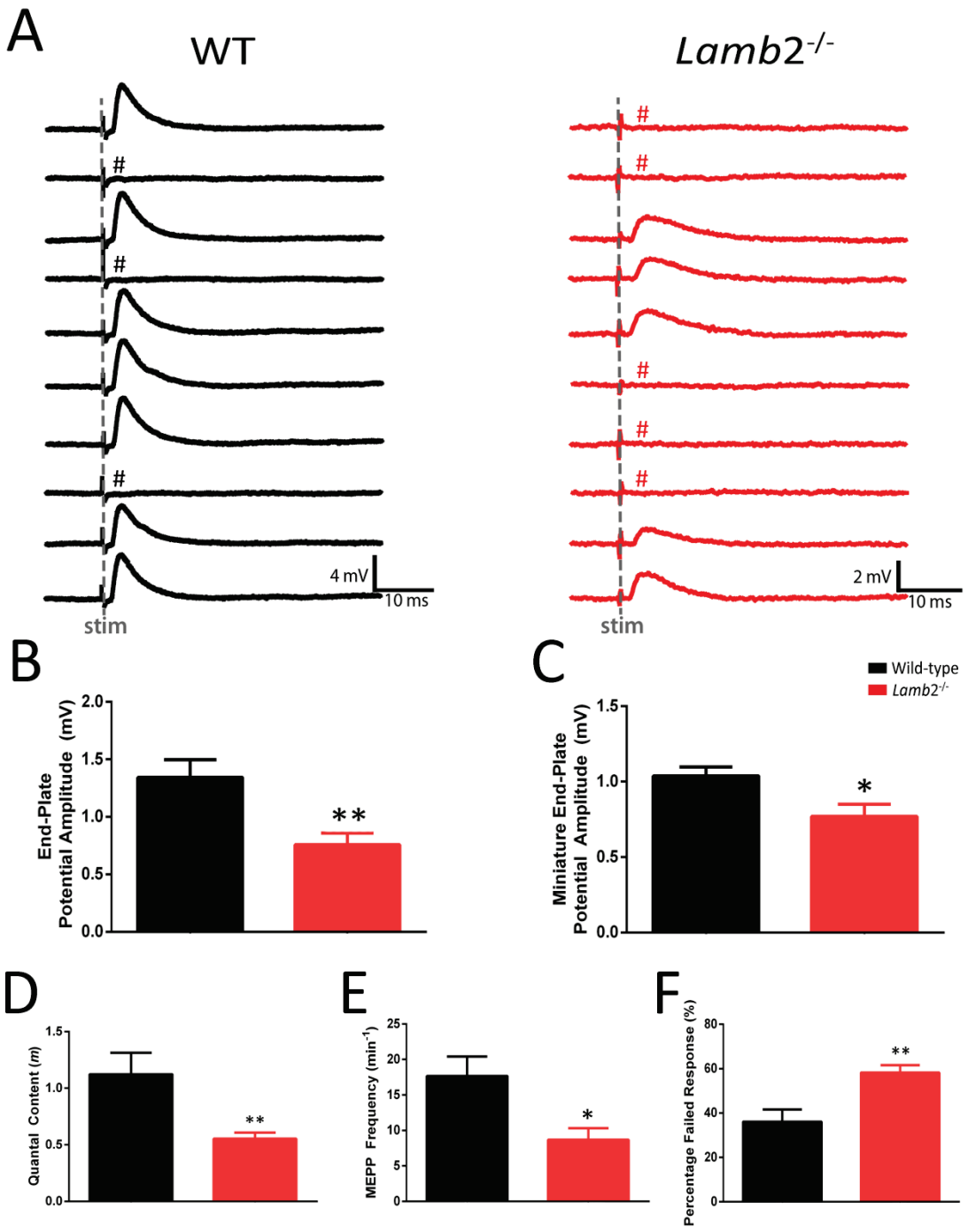

Figure 4.1 Laminin-β2 Deficient Neuromuscular Junctions presented Perturbed Neurotransmission Properties compared to Wild-type littermates in Slow Twitch Fibre Muscles

A, ten consecutive representative intracellular electrophysiological recordings from wild type (black) and laminin-β2 deficient (*Lamb2*$^{-/-}$) (red) NMJs, showing altered neurotransmission at mutant NMJs (# indicates stimuli that failed to evoke a response). ***B***, *Lamb2*$^{-/-}$ NMJs showed smaller EPP amplitudes ($P < 0.01$), and ***C***, MEPP amplitudes ($P < 0.05$) than those observed at wild-type NMJs ***D***, *Lamb2*$^{-/-}$ NMJs demonstrated significantly decreased quantal content compared to wild-type NMJs ($P < 0.01$). ***E***, Decreased spontaneous release frequency was observed at

mutant NMJs ($P < 0.05$). ***F***, Mutant NMJs also presented significantly higher levels of intermittence than wild-type littermates ($P < 0.01$). Values presented in histograms (B-F) are means ± SEM. Unpaired *t*-test was used to test for significance. For wild-type ($n = 8$) and *lamb*2$^{-/-}$ ($n = 10$) NMJs.

4.3.2 Transmitter Release during High Frequency Stimulation is altered in Laminin-β2 Deficient Neuromuscular Junctions when Compared to Wild-types

We compared vesicular dynamics at the active zone of *lamb*2$^{-/-}$ NMJs compared with wild-type NMJs by applying high frequency stimulation (50 Hz for 20 s) and recording quantal content. As shown in Figure 4.2*A*, *lamb*2$^{-/-}$ NMJs displayed significantly increased depression during high frequency stimuli (50 Hz for 20 s) compared to wild-type NMJs (wild-type; 73.07 ± 4.17%, n = 5 vs. *lamb*2$^{-/-}$; 35.50 ± 8.59%, n = 6 $P < 0.005$, Figure 4.2*B*). The potentiation observed in wild-type NMJs during and immediately after high frequency stimuli was impaired at mutant synapses with wild-type showing higher mean EPP amplitudes post high frequency stimuli (wild-type; 134.7 ± 13.06%, n = 5 vs. *lamb*2$^{-/-}$; 44.44 ± 6.40%, n = 6, $P < 0.001$, Figure 4.2*C*), suggesting a possible decrease in vesicular availability to the active zone or altered Ca^{2+} handling in mutant NMJs. Wild-type NMJs demonstrate significantly higher potentiation with faster recovery back to baseline. By contrast, *lamb*2$^{-/-}$ NMJs displayed lower facilitation in comparison to wild-type (wild-type; 109.30 ± 3.49%, n = 5 vs. *lamb*2$^{-/-}$; 52.15 ± 8.26%, n = 6, $P < 0.001$, Figure 4.2*D*). These findings suggest altered vesicular dynamics at *lamb*2$^{-/-}$ NMJs, resulting in higher levels of depression during and after high frequency stimulation.

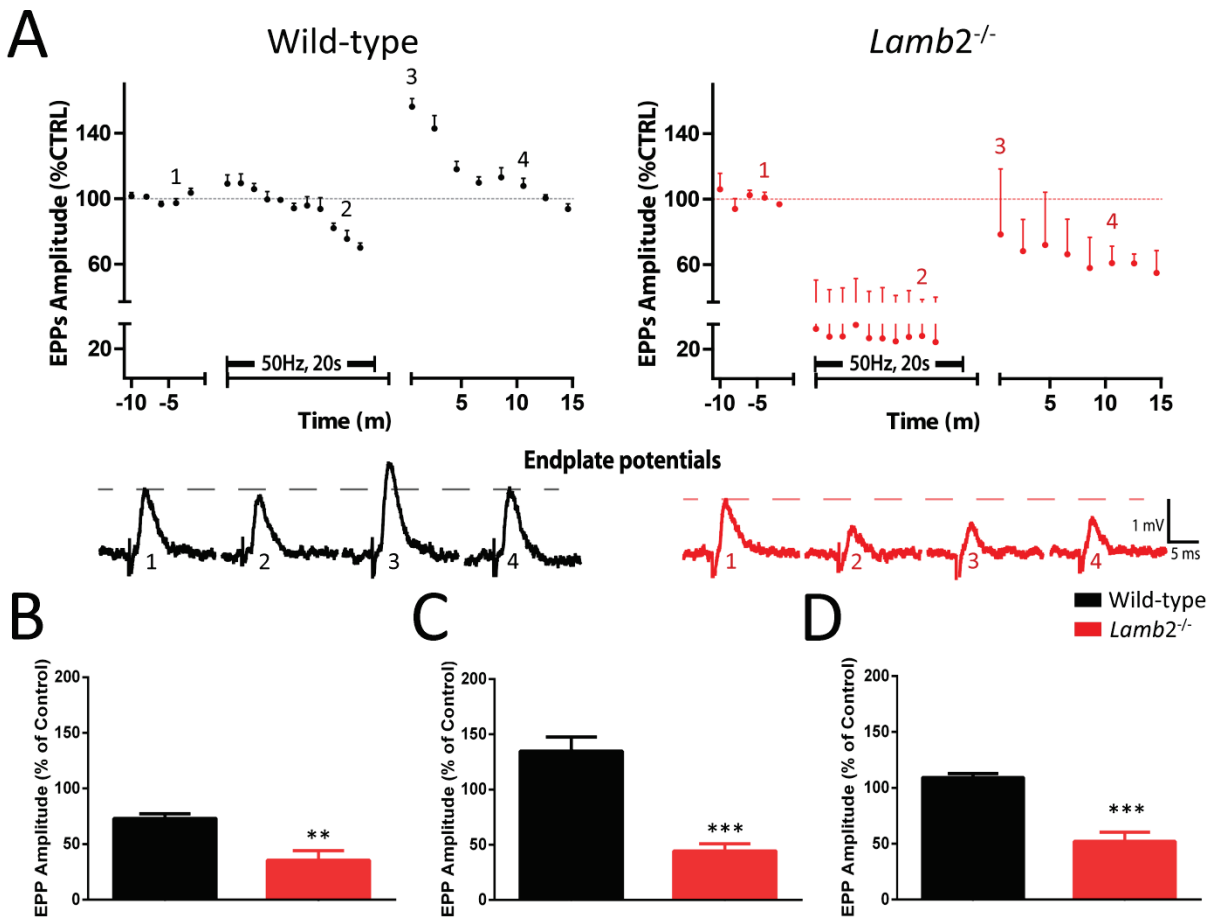

Figure 4.2 Laminin-β2 deficient NMJs undergo significantly higher levels of Depression and Demonstrate Altered Synaptic Plasticity

A, *Top*, Changes in EPP amplitude before, during and post high frequency stimulus. Period of high-frequency stimulation is indicated. *Bottom*, Examples of EPPs induced by stimulation before, during, post high frequency stimulation and ten minutes after high frequency stimulus. Grey dashed line represents control values (100%). ***B***, *Lamb2*$^{-/-}$ NMJs demonstrate significantly higher levels of synaptic depression induced by high frequency stimulus (P < 0.005). ***C***, Post high frequency stimulus, *lamb2*$^{-/-}$ NMJs display decreased synaptic facilitation compared to wild-type littermates (P < 0.001). ***D***, Long-term plasticity was impaired at *lamb2*$^{-/-}$ NMJs (P < 0.001). Wild-type, n = 5 and *lamb2*$^{-/-}$, n = 6.

4.3.3 Perisynaptic Schwann cell Excitability is decreased at Laminin-β2 Deficient Neuromuscular Junctions in response to High Frequency Stimuli

A primary role of PSCs at the NMJ is thought to involve the detection and decoding of synaptic activity at the NMJ (Jahromi *et al.*, 1992; Robitaille, 1995). In order to examine whether PSCs play a role in the decreased transmitter release observed at *lamb*2$^{-/-}$ NMJs, we investigated PSC excitability using the same high frequency stimuli parameters (50 Hz for 20 s). High frequency stimulus elicited a rapid changes in Ca^{2+} response (%∆F/F0) in wild-type PSCs (103.97 ± 12.65% ∆F/F0, *n* = 13, Figure 4.3A). By contrast, PSCs at *lamb*2$^{-/-}$ NMJs displayed poor responses to the same high frequency stimulus, with prolonged response times and decreased Ca^{2+} response amplitudes (50 ± 18.33% ∆F/F0, *n* = 6, Figure 4.3*B*). The change in Ca^{2+} response was found to be significantly lower at *lamb*2$^{-/-}$ NMJs than at wild-type littermates ($P < 0.05$, Figure 4.3*C*). In addition to these findings, we observed a decrease in the number of responding PSCs at each NMJ in *lamb*2$^{-/-}$ mice ($P < 0.05$, Figure 4.3*D*). These findings correspond with the poor synaptic response to high frequency stimuli observed at *lamb*2$^{-/-}$ NMJs (Figure 4.2), suggesting that the poor response of PSCs at mutant NMJs may be influencing the neurotransmission properties at *lamb*2$^{-/-}$ NMJs or vice versa.

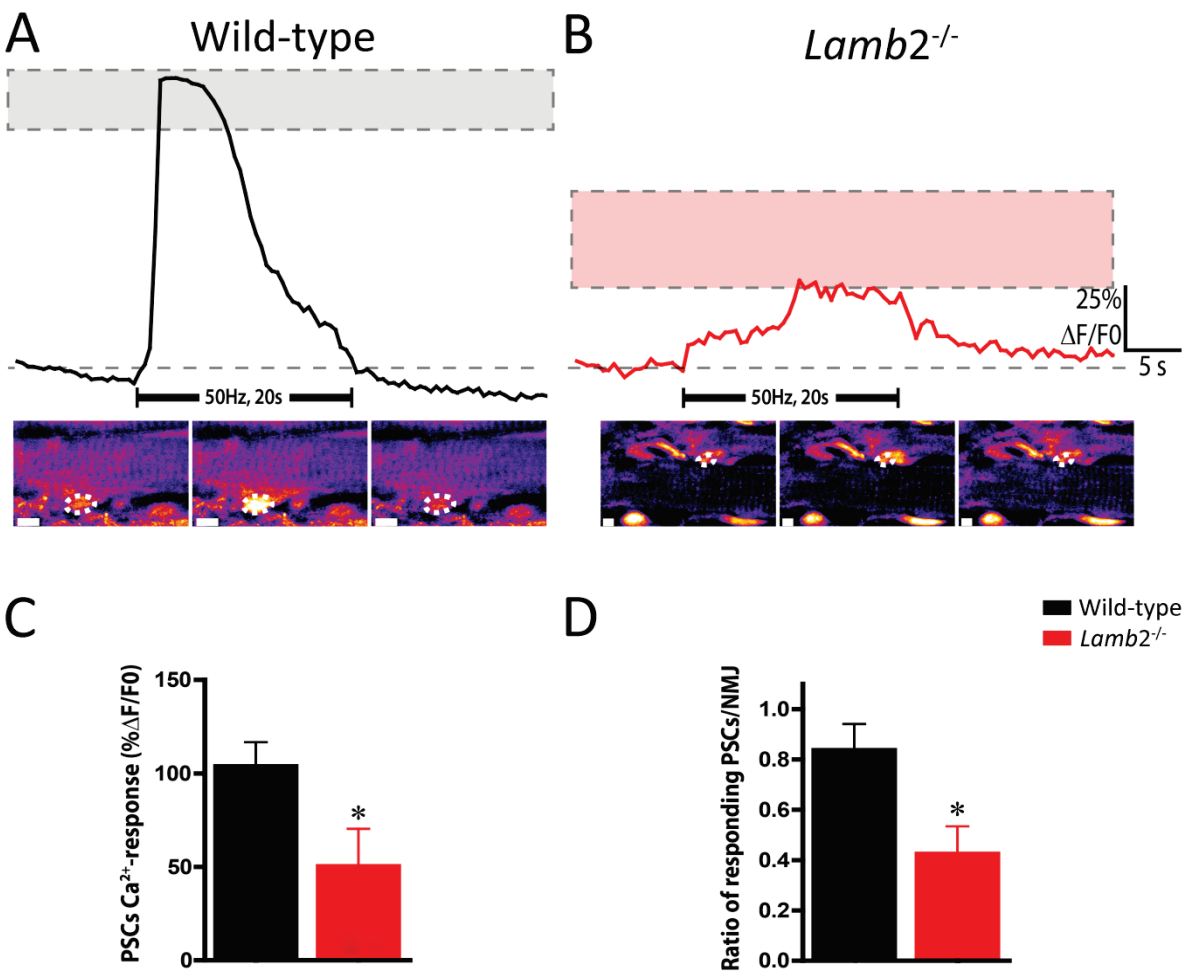

Figure 4.3 Perisynaptic Schwann Cell Excitability is decreased at Laminin-β2 Deficient Neuromuscular Junctions in response to High Frequency Stimuli

A, demonstrates the rapid response of wild-type PSCs to endogenous neurotransmitter release after high frequency stimulus (indicated on sample PSC response). ***B***, PSCs at *lamb2*$^{-/-}$ NMJs show poor response to the same high frequency stimulus, with visually slower response times and decreased amplitude of response (%ΔF/F0). Grey dashed line represents basal fluorescence with dashed boxes representing mean values of change in Ca^{2+} responses for the respective genotype. Corresponding snapshots of Ca^{2+} response for PSCs at wild-type and *lamb2*$^{-/-}$ NMJs can be seen below A and B respectively (PSCs are indicated by dotted circles). ***C***, The change in Ca^{2+} response (%ΔF/F0) is significantly smaller at *lamb2*$^{-/-}$ NMJs than wild-type littermates ($P < 0.05$). ***D***, the ratio of responding PSCs at each NMJ was also significantly lower at mutant NMJs ($P < 0.05$). Wild-type, $n = 13$ and *lamb2*$^{-/-}$, $n = 6$.

4.3.4 Perisynaptic Schwann Cell activation is Mediated by Purinergic Receptors at Wild-type and *Lamb2*$^{-/-}$ Neuromuscular Junctions

We next examined the effect of purinergic transmission (P_{2Y}Rs) at P14-P16 soleus, since it has recently been shown that purinergic receptors on PSCs have an important role in regulating transmitter release from motor nerve terminals during development of NMJs (Todd & Robitaille, 2006; Darabid *et al.*, 2013). The significance of purinergic transmission on PSCs was ascertained by local application of the P_{2Y}R agonist ATP (10 μM) on PSCs at the NMJ. Local application of ATP resulted in matching Ca^{2+} responses between *lamb2*$^{-/-}$ PSCs and wild-type littermates (compare Figure 4.4*A* and 4.4*B*). Both genotypes presented rapid responses with similar changes in amplitude after application of ATP (wild-type; 295.4 ± 44.12% ΔF/F0, n = 27 vs. *lamb2*$^{-/-}$; 350 ± 38.24% ΔF/F0, n = 31, P > 0.05, Figure 4.4*C*). The ratio of responding PSCs per NMJ investigated was the same at wild-type and *lamb2*$^{-/-}$ NMJs (wild-type; 0.96 ± 0.03 PSCs/NMJ, n = 27 vs. *lamb2*$^{-/-}$; 0.98 ± 0.03 PSCs/NMJ, n = 31, P > 0.05, Figure 4.4*D*). These results indicate no change in the level of purinergic influence between *lamb2*$^{-/-}$ and wild-type PSCs.

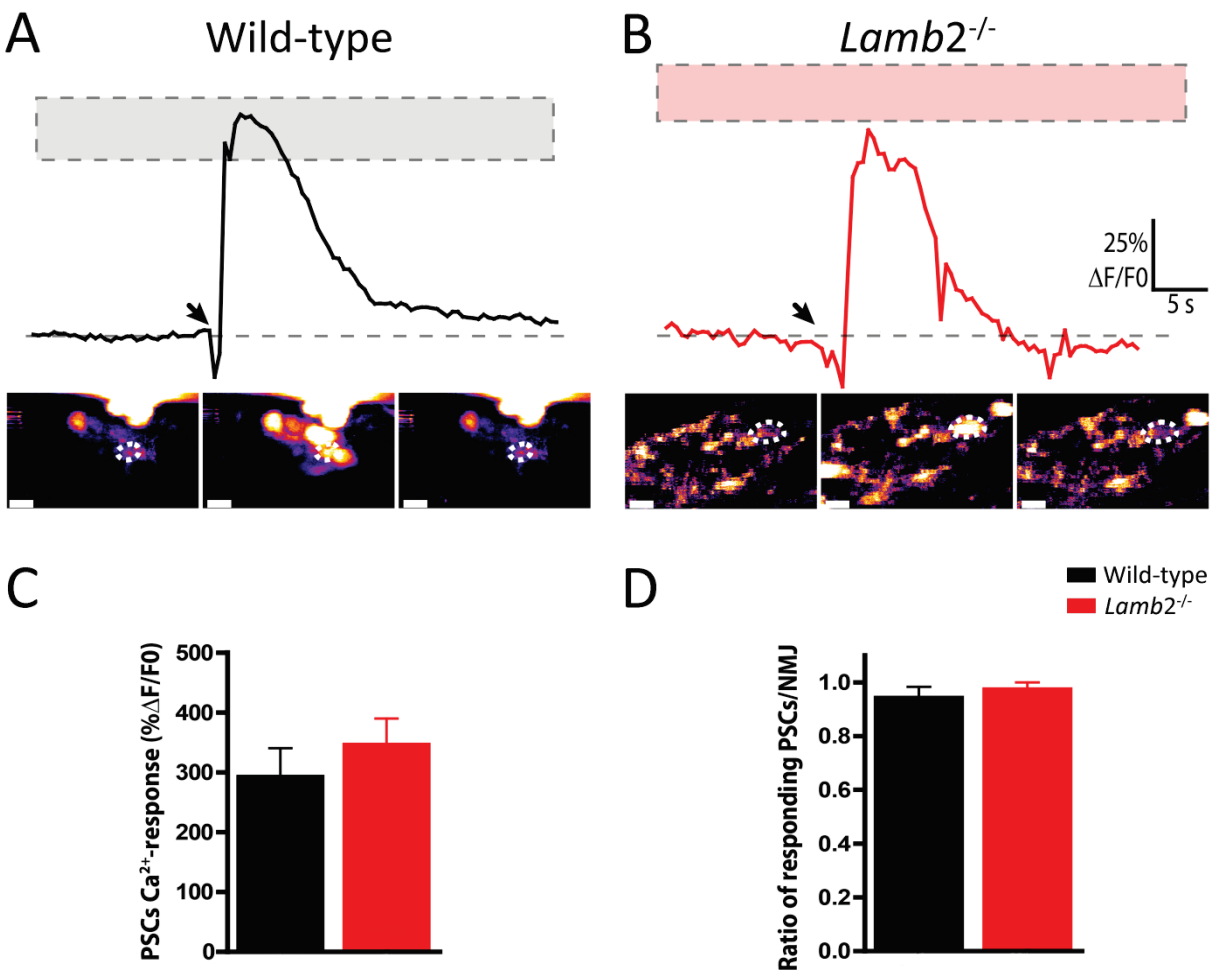

Figure 4.4 Perisynaptic Schwann Cells at Laminin-β2 demonstrate normal Response to Local Application of ATP

Both ***A***, wild-type and ***B***, *lamb*2$^{-/-}$ NMJs present comparable responses to local application of ATP (10 μM) (application indicated by arrow). Grey dashed line represents basal fluorescence with dashed boxes representing mean values of change in Ca^{2+} responses for the respective genotype. Corresponding snapshots of Ca^{2+} response for PSCs at wild-type and *lamb*2$^{-/-}$ NMJs can be seen below A and B respectively (PSCs are indicated by dotted circles). ***C***, No significant difference in Ca^{2+} response (%ΔF/F0) was observed between genotypes ($P > 0.05$). ***D***, the ratio of responding PSCs at each NMJ was not significantly different between genotypes. Wild-type, $n = 27$ and *lamb*2$^{-/-}$, $n = 31$.

4.3.5 Perisynaptic Schwann Cell activation by Muscarinic Receptors is reduced at *Lamb2*$^{-/-}$ Neuromuscular Junctions

The muscarinic receptors (mAChRs) have been shown to be the main receptor system by which matured PSCs regulate neurotransmission in adult NMJs (Rochon *et al.*, 2001). As shown in Figure 4.5*A*, local application of muscarine elicited a strong rapid PSC Ca^{2+} response at wild-type NMJs. By contrast, Figure 4.5*B* shows that PSCs at *lamb2*$^{-/-}$ NMJs have significantly lower responses to local application of muscarine. Analysis of the changes in Ca^{2+} response confirm this, with PSCs at mutant NMJs displaying significantly lower changes in Ca^{2+} levels (wild-type; 172.50 ± 34.17% ΔF/F0, n = 34 vs. *lamb2*$^{-/-}$; 70.83 ± 18.33% ΔF/F0, n = 37, $P < 0.005$, Figure 4.5*C*). The ratio of responding PSCs at each NMJ was also significantly lower at mutant NMJs (wild-type; 0.78 ± 0.06 PSCs/NMJ, n = 27 vs. *lamb2*$^{-/-}$; 0.49 ± 0.09 PSCs/NMJ, n = 31, $P < 0.005$, Figure 4.5*D*). These results suggest that the mature wild-type PSCs are more responsive to ACh via the muscarinic receptor than their *lamb2*$^{-/-}$ littermates, indicating persistent plasticity of PSCs at mutant NMJs.

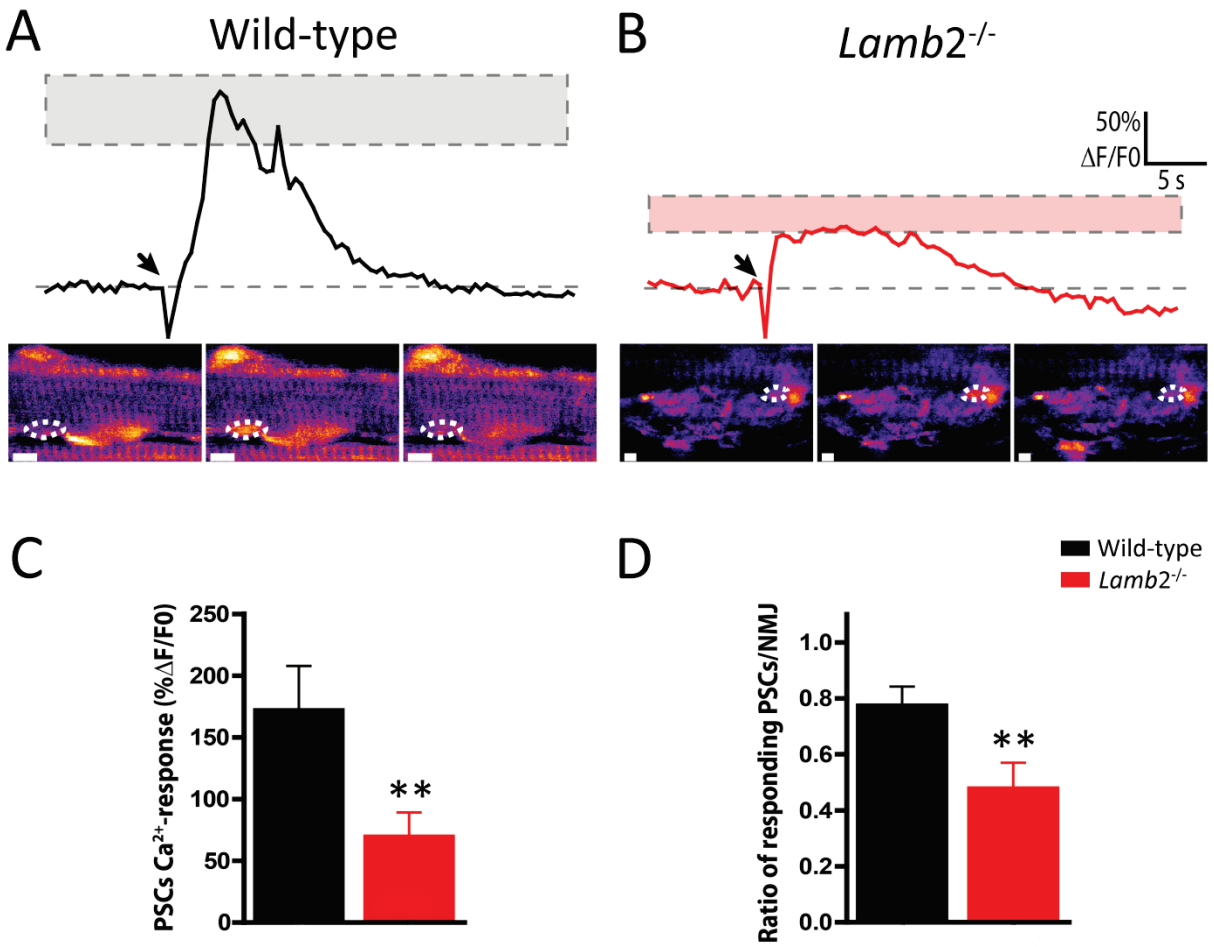

Figure 4.5 Perisynaptic Schwann Cell Excitability is decreased at Laminin-β2 Deficient Neuromuscular Junctions in Response to Local Application of Muscarine

A, wild-type PSCs demonstrate rapid response to local application of muscarine (10 μM) (application indicated by arrow). ***B***, PSCs at *lamb2*$^{-/-}$ NMJs demonstrate poor responses to muscarine application. Grey dashed line represents basal fluorescence with dashed boxes representing mean values of change in Ca^{2+} responses for the respective genotype. Corresponding snapshots of Ca^{2+} response for PSCs at wild-type and *lamb2*$^{-/-}$ NMJs can be seen below A and B respectively (PSCs are indicated by dotted circles). ***C***, The change in Ca^{2+} response (%ΔF/F0) is significantly smaller at *lamb2*$^{-/-}$ NMJs than wild-type littermates ($P < 0.005$). ***D***, the ratio of responding PSCs at each NMJ was also significantly lower at mutant NMJs ($P < 0.005$). Wild-type, $n = 34$ and *lamb2*$^{-/-}$, $n = 37$.

4.3.6 Perisynaptic Schwann Cells at *Lamb2*$^{-/-}$ Neuromuscular Junctions display Perturbed Morphological Distribution

Preliminary findings based on immuno-histochemical studies conducted by our collaborators (Houssam Darabid; Robitaille laboratory), indicate unusual distribution of PSCs at *lamb2*$^{-/-}$ NMJs. As shown in Figure 4.6, wild-type NMJs demonstrate good co-localisation of pre- and postsynaptic regions. The entire presynaptic region is capped by multiple PSCs that may aid in stability of the functional properties observed at wild-type NMJs. Mutant NMJs on the other hand, demonstrate decreased co-localisation of pre- and postsynaptic regions. In addition to this finding, we observed 'naked' AChR end-plate regions that were sparse of both presynaptic nerve terminals and PSCs. This irregular distribution may suggest maintained dynamic movement of PSCs at mutant NMJs leading to invasion of the synaptic cleft, while wild-type PSCs become more static in conjunction with the increase in stability as the NMJ reaches maturation(Noakes *et al.*, 1995a).

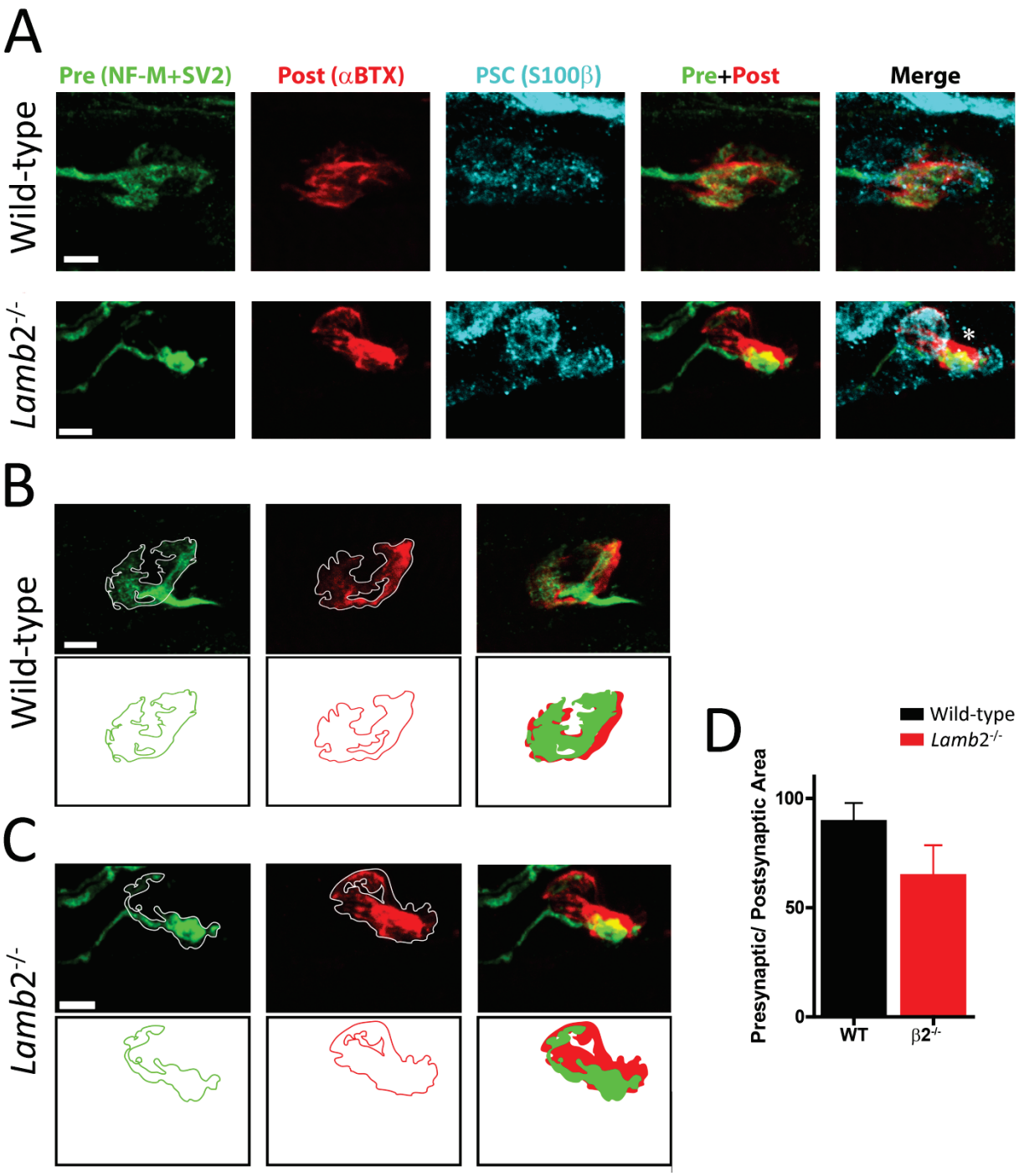

Figure 4.6 Immunohistochemical Labelling of Perisynaptic Schwann Cells at Wild-type and *Lamb2*$^{-/-}$ Neuromuscular Junctions

A, Labelling of presynaptic terminals (green), postsynaptic AChRs (red), and PSCs (blue) of mono-innervated (P14-P16) soleus NMJs from wild-type (top row) and *lamb2*$^{-/-}$ (bottom row) mice. Pre + Post and merge panels demonstrate co-localisation of the cellular bodies that comprise the NMJ. Multiple PSCs (blue) cap the presynaptic terminal at NMJs of both genotypes. Also note that at wild-type NMJs, multiple PSCs (blue) covered the entire postsynaptic end-plate area (red), while at mutant NMJs there is a 'naked' region (indicated by *; *lamb2*$^{-/-}$ merge panel). Co-localisation of pre- (green) and postsynaptic

(red) regions at ***B***, wild-type and ***C***, *lamb*2$^{-/-}$ NMJs. Rendering shows an evidently larger area of postsynaptic area not covered by the presynaptic area at mutant NMJs. ***D***, analysis of co-localisation shows a trend indicating a decrease in co-localisation of pre- and postsynaptic areas at *lamb*2$^{-/-}$ NMJs. Wild-type and *lamb*2$^{-/-}$, *n* = 4. Scale bars: 5 µm. Work conducted in whole by; Darabid, H. of the Robitaille Laboratory, Univ. Montreal.

4.4 DISCUSSION

The present study has indicated a delay in switching from mainly purinergic transmission in immature PSCs to predominantly muscarinic transmission in *lamb*2$^{-/-}$ when compared to wild-type PSCs. We observed significant reductions in transmitter release which correspondingly coincided with delayed maturation of PSCs. Mutant NMJs remained dependent on the purinergic receptor signalling pathway, which has been shown to be the primary receptor signalling pathway in activation of immature PSCs. Wild-type PSCs showed increasing dependency on muscarinic receptor signalling with a progressive and corresponding decline in purinergic contribution. Finally, our preliminary immuno-histochemical findings suggest poor arrangement of PSCs at the NMJ, which may contribute to decreased synaptic efficacy at *lamb*2$^{-/-}$ NMJs. We propose that the loss of laminin-β2 results in delayed maturation of PSCs at the NMJ, resulting in poor synaptic properties stemming from the functional and morphological traits of immature PSCs.

4.4.1 Laminin-β2 Deficiency Induced a decrease in Neurotransmission when Compared to Wild-type Junctions

Our electrophysiological recordings from the soleus NMJs are consistent with previously reported decreased neurotransmission in the diaphragm of *lamb*2$^{-/-}$ NMJs at postnatal day 18 (Knight *et al.*, 2003). Knight *et al.* (2003) observed a 15-fold decrease in the release frequency of spontaneous transmitter with no difference in quantal size at *lamb*2$^{-/-}$ NMJs, a finding attributed to reduced numbers of functional release sites due to poorly formed presynaptic terminals at mutant NMJs. The present study observed only a 50% decrease in spontaneous release frequency and decreased quantal size at *lamb*2$^{-/-}$ NMJs. These subtle differences in findings may be due to the muscle fibre types used in the investigations, with the soleus, a slow twitch fibre type muscle, perhaps able to sustain neurotransmission at low frequencies more effectively than the mixed fibre type diaphragm muscle. To ensure consistency with our electrophysiological studies we compared transmission in the diaphragm of *lamb*2$^{-/-}$ and wild-type NMJs from animals that we examined the soleus NMJs and obtained consistent results with those reported by Knight *et al.*, (2003). We advanced our understanding by demonstrating that the reason for poor neurotransmission at *lamb*2$^{-/-}$ NMJs may be due to a change in calcium channel subtype expression (see Chapter 3). Furthermore the loss of laminin-β2 has been shown to lead to invasion of the synaptic cleft by Schwann cell processes (Noakes *et al.*, 1995a; Patton *et al.*, 1998), with laminin-521, containing the β2 chain, thought to directly prevent invasion of the synaptic cleft by Schwann cells (Cho *et al.*, 1998; Patton *et al.*, 1998). Thus the defects in

neurotransmission associated with loss of laminin-β2 may be partly attributed to the entry of Schwann cell processes into the cleft as a result of altered PSC activity. However, we do not know whether the decline in neurotransmission leads to Schwann cell invasion of the synaptic cleft of already inactive release sites or that the Schwann cell invasion initiates decline in neurotransmission.

4.4.2 Laminin-β2 Deficient Neuromuscular Junctions respond differently in the Release of Transmitter during the Demands of High Frequency Stimulation

We compared the capacity of *lamb2*$^{-/-}$ and wild-type NMJs in the soleus preparation to sustain neurotransmission during high frequency stimulus. High frequency stimulation mimics tonic firing of the developing motor neurons innervating the soleus (Navarrete & Vrbová, 1983; Gorassini *et al.*, 2000; Buffelli *et al.*, 2002; Eken *et al.*, 2008). The activity of soleus motor units has been shown to progress from phasic short bursting activity to tonic activity after the first two weeks postnatal (Navarrete & Vrbová, 1983; Westerga & Gramsbergen, 1994; Buffelli *et al.*, 2002; Eken *et al.*, 2008), which coincides with maturation of the cellular elements comprising the NMJ. This change in input activity is associated with a change in muscle fibre type expression and consequently the development of the slow twitch fibre properties observed at the soleus. Studies have shown that altering the motor unit activity can inhibit the conversion of fast twitch fibre type IIA into slow twitch fibres type I in developing rodent soleus (Blewett & Elder, 1993; Elder & Toner, 1998). The decreased motor unit activity at *lamb2*$^{-/-}$ NMJs, reported here, may result in maintained presence of type IIA fibres which are not energy efficient and fatigue resistant. Thus the soleus of *lamb2*$^{-/-}$ mice are not functionally capable of handling the tonic impulses required of a healthy soleus in providing reliable postural support.

Here we show clear short and long-term deficits in neurotransmission at the NMJs of *lamb2*$^{-/-}$ mice. Mutant NMJs demonstrated a two-fold higher level of depression, which suggests that the terminals are not capable of sustaining tonic firing at high frequency, a demand required to be fulfilled by healthy soleus muscle in maintaining posture. Previous literature has shown a dispersal of synaptic vesicles at mutant NMJs, thus under high frequency stimulus *lamb2*$^{-/-}$ NMJs undergo severe depletion of the synaptic vesicles in the readily releasable pool (Noakes *et al.*, 1995a; Knight *et al.*, 2003). After high frequency stimulus, wild-type NMJs demonstrated potentiation due to priming of the nerve terminal by residual calcium that enters during successive stimuli and via activation of the Ca^{2+} calmodulin protein kinase II (CaMKII) phosphorylation of synapsin I (Huttner & Greengard, 1979). Mutant NMJs displayed a 70% reduction in facilitation, indicating impaired priming and decreased availability of synaptic

vesicles due to poor synaptic vesicle recycling to replenish the readily releasable pool. Furthermore, mutant NMJs displayed a prolonged recovery from depression adding support to the suggestion that vesicular recycling or transport/translocation impairment is responsible for the decrease in transmitter release. Overall the present findings indicate that supply of vesicles to the active zone cannot keep up with the demand imposed by frequent stimulation in the laminin-β2 deficient NMJs.

4.4.3 Perisynaptic Schwann Cell Excitability is decreased at Laminin-β2 Deficient Neuromuscular Junctions in response to High Frequency Stimuli

Based on our functional findings, *lamb*2$^{-/-}$ NMJs are not capable of dealing with high frequency tonic stimulus patterns. PSCs are able to modulate neurotransmission by detecting and decoding synaptic activity thus enhancing or depressing transmitter release (Jahromi *et al.*, 1992; Robitaille, 1995). This modulation is thought to be mediated by calcium handling involving PSC membrane receptors such as purinergic and muscarinic (Jahromi *et al.*, 1992; Reist & Smith, 1992). Under high frequency activity the PSCs at mutant NMJs displayed significantly smaller Ca^{2+} responses (~50% of wild-type responses), suggesting poor PSC excitability by the release of endogenous neurotransmitter from the presynaptic terminal. The number of PSCs responding to the stimuli was also found to be decreased at mutant NMJs. These findings suggest a correlation between the poor PSC excitability at *lamb*2$^{-/-}$ NMJs and the perturbed neurotransmission properties observed. We suggest that PSCs at *lamb*2$^{-/-}$ are not be able to detect and decode the 'foreign' high frequency input as they may not possess the correct signalling receptors to be activated by endogenous neurotransmitter under high frequency conditions. The vesicles within motor nerve terminals store a number of transmitters including ACh and ATP, which are released during stimulation resulting in not only activation of postsynaptic receptors but also presynaptic receptors to enhance or auto-inhibit further release of transmitters (Bennett *et al.*, 1991). PSCs also harbour these receptors which when activated alter their excitability and thus effect the micro-extracellular environment of neurons and terminals. The decrease in transmitter release from the nerve terminals of *lamb*2$^{-/-}$ NMJs may contribute to the lower excitability of PSCs with subsequent lower feedback to the nerve terminals.

4.4.4 Perisynaptic Schwann Cells at *Lamb2*$^{-/-}$ Neuromuscular Junctions demonstrate normal Purinergic Signalling with poor Excitability via the Muscarinic Receptor Signalling Pathway

In the present study we have shown that there is no difference in purinergic influence on neurotransmission between the developing wild-type and *lamb2*$^{-/-}$ NMJs. Robitaille and colleagues have previously examined the development and maturation of the receptor signalling pathways of PSCs. At developing NMJs, PSCs are almost completely activated via the purinergic receptors (P_{2Y}Rs) while at matured NMJs transmission is modulated via a combination of purinergic and muscarinic receptors (Rochon *et al.*, 2001; Darabid *et al.*, 2013). Here we found comparable PSC Ca^{2+} responses after local application of the purinergic receptor agonist (ATP) at wild-type and *lamb2*$^{-/-}$ NMJs, suggesting no difference in the receptor signalling pathway mediating activation of PSCs during development. Application of muscarine elicited poor responses at mutant NMJs, while PSCs at wild-type NMJs demonstrated a greater responsiveness. Investigation of the mAChR signalling pathway at *lamb2*$^{-/-}$ NMJs showed defective excitability of mutant PSCs, with less cells responding compared to PSCs at wild-type NMJ. These findings suggest that wild-type PSCs have developed suitable dependence on both the purinergic and muscarinic receptor pathways as expected at a matured NMJ. By contrast, PSCs at *lamb2*$^{-/-}$ NMJs demonstrated maintained dependence on purinergic receptor signalling, a characteristic of PSCs at immature NMJs. Darabid *et al.* (2013) demonstrated the presence of functional mAChRs at developing NMJs, however these receptors did not contribute to synaptic activation of PSCs. The study went on to propose that the absence of mAChRs in proximity to active zones may be responsible for the lack of involvement in synaptic-induced PSC activation at developing NMJs.

4.4.5 Perisynaptic Schwann Cells at *Lamb2*$^{-/-}$ Neuromuscular Junctions display Perturbed Morphological Distribution

It has previously been shown that the development of the postsynaptic end-plate region in *lamb2*$^{-/-}$ NMJs remains immature (see Chapter 3). Mutant mice displayed smaller end-plate regions as well as poor morphological development, with maintained diffuse plaque-like structure compared to the convoluted wild-type end-plate region. The preliminary immunohistochemistry study conducted by Houssam Darabid (Robitaille Laboratory, Univ. Montreal), again highlights perturbed morphology of *lamb2*$^{-/-}$ NMJs and the associated PSCs. Wild-type NMJs, presented good co-localisation of pre- and postsynaptic regions. Of note, the entire presynaptic terminal was completely covered by multiple PSCs, this

close interaction between PSCs and pre-/ postsynaptic structures likely facilitates communication and thus promotes efficient modulation of neurotransmission. By contrast, *lamb*2$^{-/-}$ NMJs appear to show lesser co-localisation of pre- and postsynaptic regions. In addition to this it was noted that some regions of the presynaptic terminal contained regions bare of PSCs. These 'naked' regions may in part lead to poor detection of synaptic signals and subsequently lower levels of neuromodulation at mutant NMJs. We propose that these abnormal PSC and NMJ morphologies may be due to the immature phenotype of *lamb*2$^{-/-}$ NMJs. During development, PSCs are highly dynamic with movement and are constantly extending and retracting processes in response to neural signalling (Brill *et al.*, 2011). As PSCs mature they become more compartmentalised and territorial of regions which envelop the presynaptic terminal. This progressive loss of dynamism is associated with an increase in NMJ stability and enhanced reliability of neurotransmission. Thus, it is likely that the maintained dynamism contributes to irregular PSC distribution at the presynaptic terminal, subsequently resulting in poor ability of mutant PSCs to reliably detect and decode neurotransmission at *lamb*2$^{-/-}$ NMJs.

4.5 CONCLUSION

Deletion of laminin-β2 at the NMJ results in functional and morphological changes at the pre- and postsynaptic regions, as well as in the PSCs themselves. In comparing these changes with NMJs from wild-type littermates, we noted a decrease in quantal content which was attributed to a decrease in the number of active release sites. These functional observations were supported by previous morphological findings, which indicated a decrease in the number of active zones. Also it was noted that the laminin-β2 deficient NMJs had fewer PSCs associated with nerve terminal structures with some even being 'naked'. Terminal structures without the proper support of PSCs may be destined to be eliminated. Communication between nerve terminal structures and PSCs may play a vital role in the development of properly functioning synapses. It is not clear what comes first, the decrease in transmission or the decline in PSCs numbers and/or function. These observations suggest that laminin-β2 is involved in establishing mature and structured PSCs that are capable of detecting and decoding synaptic activity, which consequentially possess the ability to appropriately modulate neurotransmission.

CHAPTER 5

Functional Analysis of Neurotransmission in Laminin-α4 Deficient Mice during Development

ABSTRACT

Synaptic basal lamina such as laminin-421 (α4β2γ1), mediate differentiation of the neuromuscular junction (NMJ). Laminins interact with other synaptic molecules to provide stability and ensure precise alignment of the pre- and postsynaptic specialisations. Targeted mutation of the *lama4* gene does not alter NMJ morphogenesis, with normal formation and numbers of active zones and junctional folds. However, mice deficient in laminin-α4 (*lama*4$^{-/-}$) display disruptions in the precise alignment of active zones and postsynaptic folds at the NMJ. The functional consequences of laminin-α4 loss have not been previously examined. The present study investigated the differences in neurotransmission during early development and maturation of the NMJ in *lama*4$^{-/-}$ and wild-type mice. Our results indicated clear changes in neurotransmission between mutant and wild-type NMJs involving pre- and postsynaptic differences. In *lama*4$^{-/-}$ NMJs we observed a significant decrease in miniature end-plate potentials (MEPPs) frequency and an increase in the mean amplitude of MEPPs. In *lama*4$^{-/-}$ NMJs we observed a significant decrease in quantal content which was wholly explained by an increase in intermittence of evoked transmitter release, as mean amplitude of end-plate potentials increased in mutants (when failures were excluded from analysis). Mutants also displayed significantly higher levels of synaptic depression under high frequency stimulus and altered paired pulse facilitation compared to wild-type littermates. Analysis of the binomial parameters of neurotransmitter release demonstrated a decrease in quantal release as a result of a decrease in the number of active release sites but not in the probability of transmitter release. Our findings demonstrate altered distribution and expression of presynaptic components associated with active zones, specifically an increase in the number of synaptic vesicles and a decrease in the density of the fluorescently labelled Bassoon at the active zone region. From these findings we conclude that laminin-α4 is critical for alignment of active zone elements like Bassoon and the ready releasable pool of vesicles with the high density of post-synaptic AChRs found at the crests of the postsynaptic folds. Our results suggest that the fewer active release sites may compensate for the deficits of the *lama*4$^{-/-}$ NMJs by postsynaptic alterations.

5.1 INTRODUCTION

Signalling and adhesion molecules such as laminin-421 (α4β2γ1) have been shown to play an integral role in the organisation of the neuromuscular junction (NMJ) (Noakes *et al.*, 1995a; Cho *et al.*, 1998; Patton *et al.*, 1998). The laminin-α4 chain, found concentrated specifically at the synaptic cleft from embryonic day 14, has been shown to be important for co-localisation of pre- and postsynaptic specialisations (Miner *et al.*, 1997; Patton, 2000; Patton *et al.*, 2001; Carlson *et al.*, 2010). Mice deficient in laminin-α4 (*lama*4$^{-/-}$) undergo normal synaptogenesis, with similar formation and number of active zones as well as normal postsynaptic membrane folding, as seen at wild-type NMJs (Patton *et al.*, 2001). Notably however, the precise apposition of active zones and postsynaptic folds fails to develop at *lama*4$^{-/-}$ NMJs, with over 70% of active zone regions displaying misalignment to postsynaptic specialisations (Patton *et al.*, 2001). These findings indicate that the laminin-α4 chain does not play a role in the formation and development of specific synaptic components. This hypothesis is supported by the presence of laminin-α4 in highest concentrations between postsynaptic folds rather than at the crest of the folds, suggesting it likely plays an instructive role in the placement of postsynaptic specialisations such as acetylcholine receptors (AChRs), by signalling regions where active zones or folds should not form during development.

The NMJs of *lama*4$^{-/-}$ mice do not display severe morphological defects and abnormalities when compared to mice lacking laminin-β2 (*lamb*2$^{-/-}$) (Patton *et al.*, 2001). Mice lacking laminin-α4 appear healthy and grow at a rate similar to wild-type littermates, whereas *lamb*2$^{-/-}$ mice display stunted growth and die after weaning. This may be a result of the laminin-β2 chain being present in all three heterotrimers found specifically in the synaptic basal lamina, while the laminin-α4 chain is present only in laminin- 421 (Patton, 2000; Carlson *et al.*, 2010). Patton *et al.* (2001), found that at two months of age mice deficient in laminin-α4 displayed uncoordinated hindlimb movement when held by the tail, and were noted to occasionally drag their hindlimbs when walking, suggestive of neuromuscular dysfunction. Histological analysis showed no evident signs of myopathy or dystrophy in muscle fibres with preserved size and shape, as well as normal contractile properties in *lama*4$^{-/-}$ mice (Patton et al., 2001). However, no studies have yet investigated the functional capacity of neurotransmission at *lama*4$^{-/-}$ NMJs.

Given that literature has focused largely upon the morphological changes associated with loss of laminin-α4, the present study examined the functional neurotransmission properties at *lama*4$^{-/-}$ NMJs during development and maturation. Here, we functionally measured neurotransmission using electrophysiology to characterise these properties during development, from postnatal day 8 (P8) to postnatal day 18 (P18). We observed alterations in neurotransmission at *lama*4$^{-/-}$ NMJs at P8, which became more apparent by P18. Perturbations observed were comparable in each of the muscle fibre types investigated at P18. We also show that these functional changes are associated with a change in morphology of the pre- and postsynaptic regions, specifically we observed an increase in synaptic vesicle staining and a decrease in the active zone marker density. Our findings suggest modifications at both the pre- and postsynaptic regions, as a long-term compensatory response to the misalignment observed at *lama*4$^{-/-}$ NMJs.

5.2 METHODS

5.2.1 Ethics approval

The University of Queensland Animal Care and Ethics Committee approved all procedures undertaken (Ethics number 152/12) and were in accordance with the Queensland Government Animal Research Act 200, associated Animal Care and Protection Regulations (2002 and 2008), as well as the Australian Code for the Care and Use of Animals for Scientific Purposes, 8th Edition (National Health and Medical Research Council, 2013).

5.2.2 Animals

Wild-type mice (with two normal copies of all laminin genes) and homozygous mutant mice (with no normal copies of the *lama*4 gene) were used in this investigation. Mice were obtained from the mating of homozygous males and females and maintained on a defined C57BL/6-129SvJ genetic background. Mice of either sex were used in this study and age-matched for postnatal days 8 and 18. Mice were anaesthetised with rising concentrations of carbon dioxide and then killed by cervical dislocation. A minimum of five age-matched pairs was used at each age group for both electrophysiological and histological procedures detailed below.

5.2.3 Electrophysiology

Tissue Preparation

Diaphragm, *extensor digitorum longus* (EDL) and *soleus* (SOL) muscles with associated innervating nerves were dissected free and pinned to the bottom of a Sylgard-coated recording chamber. The preparation was perfused at a rate of 3 mL min^{-1} with Tyrode solution (composition (mM): NaCl 123.4; KCl 4.7; NaH_2PO_4 1.3; $NaHCO_3$ 16.3; $MgCl_2$ 1.0; glucose 7.8; $CaCl_2$ 0.1 - 0.3; pH 7.3). The reservoir supplying the bath was continuously gassed with 95% O_2 and 5% CO_2 and maintained at room temperature 22 ± 2^{0}C. All reagents unless specified were supplied by Sigma Chemicals Australia.

Electrical Stimulation

The innervating nerve supplying the associated muscle was gently sucked into a glass pipette filled with Tyrode solution. This pipette acted as a stimulating electrode utilising two silver chloride wires, one passing within the pipette as a positive electrode and the other outside as the negative electrode. The phrenic nerve was stimulated with square wave pulses of 15-20 V intensity, 0.08 ms duration at a frequency of 0.2 Hz, using a Grass Instruments stimulator (SD48) coupled to a Grass stimulus isolator (SIU5).

Extracellular Recordings

Extracellular recordings of nerve terminal impulses (NTI), end-plate currents (EPCs) and miniature end-plate currents (MEPCs) were obtained, as previously described (Knight *et al.*, 2003). In brief, coarse glass micropipettes (2-10 µm in diameter) filled with Tyrode solution were positioned on the surface of muscle fibres until sharp rise times of less than 1 ms were detected for both EPCs and MEPCs. The frequency of EPCs and MEPCs were carefully monitored while the electrode was lowered as electrode pressure may give rise to increased frequency of spontaneous activity (Fatt & Katz, 1952; Bennett *et al.*, 1986a; Bennett *et al.*, 1986b). After a recording site was located the stimulus was ceased for a five-minute period before commencing recordings of EPCs and MEPCs. This allowed for replenishment of vesicular pools at the nerve terminals. Five to six recording sites were selected from each muscle preparation with 100-200 stimulations and at least 30 MEPCs recorded at each site.

Intracellular Recordings

Fine tipped glass microelectrodes (30 to 50 MΩ) filled with 2 M KCl were used to record end-plate potentials (EPPs), miniature end-plate potentials (MEPPs) and resting membrane potentials (RMPs). Recorded signals were amplified using an Axoclamp 2B amplifier (Axon Instruments, USA) and digitised to 20-40 kHz sampling rate using MacLab system and Scope software (Version 3.5.5, ADInstruments, CO, USA). Electrodes were manipulated to impale muscle fibres within 0.5 mm of the end-plate region. Proximity to end-plate regions was confirmed through analysis of EPP and MEPP rise times, sites with rise times greater than 1.5 ms were rejected for wild-type mice and times greater than 2 ms rejected for mutant mice. During recordings the initial resting membrane potential (RMP) values were in the range of 70-80 mV with these values undergoing a gradual decrease to steady values between 55-65 mV. Recordings were terminated if the RMP fluctuated by more than 10% from the steady values.

Paired Pulse Facilitation

The facilitation of wild-type and mutant NMJs was investigated by applying twin pulse stimuli at 10, 20, 40 and 60 ms delays with Tyrode solution containing 0.3 mM [Ca^{2+}] and 1 mM [Mg^{2+}]. The degree of facilitation was evaluated using the facilitation index (*fi*): *fi* = A_2/A_1 where A_2 is the average of the EPP amplitudes elicited by the second stimulus and A_1 is the average of the EPP amplitudes elicited by the first stimulus. A total of six wild-type and six laminin-α4 deficient mice were studied at both age groups.

5.2.4 Wholemount Immunohistochemistry

Diaphragm muscles were dissected free from wild-type and mutant mice at P18. The muscles were incubated with Alexa Fluor 555 α-bungarotoxin (αBTX) for 30 minutes followed by washing with Tyrode solution. The tissues were then fixed with 2% paraformaldehyde in 0.1 M phosphate buffered saline, pH 7.4 (PBS) at room temperature for 20 minutes followed by consecutive washing with PBS. Immunofluorescence double staining was performed to determine the localisation and distribution of presynaptic components such as the active zone marker; Bassoon, and synaptic vesicles with respect to postsynaptic AChRs in diaphragm muscles. The fixed diaphragm muscles were blocked with PBS containing 2% bovine serum albumin (BSA), 2% goat serum and 0.5% Triton X-100 (TX-100). The muscles were then incubated with the following primary antibodies overnight at 4^0C; mouse anti-Bassoon (Enzo Life Sciences; SAP7F407 clone; Nishimune *et al*., 2004; Chen *et al*., 2011), and mouse anti-SV2 (Developmental Studies Hybridoma Bank; Knight *et al.*, 2003; Chen *et al.*, 2012). The tissues were rinsed with 0.5% TX-100 prior to incubation with the appropriate Alexa Fluor 488-conjugated secondary antibodies (Molecular Probes, Invitrogen, Eugene OR, USA) at 4^0C for 5 hours. The tissues were then washed with PBS, mounted in Prolong Gold anti-fade reagent (Molecular Probes, Invitrogen) and cover-slipped.

5.2.5 Image Acquisition and Analysis

Tissues were imaged with an Olympus Fluoview FV1000 confocal laser scanning microscope, equipped with two excitation diode laser lines (473 nm and 559 nm) running on Fluoview FV10-ASW software version 01.07C. Images were taken at a resolution of 1024 by 1024 pixels, using a 100x/ 1.35 NA Oil Iris UPlan-Apochromat objective with a Z-step size of 0.3 µm. Images were captured using identical laser power levels, photomultiplier gain levels, scanning speed and pinhole size amongst different slides using the same antibody. Imaris x64 7.1.0. (Bitplane, South Windsor, CT, USA) was used to analyse Z-stacked images for volume measurement of synaptic vesicles and postsynaptic end-plate. Synaptic vesicles targeted by mouse anti-SV2, stained with Alexa Fluor 488-conjugated secondary antibody and postsynaptic AChR end-plates stained with Alexa Fluor 555 αBTX, were reconstructed into 3-dimension (3D) using a surface-rendering algorithm based on local contrast in fluorescent z-stacks as previously described (Caillol *et al.*, 2012; Fogarty *et al.*, 2013). The density of synaptic vesicles at each junction was then determined by dividing the volume of the 3D reconstruced SV2-stained region over the 3D reconstructed end-plate volumes. The end-plate volume is defined as the entire 3D reconstructed end-plate inclusive of interstitial spaces.

The density of active zones as labelled by the presynaptic active zone marker, Bassoon was analysed from the captured Z-stack images. Fiji software was utilised to perform auto threshold on the Bassoon stained images, which then allowed for counting of number of Bassoon puncta objectively, as previously described in Chen *et al.* (2012). The density of Bassoon puncta was determined by dividing the number of Bassoon puncta at each junction over the area of the corresponding end-plates. The area of the end-plates were measured using Image J software (Abramoff *et al.*, 2004). All image analysis was completed under double blinded conditions. Student's *t*-tests were used to quantitatively compare the expression of these NMJ components between wild-type and mutant junctions at P18. Results are expressed as mean ± SEM with statistical significance accepted at $P < 0.05$.

5.2.6 Data Analysis

Extracellular recording sites were analysed if the frequency of EPCs and MEPCs did not change as a result of electrode pressure and if a single EPC was recorded within the first ten stimuli. Intracellular recordings were included if at least 100 EPPs and 30 MEPPs were recorded. Quantal content $(\bar{m})$ was determined using method of failures (Del Castillo & Katz, 1954b): $\bar{m}$ = $\log_e$ (number of stimuli/ number of failures) utilising intracellular electrophysiological recordings. Binomial parameters were calculated from intracellular recording data using methods previously described by Bennett and Florin (1974). The rise times, decay times, amplitude and frequency of evoked and spontaneous releases were calculated and tabulated for each experimental group. Unpaired two-tailed *t*-tests were performed to compare mean values of wild-type and *lama4*$^{-/-}$ mice. Results are expressed as mean ± SEM with statistical significance accepted at $P < 0.05$.

5.3 RESULTS

5.3.1 Loss of Laminin-α4 resulted in altered Spontaneous and Evoked Transmitter Release

The present study investigated the potential changes in neurotransmission properties that may arise from the misalignment of pre- and postsynaptic specialisation observed in *lama*4$^{-/-}$ NMJs. As this misalignment of synaptic specialisations occur from as early as P12, we examined NMJs from postnatal day 8 (immature) to postnatal day 18 (mature) (Balice-Gordon *et al.*, 1993; Balice-Gordon & Lichtman, 1993; Balice-Gordon, 1997; Culican *et al.*, 1998; Marques *et al.*, 2000; Patton *et al.*, 2001). At both age groups the resting membrane potential recorded via intracellular electrophysiology was comparable to that of age-matched wild-type muscle fibres (Table 5.1). Analysis of spontaneous transmitter release, showed a significant increase in MEPP amplitude at both P8 ($P < 0.05$) and P18 ($P < 0.01$) at *lama*4$^{-/-}$ NMJs compared to wild-types of the same age (Table 5.1, Figure 5.1*A* and 5.1*B*). At P8, both wild-type and mutant NMJs displayed a low frequency in spontaneous transmitter release. Difference in MEPP frequency become evident at P18 when the rate significantly increased from 3.45 ± 0.43 to 18.73 ± 2.65 min^{-1} ($P < 0.001$) in the wild-type NMJs and for the *lama*4$^{-/-}$ NMJs MEPP frequency significantly increased from 2.56 ± 0.52 to 8.68 ± 0.76 min^{-1} ($P < 0.0001$, Table 5.1). A comparison of the relative change between *lama*4$^{-/-}$ NMJs and wild-type MEPP frequency indicated a greater increase in the wild-type NMJs (5.4 fold increase in the wild-type compared with a 3.4 fold increase in the *lama*4$^{-/-}$ NMJs) ($P < 0.01$, Table 5.1). We observed an increase of 60% in MEPP time course (rise time and decay time) at P8 mutant NMJs compared to wild-type ($P < 0.01$) (Figure 5.1*A*; compare black to red spontaneous traces). By P18, *lama*4$^{-/-}$ NMJs showed a decrease in MEPP time course but were still significantly longer than those observed at wild-type NMJs ($P < 0.05$). This increased time may be a result of decreased levels of acetylcholinesterase (AChE) in the synaptic cleft, which is necessary for the breakdown of bound ACh at the postsynaptic AChRs and/or a more diffuse distribution of AChRs, or potentially a broader delay in the release of transmitter release from active zones.

Evoked transmitter release was examined under conditions of low probability of release (0.3 mM Ca^{2+} and 1.0 mM Mg^{2+}). Comparison of the distributions of EPP amplitude and frequency of observations for wild-type and *lama*4$^{-/-}$ NMJs indicated positively skewed distribution with a large number of stimuli failing to evoke an EPP in both *lama*4$^{-/-}$ and wild-type NMJs, at both ages (Figure 5.1*A*). Mutants however had higher levels of failures with

a slightly greater tail in the distribution indicative of greater EPP amplitudes being registered. Mutant NMJs displayed higher EPP amplitudes compared to wild-type (Figure 5.1*A*; compare black evoked to red evoked traces). Importantly, we observed a significant increase in intermittence of transmitter release at *lama*4$^{-/-}$ NMJs compared to wild-type. At P8, the failure rate of evoked response for mutant NMJs was 53.47 ± 2.81% compared to 29.28 ± 3.26% for wild-type, a 82.6% higher failure rate ($P < 0.0001$, Table 5.1). As the NMJ matured, the rate of failures increased at wild-type NMJs to 43.73 ± 3.24%, while *lama*4$^{-/-}$ NMJs maintained a failure rate of 58.30 ± 3.17%, which was 33.3% higher in intermittence than the wild-type ($P < 0.01$, Table 5.1 & Figure 5.1*B*).

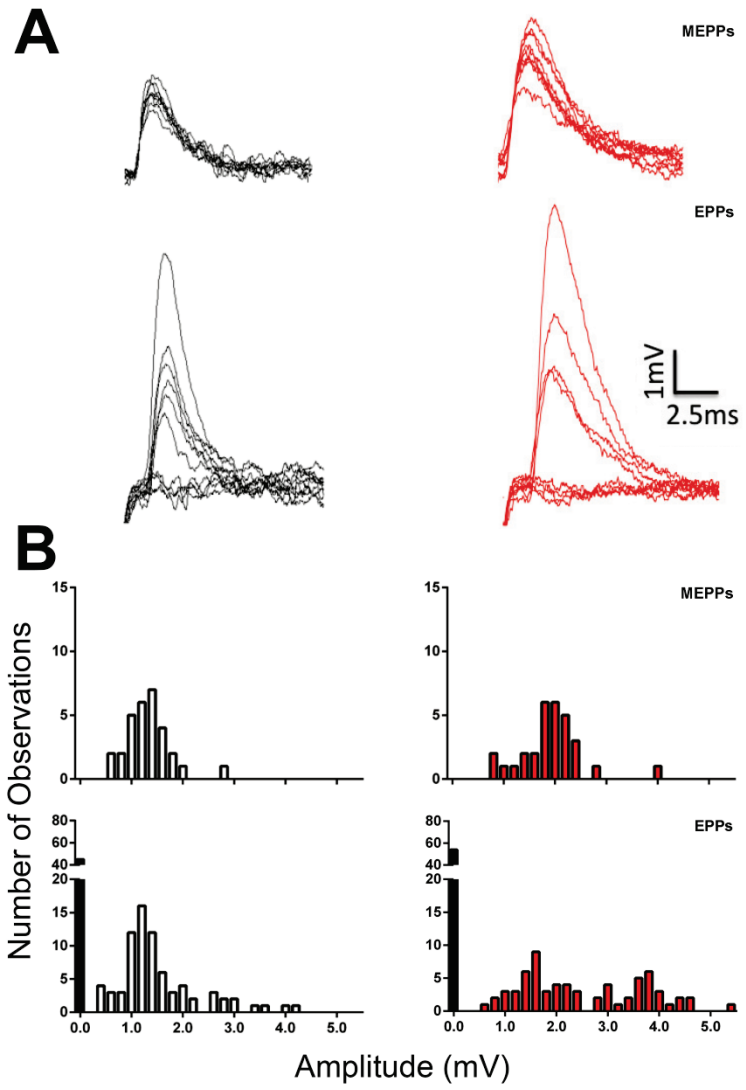

Figure 5.1 Intracellular Recordings from Wild-type and *Lama4*$^{-/-}$ Neuromuscular Junctions in Diaphragm Muscle at Postnatal Day 18

A, sample traces of MEPPs (10 consecutive spontaneous recordings) and EPPs (10 consecutive evoked recordings) from wild-type (black traces) and *lama4*$^{-/-}$ (red traces) NMJs. ***B***, frequency histograms were constructed based on recordings of spontaneous (top row) and evoked (bottom row) amplitude recordings for wild-type (black hollowed bars) and mutant NMJs (red hollowed bars) respectively. Histograms shown are from a single NMJ recording from each genotype that exemplifies distributions observed in this study. Distribution of both MEPP and EPP responses displayed a rightward skew at *lama4*$^{-/-}$ NMJs compared to wild-type, indicating an increased number of higher amplitude responses observed at mutant junctions. As indicated by solid black bars, *lama4*$^{-/-}$ NMJs displayed higher rate of failures in response to stimuli compared to wild-type.

Table 5.1. Comparison of Neurotransmission in the Diaphragm Muscle using Intracellular Electrophysiological Recordings

	Age (Postnatal days)			
	P8		P18	
Genotype	Wild-type	*Lama4*$^{-/-}$	Wild-type	*Lama4*$^{-/-}$
n number	5	6	5	6
Number of junctions				
MEPP	32	45	40	48
EPP	30	44	41	50
RMP (mV)	-57.29 ± 1.43	-59.27 ± 0.90	-56.33 ± 0.73	-58.60 ± 1.29
MEPP Amplitude (mV)	0.88 ± 0.05	1.09 ± 0.06*	0.95±0.04	1.18 ± 0.06**
MEPP time course (ms)	6.14 ± 0.24	9.83 ± 0.54**	6.04 ± 0.39	7.11± 0.37*
MEPP rise time (ms)	1.31 ± 0.01	1.56 ± 0.10	1.64 ± 0.04	1.44 ± 0.10
MEPP decay time (ms)	4.83 ± 0.24	8.27 ± 0.52**	4.38 ± 0.32	5.56 ± 0.30*
MEPP frequency (min^{-1})	3.45 ± 0.43	2.56 ± 0.52	18.73 ± 2.65	8.68 ± 0.76**
Percentage Failures (%)	29.28 ± 3.26	53.47 ± 2.81****	43.73 ± 3.24	58.30 ± 3.17**

* $P < 0.05$; ** $P < 0.01$; **** $P < 0.0001$

5.3.2 Loss of Laminin-α4 did not alter Action Potential Conduction

The higher intermittence of transmitter release observed at *lama*4$^{-/-}$ NMJs may be due to an impairment of action potential propagation along the nerve terminals. Patton *et al.* (1997) have previously shown the presence of laminin-α4 at the basal lamina of the peri-neural sheathing of peripheral nerve branches. Thus loss of laminin-α4 may result in failure of action potential to conduct along the motor axon and subsequently lead to the higher intermittence of transmitter release we observed in the present study. To address this possibility we used focal extracellular recordings to observe the nerve terminal impulse (NTI) at mutant NMJs at both P8 and P18. We found normal presence of NTIs with no variation or intermittence at both mutant and wild-type NMJs (Figure 5.2*A*, evoked responses). These findings suggest no significant change in conductance of action potentials at *lama*4$^{-/-}$ NMJs, therefore the observed increased intermittence of release is not due to a failure of action potential invasion of the presynaptic terminal but more likely due to failure of the depolarisation-secretion mechanisms. At both age groups investigated the latency at *lama*4$^{-/-}$ NMJs averaged 14.5% slower than those measured at wild-type junctions ($P > 0.05$, Table 5.2). This difference prompted us to closely examine for changes in the time course of MEPCs and EPCs during development and maturation of *lama*4$^{-/-}$ and wild-type NMJs.

Analysis of spontaneous release demonstrated an evident increase in MEPC amplitude at *lama*4$^{-/-}$ NMJs compared to wild-types. During early development, the MEPC amplitude of wild-type NMJs was 20% lower at 122.4 ± 5.73 μV compared to 147.1 ± 13.74 μV at *lama*4$^{-/-}$ NMJs ($P < 0.05$, Table 5.2). By P18, the difference in MEPC amplitude rose to 52%, with wild-type at 106.1 ± 5.89 μV compared to *lama*4$^{-/-}$ NMJs at 162.1 ± 12.50 μV ($P < 0.01$) (Table 5.2 & Figure 5.2). We also observed an increase in MEPC time course at *lama*4$^{-/-}$ NMJs compared to wild-type NMJs, which increased further with maturation (P8; $P < 0.05$, P18; $P < 0.01$). MEPC rise time was significantly greater for P18 mutant NMJs compared to wild-type NMJs (wild-type; 0.26 ± 0.01 ms, $n = 6$ vs. *lama*4$^{-/-}$; 0.30 ± 0.01, $n = 7$, $P < 0.001$). EPC amplitude was significantly increased at *lama*4$^{-/-}$ NMJs compared to wild-type, again becoming more evident as the NMJs reached maturation. At P8, wild-type displayed mean EPC amplitudes of 230.2 ± 10.8 μV compared to 281.0 ± 16.8 μV at *lama*4$^{-/-}$ NMJs ($P < 0.05$). By P18, mutant responses increased by 76% to 494.7 ± 58.8 μV while wild-type EPC amplitude was maintained at 233.0 ± 19.6 μV ($P < 0.001$, Table 5.2 & Figure 5.2*A*). These changes were clearly evident by a rightward shift in the examples of mean EPC amplitude versus number of observation histograms shown in Figure 5.2*B*. Corresponding with this increase in EPC amplitude, we noted an increase in the rise time at P8 (wild-type; 0.64 ± 0.01 ms vs. *lama*4$^{-/-}$; 0.82 ± 0.03 ms, $P < 0.001$) and P18 (wild-type; 0.52 ± 0.02 ms vs. *lama*4$^{-/-}$; 0.63 ± 0.01 ms, $P < 0.01$).

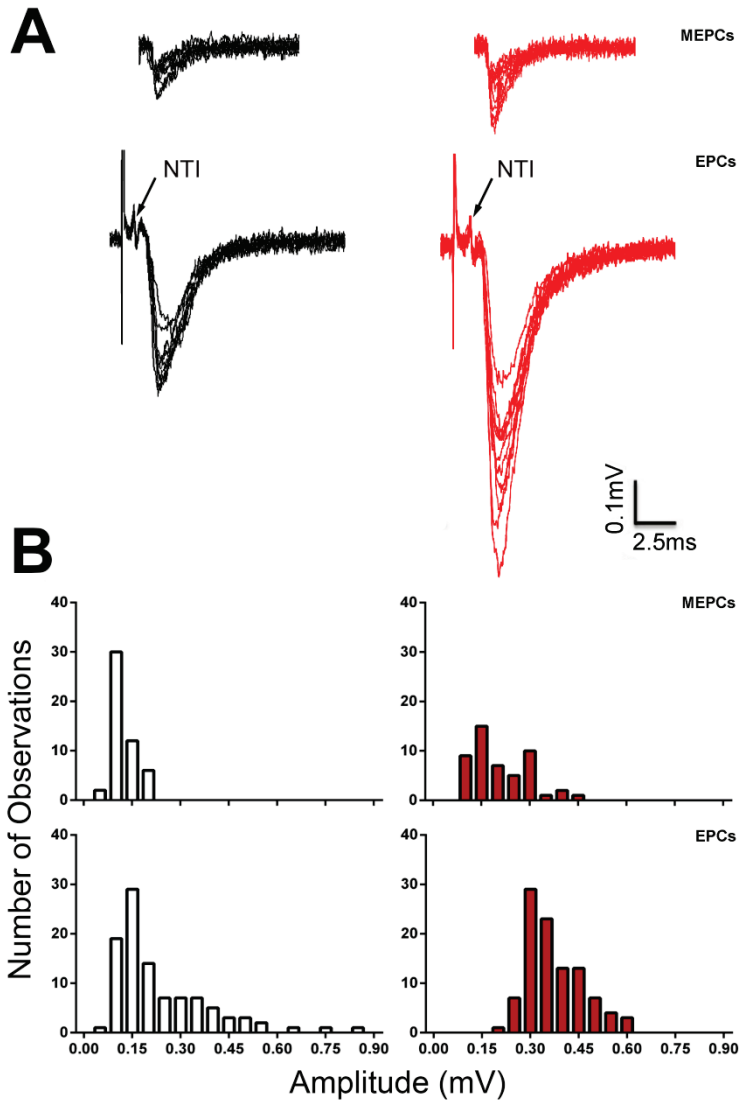

Figure 5.2 Extracellular Recordings from Wild-type and *Lama4*$^{-/-}$ Neuromuscular Junctions in the Diaphragm Muscle at Postnatal Day 18

A, sample traces of MEPCs (10 consecutive spontaneous recordings) and EPCs (10 consecutive evoked recordings) from wild-type (black traces) and *lama4*$^{-/-}$ (red traces) NMJs. Note the presence of the nerve terminal impulse (NTI), which displayed no variation or intermittence in both wild-type and mutant recordings. Frequency histograms were constructed based on ***B***, recordings of spontaneous (top) and evoked amplitude (bottom) recordings for wild-type (black) and mutant (red) NMJs respectively. Histograms shown are from a single NMJ recording from each genotype that exemplifies distributions observed in this study. Distribution of both MEPC and EPC responses displayed a rightward shift in the mode of *lama4*$^{-/-}$ NMJs compared to wild-type, indicating an increased number in higher amplitude responses observed at mutant junctions.

Table 5.2. Comparison of Neurotransmission in the Diaphragm Muscle using Extracellular Electrophysiological Recordings

	Age (Postnatal days)			
	P8		P18	
Genotype	Wild-type	*Lama4*$^{-/-}$	Wild-type	*Lama4*$^{-/-}$
n number	5	6	6	7
Number of junctions				
MEPC	35	42	54	50
EPC	35	42	47	42
EPC Amplitude (μV)	230.2 ± 10.8	281.0 ± 16.8*	233.0 ± 19.6	494.7 ± 58.8***
EPC rise time (ms)	0.64 ± 0.01	0.82 ± 0.03***	0.52 ± 0.02	0.63 ± 0.01**
Latency (ms)	0.75 ± 0.03	0.85 ± 0.04	0.48 ± 0.02	0.56 ± 0.04
MEPC Amplitude (μV)	122.4 ± 5.73	147.1 ± 13.74*	106.1 ± 5.89	162.1 ± 12.50**
MEPC time course (ms)	5.68 ± 0.5	8.49 ± 0.7*	3.61 ± 0.1	4.46 ± 0.2**
MEPC rise time (ms)	0.36 ± 0.01	0.44 ± 0.03	0.26 ± 0.01	0.30 ± 0.01***

* $P < 0.05$; ** $P < 0.01$; *** $P < 0.001$

5.3.3 Quantal Content is reduced at Laminin-α4 Deficient Neuromuscular Junctions

We next performed quantal analysis of the binomial parameters of release at wild-type and *lama*4$^{-/-}$ NMJs under conditions of low release probability to determine if the lower evoked transmitter release was due to a reduction in the probability of transmitter release at each release site or a reduction in the number of active release sites. Quantal content was calculated using the methods of failure due to the high intermittence of transmitter release observed at both wild-type and mutant NMJs (see Methods, Del Castillo and Katz (1954b)). Transmitter release was highly intermittent and variable between release sites at both wild-type and *lama*4$^{-/-}$ NMJs, as has been observed previously in a number of different wild-type preparations (Bennett & Lavidis, 1979; Bennett *et al.*, 1986b; Walmsley *et al.*, 1988; Lavidis & Bennett, 1992, 1993). Due to the high failure rate of transmitter release at most terminals in 0.3 mM calcium, a binomial analysis of transmitter release was only possible in the most active nerve terminals. Quantal content at *lama*4$^{-/-}$ NMJs was normalised to the mean quantal content value of wild-type NMJs at the corresponding age group (Figure 5.3). At P18, we observed a significant reduction in the quantal content ($\bar{m}$) at laminin-α4 deficient NMJs to 62.92 ± 4.74% of $\bar{m}$ at age-matched wild-types (P < 0.01, Student's *t*-test, Figure 5.3). We observed a no significant change in the average probability ($\bar{p}$) of release at mutant and wild-type NMJs (P > 0.05, Student's *t*-test, Figure 5.3). The reduction in $\bar{m}$ at *lama*4$^{-/-}$ NMJs was due to a decrease in the number of active release sites (n) to 57.58 ± 3.43% of that calculated for wild-type NMJs (P < 0.01, Student's *t*-test, Figure 5.3).

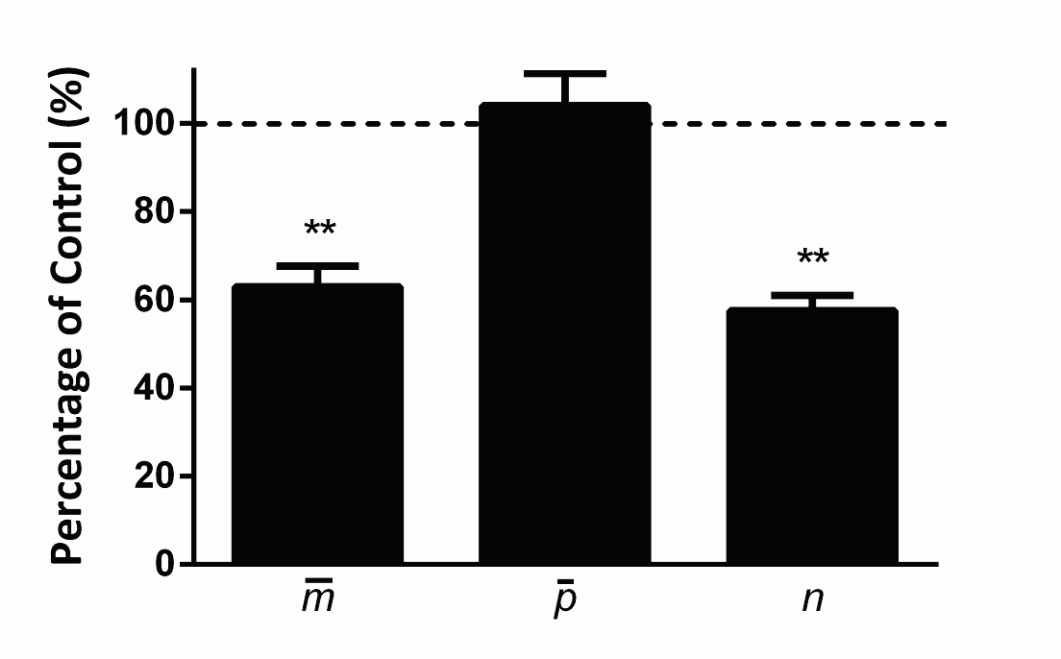

Figure 5.3 The Quantal Content was reduced in Diaphragm Muscles of *Lama*4$^{-/-}$ mice at Postnatal Day 18

Histogram of normalised binomial parameters of neurotransmitter release using data obtained from intracellular electrophysiology recordings of P18 diaphragm muscles. Data is normalised to binomial parameters obtained from P18 wild-type recordings, which represent control values (100%) as indicated by the dashed line. The results demonstrate a significant decrease in quantal content (** $P < 0.01$) at mutant NMJs, which is due to a decrease in the number of release sites (** $P < 0.01$). The probability of release was not significantly altered at *lama*4$^{-/-}$ NMJs compared to age-matched wild-type littermates ($P > 0.05$).

5.3.4 Quantal Content is reduced at Laminin-α4 Deficient Neuromuscular Junctions to a similar extent in Slow and Fast Muscle Fibre Types

Patton *et al.* (2001) previously reported uncoordinated hindlimb movement at *lama*4$^{-/-}$ NMJs, which is indicative of muscular dysfunction. We functionally investigated the properties of hindlimb muscles of two different fibre types (Soleus; type I and EDL; type II) and compared our findings with observations made from the mixed fibre type diaphragm muscle. We observed similar changes in quantal content between the three muscles examined, as indicated by the distribution of MEPPs and EPPs shown in Figure 5.4*A*. Mutant NMJs displayed a rightward shift, indicating an increase in the number of higher responses observed at each muscle fibre type compared to wild-type littermates. Analysis of quantal content demonstrated similar decreases in quantal release for each of the fibre types, relative to the associated controls (EDL; $P < 0.001$, diaphragm and Sol; $P < 0.01$, Figure 5.4*B*). These findings suggest that hindlimb muscles are affected by the loss of laminin-α4 to the same degree as the diaphragm muscle, irrespective of muscle fibre type.

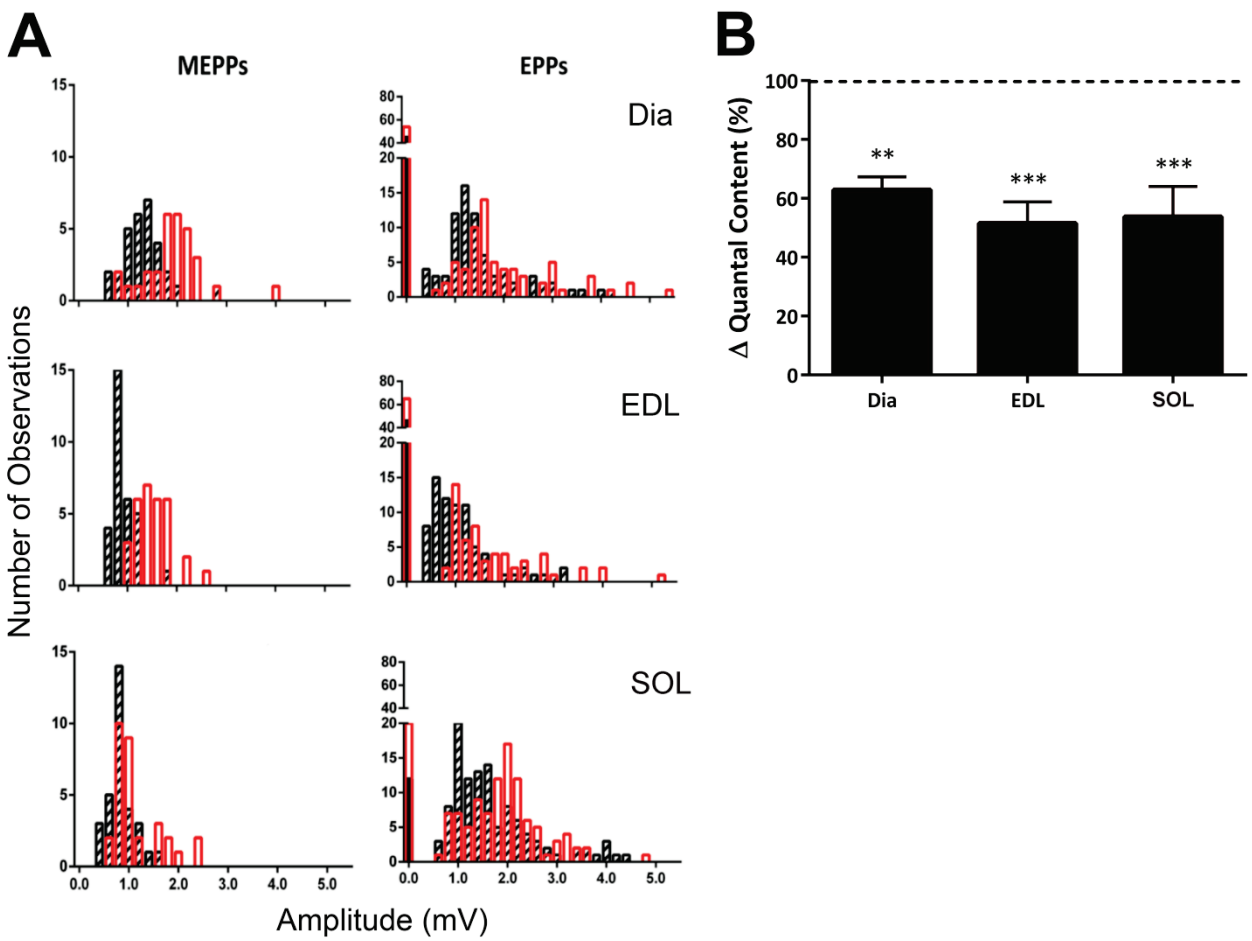

Figure 5.4 The Quantal Content was reduced at *Lama4*$^{-/-}$ Neuromuscular Junction in Muscles primarily composed of Fast or Slow Fiber Types at Postnatal Day 18

A, Frequency histograms constructed from intracellular recordings of mixed fibre (diaphragm; Dia), fast twitch fibre (EDL), and slow twitch fibre (SOL) muscles in wild-type (black striped bars) and *lama4*$^{-/-}$ (red hollowed bars) NMJs. Mutant NMJs demonstrate a rightward shift in each of the three fibre types, indicating similar changes irrespective to synaptic inputs. Significantly higher levels of intermittence were noted at *lama4*$^{-/-}$ NMJs compared to wild-type. ***B***, Quantal content was decreased by a similar degree in each of the fibre types investigated at postnatal day 18 *lama4*$^{-/-}$ NMJs compared to wild-type NMJs for corresponding muscle fibre type. Dashed line represents quantal content for wild-type of corresponding muscle fibre type (100%); ** $P < 0.01$ and *** $P < 0.001$.

5.3.5 Loss of Laminin-α4 results in altered Time Course of Facilitation

The paired pulse facilitation was examined at P18 for wild-type and mutant NMJs, by comparing the test pulse (first stimuli) with the conditioning pulse (second stimuli) to observe the degree of facilitation. Wild-type NMJs, consistently produced high levels of facilitation at 10 ms paired pulse (PP) delay, with the amplitude of the second response being approximately 30% higher than the first response (Figure 5.5). As the interval between PP increased (20-60 ms), there was a decrease in facilitation at wild-type NMJs by approximately 5% for each additional 10 ms (Figure 5.5*A* and 5.5*B*; compare black traces). The time constant for decay in facilitation for wild-type NMJs was 46 ms. By contrast, *lama*4$^{-/-}$ NMJs showed a significantly different pattern of facilitation at 10 ms interval between PPs, with mutant NMJs producing approximately 10% facilitation compared to wild-types 30% (wild-type; 1.30 ± 0.05 vs *lama*4$^{-/-}$; 1.13 ± 0.04, $P < 0.05$). As the interval between PPs increased to 60 ms facilitation increased by 3.5 times at the *lama*4$^{-/-}$ NMJs (Figure 5.5*A* and 5.5*B*; wild-type; 1.10 ± 0.03 vs. *lama*4$^{-/-}$; 1.26 ± 0.05, $P < 0.05$, $n = 6$ for both genotypes). Such changes in the dynamics of paired pulse facilitation may be indicative of alterations in the delivery of vesicles to the active zone or in the numbers of ready releasable vesicles.

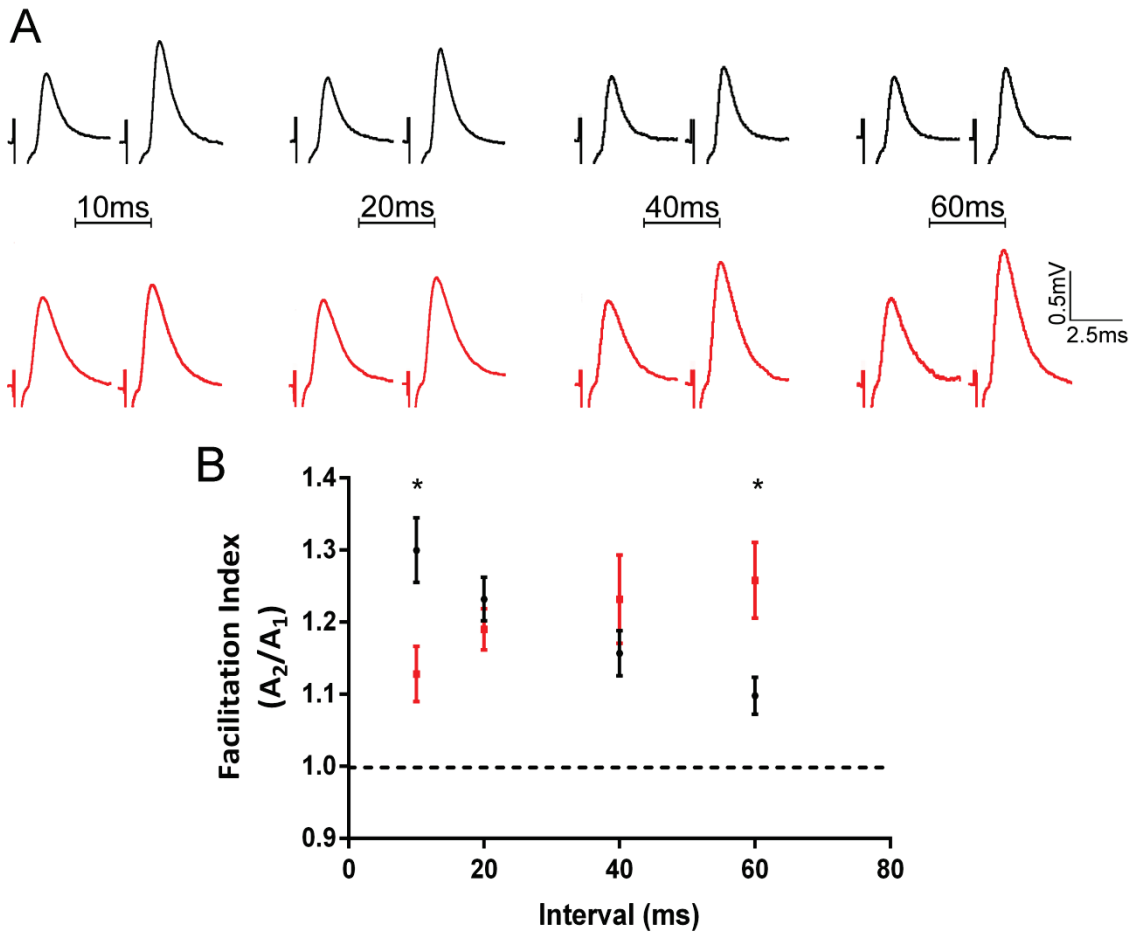

Figure 5.5 The Facilitation of Laminin-α4 Deficient Release Sites was altered to those in Wild-type Neuromuscular Junctions

A, representative sample traces of paired pulse facilitation at 10, 20, 40, and 60 ms delay for wild-type (black) and *lama4*$^{-/-}$ (red) NMJs. ***B***, plot of facilitation ratio against paired-pulse delay times for 10, 20, 40, and 60 ms delays. As delay times increased, the facilitation ratio of wild-type NMJs decreased. Mutant NMJs showed poor facilitation at 10 ms paired-pulse delay time, which was significantly lower than wild-type ($P < 0.05$). Laminin-α4 deficient NMJs consistently showed increased facilitation as paired pulse delay time increased, becoming significantly higher at 60 ms delay ($P < 0.05$). The stimulus artefact was decreased for better visibility in A. For B wild-type and *lama4*$^{-/-}$ NMJs, $n = 6$. Results are presented as mean facilitation index ± SEM.

5.3.6 Laminin-α4 Deficient Neuromuscular Junctions display Higher Levels of Synaptic Depression

Ultra-structural investigation has shown relatively normal distribution of synaptic vesicles in the juxtamembrane half of the presynaptic terminal (Patton *et al.*, 2001). Thus we next examined the synaptic ability of mutant NMJs to sustain release of synaptic vesicles in response to high frequency stimulus. Mutant NMJs underwent synaptic depression to reach a plateau (60% of baseline), which was relatively similar to responses observed at wild-type NMJs when exposed to high frequency stimulus (Figure 5.6*A*). Under these conditions, mutant NMJs underwent a rapid depression reaching a plateau within 5 pulses that was 60 % in amplitude compared with the EPP amplitude of the first pulse in the train, By contrast, wild-types reached the same plateau after fifteen stimuli (Figures 5.6*A* and 5.6*B*). This finding suggests a holding back of vesicles from release for short intervals of pulses which is eventually overcome with time. This finding is reflected in the cumulative quantal release, which showed significantly less release of quanta with each stimulus at mutant NMJs within the first second of high frequency stimulus (Figures 5.6*C* and 5.6*D*, $P < 0.05$). These findings suggest a decrease in the availability of synaptic vesicles from the readily releasable pool (RRP) at *lama*4$^{-/-}$ NMJs (Harlow *et al.*, 2001). Based on this finding, we applied a model that assumes initially all vesicles are derived from the RRP and upon its exponential depletion, the recruitment of vesicles is initiated to maintain the plateau at a steady level, as observed here in both genotypes (Elmqvist & Quastel, 1965). The RRP size can be estimated by plotting quantum content (*y*-axis) against accumulated quantum content (Figure 5.6*B*) and drawing a straight line through the declining phase; its *x*-axis intercept to give an estimate of the RRP size (Ruiz *et al.*, 2011). Using this theoretical estimate it is evident that *lama*4$^{-/-}$ NMJs display a ~40% decrease in the RRP recruited under these high frequency conditions (Figure 5.6*B*, compare dashed lines through the declining phase). It must be highlighted that this is an approximation, and under conditions of low probability of release (0.3 mM $[Ca^{2+}]_o$) it may not be a true reflection of the RRP size. This aspect of the study must be re-undertaken under physiological conditions 1-2 mM $[Ca^{2+}]_o$ to obtain a more accurate estimation, however the present findings do raise interesting questions in regards to the availability of synaptic vesicles when higher demands are place on mutant NMJs.

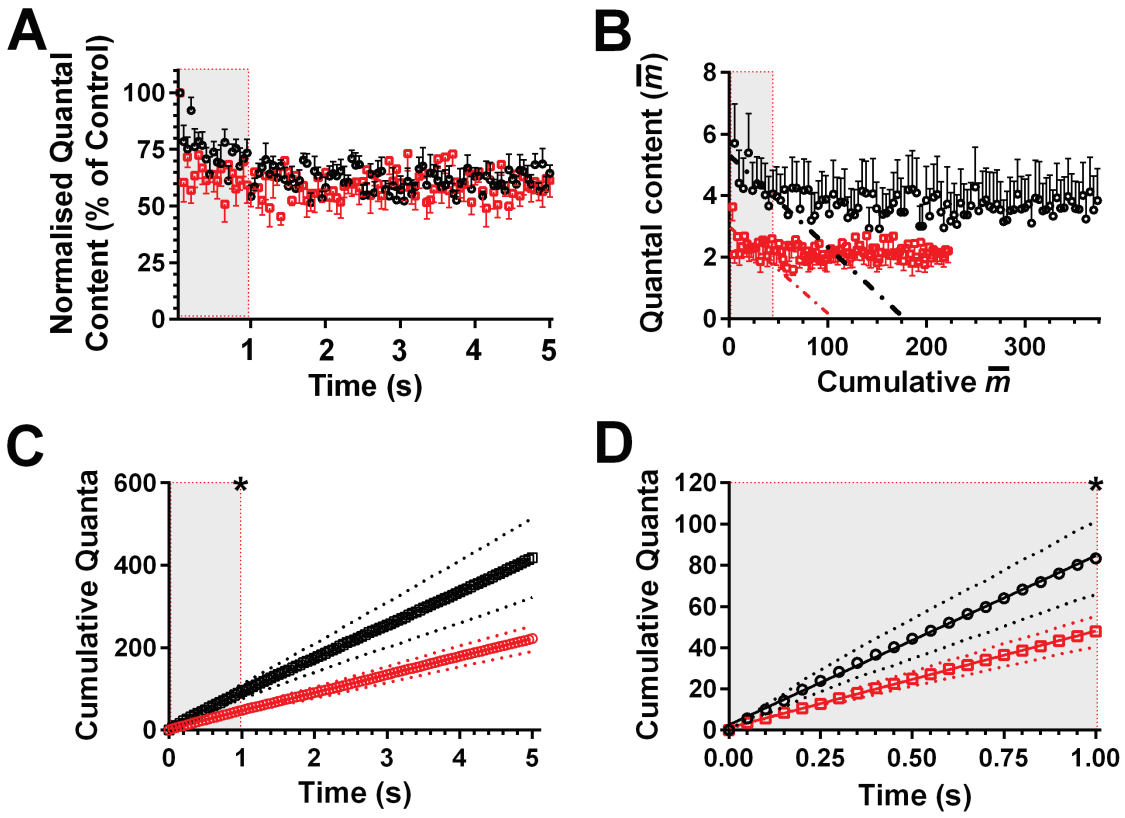

Figure 5.6 *Lama4*$^{-/-}$ Neuromuscular Junctions have lower Cumulative Quantal Release during High Frequency Stimulation

A, L*ama4*$^{-/-}$ NMJs (red) undergo the same degree of depression as wild-type NMJs (black) under trains of high frequency stimulus (20 Hz for 5 seconds). ***B***, the cumulative quantal release begins and is maintained significantly lower than that observed at wild-type NMJs throughout high frequency stimulus ($P < 0.05$). Dashed lines represent estimations of RRP size by plotting $\bar{m}$ (*y*-axis) versus cumulative $\bar{m}$ (*x*-axis) and linearly extrapolating the initial decline to the *x*-axis (wild-type; black, ~175 vs. *lama4*$^{-/-}$; red, ~100) ***C***, within the first second of the five second 20 Hz train, mutant NMJs displayed significantly lower quantal release as highlighted in ***D*** ($P < 0.05$). The grey shaded regions indicate the rapid decline in quantal release observed at *lama4*$^{-/-}$ NMJs within the first second of high frequency stimulus. Values are presented as mean ± SEM; * $P < 0.05$.

5.3.7 Altered Expression of Presynaptic Active Zone components at *Lama4*$^{-/-}$ Neuromuscular Junctions

We next examined the arrangement of pre- and postsynaptic regions using immunohistochemistry at P18 wild-type and *lama*4$^{-/-}$ NMJs. In particular we investigated the distribution of synaptic vesicles as our functional findings suggest deficits in replenishment of vesicles during evoked release, in particular under high frequency conditions. The distribution of synaptic vesicles labelled with SV2 at the presynaptic terminal in relation to the AChR end-plate region labelled with αBTX was analysed (Figure 5.7*A*). We observed a significantly larger AChR end-plate volume at *lama*4$^{-/-}$ NMJs compared to wild-type littermates (wild-type; 172.9 ± 5.69 μm^3 vs. *lama*4$^{-/-}$; 227.2 ± 6.67 μm^3, $P < 0.0001$, $n = 143$ and 148 respectively, Figure 5.7*B*). Mutant NMJs also displayed significantly higher SV2 volumes compared to wild-type NMJs (wild-type; 78.97 ± 2.57 μm^3 vs. *lama*4$^{-/-}$; 107.6 ± 3.53 μm^3, $P < 0.0001$, Figure 5.7*C*). The density of SV2 in relation to end-plate volume at mutant NMJs was also significantly larger compared to wild-type NMJs (wild-type; 0.47 ± 0.01 SV2 μm^3/ AChR μm^3 vs. *lama*4$^{-/-}$; 0.51 ± 0.01 SV2 μm^3/ AChR μm^3, $P < 0.05$, Figure 5.7*D*), due to the proportional increase in size of both the pre- and postsynaptic regions. These findings suggest that both the pre- and postsynaptic regions of *lama*4$^{-/-}$ NMJs are significantly larger in size than age-matched wild-type littermates.

As our functional analysis of binomial parameters indicated a decrease in the number of active release sites, we next investigated the expression of active zone proteins at the NMJ of P18 wild-type and *lama*4$^{-/-}$ mice. This was undertaken by quantitatively analysing the punctate density of the active zone marker Bassoon in relation to postsynaptic AChR end-plates (Figure 5.8). At wild-type and *lama*4$^{-/-}$ NMJs, Bassoon was well expressed throughout the entire end-plate area (Figure 5.8*A*). We noted a significant increase in the end-plate area at mutant NMJs compared to wild-type littermates (wild-type; 137.3 ± 4.49 μm^2, $n = 3$, NMJs = 65 vs. *lama*4$^{-/-}$; 173.4 ± 7.16 μm^2, $n = 3$, NMJs = 72, Figure 5.8*B*). Bassoon punctate were also significantly higher at mutant NMJs (wild-type; 229.0 ± 7.40, $n = 3$, NMJs = 64 vs. *lama*4$^{-/-}$; 253.1 ± 9.19, $n = 3$, NMJs = 71, Figure 5.8*C*). However, normalisation of Bassoon puncta to end-plate area, displayed a significantly lower density at *lama*4$^{-/-}$ NMJs compared to wild-type littermates (wild-type; 1.73 ± 0.06 puncta/ μm^2 vs. *lama*4$^{-/-}$; 1.53 ± 0.06 puncta/ μm^2, Figure 5.8*D*). These findings indicate that Bassoon is still present but the loss of laminin-α4 results in decreased expression density of the active zone marker Bassoon.

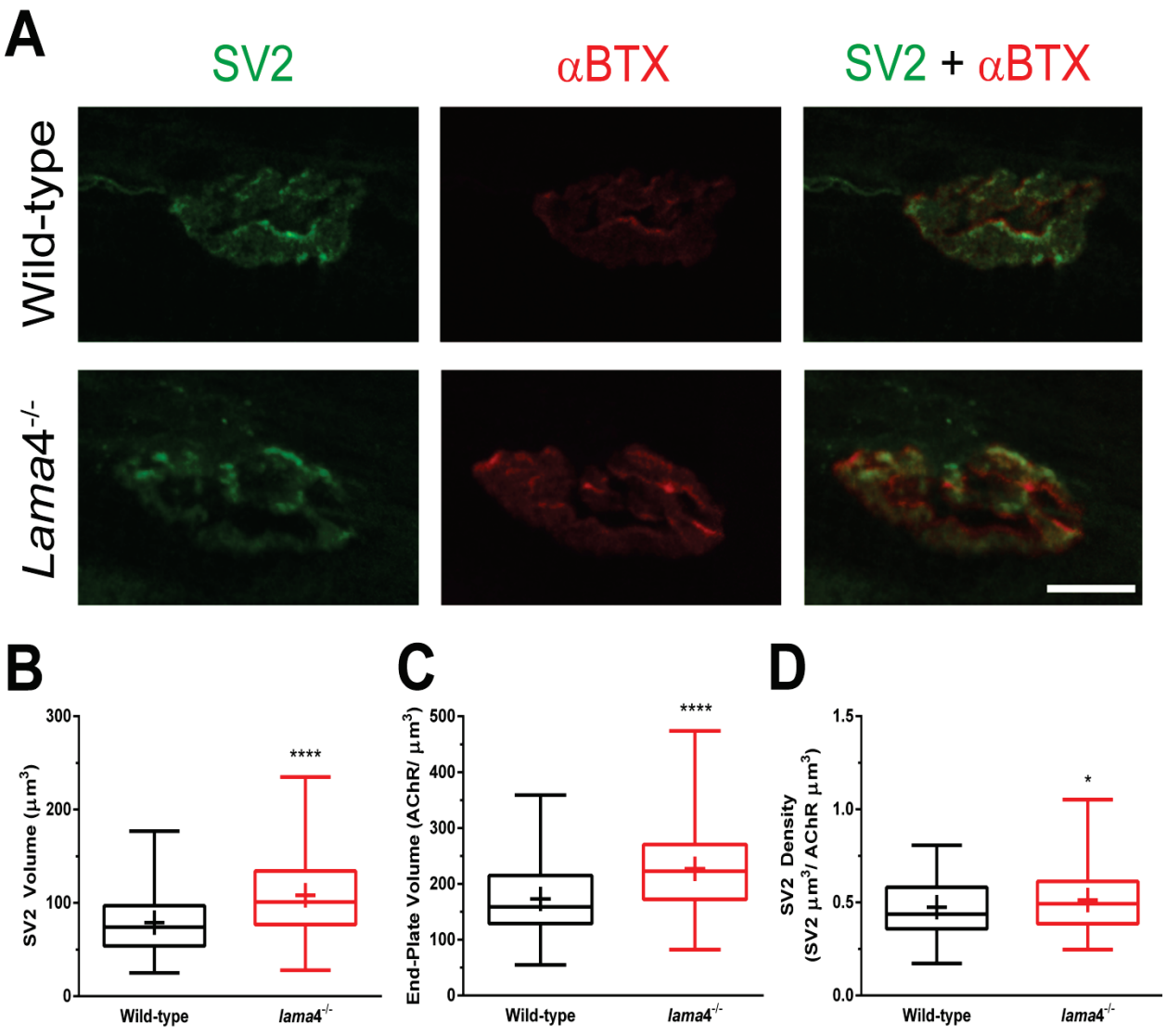

Figure 5.7 Laminin-α4 Deficient mice demonstrated increased Expression and normal Co-localisation of Synaptic Vesicles to Acetylcholine Receptors

A, representative immuno-staining of NMJs from postnatal day 18 wild-type and *lama*4$^{-/-}$ mice. Confocal microscopy was undertaken on wholemount diaphragm muscles co-stained with SV2 antibodies (green) and conjugated aBTX (red). Wild-type and mutant NMJs demonstrate good co-localisation of synaptic vesicles in relation to postsynaptic AChR end-plates. ***B***, *lama*4$^{-/-}$ NMJs possessed significantly larger AChR end-plate volumes compared to wild-types. ***C***, the volume of synaptic vesicles, measured using staining for SV2, was again significantly higher at mutant terminals. ***D***, mutant NMJs possessed a higher density of SV2 when vesicle volume was normalised to the AChR end-plate volume. For B-D; boxplots display median with 25-75% box, max-min whiskers, with mean values for parameters represented by '+' for each genotype. B-D; wild-type, *n* = 3, NMJs = 143, and *lama*4$^{-/-}$, *n* = 3, NMJs = 148; significance is indicated for mean values for each genotype per parameter quantified * $P < 0.05$, **** $P < 0.0001$. Scale bar: 10 µm.

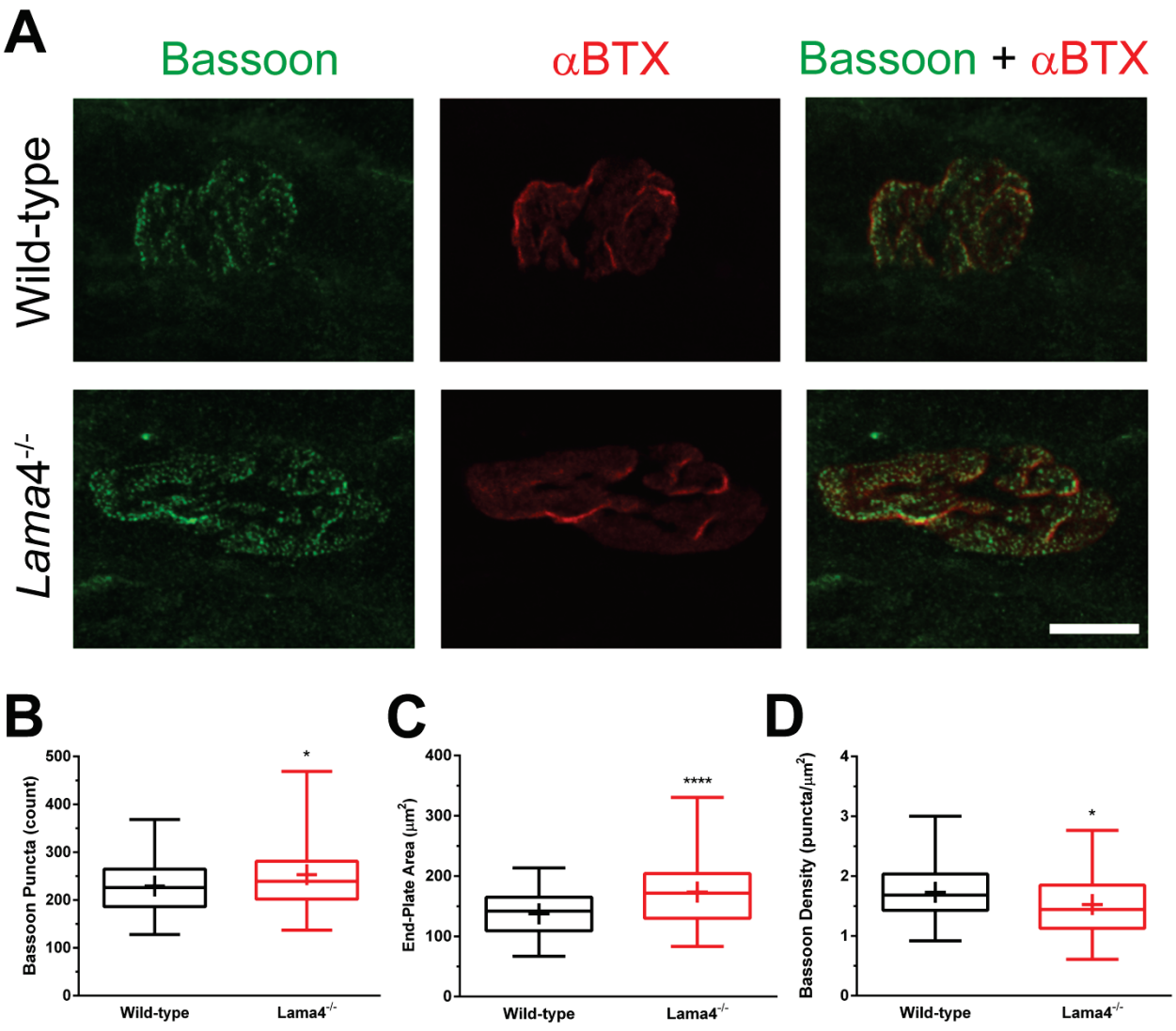

Figure 5.8 Decreased Bassoon Density at *Lama4*$^{-/-}$ Neuromuscular Junctions compared to Wild-type Junctions at Postnatal Day 18

A, Left panels stained for the active zone marker Bassoon, middle panels show AChRs labelled with αBTX, and right panels displaying merged staining. At P18, wild-type and *lama4*$^{-/-}$ NMJs showed similar patterns of Bassoon staining, with good co-localisation to AChRs. ***B***, quantification of staining showed a higher number of Bassoon puncta at mutant terminals. ***C***, end-plate area was also enlarged at lama4$^{-/-}$ NMJs. ***D***, Bassoon density was decreased at mutant NMJs. For B-D; boxplots display median with 25-75% box, max-min whiskers, with mean values for parameters represented by '+' for each genotype. B-D; wild-type, *n* = 3, NMJs = 65, and *lama4*$^{-/-}$, *n* = 3, NMJs = 72; significance is indicated for mean values for each genotype per parameter quantified * $P < 0.05$, **** $P < 0.0001$. Scale bar: 10 μm.

5.3.8 Early Signs of Ageing are observed at *Lama4*$^{-/-}$ End-Plates

Our immunohistochemistry studies raised an interesting observation in regards to the changes in morphology of hindlimb muscles. Preliminary immunohistochemistry work on two-three month old *lama4*$^{-/-}$ NMJs has shown clear signs of perturbed postsynaptic morphology (Figure 5.9). At P18, mutant NMJs began to show irregular postsynaptic morphology, with early signs of AChR regions separating and 'budding' off from the end-plate (Figure 5.9, see bottom left panels). Age-matched wild-type NMJs displayed strong convolution of the postsynaptic area and nerve terminal arbors overlayed the end-plate region (Figure 5.9, top left panels). By two-three months of age, we observed an increase in the number of end-plate regions showing small islands, as well as irregular convolutions and elongated end-plate regions at mutant NMJs compared to wild-type littermates (Figure 5.9, compare right panels). Together these findings indicate that loss of laminin-α4 may in fact result in a poorly maintained NMJ, which culminates in premature disassembly of the postsynaptic AChR end-plate.

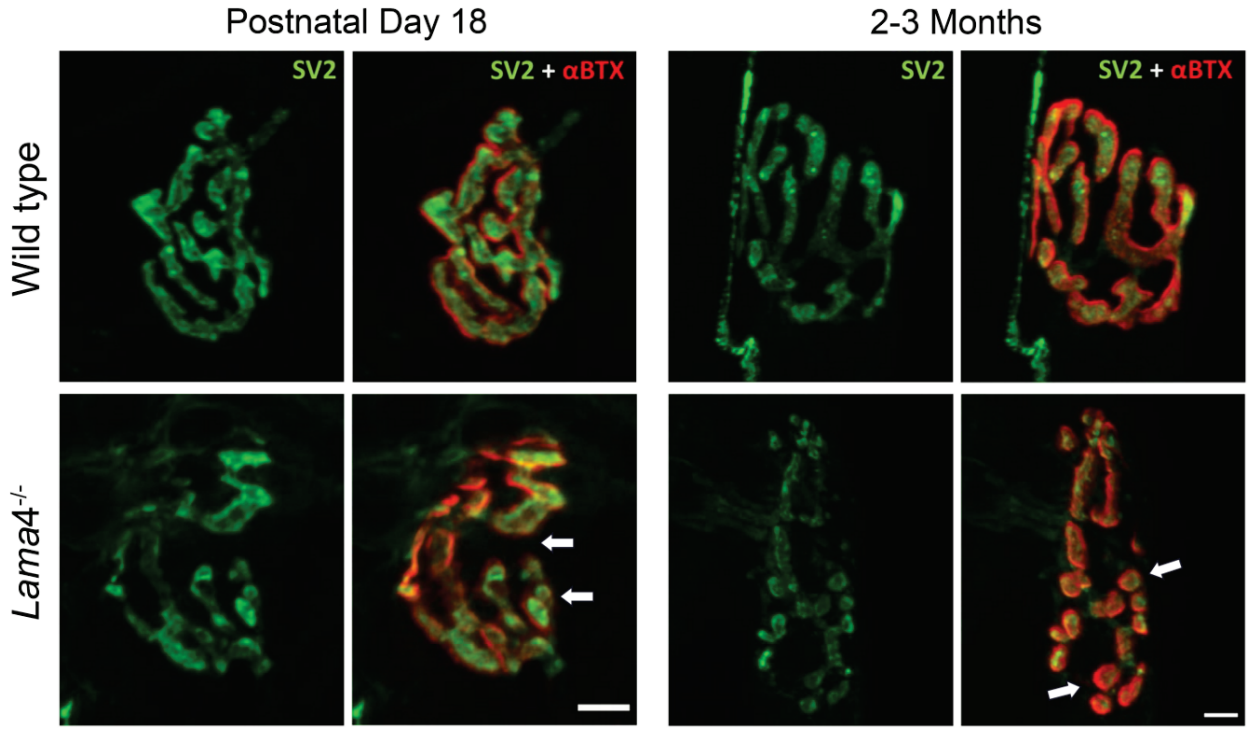

Figure 5.9 *Lama*4$^{-/-}$ Neuromuscular Junctions display signs of Premature Disassembly compared to Age-matched Wild-type Junctions in EDL Muscles

Wild-type and *lama*4$^{-/-}$ NMJs from EDL muscles at postnatal day 18 and 2-3 months of age, stained for presynaptic SV2 (green fluorescence) and postsynaptic AChR end-plates with αBTX (red fluorescence). Both genotypes present good co-localisation of pre- and postsynaptic regions. *Lama*4$^{-/-}$ NMJs begin to display perturbed morphology of the end-plates at P18. At 2-3 months of age, *lama*4$^{-/-}$ NMJs show signs of fragmentation indicative of a disassembling end-plate, a process normally associated with ageing NMJs. By contrast, wild-type NMJs maintained their structural integrity at the both age groups with no evident signs of fragmentation or disassembly. Scale bars: 5 μm.

5.4 DISCUSSION

Loss of laminin-α4 results in misalignment of pre- and postsynaptic specialisations at the skeletal NMJ (Patton *et al.*, 2001). Previous study has focused upon morphological changes in *lama*4$^{-/-}$ NMJs, with little examination of functional consequences associated with these changes. Here, we have provided the first functional characterisation of neurotransmission properties at *lama*4$^{-/-}$ NMJs from early development (P8) to maturity (P18). We observed evident alterations to neurotransmission at laminin-α4 deficient NMJs compared to wild-type junctions that can be explained by the reported morphological differences, with similar functional differences observed in all three muscles examined. Quantal content decreased at *lama*4$^{-/-}$ NMJs due to a decrease in the number of active release sites. Facilitation in transmitter release induced by paired pulse stimulation was reduced for short PP intervals but significantly increased as the PP interval increased. Depression in transmitter release induced by high frequency stimulation increased in the *lama*4$^{-/-}$ NMJs. Utilising immunohistochemistry, we demonstrated an increase in the volume of SV2 at the presynaptic terminal as well as an enlarged postsynaptic region at mutant NMJs. In addition to this we observed a decrease in the active zone marker Bassoon at the presynaptic nerve terminal. Together these findings suggest modifications to both pre- and postsynaptic elements at NMJs lacking laminin-α4.

5.4.1 Altered Spontaneous Release Properties suggest Presynaptic and Postsynaptic Modifications

At both P8 and P18, mutant NMJs displayed a lower frequency of spontaneous release compared to wild-type littermates, a finding observed in each of the muscle fibre types investigated. The loss of laminin-β2, another laminin chain that comprises the laminin-421 heterotrimer, also resulted in significantly decreased spontaneous release (Noakes *et al.*, 1995a; Knight *et al.*, 2003). Investigators suggested that this decrease in MEPP frequency was due to presynaptic alterations (Robitaille & Tremblay, 1989; Knight *et al.*, 2003). Interestingly, loss of laminin-β2 did not result in increased MEPP amplitude that was observed in the present study on *lama*4$^{-/-}$ NMJs. Here we observed significantly larger quantal size at *lama*4$^{-/-}$ NMJs compared to wild-type at both ages investigated. Kriebel and Gross (1974), hypothesised based on the first reports of sub-quantal MEPPs, that MEPPs are composed of the synchronous release of multiple vesicles. Alternative hypotheses, suggest that larger MEPPs represent the whole release of transmitter from a single vesicle, while sub-quanta

occur as a result of short spurts of transmitter. The release of spontaneous transmitter resulting in larger than normal MEPPs has previously been observed in multiple models, including the $SOD1^{G93A}$ model of ALS (Liley, 1957; Alkadhi, 1989; Sellin *et al.*, 1996; Rocha *et al.*, 2013). These 'giant' MEPPs are caused by the single release of a large volume of ACh, which saturates AChRs at the postsynaptic membrane. It is possible that these giant MEPPs occur as a result of giant vesicles releasing their transmitter, these arise infrequently (less than 1 out of 50 releases). Higher concentrations of ACh may result in lateral diffusion after release, which subsequently activates further AChRs resulting in a prolonged period of current at the end-plate region. Increased prevalence of abnormally large MEPPs has been noted under pathological conditions such as nerve terminal degeneration, NMJ remodelling and motor end-plate diseases (Birks *et al.*, 1960; Miledi, 1960; Weinstein, 1980).

These large MEPPs may be a consequence of impaired processing of recycled vesicles, with the formation of bulk endocytotic structures which may be released before budding into smaller vesicles by dynamin. This phenomenon has been described to occur during high levels of exocytosis (Harper *et al.*, 2011). Changes in vesicle filling may perhaps be an adaptive mechanism brought about by the misalignment seen at *lama*$4^{-/-}$ NMJs. Decreased AChE, the enzyme responsible for degrading bound ACh, could also produce large MEPP amplitudes with more transmitter likely to activate AChRs at the end-plate. The prolonged spontaneous decay time at *lama*$4^{-/-}$ NMJs would support a decrease in AChE, resulting in altered ACh hydrolysis and subsequently a longer activation of AChRs after spontaneous release. Another possible cause for the increased MEPP amplitude is a higher density of postsynaptic AChRs. The larger end-plate volume at mutant NMJs may result in increased AChR density which means more receptors are available to bind the released transmitter. It is possible that each of the factors discussed above may be acting synergistically to contribute to the increased MEPP amplitude observed at *lama*$4^{-/-}$ NMJs. These changes however may be counter adaptive mechanisms in order to overcome the decreased quantal content we observed in this study.

5.4.2 *Lama*4$^{-/-}$ Neuromuscular Junctions display altered Properties in Evoked Transmitter Release

The present study also observed significantly increased evoked amplitudes at *lama*4$^{-/-}$ NMJs at both P8 and P18. In addition to this, we noted higher levels of intermittent transmitter release at mutant NMJs compared to wild-type littermates leading to a decrease in mean quantal content at *lama*4$^{-/-}$ NMJs. Our extracellular recordings of the NTI and EPCs indicated no intermittence in the NTI even though intermittence in EPC responses was higher in *lama*4$^{-/-}$ NMJs when compared to wild-type NMJs at P8 and P18. In addition, we noted a slightly greater latency (~14.5%) between the NTI and the start of rise in EPCs at *lama*4$^{-/-}$ NMJs compared to wild-type. In support of these findings, prior study has shown normal morphology of peripheral nerves in *lama*4$^{-/-}$ mice, thus the loss of laminin-α4 results in morphological changes isolated to the NMJ (Patton *et al.*, 2001). These findings would suggest an issue in the depolarisation-secretion coupling mechanism at the presynaptic active zones of mutant NMJs, possibly in the supply of vesicles to the active zone. There are a number of vesicular associated proteins which influence the docking and supply of ready releasable vesicles prior to calcium triggered exocytosis such as Rab, Rabphilin, and synapsin I (Li *et al.*, 1994; Li *et al.*, 1995; Sudhof, 1997; Burns *et al.*, 1998; Sudhof, 2004). Synapsin I is an interesting vesicular associated protein as it has been shown to influence the pattern of transmitter release during single and trains of stimulation. Synapsin I is closely associated with a calcium binding protein kinase (Ca^{2+}/ calmodulin-dependent protein kinase II; CaMKII), which affects the phosphorylation of synapsin I subsequent to formation of calcium micro-domains, and is thought to contribute to facilitated transmitter release (Hosaka *et al.*, 1999; Menegon *et al.*, 2006).

5.4.3 Loss of Laminin-α4 results in decreased Quantal Content due to fewer Active Release Sites

We next performed analysis of the binomial parameters of release at wild-type and *lama*4$^{-/-}$ NMJs. Our analysis confirmed that the reduction in quantal content was due primarily to a reduction in the number of active release sites at *lama*4$^{-/-}$ NMJs, with no significant change in the average probability of transmitter release from those active sites. Together our functional findings indicate the maintenance of the most active release sites, and loss of release sites with low probabilities of transmitter release. We also functionally investigated the neurotransmission properties of fast and slow twitch fibre muscles in the hindlimb of *lama*4$^{-/-}$ mice as prior research has shown deficits in hindlimb co-ordination. Patton *et al*.,

(2001) used a narrow beam to test possible changes in co-ordinated movement in *lama*4$^{-/-}$ mice. Wild-type mice were capable of crossing the beam with less than two foot slips while only 11% of *lama*4$^{-/-}$ mice were able to do so. We observed comparable decreases in quantal content irrespective of fibre type at mutant NMJs compared to wild-type littermates. These findings suggest that peripheral hindlimb muscles are affected by the loss of laminin-α4 to the same degree as the diaphragm muscle, irrespective of muscle fibre type. Our behavioural observations suggest that under lower levels of muscle activity NMJs in *lama*4$^{-/-}$ mice show no obvious deficits, however if animals are made to increase muscular activity the effects of *lama*4$^{-/-}$ on NMJs becomes evident most likely because the normal large safety factor in transmission is reduced in the *lama*4$^{-/-}$ NMJs.

5.4.4 Altered Plasticity and Replenishment of Synaptic Vesicles at *Lama*4$^{-/-}$ Neuromuscular Junctions

We used paired pulse facilitation in transmitter release to investigate short term plasticity at *lama*4$^{-/-}$ junctions. Facilitation studies employ the application of test conditioning pulses in close succession to assess intracellular calcium handling and vesicular dynamics at the active zone. The level of facilitation has been easily predicted by the time course of calcium sequestration. Unexpectedly, we observed increased facilitation at higher delay times between stimuli (40-60ms delays) with minimal facilitation occurring at lower times (10-20ms) in *lama*4$^{-/-}$ NMJs. By comparison, wild-type NMJs displayed the expected time course for decline in facilitation of 46 ms which is comparable to the value of 40 ms reported by Bennett *et al.* (1977). These findings suggest alterations in the short-term plasticity of the NMJ and possibly defective recycling of synaptic vesicles and/or the calcium handling at *lama*4$^{-/-}$ NMJs. We propose that alterations to synapsin I and its associated molecules may be responsible for the changes in neurotransmission observed at *lama*4$^{-/-}$ NMJs. The synaptic vesicle associated phosphoproteins, synapsin I, has been shown to preferentially localise to the reserve pool of synaptic vesicles (Pieribone *et al.*, 1995; Bloom *et al.*, 2003). Synapsin I maintains the reserve pool in close proximity of active zones via tethering of synaptic vesicles to the actin cytoskeleton, and regulate the availability of vesicles by releasing them in a phosphorylation dependent manner (Chi *et al.*, 2001). The synapsins are targeted for phosphorylation by protein Kinase A and CaMKII to modulate neurotransmission (Huttner & Greengard, 1979; Hosaka *et al.*, 1999; Menegon *et al.*, 2006). Thus a decrease in synapsin I expression may result in altered availability of synaptic vesicles. This effect has been observed in synapsin I knockout

mice, which showed that transmitter release is increased during the first stimuli but subsequent stimuli induce a greater depression (Gaffield & Betz, 2007).

To further examine the above mentioned possibility, we conducted studies using trains of high frequency stimuli (20 Hz for 5 s) to investigate synaptic depression in mutant NMJs. The relative degree of depression was similar to that observed at wild-type NMJs, however mutants underwent a rapid decline within the first five stimuli compared to fifteen in wild-types. Both genotypes underwent depression and reached a steady plateau of transmitter release as the nerve terminal attempted to replenish the supply of synaptic vesicles at the readily reserve pool (RRP) by drawing from the recycling and reserve pools (Bennett, 2001; Rizzoli & Betz, 2004, 2005). The cumulative quanta released during the high frequency train was approximately 50% lower for the *lama*4$^{-/-}$ NMJs when compared with the wild-type NMJs. Combined, these findings suggest a decrease in the availability of synaptic vesicles from the RRP at *lama*4$^{-/-}$ NMJs (Harlow *et al.*, 2001). Knight *et al.* (2003) observed similar deficits in response to high frequency stimuli at laminin-β2 deficient NMJs, which they attributed to the reduced number of vesicles positioned at the juxtamuscular half of the terminals and therefore a decrease in delivery of vesicles to the active regions. Using theoretical estimations of the RRP recruited during the 20 Hz stimulus we observed a 40% decrease in the number of vesicles in this pool at *lama*4$^{-/-}$ NMJs. However, depletion of the RRP is not likely to be the cause of the decreased cumulative quantal release, as the number of synaptic vesicles in the RRP is thirty to forty times greater than the number of vesicles released with each stimulus (Rowley *et al.*, 2007). In addition to this, previous ultra-structural studies of *lama*4$^{-/-}$ NMJs did not observe aberrant distributions of synaptic vesicles (Patton *et al.*, 2001). These findings suggest a normal presence of synaptic vesicle numbers at mutant terminals, but the docking process may be defective resulting in altered neurotransmission. Again these defects may relate to changes in synapsin I expression, as previous study has shown that mice deficient in all three synapsins demonstrate an increase in the rate of synaptic depression during trains of stimuli (Gitler *et al.*, 2004).

5.4.5 Morphological examination of Laminin-α4 Deficient Neuromuscular Junctions revealed normal Arrangement and Localisation of Pre- and Postsynaptic Components

We next examined the arrangement of pre- and postsynaptic regions using immuno-histochemistry at P18 wild-type and *lama*4$^{-/-}$ NMJs. Our functional findings suggest changes to both pre- and postsynaptic regions at mutant NMJs. Firstly we investigated the distribution of synaptic vesicles in relation to the AChR end-plate region. We observed good co-localisation of SV2 to the AChR dense postsynaptic region at both *lama*4$^{-/-}$ and wild-type NMJs. We also observed an increase in SV2 staining at mutant terminals, indicating a greater density of vesicles at the presynaptic terminal. Caillol and colleagues (2012), have previously reported increased SV2 volume in mice with motor end-plate disease at postnatal day 19. This accumulation of synaptic vesicles is suggested to be a compensatory mechanism in response to a failure in neurotransmission (Mantilla *et al.*, 2007; Mantilla & Sieck, 2009).

Investigation of ultrastructure of mutant NMJs has demonstrated relatively normal active zone numbers and arrangement (Patton *et al.*, 2001). We observed higher numbers of Bassoon puncta at mutant nerve terminals, however when punctae were normalised to the larger end-plate area we noted a significant decrease in the density of Bassoon compared to wild-type littermates. Carlson *et al.* (2010), propose that laminin-421 (α4β2γ1) may interact with cellular surface receptors to pattern active zones and stabilise the NMJ. This is achieved via individual laminin chains ability to interact with each component, laminin-β2 with the pore forming α-subunit of VGCCs ($Ca_v\alpha$), and laminin-α4 with α3 integrin, a cell receptor located close to active zones (Cohen *et al.*, 2000; Talts *et al.*, 2000; Fujiwara *et al.*, 2001; Nishimune *et al.*, 2004; Suzuki *et al.*, 2005). Based on this it would be expected that loss of laminin-α4 would also result in decreased active zone patterning. We have previously shown a decrease in the density of Bassoon puncta at P8 which became more evident by P18 at *lamb*2$^{-/-}$ NMJs, a finding which was in agreement with previous studies (see Chapter 3; Nishimune *et al*., 2004; Chand *et al*., 2014). Our current study on *lama*4$^{-/-}$ NMJs did not demonstrate as drastic decreases that could be determined qualitatively, however we did find a significant decrease in Bassoon density using quantitative analysis. The interaction between laminin-β2 and $Ca_v\alpha$ is fundamentally important in the active zone patterning with its loss resulting in significant changes at the nerve terminal, while laminin-α4 acts more as a guiding cue via interaction with α3 integrin. Thus loss of

laminin-α4 does not drastically influence active zone number, but rather, the placement in relation to end-plate folds culminating in misapposition of pre- and postsynaptic specialisations.

There are numerous molecules involved in the development and maturation of the postsynaptic end-plate region of the NMJ. Of particular interest is dystroglycan, which has been shown to aggregate at the postsynaptic membrane in the presence of laminins-α4 and -α5 to promote maturation of the endplate (Nishimune *et al.*, 2008; Pilgram *et al.*, 2010). It has been shown that loss of laminin-α4 does not alter the expression or presence of dystroglycan and in turn has no effect on the clustering of AChRs, as supported by our immunohistochemical studies which showed normal expression levels of AChRs (Nishimune *et al.*, 2008). This is likely due to the presence of laminin-α5 which is capable of interacting with dystroglycan to maintain postsynaptic expression of AChRs. However, the end-plate regions of *lama*4$^{-/-}$ NMJs displayed altered morphological characteristics, with irregular convolution and size. We quantified both the area and volume of mutant AChR end-plates, finding significant increases compared to age-matched wild-type NMJs. Studies have previously shown that paralysis of diaphragm muscle resulted in enlarged nerve terminal and postsynaptic end-plate regions (Prakash *et al.*, 1999; Mantilla *et al.*, 2007; Mantilla & Sieck, 2009). We propose that the increased postsynaptic end-plate regions are another compensatory mechanism of the NMJ to deal with the misalignment of specialisations at mutant NMJs. It is widely believed that one of the functions of the postsynaptic folds and the voltage gated sodium channels (VGSCs) in their depths is to enhance the efficacy of neurotransmission by amplifying the potential generated by the released transmitter from the presynaptic nerve terminal. Thus an enlargement of this region could allow for a higher degree of folding and density of VGSCs, which in some part may explain the higher amplitude in spontaneous and evoked responses that we observed at *lama*4$^{-/-}$ NMJs. Laminin-α4 is produced by myotubes and inserted into the basal lamina associated with the postsynaptic specialisations (Patton, 2000). In contrast to other laminin chains expressed sub-synaptically, laminin-α4 is found in highest concentrations at the depths of folds rather than at the crest of folds (Patton *et al*., 2001). This finding suggests laminin-α4 plays an instructive role in the placement of postsynaptic specialisations, i.e. separating the postsynaptic folds themselves. Thus, NMJs deficient of laminin-α4 may lose the signal which guides precise placement of postsynaptic specialisations resulting in the misapposition observed by others at *lama*4$^{-/-}$ NMJs.

In addition to this, our preliminary immunohistochemistry studies raised interesting observations in regards to altered NMJ morphology of two-three month old *lama*4$^{-/-}$ mice. We observed an increase in the number of end-plate regions showing small islands, as well as irregular convolutions and elongated end-plate regions at mutant NMJs compared to wild-type littermates. Together these findings indicate that loss of laminin-α4 may in fact result in poorly maintained NMJs, which culminates in premature disassembly of the postsynaptic AChR end-plate.

5.5 CONCLUSION

In summary, this investigation is the first to demonstrate the functional consequences associated with the loss of laminin-α4 at the NMJ. Laminin-α4 acts as a trans-synaptic coordinator via interactions with pre- and postsynaptic cell surface receptors which align specialisations of these regions. Loss of laminin-α4 results in altered neurotransmission, with decreased quantal content irrespective of muscle fibre type and compromised vesicular supply to the immediate area of the active zone. These functional changes lead to hindlimb weakness when the NMJs are intensely stimulated, indicative of a possible reduction in the safety factor of neurotransmission. We also demonstrate altered expression of synaptic vesicles and active zone components at the presynaptic nerve terminal. In addition to this, we noted enlarged postsynaptic AChR end-plates at mutant NMJs. I propose that these morphological and functional changes are compensatory responses to the early misalignment in pre- and postsynaptic specialisations observed at *lama*4$^{-/-}$ NMJs.

CHAPTER 6

General Discussion

6.1 Thesis Summary

This thesis has made a number of important observations, which have greatly contributed to our understanding of the functional importance of laminins-α4 and –β2 in developing and matured NMJs. The findings demonstrate that the loss of laminin-β2 resulted in a delay or cessation in maturation of each of the three key structures comprising the NMJ; the presynaptic terminal, perisynaptic Schwann cells, and the postsynaptic end-plate. Specifically *lamb*2$^{-/-}$ NMJs failed to undergo a developmental switch in VGCCs mediating transmitter release resulting in disorganisation of active zone proteins at the presynaptic terminal, and also contributing to the deficits in neurotransmission observed at laminin-β2 deficient NMJs. Laminin-β2 may also play a role in the maturation of the postsynaptic apparatus, as the majority of AChR end-plates studied in this thesis were of the immature plaque-like form. Functional examination of perisynaptic Schwann cells at *lamb*2$^{-/-}$ NMJs also demonstrated a delay or cessation in development. Mutant PSCs remained reliant on the developmental purinergic signalling pathway rather than switching to muscarinic signalling. The PSCs of *lamb*2$^{-/-}$ NMJs displayed irregular responses to stimuli, suggesting severe perturbations in decoding neurotransmission signals and thus failing to achieve their functional role as neuronal support cells. Combined, these findings suggest that laminin-β2 is an integral synaptic component necessary for the proper development and maturation of the neuromuscular junction. Furthermore, this is the first study to functionally characterise the neurotransmission properties of laminin-α4 deficient NMJs. The NMJs of *lama*4$^{-/-}$ mice presented early perturbations in transmission which progressed as the NMJ matured. These findings allow us to better understand the functional consequences associated with loss of laminins-α4 and -β2, and their interactions with molecular components of the neuromuscular junction. This chapter will summarise the findings from this thesis in context with both the general literature and other work performed within our laboratory.

6.2 The Functional Consequence of Laminin-β2 loss at the Developing Neuromuscular Junction

In agreement with previous literature, we observed significant impairment of neurotransmission at the NMJs of laminin-β2 deficient mice (Noakes *et al.*, 1995a; Knight *et al.*, 2003). The study by Knight *et al.*, (2003) reported altered functional transmission properties between wild-type and *lamb*2$^{-/-}$ NMJs at early stages of development (P8), with mutants later showing drastic decreases in quantal transmitter release by P18. It was proposed that this reduction was due to a failure in the depolarisation-secretion coupling mechanism, a process driven by the influx of calcium into the nerve terminal after arrival of the action potential. One of the key findings of the present study was a clear decrease in calcium sensitivity at the NMJ of *lamb*2$^{-/-}$ mice at P18 compared to wild type littermates. We suggest that this decreased calcium sensitivity is a result of decreased overlap in calcium domains effectively reducing the calcium concentration around synaptotagmin close to the active zone (Augustine, 1990; Augustine *et al.*, 1992). Altered VGCC distribution and/or channel subtypes involved in mediating transmitter release may contribute to this reduced domain overlap, with P/Q-type VGCCs suggested to be more proximal to active zones than N-type VGCCs (Rosato-Siri *et al.*, 2002; Nudler *et al.*, 2003; Urbano *et al.*, 2003; Nishimune *et al.*, 2012). Interestingly loss of laminin-β2 did not influence the VGCCs involved in mediation of transmitter release at the NMJs during early development (P8). Both wild-type and mutant NMJs demonstrated similar dependence on N- and P/Q-type VGCCs at this stage in development. By postnatal day 18, wild-type mice demonstrated an evident shift towards P/Q-type VGCCs mediated transmitter release with N-type channels playing a supporting role. By contrast, *lamb*2$^{-/-}$ NMJs displayed maintained dependence on N-type VGCCs with P/Q-type channels playing a minor role in mediating transmitter release. These functional changes were supported by our immunohistochemical findings.

During early development, both wild-type and mutant NMJs displayed similar expression of N-type VGCC puncta staining with lesser P/Q-type VGCCs. This was confirmed by our quantitative analysis, which showed higher total N-type VGCC puncta compared to total P/Q-type VGCC puncta. This finding is in support of prior literature which states that, N-type VGCC are more abundant at the nerve terminal than P/Q-type channels during early development of the NMJ (Rosato-Siri *et al.*, 2002). The N-type VGCCs are however located more distal to active zones compared to P/Q-type VGCCs, resulting in further diffusion distance for Ca^{2+} to reach the active zones and initiate propagation of

neurotransmission. As a result of their distal proximity to active zones, N-type VGCCs are purported to be involved in fine tuning calcium influx depending on stimulus patterns, while P/Q-type VGCCs are directly involved in bulk release. This hypothesis suits the functional demands required of a developing mammalian NMJ, as maturation generally leads to more locomotive activity. At P18, wild-type NMJs demonstrate an evident increase in expression of P/Q-type VGCCs, while *lamb2*$^{-/-}$ NMJs maintained presence of N-type VGCCs. Given this finding and the hypothesis described above it is plausible that the poor mobility of *lamb2*$^{-/-}$ mice may be attributed in part to the maintained dependence on N-type VGCCs, which are not capable of sufficient release to facilitate proper locomotive ability.

The findings presented in this thesis demonstrate that loss of laminin-β2 resulted in altered distribution of molecular components known to associate with VGCCs. We propose that laminin-β2 interacts with P/Q-VGCCs to aid in organisation and stability of the active zone. Nishimune and colleagues (2012) showed similar expression patterns of both P/Q-type VGCCs and the active zone protein Bassoon across the end-plate and within the depths of gutters themselves. This finding suggests close interaction and localisation between P/Q-type VGCCs and active zones, which allows Bassoon to directly modulate P/Q-type VGCCs in a similar fashion to RIM1 on VGCCs by supressing inactivation of the channel to allow longer opening times and augment Ca^{2+} influx (Kiyonaka *et al.*, 2007; Kaeser *et al.*, 2011; Nishimune *et al.*, 2012). Previous literature has demonstrated interactions between active zone proteins and the β-subunit of VGCCs acts as scaffolds to aid in stability and anchoring of active zone complexes (Chen *et al.*, 2011; Billings *et al.*, 2012). Together these findings show a close interaction of active zone components and P/Q-type VGCCs, which suggests a role in anchoring of the active zone complexes, and thus they likely play a significant role in the structural integrity of the mature NMJ. We propose that this enhancement of structural integrity during maturation coincides with the functional switch from N- to P/Q-type VGCC mediated transmitter release, a process which is defective at *lamb2*$^{-/-}$ NMJs.

Nishimune *et al*., (2004) used *in vitro* studies to demonstrate that laminin-β2 is capable of binding directly to VGCCs. Thus, loss of laminin-β2 could result in dispersal of P/Q-type VGCCs, as supported by the functional and morphological findings presented in this thesis. While the same study demonstrated laminin-β2 is also capable of binding to N-type VGCCs, we propose that the interaction with P/Q-type VGCCs is critical for maturation and active zone stability *in vivo*. The functional switch in VGCC mediation of transmitter

release may also benefit the stability of active zones and the NMJ itself. Maintained presence of N-type and lesser P/Q-type VGCCs in *lamb*2$^{-/-}$ mice, as demonstrated in our studies, may result in poor active zone stability as the mutant NMJ develops. By contrast wild-type mice showed higher levels of P/Q-type VGCCs and therefore a more stable matured active zone complex at P18. Together the findings of the studies conducted herein suggest that laminin-β2 is an integral synaptic component necessary for the proper development and maturation of both the pre- and postsynaptic elements of the NMJ.

6.3 Perisynaptic Schwann cell activity at the Neuromuscular Junctions of Laminin-β2 Deficient mice

Literature has shown PSCs are capable of regulating the development and functional properties of NMJs, as well as responding to perturbations at the NMJ effectively attempting to compensate for such perturbations (Miledi & Slater, 1968; Georgiou *et al.*, 1994; Robitaille, 1998; Feng & Ko, 2008; Todd *et al.*, 2010). During development, PSCs are plastic and are capable of directing processes to regulate the function of NMJs by pruning inactive sites during the elimination stage of development. Robitaille and colleagues have shown PSCs are capable of detecting and modulating synaptic transmission via purinergic and muscarinic signalling receptors during different stages of NMJ development (Rochon *et al.*, 2001; Darabid *et al.*, 2013). Such signalling may be responsible for regulating the level of interposition of Schwann cell finger like projections within the synaptic cleft (Bennett *et al.*, 1989). The loss of laminin-β2 results in invasion of the synaptic cleft by perisynaptic Schwann cell processes, with a fifteen fold increase in the direct apposition of PSCs to the basal lamina (Noakes *et al.*, 1995a; Patton *et al.*, 1998). Investigators propose that laminin-521, possessing the laminin-β2 chain, actively inhibits the invasion of the synaptic cleft by PSC processes. Thus laminin-β2 may serve to maintain the integrity of pre- and postsynaptic components and ensure that these synaptic elements are not disrupted by PSC processes. We are the first to functionally characterise the activity and capacity of PSCs at *lamb*2$^{-/-}$ NMJs. Interestingly we found mutant PSCs generally demonstrated immature phenotypes, with irregular responses to stimuli. During development, PSCs influence transmission by purinergic signalling which later switches to muscarinic signalling (Darabid *et al.*, 2013). The purinergic agonist, ATP, is co-released with ACh from the nerve terminal and from activated skeletal muscle (De Lorenzo *et al.*, 2006; Burnstock, 2009). *Lamb*2$^{-/-}$ NMJs remained dependent on the purinergic receptor signalling pathway, which has been shown to be the primary receptor signalling pathway in activation of immature PSCs. Wild-type PSCs showed increasing dependency on

muscarinic receptor signalling with a progressive and corresponding decline in purinergic contribution. These findings strongly indicate a failure in the developmental switch of signalling receptors involved in neuromodulation at mutant NMJs. The loss of laminin-β2 also coincided with higher synaptic depression after high frequency stimulation was induced at *lamb*2$^{-/-}$ NMJs. Darabid *et al*., (2013), demonstrate that PSCs are capable of detecting and decoding input stimulus and altering the activity at the NMJ to enhance or depress neurotransmission signals. Our findings suggest that PSCs at *lamb*2$^{-/-}$ NMJs are incapable of properly detecting these signals and therefore cannot aid in enhancing synaptic activity when the stimulus pattern is applied at the terminal. It is possible that mutants are not exposed to such stimulus patterns and thus the PSCs are unfamiliar with how to decode and deal with such signalling. It is yet to be elucidated if the decrease in neurotransmission precedes the alterations in PSC function or whether a decline in the latter results in poor transmission properties.

This thesis is also the first to examine neurotransmission at slow twitch fibre type muscle (soleus) from *lamb*2$^{-/-}$ mice. We found comparable trends in neurotransmission deficits to those previously reported at the diaphragm, a mixed fibre type muscle (Noakes 1995; Knight et al., 2003). The observed significant reductions in quantal release at *lamb*2$^{-/-}$ NMJs coincided with the delayed maturation of PSCs. The similarities in neurotransmission defects at both slow twitch and mixed twitch fibre type muscles suggests loss of laminin-β2 results in compromised development of NMJs leading to a decrease in the safety factor for transmission, irrespective of fibre type. We propose that the defects in transmission properties are in part due to poor PSC modulation of synaptic transmission at *lamb*2$^{-/-}$ NMJs. Or it is equally plausible, that as a consequence of the defects in neurotransmission, there is compromised maturation of the supportive PSCs. In conclusion, we propose that the loss of laminin-β2 results in delayed maturation of PSCs at the NMJ, resulting in poor synaptic properties stemming from the functional and morphological traits of immature PSCs. This hypothesis will have to be further tested. A possible experiment would be to chronically inhibit the muscarinic receptors with atropine during the developmental period P0 to P15 on wild-type NMJs and examine the changes in neurotransmission this produces.

6.4 The Functional consequence of Laminin-α4 loss at the Developing Neuromuscular Junction

This study was the first to functionally characterise the neurotransmission properties of neuromuscular junctions lacking laminin-α4. Previous studies have focused on the morphological changes associated with loss of laminin-α4, showing normal formation but misalignment of presynaptic specialisations to the postsynaptic AChR end-plate (Patton *et al.*, 2001). Laminin-α4 is found in highest concentration between the folds rather than at the crests of the folds themselves, suggesting a role in signalling where active zones or folds should not form during development, resulting in tight apposition of active zones to dense AChR clusters at the end-plate. Thus, the misalignment observed by Patton *et al.*, (2001) may be attributed to this loss of instruction during development. A previous study has observed that *lama*4$^{-/-}$ mice show uncoordinated hindlimb movement when held by the tail, suggestive of a motor deficit (Patton *et al.*, 2001). We found significant changes in neurotransmission properties from P8 in *lama*4$^{-/-}$ mice that are likely not directly due to changes in alignment of pre- and postsynaptic specialisations but rather occur as a consequence of adaptive measures taken to overcome the mutant induced defects. Mutant mice demonstrate significantly decreased quantal content in each of the fibre types investigated, suggesting loss of laminin-α4 results in similar deficits irrespective of fibre types. Immunohistochemistry showed a decrease in active zone markers and an increase in synaptic vesicles. Studies have suggested that a build-up of synaptic vesicles may be the result of impaired transmission due to a loss of interaction in the release mechanisms. What this loss of interaction is, and which molecules are involved, is yet to be elucidated but we propose that the release-machinery proteins are the likely culprits. This is supported by our findings of increased synaptic depression and perturbed facilitation which could be explained by a deficit on the ready releasable pool of vesicles. Vesicular availability relies on vesicular associated proteins such as synapsin 1, Rab3A, Rabphilin 3, dynamin and clathrin. The increase in depression and changes in facilitation in the mutant NMJs could not be explained by a decrease in vesicular density within the terminal since ultra-structural examination revealed no evidence for this. Thus neither the availability of synaptic vesicles nor their locale within the presynaptic terminal, are the reason behind the altered neurotransmission that we have observed.

6.5 Laminins form Scaffolds with Pre- and Postsynaptic Molecules to Organise Specialisation and Enhance the Integrity of the Neuromuscular Junction

Given our functional findings, it is evident that the laminins, in particular laminins-α4 and –β2 play an integral part in organisation of the NMJ. The laminin family has been shown to interact with numerous molecules at both the pre- and postsynaptic regions of the NMJ. At the presynaptic nerve terminal, VGCCs and α3 integrin have been shown to act as ligands to bind laminins-β2 and –α4 respectively which comprise the heterotrimer laminin-421 (Nishimune *et al.*, 2004; Carlson *et al.*, 2010; Chen *et al.*, 2011; Nishimune *et al.*, 2012) (Figure 6.1*A*). Interaction with the presynaptic VGCCs forms a scaffold for other presynaptic active zone molecules to anchor in close proximity to the VGCCs themselves. The laminin-α4-α3 integrin complex is suggested to allow patterning of active zones to the VGCCs linked via laminin-β2. The long arms of laminin-221 and laminin 521, interact with receptors at the postsynaptic membrane (Figure 6.1*B*). Cell surface receptors such as α-dystroglycan, agrin and integrin have also been shown to bind laminins at high affinity, and in turn bind to the actin cytoskeleton to transduce signals to the cell interior (Ervasti & Campbell, 1993; Gee *et al.*, 1993; Denzer *et al.*, 1997; Denzer *et al.*, 1998; Kammerer *et al.*, 1999; Colognato & Yurchenco, 2000; Hohenester & Yurchenco, 2013). The laminin heterotrimers, laminin-221 and laminin 521, interact with each other to form ternary nodes, which in turn allow the linkage of a laminin network (Figure 6.1*C*). The short arm domains of the laminin network interact with a type XVIII collagen network via nidogens and perlecans/agrins (Fox *et al.*, 1991; Latvanlehto *et al.*, 2010). These non-laminin molecules are involved in not only providing stability but also enabling the tethering of tissue specific growth factors (such as neuregulins) via interaction with the heparin sulfates, agrin and perlecan. Of note, the short-arm laminin-421 is not part of the laminin network that links the postsynaptic membrane to the basement membrane, due to the short arm ‘T’ shaped structure. Based on this unique structure and the findings presented here, we propose that laminin-421 plays a critical role in the organisation of the NMJ. These complex interactions allow for a link between pre- and postsynaptic regions to the basement membrane and are thought to enhance the precision, stability, and structural integrity of the NMJ, and in turn enable efficient neurotransmission.

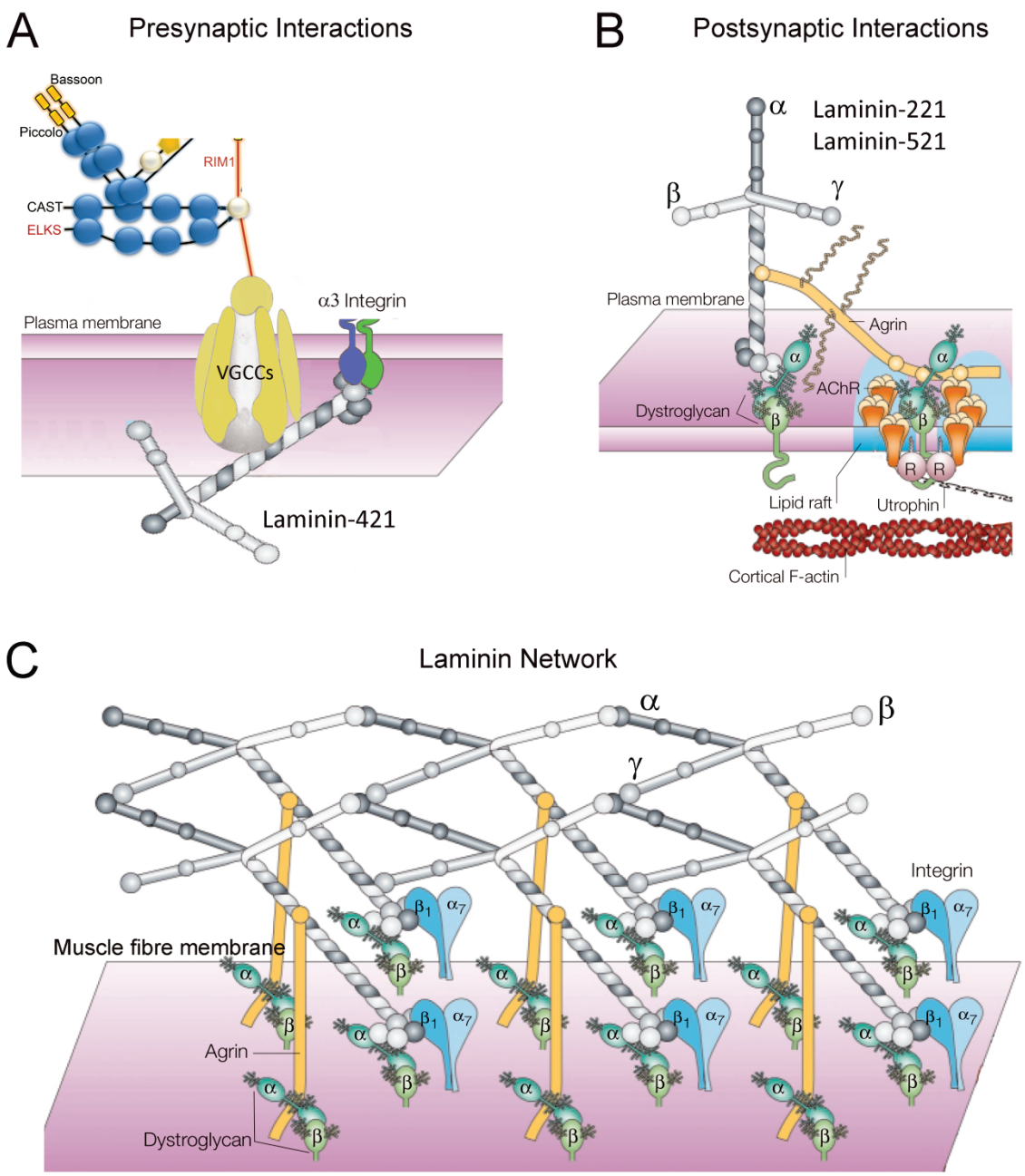

Figure 6.1 Illustration of the Molecular Interactions with Laminin Chains at the Neuromuscular Junction

A, laminin-421 binds receptors at the presynaptic region, namely $Ca_v\alpha$ subunit of VGCCs and α3 integrins via interactions with the laminin-β2 and –α4 chains respectively. This interaction aids in the stabilisation of the active zone region as well as organising and aligning the active zones to the postsynaptic specialisations. ***B***, lipid rafts act as platforms that allow concentration of molecules such as AChRs and rapsyn (R) at the postsynaptic membrane. Agrin is proposed to aggregate and anchor lipid rafts through its binding of laminins and to the dystroglycan-rapsyn complex. These complexes are then thought to interact with other molecules to connect to the cortical F-actin cytoskeleton to enhance stability of the clustered postsynaptic molecules. ***C***, diagrammatic illustration of the molecular architecture of the basement membrane. The laminin heterotrimers, laminin-221 and -521, interact to form a

network that aids in maintenance of structural integrity of the NMJ. A single α, β, and γ subunit from different heterotrimers interacts to form a ternary node. This network is then anchored to the muscle fibre membrane via interactions with integrins, α-dystroglycan and agrin as well as a number of collateral interactions with other molecules. The laminin network also interacts with a collagen network via nidogens and perlecans/agrins to scaffold the basement membrane to the postsynaptic membrane. Note, laminin-421 is not thought to be involved with this laminin network. Figures adapted from Bezakova and Ruegg (2003).

6.6 Limitation of Current Studies and Future Directions

While the studies presented within this thesis substantially further the understanding of laminins in development of the NMJ, several limitations must be noted. The knockout model used for the *lamb*2$^{-/-}$ studies allows only a limited age range to be investigated, with mice commonly dying at weaning age (P21) due to renal failure (Noakes *et al.*, 1995a; Patton *et al.*, 1997). Thus conclusive findings cannot be drawn as to whether these mutant NMJs demonstrated delayed maturation or, whether these changes indicate a complete halt in NMJ development. Patton (1998), have shown that the survival rate of *lamb*2$^{-/-}$ mice can be increased to around postnatal day 40 if mice are fed a special high fat diet after weaning. A current study in our laboratory is employing a high caloric diet in order to increase the lifespan of the *lamb*2$^{-/-}$ mice to allow us to comprehensively address this issue with the currently available model. The findings thus far indicate no improvement in the functional neurotransmission properties in mutant mice, however morphological study is still underway. Present studies have been limited to investigating the role of laminin-β2 during synaptogenesis, with little known of its purpose or actions during latter stages of life. It would be interesting to investigate whether the loss of laminin-β2 at later stages of synaptogenesis or during adulthood, would result in disassembly or drastic morphological changes at the mouse NMJ. A potential tool to study these queries would be the generation of a flox *LAMB2* allele in mice, as has been successfully undertaken to create the *lama*5^{loxP} conditional mutant (Nguyen *et al.*, 2005; Nishimune *et al.*, 2008). Utilising this technique the functional changes associated with loss of laminin-β2 at various adult ages can be investigated after the NMJ has fully developed, to help in elucidating whether laminin-β2 is purely a regulator of differentiation or is involved in some capacity in the maintenance of the NMJ during ageing.

Investigation of *lama*4$^{-/-}$ NMJs utilising extracellular macro-patch electrodes raised another limitation to our study. The use of such electrodes allowed detection of currents beneath the electrode where it formed a seal with the muscle fibre. Thus the sampling properties are greatly influenced by the relative size of the NMJ in relation to the muscle fibre. Release from a small NMJ relative to the fibre size will be adequately sampled but there was a possibility that larger NMJs may not be sampled accurately. Our morphological studies indicate that the *lama*4$^{-/-}$ mice possessed larger NMJs and thus it is possible that we may have been under-sampling these junctions. While electrodes were approximately 2-10 μm in size, they still failed to detect intermittence of evoked responses at mutant NMJs. This may have been as a result of the electrodes detecting release from other

NMJs at a distance i.e. multi-terminal recording. These failures were clearly detected through the use of intracellular recordings and therefore we must highlight issues with the reliability of the extracellular recordings in this regard. I therefore limited the use of our extracellular recordings to accurately assess a number of functional parameters including the detection of nerve terminal impulses, and the timing parameters of evoked and spontaneous responses.

While we observed changes in the laminin-α4 deficient NMJs, starting at P8 which became more apparent by P18, we could not determine the exact cause of this functional deficit. Our studies proposed a change in the interaction of presynaptic release machinery. However, due to the techniques used to investigate neurotransmission and morphology we were not able to delve deeper and find the exact molecular interactions which may be altered. Molecular interactions may be synergistically enhanced in the presence of laminin-α4 and therefore are capable of efficiently releasing vesicular contents. The use of *in vitro* techniques may allow for more thorough investigation of specific presynaptic interactions which are likely affected in *lama*4$^{-/-}$ NMJs.

Finally, due to the observed decline in neurotransmission properties from P8 to P18 at *lama*4$^{-/-}$ NMJs, it would be important to investigate older ages to elucidate if any further progression of deficits occurs. The study presented in this thesis was limited to animals under or at weaning age, with no aged animals investigated. Recent study has shown irregular expression of laminin-α4 at the NMJs of aged wild type mice (Samuel *et al.*, 2012). Samuel and colleagues (2012) suggest that laminin-α4 may play a role in maintaining the NMJ during ageing, with its loss resulting in premature breakdown of the NMJ, however no functional studies were conducted to elucidate the implications of these changes on neurotransmission properties. Studies in our laboratory are underway to address this issue. We are currently characterising wild-type and *lama*4$^{-/-}$ NMJs during ageing, from three to twelve months of age, to better understand the role of laminin-α4 in the maintenance of the NMJ.

6.7 Conclusions

The laminin family, in particular laminins-α4 and -β2, are critical for the proper development of a functional neuromuscular junction, which has a high safety factor for neurotransmission. Overall, loss of either of these laminin chains resulted in functional deficits via two different pathways. Loss of laminin-β2 lead to more severe changes in functional capacity compared to those seen in laminin-α4 deficient NMJs. This may be due to the fact that laminin-β2 is present in each of the three synapse specific laminin heterotrimers, resulting in the loss of more molecular interactions than observed after the loss of a single heterotrimers as in the case of laminin-α4 knockout. The functional findings of this study are in strong agreement with the ultra-structural and molecular findings of previous literature. Importantly, we have advanced this field by our present study, which observed a functional change in the VGCCs involved in neurotransmission rather than simply a molecular interaction that aids in active zone stability. We have observed that laminin-β2 plays an integral role and interaction with each component of the NMJ. Notably, while the defects observed at *lama*4$^{-/-}$ NMJs were not as drastic compared to those shown at *lamb*2$^{-/-}$ NMJs, we were the first to functionally characterise these mice, observing subtle deficits from early age that progress but do not effect the survivability of mutants. The findings of this thesis suggest that each laminin plays a crucial and different role for the developing NMJ. Laminin-α4 appears to act as the NMJ engineer by signalling the correct placement of pre- and postsynaptic specialisations. By contrast, laminin-β2 may act as the foundation stone or support pillar for each element to be structured and anchored around. Thus loss of laminin-α4 results in a synapse with improperly localised specialisation, while loss of laminin-β2 leads to whole scale deficits in structure of the NMJ. The loss of, or change in expression of laminins-α4 or -β2 resulted in significant changes in morphology and neurotransmission at the developing neuromuscular junction.

References

Abramoff MD, Magalhaes PJ & Ram SJ. (2004). Image Processing with ImageJ. *Biophotonics International* **11,** 36-42.

Adams ME, Kramarcy N, Fukuda T, Engel AG, Sealock R & Froehner SC. (2004). Structural Abnormalities at Neuromuscular Synapses Lacking Multiple Syntrophin Isoforms. *The Journal of Neuroscience* **24,** 10302-10309.

Adler EM, Augustine GJ, Duffy SN & Charlton MP. (1991). Alien Intracellular Calcium Chelators Attenuate Neurotransmitter Release At The Squid Giant Synapse. *Journal of Neuroscience* **11,** 1496-1507.

Adolfsen B & Littleton JT. (2001). Genetic and Molecular Analysis of the Synaptotagmin Family. *Cellular and Molecular Life Sciences* **58,** 393-402.

Alkadhi K. (1989). Giant Miniature End-Plate Potentials at the Untreated and Emetine-Treated Frog Neuromuscular Junction. *Journal of Physiology* **412,** 475-491.

Augustin I, Rosenmund C, Sudhof TC & Brose N. (1999). Munc13-1 is Essential for Fusion Competence of Glutamatergic Synoptic Vesicles. *Nature* **400,** 457-461.

Augustine GJ. (1990). Regulation of Transmitter Release at the Squid Giant Synapse by Presynaptic Delayed Rectifier Potassium Current. *Journal of Physiology-London* **431,** 343-364.

Augustine GJ, Adler EM & Charlton MP. (1991). The Calcium Signal for Transmitter Secretion from Presynaptic Nerve Terminals. *Annals of the New York Academy of Sciences* **635,** 365-381.

Augustine GJ, Adler EM, Charlton MP, Hans M, Swandulla D & Zipser K. (1992). Presynaptic Calcium Signals During Neurotransmitter Release- Detection with Fluorescent Indicators and Other Calcium Chelators. *Journal of Physiology-Paris* **86,** 129-134.

Augustine GJ & Charlton MP. (1986). Calcium Dependence of Presynaptic Calcium Current and Postsynaptic Response at the Squid Giant Synapse. *Journal of Physiology-London* **381,** 619-640.

Auld DS & Robitaille R. (2003). Perisynaptic Schwann Cells at the Neuromuscular Junction: Nerve- and Activity-Dependent Contributions to Synaptic Efficacy, Plasticity, and Reinnervation. *The Neuroscientist* **9,** 144-157.

Aumailley M, Bruckner-Tuderman L, Carter WG, Deutzmann R, Edgar D, Ekblom P, Engel J, Engvall E, Hohenester E & Jones JC. (2005). A Simplified Laminin Nomenclature. *Matrix Biology* **24,** 326-332.

Aumailley M, Timpl R & Sonnenberg A. (1990). Antibody to Integrin α6 Subunit Specifically Inhibits Cell-Binding to Laminin Fragment 8. *Experimental cell research* **188,** 55-60.

Balice-Gordon R. (1997). Age-Related Changes in Neuromuscular Innervation. *Muscle & Nerve* **5,** S83-S87.

Balice-Gordon RJ, Chua CK, Nelson CC & Lichtman JW. (1993). Gradual Loss of Synaptic Cartels Precedes Axon Withdrawal at Developing Neuromuscular Junctions. *Neuron* **11,** 801-815.

Balice-Gordon RJ & Lichtman JW. (1993). *In vivo* Observations of Pre-and Postsynaptic Changes During the Transition from Multiple to Single Innervation at Developing Neuromuscular Junctions. *The Journal of Neuroscience* **13,** 834-855.

Bauch H & Schaffer J. (2006). Optical Sections by means of "Structured Illumination": Background and Application in Fluorescence Microscopy. *Photonik International* **5,** 86-88.

Bean AJ & Scheller RH. (1997). Better Late Than Never: A Role for Rabs Late in Exocytosis. *Neuron* **19,** 751-754.

Beck K, Hunter I & Engel J. (1990). Structure and Function of Laminin: Anatomy of a Multidomain Glycoprotein. *The FASEB journal* **4,** 148-160.

Belkin AM & Stepp MA. (2000). Integrins as receptors for Laminins. *Microscopy Research and Technique* **51,** 280-301.

Bennett MR. (2001). Mechanisms of Depression of Transmitter Release at Synapses. *Neuroreport* **12,** A15-A20.

Bennett MR, & Florin T. (1974). A Statistical Analysis of the Release of Acetylcholine at Newly Formed Synapses in Striated Muscle. *Journal Physiology* **238,** 93-107.

Bennett MR, Jones P & Lavidis N. (1986a). Transmitter Secretion Varies Between Visualized Release Sites at Amphibian Neuromuscular Junctions. *Neuroscience Letters* **65,** 311-315.

Bennett MR, Karunanithi S & Lavidis N. (1991). Probabilistic Secretion of Quanta from Nerve Terminals in Toad (*Bufo Marinus*) Muscle Modulated by Adenosine. *Journal Physiology* **433,** 421-434.

Bennett MR, Fisher C, Florin T, Quine M & Robinson J. (1977). The Effect of Calcium Ions and Temperature on the Binomial Parameters that Control Acetylcholine Release by a Nerve Impulse at Amphibian Neuromuscular Synapses. *J Physiol* **271,** 641-672.

Bennett MR, Jones P & Lavidis NA. (1986b). The Probability of Quantal Secretion Along Visualized Terminal Branches at Amphibian (*Bufo marinus*) Neuromuscular Synapses. *Journal of Physiology-London* **379,** 257-&.

Bennett MR & Lavidis NA. (1979). Effect of Calcium-Ions on the Secretion of Quanta Evoked by an Impulse at Nerve-Terminal Release Sites. *Journal of General Physiology* **74,** 429-456.

Bennett MR, Lavidis NA & Lavidis-Armson F. (1989). The Probability of Quantal Secretion at Release Sites of Different Length in Toad (*Bufo Marinus*) Muscle. *Journal of Physiology* **418,** 235-249.

Betz A, Okamoto M, Benseler F & Brose N. (1997). Direct Interaction of the Rat *unc-13* Homologue Munc13-1 with the N Terminus of Syntaxin. *Journal of Biological Chemistry* **272,** 2520-2526.

Bezakova G & Ruegg MA. (2003). New Insights into the Roles of Agrin. *Nature Reviews Molecular Cell Biology* **4,** 295-309.

Billings SE, Clarke GL & Nishimune H. (2012). ELKS1 and Ca^{2+} Channel Subunit β4 Interact and Colocalize at Cerebellar Synapses. *Neuroreport* **23,** 49.

Birks R, Katz B & Miledi R. (1960). Physiological and Structural Changes at the Amphibian Myoneural Junction, in the Course of Nerve Degeneration. *Journal of Physiology* **150,** 145.

Birnbaumer L, Qin N, Olcese R, Tareilus E, Platano D, Costantin J & Stefani E. (1998). Structures and Functions of Calcium Channel β Subunits. *Journal of Bioenergetics and Biomembranes* **30,** 357-375.

Bishop DL, Misgeld T, Walsh MK, Gan W-B & Lichtman JW. (2004). Axon Branch Removal at Developing Synapses by Axosome Shedding. *Neuron* **44,** 651-661.

Blewett C & Elder GC. (1993). Quantitative EMG Analysis in Soleus and Plantaris During Hindlimb Suspension and Recovery. *Journal of Applied Physiology* **74,** 2057-2066.

Bloom O, Evergren E, Tomilin N, Kjaerulff O, Low P, Brodin L, Pieribone VA, Greengard P & Shupliakov O. (2003). Colocalization of Synapsin and Actin During Synaptic Vesicle Recycling. *Journal of Cell Biology* **161,** 737-747.

Bogen IL, Boulland JL, Mariussen E, Wright MS, Fonnum F, Kao HT & Walaas SI. (2006). Absence of Synapsin I and II is Accompanied by Decreases in Vesicular Transport of Specific Neurotransmitters. *Journal of Neurochemistry* **96,** 1458-1466.

Bowersox SS, Miljanich GP, Sugiura Y, Li C, Nadasdi L, Hoffman BB, Ramachandran J & Ko CP. (1995). Differential Blockade of Voltage-Sensitive Calcium Channels at the Mouse Neuromuscular-Junction by Novel ω-Conopeptides and ω-Agatoxin-IVA. *Journal of Pharmacology and Experimental Therapeutics* **273,** 248-256.

Brill MS, Lichtman JW, Thompson W, Zuo Y & Misgeld T. (2011). Spatial Constraints Dictate Glial Territories at Murine Neuromuscular Junctions. *Journal of Cell Biology* **195,** 293-305.

Brodin L, Low P, Gad H, Gustafsson J, Pieribone VA & Shupliakov O. (1997). Sustained Neurotransmitter Release: New Molecular Clues. *European Journal of Neuroscience* **9,** 2503-2511.

Brose N, Petrenko AG, Sudhof TC & Jahn R. (1992). Synaptotagmin: a Calcium Sensor on the Synaptic Vesicle Surface. *Science* **256,** 1021-1025.

Brown M, Jansen J & Van Essen D. (1976). Polyneuronal Innervation of Skeletal Muscle in New-Born Rats and its Elimination During Maturation. *Journal of Physiology* **261,** 387-422.

Buffelli M, Busetto G, Cangiano L & Cangiano A. (2002). Perinatal Switch from Synchronous to Asynchronous Activity of Motoneurons: Link with Synapse Elimination. *Proceedings of the National Academy of Sciences* **99,** 13200-13205.

Burns ME, Sasaki T, Takai Y & Augustine GJ. (1998). Rabphilin-3A: a Multifunctional Regulator of Synaptic Vesicle Traffic. *Journal of General Physiology* **111,** 243-255.

Burnstock G. (2009). Purinergic Cotransmission. *Experimental physiology* **94,** 20-24.

Caillol G, Vacher H, Musarella M, Bellouze S, Dargent B & Autillo-Touati A. (2012). Motor Endplate Disease Affects Neuromuscular Junction Maturation. *European Journal of Neuroscience* **36,** 2400-2408.

Carbone E & Lux H. (1987). Kinetics and Selectivity of a Low-Voltage-Activated Calcium Current in Chick and Rat Sensory Neurones. *Journal of Physiology* **386,** 547-570.

Carlson SS, Valdez G & Sanes JR. (2010). Presynaptic Calcium Channels and Integrins are Complexed with Synaptic Cleft Laminins, Cytoskeletal Elements and Active Zone Components. *Journal of Neurochemistry* **115,** 654-666.

Castillo PE, Schoch S, Schmitz F, Sudhof TC & Malenka RC. (2002). RIM1α is Required for Presynaptic Long-Term Potentiation. *Nature* **415,** 327-330.

Castonguay A & Robitaille R. (2001). Differential Regulation of Transmitter Release by Presynaptic and Glial Ca2+ Internal Stores at the Neuromuscular Synapse. *Journal of Neuroscience* **21,** 1911-1922.

Catterall WA. (1999). Interactions of Presynaptic Ca^{2+} Channels and SNARE Proteins in Neurotransmitter Release. In *Molecular and Functional Diversity of Ion Channels and Receptors*, ed. Rudy BSP, pp. 144-159.

Ceccarelli B, Hurlbut WP & Mauro A. (1973). Turnover of Transmitter and Synaptic Vesicles at Frog Neuromuscular Junction. *Journal of Cell Biology* **57,** 499-524.

Chand, KK, Lee, KM, Schenning, MP, Lavidis, NA, and Noakes, PG. (2014) Loss of β2-laminin Alters Calcium Sensitivity and Voltage Gated Calcium Channel Maturation of Neurotransmission at the Neuromuscular Junction. *Journal of Physiology.* DOI: 10.1113/jphysiol.2014.284133

Chapman ER. (2002). Synaptotagmin: A Ca^{2+} Sensor that Triggers Exocytosis? *Nature Reviews Molecular Cell Biology* **3,** 498-508.

Charvin N, Leveque C, Walker D, Berton F, Raymond C, Kataoka M, ShojiKasai Y, Takahashi M, DeWaard M & Seagar MJ. (1997). Direct Interaction of the Calcium Sensor Protein Synaptotagmin I with a Cytoplasmic Domain of the α1A Subunit of the P/Q-type Calcium Channel. *Embo Journal* **16,** 4591-4596.

Chen J, Billings SE & Nishimune H. (2011). Calcium Channels Link the Muscle-Derived Synapse Organizer Laminin β2 to Bassoon and CAST/Erc2 to Organize Presynaptic Active Zones. *Journal of Neuroscience* **31,** 512-525.

Chen J, Mizushige T & Nishimune H. (2012). Active Zone Density is Conserved During Synaptic Growth but Impaired in Aged Mice. *Journal of Comparative Neurology* **520,** 434-452.

Chen YA & Scheller RH. (2001). SNARE-Mediated Membrane Fusion. *Nature Reviews Molecular Cell Biology* **2,** 98-106.

Chi P, Greengard P & Ryan TA. (2001). Synapsin Dispersion and Reclustering During Synaptic Activity. *Nature Neuroscience* **4,** 1187-1193.

Chiu AY & Sanes JR. (1984). Development of Basal Lamina in Synaptic and Extrasynaptic Portions of Embryonic Rat Muscle. *Developmental Biology* **103,** 456-467.

Cho SI, Ko J, Patton BL, Sanes JR & Chiu AY. (1998). Motor Neurons and Schwann Cells Distinguish Between Synaptic and Extrasynaptic Isoforms of Laminin. *Journal of Neurobiology* **37,** 339-358.

Cohen MW, Hoffstrom BG & DeSimone DW. (2000). Active Zones on Motor Nerve Terminals Contain α3β1 Integrin. *Journal of Neuroscience* **20,** 4912-4921.

Cohn RD, Herrmann R, Sorokin L, Wewer UM & Voit T. (1998). Laminin alpha 2 chain-deficient congenital muscular dystrophy - Variable epitope expression in severe and mild cases. *Neurology* **51,** 94-100.

Cohn RD, Herrmann R, Wewer UM & Voit T. (1997). Changes of Laminin β2 Chain Expression in Congenital Muscular Dystrophy. *Neuromuscular Disorders* **7,** 373-378.

Colognato H & Yurchenco PD. (2000). Form and Function: the Laminin Family of Heterotrimers. *Developmental Dynamics* **218,** 213-234.

Correia-de-Sa P, Timoteo MA & Ribeiro JA. (2000a). A(2A) Adenosine Receptor Facilitation of Neuromuscular Transmission: Influence of Stimulus Paradigm on Calcium Mobilization. *Journal of Neurochemistry* **74,** 2462-2469.

Correia-de-Sa P, Timoteo MA & Ribeiro JA. (2000b). Influence of Stimulation on Ca2+ Recruitment Triggering H-3 Acetylcholine Release from the Rat Motor-Nerve Endings. *European Journal of Pharmacology* **406,** 355-362.

Couteaux R & Pecot-Dechavassine M. (1974). Les Zones Spécialisées des Membranes Présynaptiques. *Comptes Rendus de l'Academie des Sciences Paris* **278,** I-293.

Creazzo TL & Sohal GS. (1983). Neural Control of Embryonic Acetylcholine Receptor and Skeletal Muscle. *Cell and Tissue Research* **228,** 1-12.

Crowder KM, Gunther JM, Jones TA, Hale BD, Zhang HZ, Peterson MR, Scheller RH, Chavkin C & Bajjalieh SM. (1999). Abnormal Neurotransmission in Mice Lacking Synaptic Vesicle Protein 2A (SV2A). *Proceedings of the National Academy of Sciences of the United States of America* **96,** 15268-15273.

Culican SM, Nelson CC & Lichtman JW. (1998). Axon Withdrawal During Synapse Elimination at the Neuromuscular Junction is Accompanied by Disassembly of the Postsynaptic Specialization and Withdrawal of Schwann Cell Processes. *Journal of Neuroscience* **18,** 4953-4965.

Currie KP & Fox AP. (1997). Comparison of N-and P/Q-Type Voltage-Gated Calcium Channel Current Inhibition. *Journal of Neuroscience* **17,** 4570-4579.

Currie KP & Fox AP. (2002). Differential Facilitation of N-and P/Q-Type Calcium Channels During Trains of Action Potential-Like Waveforms. *Journal of Physiology* **539,** 419-431.

Darabid H, Arbour D & Robitaille R. (2013). Glial Cells Decipher Synaptic Competition at the Mammalian Neuromuscular Junction. *Journal of Neuroscience* **33,** 1297-1313.

David G & Barrett EF. (2000). Stimulation-Evoked Increases in Cytosolic [Ca^{2+}] in Mouse Motor Nerve Terminals are Limited by Mitochondrial Uptake and are Temperature-Dependent. *Journal of Neuroscience* **20,** 7290-7296.

Davletov BA & Sudhof TC. (1993). A Single C_2 Domain from Synaptotagmin-I is Sufficient for High-Affinity Ca^{2+}/Phospholipid Binding. *Journal of Biological Chemistry* **268,** 26386-26390.

Day NC, Wood SJ, Ince PG, Volsen SG, Smith W, Slater CR & Shaw PJ. (1997). Differential Localization of Voltage-Dependent Calcium Channel α_1 Subunits at the Human and Rat Neuromuscular Junction. *Journal of Neuroscience* **17,** 6226-6235.

De Camilli P, Cameron R & Greengard P. (1983). Synapsin-I (Protein-I), a Nerve Terminal-Specific Phosphoprotein. I. its General Distribution in Synapses of the Central and Peripheral Nervous-System Demonstrated by Immunofluorescence in Frozen and Plastic Sections. *Journal of Cell Biology* **96,** 1337-1354.

De Laet A, Adriaensen D, Van Bogaert PP, Scheuermann D & Timmermans JP. (2002). Immunohistochemical Localization of Voltage-Activated Calcium Channels in the Rat Oesophagus. *Neurogastroenterology & Motility* **14,** 173-181.

De Lorenzo S, Veggetti M, Muchnik S & Losavio A. (2006). Presynaptic Inhibition of Spontaneous Acetylcholine Release Mediated by P2Y Receptors at the Mouse Neuromuscular Junction. *Neuroscience* **142,** 71-85.

DeChiara TM, Bowen DC, Valenzuela DM, Simmons MV, Poueymirou WT, Thomas S, Kinetz E, Compton DL, Rojas E, Park JS, Smith C, DiStefano PS, Glass DJ, Burden SJ & Yancopoulos GD. (1996). The Receptor Tyrosine Kinase MuSK is Required for Neuromuscular Junction Formation In Vivo. *Cell* **85,** 501-512.

Deguchi-Tawarada M, Inoue E, Takao-Rikitsu E, Inoue M, Kitajima I, Ohtsuka T & Takai Y. (2006). Active Zone Protein CAST is a Component of Conventional and Ribbon Synapses in Mouse Retina. *Journal of Comparative Neurology* **495,** 480-496.

Deguchi-Tawarada M, Inoue E, Takao-Rikitsu E, Inoue M, Ohtsuka T & Takai Y. (2004). CAST2: Identification and Characterization of a Protein Structurally Related to the Presynaptic Cytomatrix Protein CAST. *Genes to Cells* **9,** 15-23.

Del Castillo J & Katz B. (1954a). The Effect of Magnesium on the Activity of Motor Nerve Endings. *Journal of Physiology* **124,** 553-559.

Del Castillo J & Katz B. (1954b). Quantal Components of the End-Plate Potential. *Journal of Physiology-London* **124,** 560-573.

Delwel GO, Hogervorst F & Sonnenberg A. (1996). Cleavage of the alpha 6A subunit is essential for activation of the alpha 6A beta 1 integrin by phorbol 12-myristate 13-acetate. *Journal of Biological Chemistry* **271,** 7293-7296.

Denzer AJ, Brandenberger R, Gesemann M, Chiquet M & Ruegg MA. (1997). Agrin Binds to the Nerve–Muscle Basal Lamina via Laminin. *Journal of Cell Biology* **137,** 671-683.

Denzer AJ, Schulthess T, Fauser C, Schumacher B, Kammerer RA, Engel J & Ruegg MA. (1998). Electron Microscopic Structure of Agrin and Mapping of its Binding Site in Laminin-1. *The EMBO journal* **17,** 335-343.

Depetris RS, Nudler SI, Uchitel OD & Urbano FJ. (2008). Altered Synaptic Synchrony in Motor Nerve Terminals Lacking P/Q-Calcium Channels. *Synapse* **62,** 466-471.

DiAntonio A, Parfitt KD & Schwarz TL. (1993). Synaptic Transmission Persists in Synaptotagmin Mutants of Drosophila. *Cell* **73,** 1281-1290.

Dieck St, Sanmartí-Vila L, Langnaese K, Richter K, Kindler S, Soyke A, Wex H, Smalla K-H, Kämpf U & Fränzer J-T. (1998). Bassoon, a Novel Zinc-Finger Cag/Glutamine-Repeat Protein Selectively Localized at the Active Zone of Presynaptic Nerve Terminals. *Journal of Cell Biology* **142,** 499-509.

Dodge FA & Rahamimoff R. (1967). Co-Operative Action of Calcium Ions in Transmitter Release at the Neuromuscular Junction. *Journal of Physiology-London* **193,** 419-&.

Dunlap K, Luebke JI & Turner TJ. (1995). Exocytotic Ca^{2+} Channels in Mammalian Central Neurons. *Trends in Neurosciences* **18,** 89-98.

Einstein R & Lavidis N. (1984). The Dependence of Excitatory Junction Potential Amplitude on the External Calcium Concentration in Narcotic Tolerant Mouse Vas Deferens. *British Journal of Pharmacology* **83,** 853-861.

Eken T, Elder GC & Lømo T. (2008). Development of Tonic Firing Behavior in Rat Soleus Muscle. *Journal of Neurophysiology* **99,** 1899-1905.

Elder GC & Toner LV. (1998). Muscle Shortening Induced by Tenotomy does not Reduce Activity Levels in Rat Soleus. *Journal of Physiology* **512,** 251-265.

Elmqvist D & Quastel D. (1965). A Quantitative Study of End-Plate Potentials in Isolated Human Muscle. *Journal of Physiology* **178,** 505.

Erickson SL, O'Shea KS, Ghaboosi N, Loverro L, Frantz G, Bauer M, Lu LH & Moore MW. (1997). Erbb3 is Required for Normal Cerebellar and Cardiac Development: a Comparison with Erbb2-and Heregulin-Deficient Mice. *Development* **124,** 4999-5011.

Eroglu C & Barres BA. (2010). Regulation of Synaptic Connectivity by Glia. *Nature* **468,** 223-231.

Ertel EA, Campbell KP, Harpold MM, Hofmann F, Mori Y, Perez-Reyes E, Schwartz A, Snutch TP, Tanabe T, Birnbaumer L, Tsien RW & Catterall WA. (2000). Nomenclature of Voltage-Gated Calcium Channels. *Neuron* **25,** 533-535.

Ervasti JM & Campbell KP. (1993). A Role for the Dystrophin-Glycoprotein Complex as a Transmembrane Linker Between Laminin and Actin. *Journal of Cell Biology* **122,** 809-823.

Evergren E, Benfenati F & Shupliakov O. (2007). The Synapsin Cycle: a View from the Synaptic Endocytic Zone. *Journal of Neuroscience Research* **85,** 2648-2656.

Fambrough DM, Devreotes PN, Gardner JM & Card DJ. (1979). The Life History of Acetylcholine Receptors. *Progress in Brain Research* **49,** 325-334.

Fatt P & Katz B. (1952). Spontaneous Subthreshold Activity at Motor Nerve Endings. *Journal of Physiology-London* **117,** 109-128.

Fatt P & Katz B. (1953). The Electrical Properties of Crustacean Muscle Fibres. *Journal of Physiology-London* **120,** 171-&.

Fdez E & Hilfiker S. (2006). Vesicle Pools and Synapsins: New Insights Into Old Enigmas. *Brain Cell Biology* **35,** 107-115.

Feng Z & Ko C-P. (2007). Neuronal Glia Interactions at the Vertebrate Neuromuscular Junction. *Current Opinion in Pharmacology* **7,** 316-324.

Feng Z & Ko C-P. (2008). The Role of Glial Cells in the Formation and Maintenance of the Neuromuscular Junction. *Annals of the New York Academy of Sciences* **1132,** 19-28.

Fenster SD, Chung WJ, Zhai R, Cases-Langhoff C, Voss B, Garner AM, Kaempf U, Kindler S, Gundelfinger ED & Garner CC. (2000). Piccolo, a Presynaptic Zinc Finger Protein Structurally Related to Bassoon. *Neuron* **25,** 203-214.

Fernandez-Chacon R, Shin OH, Konigstorfer A, Matos MF, Meyer AC, Garcia J, Gerber SH, Rizo J, Sudhof TC & Rosenmund C. (2002). Structure/Function Analysis of Ca^{2+} Binding to the C_2A Domain of Synaptotagmin 1. *Journal of Neuroscience* **22,** 8438-8446.

Fertuck HC & Salpeter MM. (1974). Localization of Acetylcholine Receptor by 125I-Labeled α-Bungarotoxin Binding at Mouse Motor Endplates. *Proceedings of the National Academy of Sciences* **71,** 1376-1378.

Fertuck HC & Salpeter MM. (1976). Quantitation of Junctional and Extrajunctional Acetylcholine Receptors by Electron Microscope Autoradiography After (125) I-α-Bungarotoxin Binding at Mouse Neuromuscular Junctions. *Journal of Cell Biology* **69,** 144-158.

Fogarty MJ, Hammond LA, Kanjhan R, Bellingham MC & Noakes PG. (2013). A Method for the Three-Dimensional Reconstruction of Neurobiotin™-Filled Neurons and the Location of their Synaptic Inputs. *Frontiers in Neural Circuits* **7**.

Fogelson AL & Zucker RS. (1985). Presynaptic Calcium Diffusion from Various Arrays of Single Channels - Implications for Transmitter Release and Synaptic Facilitation. *Biophysical Journal* **48,** 1003-1017.

Fourcaudot E, Gambino F, Humeau Y, Casassus G, Shaban H, Poulain B & Luethi A. (2008). cAMP/PKA Signaling and RIM1α Mediate Presynaptic LTP in the Lateral Amygdala. *Proceedings of the National Academy of Sciences of the United States of America* **105,** 15130-15135.

Fox A, Nowycky M & Tsien R. (1987). Kinetic and Pharmacological Properties Distinguishing Three Types of Calcium Currents in Chick Sensory Neurones. *Journal of Physiology* **394,** 149-172.

Fox J, Mayer U, Nischt R, Aumailley M, Reinhardt D, Wiedemann H, Mann K, Timpl R, Krieg T & Engel J. (1991). Recombinant Nidogen Consists of Three Globular Domains and Mediates Binding of Laminin to Collagen Type IV. *The EMBO Journal* **10,** 3137.

Fratantoni SA, Weisz G, Pardal AM, Reisin RC & Uchitel OD. (2000). Amyotrophic Lateral Sclerosis IGg-Treated Neuromuscular Junctions Develop Sensitivity to L-Type Calcium Channel Blocker. *Muscle & Nerve* **23,** 543-550.

Fujiwara H, Kikkawa Y, Sanzen N & Sekiguchi K. (2001). Purification and Characterization of Human Laminin-8. *Journal of Biological Chemistry* **276,** 17550-17558.

Fukunaga H, Engel AG, Lang B, Newsom-Davis J & Vincent A. (1983). Passive Transfer of Lambert-Eaton Myasthenic Syndrome with IGg from Man to Mouse Depletes the Presynaptic Membrane Active Zones. *Proceedings of the National Academy of Sciences* **80,** 7636-7640.

Fukuoka T, Engel AG, Lang B, Newsom-Davis J, Prior C & W-Wray D. (1987). Lambert-Eaton Myasthenic Syndrome: I. Early Morphological Effects of IGg on the Presynaptic Membrane Active Zones. *Annals of Neurology* **22,** 193-199.

Gaffield MA & Betz WJ. (2007). Synaptic Vesicle Mobility in Mouse Motor Nerve Terminals with and without Synapsin. *Journal of Neuroscience* **27,** 13691-13700.

Gautam M, Noakes PG, Moscoso L, Rupp F, Scheller RH, Merlie JP & J.R. S. (1996). Defective Neuromuscular Synaptogenesis in Agrin-Deficient Mutant Mice. *Cell* **85,** 525-535

Gautam M, Noakes PG, Mudd J, Nichol M, Chu GC, Sanes JR & Merlie JP. (1995). Failure of Postsynaptic Specialization to Develop at Neuromuscular Junctions of Rapsyn-Deficient Mice. *Nature* **377,** 232-236.

Gee SH, Blacher R, Douville P, Provost P, Yurchenco P & Carbonetto S. (1993). Laminin-Binding Protein 120 from Brain is Closely Related to the Dystrophin-Associated Glycoprotein, Dystroglycan, and Binds with High Affinity to the Major Heparin Binding Domain of Laminin. *Journal of Biological Chemistry* **268,** 14972-14980.

Georgiou J, Robitaille R, Trimble WS & Chariton MP. (1994). Synaptic Regulation of Glial Protein Expression *In Vivo*. *Neuron* **12,** 443-455.

Geppert M, Bolshakov VY, Siegelbaum SA, Takei K, Decamilli P, Hammer RE & Sudhof TC. (1994a). The Role of Rab3a in Neurotransmitter Release. *Nature* **369,** 493-497.

Geppert M, Goda Y, Hammer RE, Li C, Rosahl TW, Stevens CF & Sudhof TC. (1994b). Synaptotagmin-I - a Major Ca^{2+} Sensor for Transmitter Release at a Central Synapse. *Cell* **79,** 717-727.

Gerona RRL, Larsen EC, Kowalchyk JA & Martin TFJ. (2000). The C Terminus of SNAP25 is Essential for Ca^{2+}-Dependent Binding of Synaptotagmin to SNARE Complexes. *Journal of Biological Chemistry* **275,** 6328-6336.

Gertler RA & Robbins N. (1978). Difference in Neuromuscular Transmission in Red and White Muscles. *Brain research* **142,** 160-164.

Gervasio OL & Phillips WD. (2005). Increased Ratio of Rapsyn to ACh Receptor Stabilizes Postsynaptic Receptors at the Mouse Neuromuscular Synapse. *Journal of Physiology* **562,** 673-685.

Ghazanfari N, Fernandez KJ, Murata Y, Morsch M, Ngo ST, Reddel SW, Noakes PG & Phillips WD. (2011). Muscle Specific Kinase: Organiser of Synaptic Membrane Domains. *International Journal of Biochemistry and Cell Biology* **43,** 295-298.

Gitler D, Takagishi Y, Feng J, Ren Y, Rodriguiz RM, Wetsel WC, Greengard P & Augustine GJ. (2004). Different Presynaptic Roles of Synapsins at Excitatory and Inhibitory Synapses. *Journal of Neuroscience* **24,** 11368-11380.

Glass DJ, Bowen DC, Stitt TN, Radziejewski C, Bruno J, Ryan TE, Gies DR, Shah S, Mattsson K, Burden SJ, DiStefano PS, Valenzuela DM, DeChiara TM & Yancopoulos GD. (1996). Agrin Acts via a MuSK Receptor Complex. *Cell* **85,** 513-523.

Gorassini M, Eken T, Bennett DJ, Kiehn O & Hultborn H. (2000). Activity of Hindlimb Motor Units During Locomotion in the Conscious Rat. *Journal of Neurophysiology* **83,** 2002-2011.

Grady RM, Zhou H, Cunningham JM, Henry MD, Campbell KP & Sanes JR. (2000). Maturation and Maintenance of the Neuromuscular Synapse: Genetic Evidence for Roles of the Dystrophin-Glycoprotein Complex. *Neuron* **25,** 279-293.

Graf ER, Valakh V, Wright CM, Wu C, Liu Z, Zhang YQ & DiAntonio A. (2012). RIM Promotes Calcium Channel Accumulation at Active Zones of the Drosophila Neuromuscular Junction. *Journal of Neuroscience* **32,** 16586-16596.

Green TL, Hunter DD, Chan W, Merlie JP & Sanes JR. (1992). Synthesis and Assembly of the Synaptic Cleft Protein S-Laminin by Cultured-Cells. *Journal of Biological Chemistry* **267,** 2014-2022.

Greengard P, Valtorta F, Czernik AJ & Benfenati F. (1993). Synaptic Vesicle Phosphoproteins and Regulation of Synaptic Function. *Science* **259,** 780-785.

Griffin JW & Thompson WJ. (2008). Biology and Pathology of Nonmyelinating Schwann Cells. *Glia* **56,** 1518-1531.

Gu Y & Hall ZW. (1988). Immunological Evidence for a Change in Subunits of the Acetylcholine Receptor and Denervated Rat Muscle. *Neuron* **1,** 117-125.

Hanley T & Merlie JP. (1991). Transgene detection in unpurified mouse tail DNA by polymerase chain reaction. *Biotechniques* **10,** 56-56.

Harlow ML, Ress D, Stoschek A, Marshall RM & McMahan UJ. (2001). The Architecture of Active Zone Material at the Frog's Neuromuscular Junction. *Nature* **409,** 479-484.

Harper CB, Martin S, Nguyen TH, Daniels SJ, Lavidis NA, Popoff MR, Hadzic G, Mariana A, Chau N & McCluskey A. (2011). Dynamin Inhibition Blocks Botulinum Neurotoxin Type A Endocytosis in Neurons and Delays Botulism. *Journal of Biological Chemistry* **286,** 35966-35976.

Hata K, Polo-Parada L & Landmesser LT. (2007). Selective Targeting of Different Neural Cell Adhesion Molecule Isoforms During Motoneuron Myotube Synapse Formation in Culture and the Switch from an Immature to Mature form of Synaptic Vesicle Cycling. *Journal of Neuroscience* **27,** 14481-14493.

Haucke V, Neher E & Sigrist SJ. (2011). Protein Scaffolds in the Coupling of Synaptic Exocytosis and Endocytosis. *Nature Reviews Neuroscience* **12,** 127-138.

Helbling-Leclerc A, Zhang X, Topaloglu H, Cruaud C, Tesson F, Weissenbach J, Tomé FM, Schwartz K, Fardeau M & Tryggvason K. (1995). Mutations in the Laminin α2-Chain Gene (*LAMA*2) Cause Merosin–Deficient Congenital Muscular Dystrophy. *Nature genetics* **11,** 216-218.

Henneberger C, Papouin T, Oliet SH & Rusakov DA. (2010). Long-Term Potentiation Depends on Release of D-Serine from Astrocytes. *Nature* **463,** 232-236.

Henry MD & Campbell KP. (1996). Dystroglycan: An Extracellular Matrix Receptor Linked to the Cytoskeleton. *Current Opinion in Cell Biology* **8,** 625-631.

Heuser J, Reese T, Dennis M, Jan Y, Jan L & Evans L. (1979). Synaptic Vesicle Exocytosis Captured by Quick Freezing and Correlated with Quantal Transmitter Release. *Journal of Cell Biology* **81,** 275-300.

Heuser JE & Reese TS. (1973). Evidence for Recycling of Synaptic Vesicle Membrane During Transmitter Release at Frog Neuromuscular Junction. *Journal of Cell Biology* **57,** 315-344.

Hibino H, Pironkova R, Onwumere O, Vologodskaia M, Hudspeth AJ & Lesage F. (2002). RIM Binding Proteins (RBPs) Couple Rab3-Interacting Molecules (RIMs) to Voltage-Gated Ca^{2+} Channels. *Neuron* **34,** 411-423.

Hida Y & Ohtsuka T. (2010). CAST and ELKS Proteins: Structural and Functional Determinants of the Presynaptic Active Zone. *Journal of Biochemistry* **148,** 131-137.

Hillyard DR, Monje VD, Mintz IM, Bean BP, Nadasdi L, Ramachandran J, Miljanich G, Azimizoonooz A, McIntosh JM, Cruz LJ, Imperial JS & Olivera BM. (1992). A New Conus Peptide Ligand For Mammalian Presynaptic Ca2+ Channels. *Neuron* **9,** 69-77.

Hohenester E & Yurchenco PD. (2013). Laminins in Basement Membrane Assembly. *Cell Adhesion and Migration* **7,** 56-63.

Horton RM, Manfredi AA & Conti-Tronconi BM. (1993). The'embryonic' gamma Subunit of the Nicotinic Acetylcholine Receptor is Expressed in Adult Extraocular Muscle. *Neurology* **43,** 983-983.

Hosaka M, Hammer RE & Sudhof TC. (1999). A Phospho-Switch Controls the Dynamic Association of Synapsins with Synaptic Vesicles. *Neuron* **24,** 377-387.

Hosaka M & Sudhof TC. (1998). Synapsin III, a Novel Synapsin with an Unusual Regulation by Ca^{2+}. *Journal of Biological Chemistry* **273,** 13371-13374.

Hosoi N, Sakaba T & Neher E. (2007). Quantitative Analysis of Calcium-Dependent Vesicle Recruitment and its Functional Role at the Calyx of Held Synapse. *Journal of Neuroscience* **27,** 14286-14298.

Hosono R, Hekimi S, Kamiya Y, Sassa T, Murakami S, Nishiwaki K, Miwa J, Taketo A & Kodaira KI. (1992). The *unc-18* Gene Encodes a Novel Protein Affecting the Kinetics of Acetylcholine Metabolism in the Nematode *Caenorhabditis elegans*. *Journal of Neurochemistry* **58,** 1517-1525.

Hosono R & Kamiya Y. (1991). Additional Genes which Result in an Elevation of Acetylcholine Levels by Mutations in *Caenorhabditis elegans*. *Neuroscience Letters* **128,** 243-244.

Hubbard JI, Jones SF & Landau EM. (1968). On Mechanism by which Calcium and Magnesium Affect Release of Transmitter by Nerve Impulses. *Journal of Physiology-London* **196,** 75-&.

Hughes BW, Kusner LL & Kaminski HJ. (2006). Molecular Architecture of the Neuromuscular Junction. *Muscle & nerve* **33,** 445-461.

Hunter DD, Shah V, Merlie JP & Sanes JR. (1989). A Laminin-like Adhesive Protein Concentrated in the Synaptic Cleft of the Neuromuscular-Junction. *Nature* **338,** 229-234.

Hurlbut W & Ceccarelli B. (1973). Transmitter Release and Recycling of Synaptic Vesicle Membrane at the Neuromuscular Junction. *Advances in cytopharmacology* **2,** 141-154.

Huttner WB & Greengard P. (1979). Multiple Phosphorylation Sites in Protein I and their Differential Regulation by Cyclic AMP and Calcium. *Proceedings of the National Academy of Sciences* **76,** 5402-5406.

Hvalby Ø, Jensen V, Kao H-T & Walaas SI. (2006). Synapsin-Regulated Synaptic Transmission from Readily Releasable Synaptic Vesicles in Excitatory Hippocampal Synapses in Mice. *Journal of Physiology* **571,** 75-82.

Ido H, Harada K, Futaki S, Hayashi Y, Nishiuchi R, Natsuka Y, Li S, Wada Y, Combs AC & Ervasti JM. (2004). Molecular Dissection of the α-Dystroglycan-and Integrin-Binding Sites within the Globular Domain of Human Laminin-10. *Journal of Biological Chemistry* **279,** 10946-10954.

Ido H, Nakamura A, Kobayashi R, Ito S, Li S, Futaki S & Sekiguchi K. (2007). The Requirement of the Glutamic Acid Residue at the Third Position from the Carboxyl Termini of the Laminin γ Chains in Integrin Binding by Laminins. *Journal of Biological Chemistry* **282,** 11144-11154.

Inchauspe CG, Martini FJ, Forsythe ID & Uchitel OD. (2004). Functional Compensation of P/Q by N-Type Channels Blocks Short-Term Plasticity at the Calyx of Held Presynaptic Terminal. *Journal of Neuroscience* **24,** 10379-10383.

Iwasaki S, Momiyama A, Uchitel OD & Takahashi T. (2000). Developmental Changes in Calcium Channel Types Mediating Central Synaptic Transmission. *Journal of Neuroscience* **20,** 59-65.

Jahn R & Grubmuller H. (2002). Membrane Fusion. *Current Opinion in Cell Biology* **14,** 488-495.

Jahromi BS, Robitaille R & Charlton MP. (1992). Transmitter Release Increases Intracellular Calcium in Perisynaptic Schwann Cells In Situ. *Neuron* **8,** 1069-1077.

Janz R, Goda Y, Geppert M, Missler M & Sudhof TC. (1999). SV2A and SV2B Function as Redundant Ca^{2+} Regulators in Neurotransmitter Release. *Neuron* **24,** 1003-1016.

Janz R, Hofmann K & Sudhof TC. (1998). SVOP, an Evolutionarily Conserved Synaptic Vesicle Protein Suggests Novel Transport Functions of Synaptic Vesicles. *Journal of Neuroscience* **18,** 9269-9281.

Jenkinson DH. (1957). The Nature of the Antagonism Between Calcium and Magnesium Ions at the Neuromuscular Junction. *Journal of Physiology-London* **138,** 434-444.

Jo SA, Zhu X, Marchionni MA & Burden SJ. (1995). Neuregulins are Concentrated at Nerve-Muscle Synapses and Activate ACh–Receptor Gene Expression. *Nature* **373,** 158-161.

Johnson AM & Connor NP. (2011). Effects of Electrical Stimulation on Neuromuscular Junction Morphology in the Aging Rat Tongue. *Muscle & Nerve* **43,** 203-211.

Johnson SL, Franz C, Kuhn S, Furness DN, Ruttiger L, Munkner S, Rivolta MN, Seward EP, Herschman HR, Engel J, Knipper M & Marcotti W. (2010). Synaptotagmin IV Determines the Linear Ca^{2+} Dependence of Vesicle Fusion at Auditory Ribbon Synapses. *Nature Neuroscience* **13,** 45-U201.

Johnston PA, Archer BT, Robinson K, Mignery GA, Jahn R & Sudhof TC. (1991). Rab3a Attachment to the Synaptic Vesicle Membrane Mediated by a Conserved Polyisoprenylated Carboxy-Terminal Sequence. *Neuron* **7,** 101-109.

Jorgensen EM, Hartwieg E, Schuske K, Nonet ML, Jin YS & Horvitz HR. (1995). Defective Recycling of Synaptic Vesicles in Synaptotagmin Mutants of *Caenorhabditis elegans*. *Nature* **378,** 196-199.

Jovanovic JN, Benfenati F, Siow YL, Sihra TS, Sanghera JS, Pelech SL, Greengard P & Czernik AJ. (1996). Neurotrophins Stimulate Phosphorylation of Synapsin I by MAP Kinase and Regulate Synapsin I-Actin Interactions. *Proceedings of the National Academy of Sciences of the United States of America* **93,** 3679-3683.

Jun K, Piedras-Renteria ES, Smith SM, Wheeler DB, Lee SB, Lee TG, Chin HM, Adams ME, Scheller RH, Tsien RW & Shin HS. (1999). Ablation of P/Q-Type Ca2+ Channel Currents, Altered Synaptic Transmission, and Progressive Ataxia in Mice Lacking the 1a-Subunit. *Proceedings of the National Academy of Sciences of the United States of America* **96,** 15245-15250.

Juranek J, Mukherjee K, Rickmann M, Martens H, Calka J, Südhof TC & Jahn R. (2006). Differential Expression of Active Zone Proteins in Neuromuscular Junctions Suggests Functional Diversification. *European Journal of Neuroscience* **24,** 3043-3052.

Kaeser PS, Deng L, Wang Y, Dulubova I, Liu X, Rizo J & Suedhof TC. (2011). RIM Proteins Tether Ca^{2+} Channels to Presynaptic Active Zones via a Direct PDZ-Domain Interaction. *Cell* **144,** 282-295.

Kaeser PS, Kwon H-B, Chiu CQ, Deng L, Castillo PE & Suedhof TC. (2008). RIM1α and RIM1β Are Synthesized from Distinct Promoters of the *RIM1* Gene to Mediate Differential But Overlapping Synaptic Functions. *Journal of Neuroscience* **28,** 13435-13447.

Kammerer RA, Schulthess T, Landwehr R, Schumacher B, Lustig A, Yurchenco PD, Ruegg MA, Engel J & Denzer AJ. (1999). Interaction of Agrin with Laminin Requires a Coiled-Coil Conformation of the Agrin-Binding Site within the Laminin γ1 Chain. *The EMBO Journal* **18,** 6762-6770.

Kao H-T, Porton B, Czernik AJ, Feng J, Yiu G, Häring M, Benfenati F & Greengard P. (1998). A Third Member of the Synapsin Gene Family. *Proceedings of the National Academy of Sciences* **95,** 4667-4672.

Kao HT, Porton B, Hilfiker S, Stefani G, Pieribone VA, DeSalle R & Greengard P. (1999). Molecular Evolution of the Synapsin Gene Family. *Journal of Experimental Zoology* **285,** 360-377.

Kasai H, Aosaki T & Fukuda J. (1987). Presynaptic Calcium-antagonist ω-Conotoxin Irreversibly Blocks N-Type Calcium-Channels in Chick Sensory Neurons. *Neuroscience Research* **4,** 228-235.

Katz B & Miledi R. (1965). The measurement of synaptic delay, and the time course of acetylcholine release at the neuromuscular junction. *Proceedings of the Royal Society of London Series B Biological Sciences* **161,** 483-495.

Katz B & Miledi R. (1973). The Binding of Acetylcholine to Receptors and its Removal from the Synaptic Cleft. *J Physiol* **231,** 549.

Katz E, Ferro PA, Weisz G & Uchitel OD. (1996). Calcium Channels Involved in Synaptic Transmission at the Mature and Regenerating Mouse Neuromuscular Junction. *Journal of Physiology-London* **497,** 687-697.

Katz E, Protti DA, Ferro PA, Siri R, Marcelo D & Uchitel OD. (1997). Effects of Ca2+ Channel Blocker Neurotoxins on Transmitter Release and Presynaptic Currents at the Mouse Neuromuscular Junction. *British journal of pharmacology* **121,** 1531-1540.

Katz LC & Shatz CJ. (1996). Synaptic Activity and the Construction of Cortical Circuits. *Science* **274,** 1133-1138.

Keith RK, Poage RE, Yokoyama CT, Catterall WA & Meriney SD. (2007). Bidirectional Modulation of Transmitter Release by Calcium Channel/Syntaxin Interactions *In Vivo*. *Journal of Neuroscience* **27,** 265-269.

Kidokoro Y. (2003). Roles of SNARE Proteins and Synaptotagmin I in Synaptic Transmission: Studies at the Drosophila Neuromuscular Synapse. *Neurosignals* **12,** 13-30.

Kim DK & Catterall WA. (1997). Ca^{2+}-Dependent and-Independent Interactions of the Isoforms of the α_{1A} Subunit of Brain Ca^{2+} Channels with Presynaptic SNARE Proteins. *Proceedings of the National Academy of Sciences* **94,** 14782-14786.

Kiyonaka S, Wakamori M, Miki T, Uriu Y, Nonaka M, Bito H, Beedle AM, Mori E, Hara Y, De Waard M, Kanagawa M, Itakura M, Takahashi M, Campbell KP & Mori Y. (2007). RIM1 Confers Sustained Activity and Neurotransmitter Vesicle Anchoring to Presynaptic Ca^{2+} Channels. *Nature Neuroscience* **10,** 691-701.

Klugbauer N, Marais E & Hofmann F. (2003). Calcium Channel Alpha(2)Delta Subunits: Differential Expression, Function, and Drug Binding. *Journal of Bioenergetics and Biomembranes* **35,** 639-647.

Knight D, Tolley LK, Kim DK, Lavidis NA & Noakes PG. (2003). Functional Analysis of Neurotransmission at β2-laminin Deficient Terminals. *Journal of Physiology-London* **546,** 789-800.

Kochubey O, Lou X & Schneggenburger R. (2011). Regulation of Transmitter Release by Ca^{2+} and Synaptotagmin: Insights from a Large CNS Synapse. *Trends in Neurosciences* **34,** 237-246.

Koh TW & Bellen HJ. (2003). Synaptotagmin I, a Ca^{2+} Sensor for Neurotransmitter Release. *Trends in Neurosciences* **26,** 413-422.

Kostyuk P. (1999). Low-Voltage Activated Calcium Channels: Achievements and Problems. *Neuroscience* **92,** 1157-1163.

Koushika SP, Richmond JE, Hadwiger G, Weimer RM, Jorgensen EM & Nonet ML. (2001). A Post-Docking Role for Active Zone Protein RIM. *Nature Neuroscience* **4,** 997-1005.

Krejci E, Coussen F, Duval N, Chatel JM, Legay C, Puype M, Vandekerckhove J, Cartaud J, Bon S & Massoulie J. (1991). Primary Structure of a Collagenic Tail Peptide of Torpedo Acetylcholinesterase: Co-Expression with Catalytic Subunit Induces the Production of Collagen-Tailed Forms in Transfected Cells. *Embo Journal* **10,** 1285-1293.

Krejci E, Thomine S, Boschetti N, Legay C, Sketelj J & Massoulie J. (1997). The Mammalian Gene of Acetylcholinesterase-Associated Collagen. *Journal of Biological Chemistry* **272,** 22840-22847.

Kriebel ME & Gross CE. (1974). Multimodal Distribution of Frog Miniature Endplate Potentials in Adult, Denervated, and Tadpole Leg Muscle. *The Journal of General Physiology* **64,** 85-103.

Kuffler DP. (1986). Thickness of the Basal Lamina at the Frog Neuromuscular Junction. *Journal of Comparative Neurology* **250,** 236-244.

Kuffler S & Yoshikami D. (1975). The Number of Transmitter Molecules in a Quantum: an Estimate from Iontophoretic Application of Acetylcholine at the Neuromuscular Synapse. *Journal of Physiology* **251,** 465-482.

Lacinova L. (2005). Voltage-Dependent Calcium Channels. *General physiology and biophysics* **24 Suppl 1,** 1-78.

Land BR, Harris WV, Salpeter EE & Salpeter MM. (1984). Diffusion and Binding Constants for Acetylcholine Derived from the Falling Phase of Miniature Endplate Currents. *Proceedings of the National Academy of Sciences of the United States of America-Biological Sciences* **81,** 1594-1598.

Land BR, Salpeter EE & Salpeter MM. (1980). Acetylcholine Receptor Site Density Affects the Rising Phase of Miniature Endplate Currents. *Proceedings of the National Academy of Sciences* **77,** 3736-3740.

Lanuza MA, Garcia N, Santafe M, Gonzalez CM, Alonso I, Nelson PG & Tomas J. (2002). Pre- and Postsynaptic Maturation of the Neuromuscular Junction During Neonatal Synapse Elimination Depends on Protein Kinase C. *Journal of Neuroscience Research* **67,** 607-617.

Latvanlehto A, Fox MA, Sormunen R, Tu H, Oikarainen T, Koski A, Naumenko N, Shakirzyanova A, Kallio M, Ilves M, Giniatullin R, Sanes JR & Pihlajaniemi T. (2010). Muscle-derived collagen XIII regulates maturation of the skeletal neuromuscular junction. *Journal of Neuroscience* **30,** 12230-12241.

Lavidis N & Bennett M. (1992). Probabilistic Secretion of Quanta from Visualized Sympathetic Nerve Varicosities in Mouse Vas Deferens. *Journal of Physiology* **454,** 9-26.

Lavidis N & Bennett M. (1993). Probabilistic Secretion of Quanta from Successive Sets of Visualized Varicosities Along Single Sympathetic Nerve Terminals. *Journal of the Autonomic Nervous System* **43,** 41-50.

Li C, Takei K, Geppert M, Daniell L, Stenius K, Chapman ER, Jahn R, De Camilli P & Sudhof TC. (1994). Synaptic Targeting of Rabphilin-3A, a Synaptic Vesicle Ca2+/Phospholipid-Binding Protein, Depends on Rab3A/3C. *Neuron* **13,** 885-898.

Li L, Chin L-S, Shupliakov O, Brodin L, Sihra TS, Hvalby O, Jensen V, Zheng D, McNamara JO & Greengard P. (1995). Impairment of Synaptic Vesicle Clustering and of Synaptic Transmission, and Increased Seizure Propensity, in Synapsin I-Deficient Mice. *Proceedings of the National Academy of Sciences* **92,** 9235-9239.

Li XM, Dong XP, Luo SW, Zhang B, Lee DH, Ting AK, Neiswender H, Kim CH, Carpenter-Hyland E, Gao TM, Xiong WC & Mei L. (2008). Retrograde Regulation of Motoneuron Differentiation by Muscle □Catenin. *Nature Neuroscience* **11,** 262-268.

Libby RT, Lavallee CR, Balkema GW, Brunken WJ & Hunter DD. (1999). Disruption of Laminin β2 Chain Production Causes Alterations in Morphology and Function in the CNS. *Journal of neuroscience* **19,** 9399-9411.

Liley A. (1957). Spontaneous Release of Transmitter Substance in Multiquantal Units. *Journal of Physiology* **136,** 595-605.

Lin W, Sanchez HB, Deerinck T, Morris JK, Ellisman M & Lee K-F. (2000). Aberrant development of motor axons and neuromuscular synapses in erbB2-deficient mice. *Proceedings of the National Academy of Sciences* **97,** 1299-1304.

Lin WC, Burgess RW, Dominguez B, Pfaff SL, Sanes JR & Lee KF. (2001). Distinct Roles of Nerve and Muscle in Postsynaptic Differentiation of the Neuromuscular Synapse. *Nature* **410,** 1057-1064.

Littleton JT, Bellen HJ & Perin MS. (1993). Expression of Synaptotagmin in Drosophila Reveals Transport and Localization of Synaptic Vesicles to the Synapse. *Development* **118,** 1077-1088.

Liu JX, Brannstrom T, Andersen PM & Pedrosa-Domellof F. (2011). Different Impact of ALS on Laminin Isoforms in Human Extraocular Muscles Versus Limb Muscles. *Investigative Ophthalmology and Visual Sciences* **52,** 4842-4852.

Llinas R, Sugimori M, Lin JW & Cherksey B. (1989). Blocking and Isolation of a Calcium-Channel from Neurons in Mammals and Cephalopods Utilizing a Toxin Fraction (Ftx) from Funnel-Web Spider Poison. *Proceedings of the National Academy of Sciences of the United States of America* **86,** 1689-1693.

Llinas R, Sugimori M & Silver R. (1992). Microdomains of High Calcium Concentration in a Presynaptic Terminal. *Science* **256,** 677-679.

Love FM & Thompson WJ. (1998). Schwann Cells Proliferate at Rat Neuromuscular Junctions During Development and Regeneration. *Journal of Neuroscience* **18,** 9376-9385.

Mackler JM, Drummond JA, Loewen CA, Robinson IM & Reist NE. (2002). The C_2B Ca^{2+}-Binding Motif of Synaptotagmin is Required for Synaptic Transmission *In Vivo*. *Nature* **418,** 340-344.

Madhavan R & Peng HB. (2005). Molecular Regulation of Postsynaptic Differentiation at the Neuromuscular Junction. *IUBMB life* **57,** 719-730.

Madhavan R, Zhao XT, Ruegg MA & Peng HB. (2005). Tyrosine phosphatase regulation of MuSK-dependent acetylcholine receptor clustering. *Molecular Cell Neuroscience* **28,** 403-416.

Mantilla C, Rowley K, Zhan W-Z, Fahim M & Sieck G. (2007). Synaptic Vesicle Pools at Diaphragm Neuromuscular Junctions Vary with Motoneuron Soma, not Axon Terminal, Inactivity. *Neuroscience* **146,** 178-189.

Mantilla CB & Sieck GC. (2009). Neuromuscular Adaptations to Respiratory Muscle Inactivity. *Respiratory Physiology Neurobiology* **169,** 133-140.

Marnay A & Nachmansohn D. (1938). Choline Esterase in Voluntary Muscle. *Journal of Physiology-London* **92,** 37-47.

Marques MJ, Conchello J-A & Lichtman JW. (2000). From Plaque to Pretzel: Fold Formation and Acetylcholine Receptor Loss at the Developing Neuromuscular Junction. *The Journal of Neuroscience* **20,** 3663-3675.

Martin PT, Kaufman SJ, Kramer RH & Sanes JR. (1996). Synaptic Integrins in Developing, Adult, and Mutant Muscle: Selective Association of α1, α7A, and α7B Integrins with the Neuromuscular Junction. *Developmental Biology* **174,** 125-139.

Martin PT & Sanes JR. (1995). Role for a Synapse-Specific Carbohydrate in Agrin-Induced Clustering of Acetylcholine Receptors. *Neuron* **14,** 743-754.

Martin PT & Sanes JR. (1997). Integrins Mediate Adhesion to Agrin and Modulate Agrin Signaling. *Development* **124,** 3909-3917.

Martinou JC & Merlie JP. (1991). Nerve-Dependent Modulation of Acetylcholine Receptor Epsilon-Subunit Gene Expression. *Journal of Neuroscience* **11,** 1291-1299.

Maselli R, Ng J, Anderson J, Cagney O, Arredondo J, Williams C, Wessel H, Abdel-Hamid H & Wollmann R. (2009). Mutations in *LAMB2* Causing a Severe Form of Synaptic Congenital Myasthenic Syndrome. *Journal of Medical Genetics* **46,** 203-208.

Massoulié J & Millard CB. (2009). Cholinesterases and the Basal Lamina at Vertebrate Neuromuscular Junctions. *Current Opinion in Pharmacology* **9,** 316-325.

McCleskey EW & Almers W. (1985). The Ca Channel in Skeletal Muscle is a Large Pore. *Proceedings of the National Academy of Sciences* **82,** 7149-7153.

McKee KK, Harrison D, Capizzi S & Yurchenco PD. (2007). Role of Laminin Terminal Globular Domains in Basement Membrane Assembly. *Journal of Biological Chemistry* **282,** 21437-21447.

McMahan UJ, Sanes JR & Marshall LM. (1978). Cholinesterase is Associated with Basal Lamina at Neuromuscular-Junction. *Nature* **271,** 172-174.

Menegon A, Bonanomi D, Albertinazzi C, Lotti F, Ferrari G, Kao H-T, Benfenati F, Baldelli P & Valtorta F. (2006). Protein Kinase A-Mediated Synapsin I Phosphorylation is a Central Modulator of Ca^{2+}-Dependent Synaptic Activity. *Journal of Neuroscience* **26,** 11670-11681.

Meriney SD & Dittrich M. (2013). Organization and Function of Transmitter Release Sites at the Neuromuscular Junction. *Journal of Physiology* **591,** 3159-3165.

Miledi R. (1960). Properties Of Regenerating Neuromuscular Synapses In The Frog. *Journal of Physiology* **154,** 190-205.

Miledi R & Slater C. (1968). Electrophysiology and Electron-Microscopy of Rat Neuromuscular Junctions after Nerve Degeneration. *Proceedings of the Royal Society of London Series B, Biological Sciences***,** 289-306.

Miner JH, Patton BL, Lentz SI, Gilbert DJ, Snider WD, Jenkins NA, Copeland NG & Sanes JR. (1997). The Laminin Alpha Chains: Expression, Developmental Transitions, and Chromosomal Locations of α1-5, Identification of Heterotrimeric Laminins 8-11, and Cloning of a Novel α3 Isoform. *Journal of Cell Biology* **137,** 685-701.

Miner JH & Yurchenco PD. (2004). Laminin Functions in Tissue Morphogenesis. *Annual Reviews of Cell and Developmental Biology* **20,** 255-284.

Mintz IM, Sabatini BL & Regehr WG. (1995). Calcium Control of Transmitter Release at a Cerebellar Synapse. *Neuron* **15,** 675-688.

Mintz IM, Venema VJ, Swiderek KM, Lee TD, Bean BP & Adams ME. (1992). P-Type Calcium Channels Blocked by the Spider Toxin ω-Aga-IVA. *Nature* **355,** 827-829.

Mittaud P, Camilleri AA, Willmann R, Erb-Vögtli S, Burden SJ & Fuhrer C. (2004). A Single Pulse of Agrin Triggers a Pathway that Acts to Cluster Acetylcholine Receptors. *Molecular and Cellular Biology* **24,** 7841-7854.

Mittelstaedt T, Alvarez-Baron E & Schoch S. (2010). RIM Proteins and their Role in Synapse Function. *Biological Chemistry* **391,** 599-606.

Moreno Davila H. (1999). Molecular and Functional Diversity of Voltage-Gated Calcium Channels. *Annals of the New York Academy of Sciences* **868,** 102-117.

Moscoso LM, Chu GC, Gautam M, Noakes PG, Merlie JP & Sanes JR. (1995). Synapse-Associated Expression of an Acetylcholine Receptor-Inducing Protein, ARIA/heregulin, and its Putative Receptors, ErbB2 and ErbB3, in Developing Mammalian Muscle. *Developmental Biology* **172,** 158-169.

Nagerl U, Novo D, Mody I & Vergara J. (2000). Binding Kinetics of Calbindin-D-28k Determined by Flash Photolysis of Caged Ca^{2+}. *Biophysical Journal* **79,** 3009-3018.

Nagwaney S, Harlow ML, Jung JH, Szule JA, Ress D, Xu J, Marshall RM & McMahan UJ. (2009). Macromolecular Connections of Active Zone Material to Docked Synaptic Vesicles and Presynaptic Membrane at Neuromuscular Junctions of Mouse. *Journal of Comparative Neurology* **513,** 457-468.

Naraghi M. (1997). T-jump Study of Calcium Binding Kinetics of Calcium Chelators. *Cell Calcium* **22,** 255-268.

Navarrete R & Vrbová G. (1983). Changes of Activity Patterns in Slow and Fast Muscles During Postnatal Development. *Developmental Brain Research* **8,** 11-19.

Neher E. (1998). Vesicle Pools and Ca^{2+} Microdomains: New Tools for Understanding their Roles in Neurotransmitter Release. *Neuron* **20,** 389-399.

Neher E & Sakaba T. (2008). Multiple Roles of Calcium Ions in the Regulation of Neurotransmitter Release. *Neuron* **59,** 861-872.

Ngo ST, Balke C, Phillips WD & Noakes PG. (2004). Neuregulin Potentiates Agrin-Induced Acetylcholine Receptor Clustering in Myotubes. *Neuroreport* **15,** 2501-2505.

Ngo ST, Cole RN, Sunn N, Phillips WD & Noakes PG. (2012). Neuregulin-1 Potentiates Agrin-Induced Acetylcholine Receptor Clustering Through Muscle-Specific Kinase Phosphorylation. *Journal of Cell Science* **125,** 1531-1543.

Ngo ST, Noakes PG & Phillips WD. (2007). Neural Agrin: A Synaptic Stabiliser. *International Journal of Biochemistry & Cell Biology* **39,** 863-867.

Nguyen NM, Kelley DG, Schlueter JA, Meyer MJ, Senior RM & Miner JH. (2005). Epithelial Laminin α5 is Necessary for Distal Epithelial Cell Maturation, VEGF Production, and Alveolization in the Developing Murine Lung. *Developmental Biology* **282,** 111-125.

Nishimune H. (2012). Molecular Mechanism of Active Zone Organization at Vertebrate Neuromuscular Junctions. *Molecular Neurobiology* **45,** 1-16.

Nishimune H, Numata T, Chen J, Aoki Y, Wang Y, Starr MP, Mori Y & Stanford JA. (2012). Active Zone Protein Bassoon Co-Localizes with Presynaptic Calcium Channel, Modifies Channel Function, and Recovers from Aging Related Loss by Exercise. *PLoS One* **7,** e38029.

Nishimune H, Sanes JR & Carlson SS. (2004). A Synaptic Laminin-Calcium Channel Interaction Organizes Active Zones in Motor Nerve Terminals. *Nature* **432,** 580-587.

Nishimune H, Valdez G, Jarad G, Moulson CL, Muller U, Miner JH & Sanes JR. (2008). Laminins Promote Postsynaptic Maturation by an Autocrine Mechanism at the Neuromuscular Junction. *Journal of Cell Biology* **182,** 1201-1215.

Nitkin RM, Smith MA, Magill C, Fallon JR, Yao Y-MM, Wallace BG & McMahan U. (1987). Identification of Agrin, a Synaptic Organizing Protein from *Torpedo* Electric Organ. *Journal Cell Biology* **105,** 2471-2478.

Noakes PG, Gautam M, Mudd J, Sanes JR & Merlie JP. (1995a). Aberrant Differentiation of Neuromuscular Junctions in Mice Lacking s-laminin/laminin β2. *Nature* **374,** 258-262.

Noakes PG, Miner JH, Gautam M, Cunningham JM, Sanes JR & Merlie JP. (1995b). The Renal Glomerulus of Mice Lacking S-laminin laminin β2: Nephrosis Despite Molecular Compensation by Laminin β1. *Nature Genetics* **10,** 400-406.

Nonet ML, Grundahl K, Meyer BJ & Rand JB. (1993). Synaptic Function is Impaired but not Eliminated in *C-Elegans* Mutants Lacking Synaptotagmin. *Cell* **73,** 1291-1305.

Nonet ML, Staunton JE, Kilgard MP, Fergestad T, Hartwieg E, Horvitz HR, Jorgensen EM & Meyer BJ. (1997). *Caenorhabditis Elegans rab-3* Mutant Synapses Exhibit Impaired Function and are Partially Depleted of Vesicles. *Journal of Neuroscience* **17,** 8061-8073.

Nudler S, Piriz J, Urbano FJ, Rosato-Siri MD, Renteria ESP & Uchitel OD. (2003). Ca2+ Channels and Synaptic Transmission at the Adult, Neonatal, and P/Q-Type Deficient Neuromuscular Junction. *Annals of the New York Academy of Sciences* **998,** 11-17.

Ohtsuka T, Takao-Rikitsu E, Inoue E, Inoue M, Takeuchi M, Matsubara K, Deguchi-Tawarada M, Satoh K, Morimoto K, Nakanishi H & Takai Y. (2002). CAST: a Novel Protein of the Cytomatrix at the Active Zone of Synapses that Forms a Ternary Complex with RIM1 and Munc13-1. *Journal of Cell Biology* **158,** 577-590.

Pagani R, Song M, McEnery M, Qin N, Tsien RW, Toro L, Stefani E & Uchitel OD. (2004). Differential expression of alpha 1 and beta subunits of voltage dependent Ca2+ channel at the neuromuscular junction of normal and P/Q Ca2+ channel knockout mouse. *Neuroscience* **123,** 75-85.

Panatier A, Vallée J, Haber M, Murai KK, Lacaille J-C & Robitaille R. (2011). Astrocytes are Endogenous Regulators of Basal Transmission at Central Synapses. *Cell* **146,** 785-798.

Pardo NE, Hajela RK & Atchison WD. (2006). Acetylcholine release at neuromuscular junctions of adult tottering mice is controlled by N-(cav2.2) and R-type (cav2.3) but not L-type (cav1.2) Ca2+ channels. *The Journal of Pharmacology and Experimental Therapeutics* **319,** 1009-1020.

Pasti L, Volterra A, Pozzan T & Carmignoto G. (1997). Intracellular calcium oscillations in astrocytes: a highly plastic, bidirectional form of communication between neurons and astrocytes in situ. *Journal of Neuroscience* **17,** 7817-7830.

Patton BL. (2000). Laminins of the Neuromuscular System. *Microscopy Research and Technique* **51,** 247-261.

Patton BL, Chiu AY & Sanes JR. (1998). Synaptic Laminin Prevents Glial Entry into the Synaptic Cleft. *Nature* **393,** 698-701.

Patton BL, Cunningham JM, Thyboll J, Kortesmaa J, Westerblad H, Edstrom L, Tryggvason K & Sanes JR. (2001). Properly Formed but Improperly Localized Synaptic Specializations in the Absence of Laminin α4. *Nature Neuroscience* **4,** 597-604.

Patton BL, Miner JH, Chiu AY & Sanes JR. (1997). Distribution and Function of Laminins in the Neuromuscular System of Developing, Adult, and Mutant Mice. *Journal of Cell Biology* **139,** 1507-1521.

Pedrosa-Domellof F, Tiger CF, Virtanen I, Thornell LE & Gullberg D. (2000). Laminin Chains in Developing and Adult Human Myotendinous Junctions. *Journal of Histochemistry & Cytochemistry* **48,** 201-209.

Perin M, Brose N, Jahn R & Südhof T. (1991). Domain Structure of Synaptotagmin (p65). *Journal of Biological Chemistry* **266,** 623-629.

Petrucci TC & Morrow JS. (1987). Synapsin-I - an Actin-Bundling Protein Under Phosphorylation Control. *Journal of Cell Biology* **105,** 1355-1363.

Piedras-Renteria ES, Pyle JL, Diehn M, Glickfeld LL, Harata NC, Cao YQ, Kavalali ET, Brown PO & Tsien RW. (2004). Presynaptic Homeostasis at CNS Nerve Terminals Compensates for lack of a Key Ca^{2+} Entry Pathway. *Proceedings of the National Academy of Sciences of the United States of America* **101,** 3609-3614.

Pieribone VA, Shupliakov O, Brodin L, Hilfikerrothenfluh S, Czernik AJ & Greengard P. (1995). Distinct Pools of Synaptic Vesicles in Neurotransmitter Release. *Nature* **375,** 493-497.

Pilgram GS, Potikanond S, Baines RA, Fradkin LG & Noordermeer JN. (2010). The Roles of the Dystrophin-Associated Glycoprotein Complex at the Synapse. *Molecular Neurobiology* **41,** 1-21.

Plomp JJ, Van Den Maagdenberg AM, Ferrari MD, Frants RR & Molenaar PC. (2003). Transmitter Release Deficits at the Neuromuscular Synapse of Mice with Mutations in the $Ca_v2.1$ α_{1A} Subunit of the P/Q-type Ca^{2+} Channel. In *Myasthenia Gravis and Related Disorders: Biomchemical Basis for Disease of the Neuromuscular Junction*, ed. Agius, pp. 29-32.

Porter BE, Weis J & Sanes JR. (1995). A motoneuron-selective stop signal in the synaptic protein S-laminin. *Neuron* **14,** 549-559.

Poskanzer KE, Marek KW, Sweeney ST & Davis GW. (2003). Synaptotagmin I is Necessary for Compensatory Synaptic Vesicle Endocytosis *In Vivo*. *Nature* **426,** 559-563.

Prakash Y, Miyata H, Zhan WZ & Sieck GC. (1999). Inactivity-Induced Remodeling of Neuromuscular Junctions in Rat Diaphragmatic Muscle. *Muscle & Nerve* **22,** 307-319.

Proszynski TJ, Gingras J, Valdez G, Krzewski K & Sanes JR. (2009). Podosomes Are Present in a Postsynaptic Apparatus and Participate in its Maturation. *Proceedings of the National Academy of Sciences of the United States of America* **106,** 18373-18378.

Proszynski TJ & Sanes JR. (2013). Amotl2 Interacts with LL5β, Localizes to Podosomes and Regulates Postsynaptic Differentiation in Muscle. *Journal of Cell Science* **126,** 2225-2235.

Protti DA & Uchitel OD. (1993). Transmitter Release and Presynaptic Ca^{2+} Currents Blocked by the Spider Toxin Omega-AGA-IVA. *Neuroreport* **5,** 333-336.

Pyle RA, Schivell AE, Hidaka H & Bajjalieh SM. (2000). Phosphorylation of Synaptic Vesicle Protein 2 Modulates Binding to Synaptotagmin. *Journal of Biological Chemistry* **275,** 17195-17200.

Qian YK, Chan AW, Madhavan R & Peng HB. (2008). The Function of Shp2 Tyrosine Phosphatase in the Dispersal of Acetylcholine Receptor Clusters. *BMC Neuroscience* **9,** 70.

Qu ZC, Apel ED, Doherty CA, Hoffman PW, Merlie JP & Huganir RL. (1996). The Synapse-Associated Protein Rapsyn Regulates Tyrosine Phosphorylation of Proteins Colocalized at Nicotinic Acetylcholine Receptor Clusters. *Molecular and Cellular Neuroscience* **8,** 171-184.

Rauvala H & Peng HB. (1997). HB-GAM (heparin-binding growth-associated molecule) and heparin-type glycans in the development and plasticity of neuron-target contacts. *Progress in Neurobiology* **52,** 127-144.

Reddy LV, Koirala S, Sugiura Y, Herrera AA & Ko C-P. (2003). Glial cells maintain synaptic structure and function and promote development of the neuromuscular junction in vivo. *Neuron* **40,** 563-580.

Redfern P. (1970). Neuromuscular Transmission in New-Born Rats. *Journal of Physiology* **209,** 701.

Regehr WG & Mintz IM. (1994). Participation of multiple calcium-channel types in transmission at single climbing fiber to purkinje-cell synapses. *Neuron* **12,** 605-613.

Reid B, Slater CR & Bewick GS. (1999). Synaptic Vesicle Dynamics in Rat Fast and Slow Motor Nerve Terminals. *Journal of Neuroscience* **19,** 2511-2521.

Reist NE, Buchanan J, Li J, DiAntonio A, Buxton EM & Schwarz TL. (1998). Morphologically docked synaptic vesicles are reduced in synaptotagmin mutants Drosophila. *Journal of Neuroscience* **18,** 7662-7673.

Reist NE & Smith SJ. (1992). Neurally Evoked Calcium Transients in Terminal Schwann Cells at the Neuromuscular Junction. *Proceedings of the National Academy of Sciences* **89,** 7625-7629.

Rickman C & Davletov B. (2003). Mechanism of Calcium-Independent Synaptotagmin Binding to Target SNAREs. *Journal of Biological Chemistry* **278,** 5501-5504.

Riethmacher D, Sonnenberg-Riethmacher E, Brinkmann V, Yamaai T, Lewin GR & Birchmeier C. (1997). Severe neuropathies in mice with targeted mutations in the ErbB3 receptor. *Nature* **389,** 725-730.

Ringelmann B, Roder C, Hallmann R, Maley M, Davies M, Grounds M & Sorokin L. (1999). Expression of Laminin α1, α2, α4, and α5 Chains, Fibronectin, and Tenascin-C in Skeletal Muscle of Dystrophic 129ReJ *dy/dy* Mice. *Experimental Cell Research* **246,** 165-182.

Rizzoli SO & Betz WJ. (2004). The Structural Organization of the Readily Releasable Pool of Synaptic Vesicles. *Science* **303,** 2037-2039.

Rizzoli SO & Betz WJ. (2005). Synaptic Vesicle Pools. *Nature Reviews Neuroscience* **6,** 57-69.

Robinson J. (1976). Estimation of Parameters for a Model of Transmitter Release at Synapses. *Biometrics* **32,** 61-68.

Robitaille R. (1995). Purinergic Receptors and their Activation by Endogenous Purines at Perisynaptic Glial Cells of the Frog Neuromuscular Junction. *Journal of Neuroscience* **15,** 7121-7131.

Robitaille R. (1998). Modulation of Synaptic Efficacy and Synaptic Depression by Glial Cells at the Frog Neuromuscular Junction. *Neuron* **21,** 847-855.

Robitaille R, Garcia ML, Kaczorowski GJ & Chariton MP. (1993). Functional Colocalization of Calcium and Calcium-Gated Potassium Channels in Control of Transmitter Release. *Neuron* **11,** 645-655.

Robitaille R & Tremblay J. (1989). Frequency and Amplitude Gradients of Spontaneous Release Along the Length of the Frog Neuromuscular Junction. *Synapse* **3,** 291-307.

Robitaille R & Tremblay J. (1991). Non-Uniform Responses to Ca^{2+} Along the Frog Neuromuscular Junction: Effects on the Probability of Spontaneous and Evoked Transmitter Release. *Neuroscience* **40,** 571-585.

Rocha MC, Pousinha PA, Correia AM, Sebastião AM & Ribeiro JA. (2013). Early Changes of Neuromuscular Transmission in the SOD1 (G93A) Mice Model of ALS Start Long before Motor Symptoms Onset. *PLoS One* **8,** e73846.

Rochon D, Rousse I & Robitaille R. (2001). Synapse–glia interactions at the mammalian neuromuscular junction. *Journal of Neuroscience* **21,** 3819-3829.

Rosato-Siri MD, Piriz J, Tropper BAG & Uchitel OD. (2002). Differential Ca2+-dependence of transmitter release mediated by P/Q- and N-type calcium channels at neonatal rat neuromuscular junctions. *European Journal of Neuroscience* **15,** 1874-1880.

Rosato-Siri MD & Uchitel OD. (1999). Calcium channels coupled to neurotransmitter release at neonatal rat neuromuscular junctions. *Journal of Physiology (Cambridge)* **514,** 533-540.

Rosenberry T. (1979). Quantitative simulation of endplate currents at neuromuscular junctions based on the reaction of acetylcholine with acetylcholine receptor and acetylcholinesterase. *Biophysical journal* **26,** 263-289.

Rousse I & Robitaille R. (2006). Calcium Signaling in Schwann Cells at Synaptic and Extra-Synaptic Sites: Active Glial Modulation of Neuronal Activity. *Glia* **54,** 691-699.

Rousse I, St-Amour A, Darabid H & Robitaille R. (2010). Synapse–Glia Interactions are Governed by Synaptic and Intrinsic Glial Properties. *Neuroscience* **167,** 621-632.

Rowley KL, Mantilla CB, Ermilov LG & Sieck GC. (2007). Synaptic Vesicle Distribution and Release at Rat Diaphragm Neuromuscular Junctions. *Journal of Neurophysiology* **98,** 478-487.

Ruiz R, Cano R, Casañas JJ, Gaffield MA, Betz WJ & Tabares L. (2011). Active Zones and the Readily Releasable Pool of Synaptic Vesicles at the Neuromuscular Junction of the Mouse. *The Journal of Neuroscience* **31,** 2000-2008.

Ryan TA, Li LA, Chin LS, Greengard P & Smith SJ. (1996). Synaptic Vesicle Recycling in Synapsin I Knock-Out Mice. *Journal of Cell Biology* **134,** 1219-1227.

Sabatini BL & Regehr WG. (1996). Timing of Neurotransmission at Fast Synapses in the Mammalian Brain. *Nature* **384,** 170-172.

Sadakata T, Itakura M, Kozaki S, Sekine Y, Takahashi M & Furuichi T. (2006). Differential Distributions of the Ca^{2+} -Dependent Activator Protein for Secretion Family Proteins (CAPS2 and CAPS1) in the Mouse Brain. *The Journal of Comparative Neurology* **495,** 735-753.

Samuel MA, Valdez G, Tapia JC, Lichtman JW & Sanes JR. (2012). Agrin and Synaptic Laminin Are Required to Maintain Adult Neuromuscular Junctions. *PLoS One* **7,** e46663.

Sanes JR. (1995). The synaptic cleft of the neuromuscular junction. *Seminars in Developmental Biology* **6,** 163-173.

Sanes JR, Apel ED, Gautam M, Glass D, GRADY R, Martin PT, Nichol MC & Yancopoulos GD. (1998). Agrin Receptors at the Skeletal Neuromuscular Junction. *Annals of the New York Academy of Sciences* **841,** 1-13.

Sanes JR, Engvall E, Butkowski R & Hunter DD. (1990). Molecular Heterogeneity of Basal Laminae: Isoforms of Laminin and Collagen IV at the Neuromuscular Junction and Elsewhere. *Journal of Cell Biology* **111,** 1685-1699.

Sanes JR & Lichtman JW. (1999). Development of the Vertebrate Neuromuscular Junction. *Annual Review of Neuroscience* **22,** 389-442.

Sanes JR & Lichtman JW. (2001). Induction, Assembly, Maturation and Maintenance of a Postsynaptic Apparatus. *Nature Reviews Neuroscience* **2,** 791-805.

Sanes JR, Marshall LM & McMahan UJ. (1978). Reinnervation of muscle fiber basal lamina after removal of myofibers. Differentiation of regenerating axons at original synaptic sites. *Journal of Cell Biology* **78,** 176-198.

Sann SB, Xu L, Nishimune H, Sanes JR & Spitzer NC. (2008). Neurite Outgrowth and *In Vivo* Sensory Innervation Mediated by a $Ca_V2.2$-Laminin β2 Stop Signal. *Journal of Neuroscience* **28,** 2366-2374.

Santafe MM, Garcia N, Lanuza MA, Uchitel OD & Tomas J. (2001). Calcium Channels Coupled to Neurotransmitter Release at Dually Innervated Neuromuscular Junctions in the Newborn Rat. *Neuroscience* **102,** 697-708.

Santafe MM, Urbano FJ, Lanuza MA & Uchitel OD. (2000). Multiple Types of Calcium Channels Mediate Transmitter Release During Functional Recovery of Botulinum Toxin Type A-Poisoned Mouse Motor Nerve Terminals. *Neuroscience* **95,** 227-234.

Sasaki M, Kleinman HK, Huber H, Deutzmann R & Yamada Y. (1988). Laminin, a Multidomain Protein. The A Chain has a Unique Globular Domain and Homology with the Basement Membrane Proteoglycan and the Laminin B Chains. *Journal of Biological Chemistry* **263,** 16536-16544.

Schiavo G, Stenbeck G, Rothman JE & Sollner TH. (1997). Binding of the Synaptic Vesicle v-SNARE, Synaptotagmin, to the Plasma Membrane t-SNARE, SNAP-25, Can Explain Docked Vesicles at Neurotoxin-Treated Synapses. *Proceedings of the National Academy of Sciences of the United States of America* **94,** 997-1001.

Schikorski T & Stevens CF. (2001). Morphological Correlates of Functionally Defined Synaptic Vesicle Populations. *Nature Neuroscience* **4,** 391-395.

Schivell AE, Batchelor RH & Bajjalieh SM. (1996). Isoform-Specific, Calcium-Regulated Interaction of the Synaptic Vesicle Proteins SV2 and Synaptotagmin. *Journal of Biological Chemistry* **271,** 27770-27775.

Schoch S & Gundelfinger ED. (2006). Molecular Organization of the Presynaptic Active Zone. *Cell and Tissue Research* **326,** 379-391.

Schuler F & Sorokin LM. (1995). Expression of Laminin Isoforms in Mouse Myogenic Cells in-Vitro and in-Vivo. *Journal of Cell Science* **108,** 3795-3805.

Sellin L, Molgo J, Törnquist K, Hansson B & Thesleff S. (1996). On the Possible Origin of "Giant or Slow-Rising" Miniature End-Plate Potentials at the Neuromuscular Junction. *Pflügers Archiv* **431,** 325-334.

Shapira M, Zhai RG, Dresbach T, Bresler T, Torres VI, Gundelfinger ED, Ziv NE & Garner CC. (2003). Unitary Assembly of Presynaptic Active Zones from Piccolo-Bassoon Transport Vesicles. *Neuron* **38,** 237-252.

Sheng ZH, Rettig J, Takahashi M & Catterall WA. (1994). Identification of a Syntaxin-Binding Site on N-Type Calcium Channels. *Neuron* **13,** 1303-1313.

Sheng ZH, Westenbroek RE & Catterall WA. (1998). Physical Link and Functional Coupling of Presynaptic Calcium Channels and the Synaptic Vesicle Docking/Fusion Machinery. *Journal of Bioenergetics and Biomembranes* **30,** 335-345.

Shi L, Butt B, Ip FC, Dai Y, Jiang L, Yung W-H, Greenberg ME, Fu AK & Ip NY. (2010). Ephexin1 is Required for Structural Maturation and Neurotransmission at the Neuromuscular Junction. *Neuron* **65,** 204-216.

Shi L, Fu AKY & Ip NY. (2012). Molecular Mechanisms Underlying Maturation and Maintenance of the Vertebrate Neuromuscular Junction. *Trends in Neurosciences* **35,** 441-453.

Sieb JP, Dorfler P, Tzartos S, Wewer UM, Ruegg MA, Meyer D, Baumann I, Lindemuth R, Jakschik J & Ries F. (1998). Congenital Myasthenic Syndromes in Two Kinships with End-Plate Acetylcholine Receptor and Utrophin Deficiency. *Neurology* **50,** 54-61.

Singer D, Biel M, Lotan I, Flockerzi V, Hofmann F & Dascal N. (1991). The Roles of the Subunits in the Function of the Calcium-Channel. *Science* **253,** 1553-1557.

Smith IW, Mikesh M, Il Lee Y & Thompson WJ. (2013). Terminal Schwann Cells Participate in the Competition Underlying Neuromuscular Synapse Elimination. *Journal of Neuroscience* **33,** 17724-17736.

Sollner T, Bennett MK, Whiteheart SW, Scheller RH & Rothman JE. (1993). A Protein Assembly-Disassembly Pathway in-Vitro That May Correspond to Sequential Steps of Synaptic Vesicle Docking, Activation, and Fusion. *Cell* **75,** 409-418.

Son YJ, Patton BL & Sanes JR. (1999). Induction of Presynaptic Differentiation in Cultured Neurons by Extracellular Matrix Components. *European Journal of Neuroscience* **11,** 3457-3467.

Sorokin LM, Pausch F, Frieser M, Kroger S, Ohage E & Deutzmann R. (1997). Developmental Regulation of the Laminin α5 Chain Suggests a Role in Epithelial and Endothelial Cell Maturation. *Developmental Biology* **189,** 285-300.

Stanley EF. (1993). Presynaptic calcium channels and the transmitter release mechanism. *Annals of the New York Academy of Sciences* **681,** 368-372.

Sudhof TC. (1997). Function of Rab3 GDP-GTP Exchange. *Neuron* **18,** 519-522.

Sudhof TC. (2004). The Synaptic Vesicle Cycle. *Annual Review of Neuroscience* **27,** 509-547.

Sudhof TC & Rizo J. (1996). Synaptotagmins: C_2-Domain Proteins that Regulate Membrane Traffic. *Neuron* **17,** 379-388.

Sugiyama J, Bowen DC & Hall ZW. (1994). Dystroglycan Binds Nerve and Muscle Agrin. *Neuron* **13,** 103-115.

Sunderland WJ, Son YJ, Miner JH, Sanes JR & Carlson SS. (2000). The Presynaptic Calcium Channel is Part of a Transmembrane Complex Linking a Synaptic Laminin (α4β2γ1) with Non-Erythroid Spectrin. *Journal of Neuroscience* **20,** 1009-1019.

Sutton RB, Fasshauer D, Jahn R & Brunger AT. (1998). Crystal Structure of a SNARE Complex Involved in Synaptic Exocytosis at 2.4 Angstrom Resolution. *Nature* **395,** 347-353.

Suzuki N, Yokoyama F & Nomizu M. (2005). Functional Sites in the Laminin Alpha Chains. *Connective Tissue Research* **46,** 142-152.

Takahashi T & Momiyama A. (1993). Different Types of Calcium Channels Mediate Central Synaptic Transmission. *Nature* **366,** 156-158.

Takai T, Noda M, Mishina M, Shimizu S, Furutani Y, Kayano T, Ikeda T, Kubo T, Takahashi H, Takahashi T & et al. (1985). Cloning, Sequencing and Expression of cDNA for a Novel Subunit of Acetylcholine Receptor from Calf Muscle. *Nature* **315,** 761-764.

Takao-Rikitsu E, Mochida S, Inoue E, Deguchi-Tawarada M, Inoue M, Ohtsuka T & Takai Y. (2004). Physical and Functional Interaction of the Active Zone Proteins, CAST, RIM1, and Bassoon, in Neurotransmitter Release. *Journal of Cell Biology* **164,** 301-311.

Takei Y, Harada A, Takeda S, Kobayashi K, Terada S, Noda T, Takahashi T & Hirokawa N. (1995). Synapsin I Deficiency Results in the Structural Change in the Presynaptic Terminals in the Murine Nervous System. *Journal of Cell Biology* **131,** 1789-1800.

Talts JF, Andac Z, Göhring W, Brancaccio A & Timpl R. (1999). Binding of the G Domains of Laminin α1 and α2 Chains and Perlecan to Heparin, Sulfatides, α-dystroglycan and Several Extracellular Matrix Proteins. *The EMBO journal* **18,** 863-870.

Talts JF, Sasaki T, Miosge N, Gohring W, Mann K, Mayne R & Timpl R. (2000). Structural and Functional Analysis of the Recombinant G Domain of the Laminin α4 Chain and its proteolytic Processing in Tissues. *Journal of Biological Chemistry* **275,** 35192-35199.

Tapia JC, Wylie JD, Kasthuri N, Hayworth KJ, Schalek R, Berger DR, Guatimosim C, Seung HS & Lichtman JW. (2012). Pervasive Synaptic Branch Removal in the Mammalian Neuromuscular System at Birth. *Neuron* **74,** 816-829.

Tarr TB, Dittrich M & Meriney SD. (2013). Are Unreliable Release Mechanisms Conserved from NMJ to CNS? *Trends in Neurosciences* **36,** 14-22.

Theiler K. (1989). *The House Mouse: Atlas of Embryonic Development*. Springer-Verlag New York.

Tiger CF & Gullberg D. (1997). Absence of laminin alpha 1 chain in the skeletal muscle of dystrophic dy/dy mice. *Muscle & Nerve* **20,** 1515-1524.

Timpl R & Brown JC. (1994). The Laminins. *Matrix Biology* **14,** 275-281.

Timpl R, Rohde H, Robey PG, Rennard SI, Foidart J-M & Martin GR. (1979). Laminin--a glycoprotein from basement membranes. *Journal of Biological Chemistry* **254,** 9933-9937.

Timpl R, Tisi D, Talts JF, Andac Z, Sasaki T & Hohenester E. (2000). Structure and Function of Laminin LG Modules. *Matrix Biology* **19,** 309-317.

Todd KJ, Darabid H & Robitaille R. (2010). Perisynaptic Glia Discriminate Patterns of Motor Nerve Activity and Influence Plasticity at the Neuromuscular Junction. *Journal of Neuroscience* **30,** 11870-11882.

Todd KJ & Robitaille R. (2006). Purinergic Modulation of Synaptic Signalling at the Neuromuscular Junction. *Pflügers Archiv* **452,** 608-614.

Torritarelli F, Villa A, Valtorta F, Decamilli P, Greengard P & Ceccarelli B. (1990). Redistribution of Synaptophysin and Synapsin-I During □-Latrotoxin Induced Release of Neurotransmitter at the Neuromuscular-Junction. *Journal of Cell Biology* **110,** 449-459.

Turney SG & Lichtman JW. (2012). Reversing the Outcome of Synapse Elimination at Developing Neuromuscular Junctions In Vivo: Evidence for Synaptic Competition and its Mechanism. *PLoS biology* **10,** e1001352.

Tzu J & Marinkovich MP. (2008). Bridging structure with function: structural, regulatory, and developmental role of laminins. *International Journal of Biochemistry and Cell Biology* **40,** 199-214.

Uchitel OD, Protti DA, Sanchez V, Cherksey BD, Sugimori M & Llinas R. (1992). P-type Voltage-Dependent Calcium Channel Mediates Presynaptic Calcium Influx and Transmitter Release in Mammalian Synapses. *Proceedings of the National Academy of Sciences of the United States of America* **89,** 3330-3333.

Urbano FJ, Piedras-Renteria ES, Jun KS, Shin HS, Uchitel OD & Tsien RW. (2003). Altered Properties of Quantal Neurotransmitter Release at Endplates of Mice Lacking P/Q-type Ca2+ Channels. *Proceedings of the National Academy of Sciences of the United States of America* **100,** 3491-3496.

Urbano FJ, Rosato-Siri MD & Uchitel OD. (2002). Calcium Channels Involved in Neurotransmitter Release at Adult, Neonatal and P/Q-Type Deficient Neuromuscular Junctions (Review). *Molecular Membrane Biology* **19,** 293-300.

Urbano FJ & Uchitel OD. (1999). L-Type Calcium Channels Unmasked by Cell-Permeant Ca2+ Buffer at Mouse Motor Nerve Terminals. *Pflügers Archiv* **437,** 523-528.

Valdez G, Tapia JC, Kang H, Clemenson GD, Jr., Gage FH, Lichtman JW & Sanes JR. (2010). Attenuation of Age-Related Changes in Mouse Neuromuscular Synapses by Caloric Restriction and Exercise. *Proceedings of the National Academy of Sciences of the United States of America* **107,** 14863-14868.

Valenzuela DM, Stitt TN, Distefano PS, Rojas E, Mattsson K, Compton DL, Nunez L, Park JS, Stark JL, Gies DR, Thomas S, Lebeau MM, Fernald AA, Copeland NG, Jenkins NA, Burden SJ, Glass DJ & Yancopoulos GD. (1995). Receptor tyrosine kinase specific for the skeletal muscle lineage: Expression in embryonic muscle, at the neuromuscular junction, and after injury. *Neuron* **15,** 573-584.

Varoqueaux F, Sigler A, Rhee JS, Brose N, Enk C, Reim K & Rosenmund C. (2002). Total Arrest of Spontaneous and Evoked Synaptic Transmission but Normal Synaptogenesis in the Absence of Munc13-Mediated Vesicle Priming. *Proceedings of the National Academy of Sciences of the United States of America* **99,** 9037-9042.

Verona M, Zanotti S, Schafer T, Racagni G & Popoli M. (2000). Changes of Synaptotagmin Interaction with t-SNARE Proteins In Vitro After Calcium/Calmodulin-Dependent Phosphorylation. *Journal of Neurochemistry* **74,** 209-221.

Vogel Z, Christian CN, Vigny M, Bauer H, Sonderegger P & Daniels MP. (1983). Laminin Induces Acetylcholine Receptor Aggregation on Cultured Myotubes and Enhances the Receptor Aggregation Activity of a Neuronal Factor. *Journal of Neuroscience* **3,** 1058-1068.

Walchsolimena C, Blasi J, Edelmann L, Chapman ER, Vonmollard GF & Jahn R. (1995). The t-SNAREs Syntaxin 1 and SNAP-25 are Present on Organelles that Participate in Synaptic Vesicle Recycling. *Journal of Cell Biology* **128,** 637-645.

Walker D, Bichet D, Campbell KP & De Waard M. (1998). A β4 Isoform-Specific Interaction Site in the Carboxyl-Terminal Region of the Voltage-Dependent Ca^{2+} Channel α_{1A} Subunit. *Journal of Biological Chemistry* **273,** 2361-2367.

Walker D & De Waard M. (1998). Subunit Interaction Sites in Voltage-Dependent Ca^{2+} Channels: Role in Channel Function. *Trends in Neurosciences* **21,** 148-154.

Wallace BG. (1989). Agrin-Induced Specializations Contain Cytoplasmic, Membrane, and Extracellular Matrix-Associated Components of the Postsynaptic Apparatus. *Journal of Neuroscience* **9,** 1294-1302.

Walmsley B, Edwards F & Tracey D. (1988). Nonuniform Release Probabilities Underlie Quantal Synaptic Transmission at a Mammalian Excitatory Central Synapse. *Journal of Neurophysiology* **60,** 889-908.

Walrond J & Reese T. (1985). Structure of Axon Terminals and Active Zones at Synapses on Lizard Twitch and Tonic Muscle Fibers. *Journal of Neuroscience* **5,** 1118-1131.

Walsh MK & Lichtman JW. (2003). In vivo time-lapse imaging of synaptic takeover associated with naturally occurring synapse elimination. *Neuron* **37,** 67-73.

Wang N, Butler JP & Ingber DE. (1993). Mechanotransduction across the Cell Surface and through the Cytoskeleton. *Science* **260,** 1124-1127.

Wang Y, Liu XR, Biederer T & Sudhof TC. (2002). A Family of Rim-Binding Proteins Regulated by Alternative Splicing: Implications for the Genesis of Synaptic Active Zones. *Proceedings of the National Academy of Sciences of the United States of America* **99,** 14464-14469.

Wang Y, Okamoto M, Schmitz F, Hofmann K & Sudhof TC. (1997). Rim is a Putative Rab3 Effector in Regulating Synaptic-Vesicle Fusion. *Nature* **388,** 593-598.

Wang Y, Sugita S & Sudhof TC. (2000). The Rim/Nim Family of Neuronal C_2 Domain Proteins- Interactions with Rab3 and a New Class of Src Homology 3 Domain Proteins. *Journal of Biological Chemistry* **275,** 20033-20044.

Weber T, Zemelman BV, McNew JA, Westermann B, Gmachl M, Parlati F, Söllner TH & Rothman JE. (1998). SNAREpins: Minimal Machinery for Membrane Fusion. *Cell* **92,** 759-772.

Weinstein S. (1980). A Comparative Electrophysiological Study of Motor End-Plate Diseased Skeletal Muscle in the Mouse. *Journal of Physiology* **307,** 453-464.

Weiss N. (2008). The N-type voltage-gated calcium channel: when a neuron reads a map. *Journal of Neuroscience* **28,** 5621-5622.

Westerga J & Gramsbergen A. (1994). Development of the EMG of the Soleus Muscle in the Rat. *Developmental Brain Research* **80,** 233-243.

Wheeler DB, Randall A & Tsien RW. (1996). Changes in action potential duration alter reliance of excitatory synaptic transmission on multiple types of Ca2+ channels in rat hippocampus. *Journal of Neuroscience* **16,** 2226-2237.

Wolpowitz D, Mason T, Dietrich P, Mendelsohn M, Talmage DA & Role LW. (2000). Cysteine-Rich Domain Isoforms of the< i> Neuregulin-1</i> Gene Are Required for Maintenance of Peripheral Synapses. *Neuron* **25,** 79-91.

Wood SJ & Slater CR. (1997). The Contribution of Postsynaptic Folds to the Safety Factor for Neuromuscular Transmission in Rat Fast- Aad Slow-Twitch Muscles. *Journal of Physiology-London* **500,** 165-176.

Wood SJ & Slater CR. (2001). Safety Factor at the Neuromuscular Junction. *Progress in Neurobiology* **64,** 393-429.

Wu H, Xiong WC & Mei L. (2010). To Build a Synapse: Signaling Pathways in Neuromuscular Junction Assembly. *Development* **137,** 1017-1033.

Xia ZP, Zhou Q, Lin JL & Liu YC. (2001). Stable SNARE Complex Prior to Evoked Synaptic Vesicle Fusion Revealed by Fluorescence Resonance Energy Transfer. *Journal of Biological Chemistry* **276,** 1766-1771.

Xiao WZ, Poirier MA, Bennett MK & Shin YK. (2001). The Neuronal t-Snare Complex is a Parallel Four-Helix Bundle. *Nature Structural Biology* **8,** 308-311.

Yoshihara M & Littleton JT. (2002). Synaptotagmin I Functions as a Calcium Sensor to Synchronize Neurotransmitter Release. *Neuron* **36,** 897-908.

Yumoto N, Wakatsuki S & Sehara-Fujisawa A. (2005). The Acetylcholine Receptor γ-to-ε Switch Occurs in Individual Endplates. *Biochemical and Biophysical Research Communication* **331,** 1522-1527.

Yurchenco P & Cheng Y-S. (1993). Self-assembly and calcium-binding sites in laminin. A three-arm interaction model. *Journal of Biological Chemistry* **268,** 17286-17299.

Yurchenco PD & Orear JJ. (1994). Basal Lamina Assembly. *Current Opinion in Cell Biology* **6,** 674-681.

Yurchenco PD & Patton BL. (2009). Developmental and Pathogenic Mechanisms of Basement Membrane Assembly. *Current Pharmaceutical Design* **15,** 1277-1294.

Zaitsev AV, Povysheva NV, Lewis DA & Krimer LS. (2007). P/Q-type, But Not N-Type, Calcium Channels Mediate Gaba Release from Fast-Spiking Interneurons to Pyramidal Cells in Rat Prefrontal Cortex. *Journal of Neurophysiology* **97,** 3567-3573.

Zenker M, Pierson M, Jonveaux P & Reis A. (2005). Demonstration of Two Novel *LAMB*2 Mutations in the Original Pierson Syndrome Family Reported 42 Years Ago. *American Journal of Medical Genetics Part A* **138,** 73-74.

Zenker M, Tralau T, Lennert T, Pitz S, Mark K, Madlon H, Dötsch J, Reis A, Müntefering H & Neumann LM. (2004). Congenital Nephrosis, Mesangial Sclerosis, and Distinct Eye Abnormalities with Microcoria: An Autosomal Recessive Syndrome. *American Journal of Medical Genetics Part A* **130,** 138-145.

Zhang B, Luo S, Wang Q, Suzuki T, Xiong WC & Mei L. (2008). LRP4 Serves as a Coreceptor of Agrin. *Neuron* **60,** 285-297.

Zhang JF, Randall AD, Ellinor PT, Horne WA, Sather WA, Tanabe T, Schwarz TL & Tsien RW. (1993). Distinctive Pharmacology and Kinetics of Cloned Neuronal Ca2+ Channels and their Possible Counterparts in Mammalian CNS neurons. *Neuropharmacology* **32,** 1075-1088.

Zheng X & Bobich JA. (1998). A Sequential View of Neurotransmitter Release. *Brain Research Bulletin* **47,** 117-128.

Zhong H, Yokoyama CT, Scheuer T & Catterall WA. (1999). Reciprocal Regulation of P/Q-type Ca^{2+} Channels by SNAP-25, Syntaxin and Synaptotagmin. *Nature Neuroscience* **2,** 939-941.

Ziskind-Conhaim L & Bennett JI. (1982). The Effects of Electrical Inactivity and Denervation on the Distribution of Acetylcholine-Receptors in Developing Rat Muscle. *Developmental Biology* **90,** 185-197.

Ziskind-Conhaim L, Inestrosa NC & Hall ZW. (1984). Acetylcholinesterase is Functional in Embryonic Rat Muscle Before its Accumulation at the Sites of Nerve Muscle Contact. *Developmental Biology* **103,** 369-377.